



**Determination of geotechnical characteristics of sensitive clay of Lac-Saint-Jean in the  
objective of prediction of retrogressive landslides**

**By**

**Sarah Jacob**

**Under the supervision of Dr. Ali Saeidi and the co-supervision of Dr. Abouzar Sadrekarimi**

**Thesis presented to the University of Quebec at Chicoutimi with a view to obtaining the degree of  
Doctor of Philosophy (Ph.D.) in engineering (Civil)**

**BOARD OF EXAMINERS:**

Dr Maxime Claprood, Professor, Department of Applied Sciences, UQAC, President of the Board

Dr. Bipul Hawlader, Professor, Department of Civil Engineering, Memorial University of Newfoundland, External Member of the Board

Dr. Ripon Hore, Senior Assistant Engineer, LGED, External Member of the Board

Dr. Ali Saeidi, Professor, Department of Applied Sciences, UQAC, Internal Member of the Board

Dr. Abouzar Sadrekarimi, Associate Professor, Department of Civil & Environmental Engineering, Western University, Internal Member  
of the Board

Québec, Canada

© Sarah Jacob, 2024

## RÉSUMÉ

Les argiles sensibles sont vulnérables à la moindre perturbation, ce qui entraîne souvent des glissements de terrain catastrophiques, les rendant hautement désastreuses et préjudiciables. Les régions de l'Est du Canada, comme le Québec et l'Ontario, possèdent d'importants dépôts de ces argiles sensibles, qui représentent une menace sérieuse pour la vie et les biens. La dégradation de la résistance des argiles sensibles est due à l'assouplissement post-pic sous contrainte, conduisant à des glissements de terrain rétrogressifs. Une conséquence majeure de ces glissements est l'ampleur des mouvements post-rupture qui y sont associés. L'évaluation de ces mouvements est essentielle dans les études de susceptibilité aux glissements de terrain. Les études existantes ont utilisé plusieurs critères pour la rétrogression, sous forme de propriétés physiques et mécaniques du sol, ainsi que certains modèles d'assouplissement sous contrainte pour définir avec précision ces mouvements. Cependant, une revue détaillée de la littérature montre qu'un critère énergétique peut évaluer ces mouvements avec une meilleure précision, et que l'historique des contraintes du sol joue un rôle significatif dans le comportement d'assouplissement sous contrainte. Cela signifie également que ces études d'évaluation des glissements de terrain devraient être accompagnées d'études de caractérisation géotechnique fournissant des informations spécifiques au site sur l'historique des contraintes du sol ainsi que sur son comportement en cisaillement. La présente étude vise à aborder le comportement complexe post-pic des argiles sensibles en cisaillement non drainé à travers un modèle mathématique et un critère énergétique, en tenant compte des propriétés physiques et mécaniques du sol. Parmi les argiles sensibles de l'Est canadien, les argiles de Laflamme sont relativement moins explorées. Ainsi, une investigation géotechnique détaillée a été menée sur les argiles de deux zones d'étude autour du Lac-Saint-Jean : Desbiens et Albanel. De plus, ces résultats sont appliqués à l'analyse de stabilité des pentes et à un critère pour les glissements de terrain rétrogressifs basé sur l'énergie de remaniement. Les résultats montrent l'importance de l'historique des contraintes dans l'assouplissement sous contrainte des argiles sensibles. À travers le modèle mathématique développé, une bonne estimation des déformations à grande échelle peut être obtenue à partir des résultats expérimentaux. Les études expérimentales et numériques montrent que les argiles de Laflamme sont surconsolidées et fortement lessivées par rapport aux argiles de Champlain. De plus, il existe des différences en termes de minéralogie, de plasticité et de composition élémentaire, principalement dues à une faible quantité de minéraux argileux, à une grande quantité de farine rocheuse résultant du broyage glaciaire du Bouclier canadien, à la surconsolidation et à l'environnement lacustre du Lac-Saint-Jean. Cela souligne la nécessité d'études spécifiques à chaque région pour analyser les glissements de terrain dans les argiles sensibles. En outre, les paramètres de résistance au cisaillement déterminés en laboratoire présentent un effet d'échelle lorsqu'ils sont appliqués aux grandes pentes en argiles sensibles. Cela est démontré par l'analyse rétrospective des pentes survenues dans la région de Desbiens et d'Albanel à l'aide d'une analyse d'équilibre limite.

Mots clés: argile sensible, glissement de terrain rétrogressif, adoucissement par déformation, caractérisation géotechnique, stabilité des pentes, photogrammétrie

## ABSTRACT

Sensitive clays are vulnerable to even the slightest of disturbance, often resulting in catastrophic landslides, making them highly disastrous and detrimental. The Eastern Canadian regions of Quebec and Ontario have large deposits of such sensitive clays which pose a serious threat to life and property. Strength degradation in sensitive clays is due to post - peak strain softening leading to retrogressive landslides. A major consequence of such landslides is the large post failure movements associated with them. Assessment of these movements is key in landslide susceptibility studies. Existing studies have used several criteria for retrogression, in the form of physical and mechanical properties of the soil as well as certain strain - softening models to accurately define these movements. However, detailed literature review shows that an energy criterion can assess these land movements with better precision and the stress history of the soil plays a significant role in the strain softening behaviour itself. This also means that such landslide assessment studies should be accompanied by geotechnical characterization studies which gives site - specific information on the stress history of the soil as well as its shear behaviour. The present study aims to address the complex post-peak behaviour of sensitive clays in undrained shear through a mathematical model and energy criterion by taking into consideration the physical and mechanical properties of the soil. Among Eastern Canadian sensitive clays, the Laflamme clays are relatively less explored and hence a detailed geotechnical investigation on clays from two study areas surrounding the Lac-Saint-Jean – Desbiens and Albanel have been conducted. Furthermore, these findings are applied to slope stability analysis and a criterion for retrogressive landslides based on remoulding energy. The results show the important role played by stress history in strain softening in sensitive clays. Through the mathematical model developed, a good estimation of large deformation strain can be made from experimental results. Experimental and numerical studies show that Laflamme clays are overconsolidated and highly leached in comparison to the Champlain clays. In addition to that there are differences in mineralogy, plasticity and elemental composition that primarily stems from low quantity of clay minerals, high amount of rock flour due to glacial grinding of the Canadian Shield, overconsolidation and lacustrine environment of the Lac-Saint-Jean. This highlights the need of region specific studies in the analysis of sensitive clay landslides. Additionally, shear strength parameters determined in the laboratory suffer a scale effect when applied to large sensitive clay slopes. This is shown by back analysis of occurred slopes in the region of Desbiens and Albanel by limit equilibrium analysis.

**Keywords:** sensitive clay, retrogressive landslide, strain softening, geotechnical characterization, slope stability, photogrammetry

## TABLE OF CONTENTS

RÉSUMÉ .....	ii
ABSTRACT .....	iii
LIST OF TABLES.....	vii
LIST OF FIGURES .....	viii
LIST OF SYMBOLS .....	x
LIST OF ABBREVIATIONS.....	xii
DEDICATION.....	xiii
ACKNOWLEDGMENTS .....	xiv
CHAPTER 1 .....	1
<b>INTRODUCTION .....</b>	<b>1</b>
1.1 General.....	1
1.2 Problem statement.....	3
1.3 Research objectives.....	5
1.4 Methodology.....	5
1.4.1 Assessment of the dependence of remoulding energy on soil properties .....	6
1.4.2 Formulation of post - peak strain softening behaviour of sensitive clays .....	6
1.4.3 Geotechnical characterization of sensitive clays.....	7
1.4.4 Evaluation of geotechnical parameters for sensitive clay slopes on large scale.....	8
1.5 Originality.....	8
1.6 Thesis outline.....	9
CHAPTER 2 .....	11
<b>Article 1: Remoulding energy as a criterion in assessing retrogressive landslides in sensitive clays – A review and its applicability to Eastern Canada.....</b>	<b>11</b>
2.1 Abstract.....	12
2.2 Introduction.....	12
2.3 Mechanism of landslides in sensitive clays .....	14
2.4 Existing criteria for retrogression in sensitive clays .....	17
2.5 Remoulding energy as a parameter for retrogressive landslides .....	20
2.5.1 Energy balance in post failure movements.....	20
2.5.2 Existing methods for determining remoulding energy .....	22
2.6 Determination of remoulding energy for sensitive clays of Eastern Canada .....	26
2.7 Discussions .....	36
2.8 Conclusions and summary .....	39
CHAPTER 3 .....	40



<b>Article 2: An exponential model for strain softening behaviour of sensitive clays.....</b>	<b>40</b>
3.1 Abstract.....	41
3.2 Introduction.....	41
3.2.1 Background.....	41
3.2.2 Existing studies on strain softening in sensitive clays.....	43
3.3 Data acquisition for model development .....	45
3.4 Development of the strain softening model .....	48
3.5 Validation of predicted remoulded strain by field data.....	57
3.5.1 Establishing a correlation between $L_R$ and predicted $\gamma_r$ .....	57
3.5.2 Validation of predicted $\gamma_r$ by other landslide data.....	58
3.5.3 Effect of topography on $L_R$ .....	61
3.6 Discussions .....	66
3.7 Conclusions.....	69
CHAPTER 4 .....	70
<b>Article 3: Geotechnical characterization of Laflamme clays from the lac-Saint-Jean basin, Quebec.....</b>	<b>70</b>
4.1 Abstract.....	71
4.2 Introduction.....	71
4.3 Geological origin and sampling.....	72
4.4 Sample preparation and testing methodology .....	74
4.4.1 Physical properties and microstructural investigations .....	74
4.4.2 Laboratory element tests .....	75
4.4.3 Undrained shear strength profiles .....	78
4.5 Experimental results .....	80
4.5.1 Index properties.....	80
4.5.2 Chemical composition and microstructural investigations.....	82
4.5.3 Laboratory element tests .....	87
4.5.4 Undrained shear strength profiles .....	94
4.6 Discussion.....	105
4.7 Conclusions.....	107
CHAPTER 5 .....	109
<b>Article 4: Evaluation of geotechnical parameters for sensitive clay slopes in Lac-Saint-Jean region using back analysis.....</b>	<b>109</b>
5.1 Abstract.....	110
5.2 Introduction.....	110
5.3 Geological background and history of landslide in study area .....	113
5.3.1 Desbiens.....	115

5.3.2 Albanel.....	119
5.4 Methodology.....	120
5.4.1 Prefailure topography of the study area .....	121
5.4.2 Estimation of geotechnical parameters on large scale.....	126
5.5 Results and interpretaions .....	128
5.5.1 Slope stability analysis.....	128
5.5.2 Overall summary .....	132
5.6 Conclusions.....	134
CHAPTER 6 .....	136
6.1 Conclusions.....	136
6.2 Recommendations.....	137
REFERENCES .....	138
PUBLICATIONS .....	150

## LIST OF TABLES

Table 2-1 Properties of Eastern Canadian sensitive clays.....	26
Table 2-2 Properties of Norwegian sensitive clays from [13] .....	28
Table 3-1 Properties of data used for model calibration .....	45
Table 3-2 Triaxial testing conditions of data used in model calibration .....	46
Table 3-3 Model parameters for the strain softening equation applied to data for calibration .....	55
Table 3-4 Landslide data used in the application of the proposed model .....	59
Table 3-5 Outline of geological conditions at each landslide location .....	62
Table 4-1 Summary of the CUI triaxial tests performed in this study .....	77
Table 4-2 Summary of the CUK0 triaxial tests performed in this study.....	78
Table 4-3 Average index properties of Desbiens and Albanel clay samples .....	82
Table 4-4 Mohr-Coulomb strength parameters.....	93
Table 5-1: Summary of properties of Desbiens and Albanel clays .....	121
Table 5-2 Model parameters used in finite element modelling for Desbiens clay slope.....	130
Table 5-3 Model parameters used in finite elemnt modelling for Albanel clay slope .....	131

## LIST OF FIGURES

Figure 1-1 Post - peak strain softening behaviour in sensitive clays .....	7
Figure 2-1 Mechanism of flowslides with rotational failure surfaces (adapted from [52]) .....	15
Figure 2-2 Mechanism of spreads in which the failure surface is almost horizontal forming horsts and grabens (adapted from [52]) .....	16
Figure 2-3 Illustration of quickness test: (a) empty cylinder into which clay is poured (b) cylinder is slowly lifted upwards (c) remoulded clay slumps (adapted from [57]) .....	20
Figure 2-4 Distribution of post-failure potential energy (adapted from [61]) .....	21
Figure 2-5 Energy distribution for (a) purely ductile material and (b) highly brittle material .....	22
Figure 2-6 Experimental investigations of remoulding by Tavenas et al., (1983) (a) Free fall test, (b) Impact test, (c) Extrusion test, and (d) Shearing test (adapted from [63]) .....	24
Figure 2-7 Ideal shear stress - shear strain curve used to calculate remoulding energy (adapted from [64]) ...	25
Figure 2-8 Shear stress - rotation curve according to [65] .....	26
Figure 2-9 Exponential extrapolation of DSS curves until remoulded shear strength to obtain $\gamma_r$ .....	29
Figure 2-10 Variations of remoulding energy for Eastern Canadian clays with (a) liquidity index, (b) plasticity index and (c) preconsolidation pressure .....	32
Figure 2-11 Comparison of remoulding energy of Eastern Canadian and Norwegian clays and their dependence on (a) liquidity index and (b) plasticity index .....	33
Figure 2-12 Post-peak strain softening curves from DSS results of selected Eastern Canadian sites (solid lines represent the laboratory data and dashed lines show the exponential extrapolations) .....	35
Figure 2-13 Remoulding energy at various degrees of remoulding index obtained from DSS results (solid lines represent the laboratory data and dashed lines show the exponential extrapolations). .....	36
Figure 3-1 Retrogressive failure morphology in (a) flowslides and (b) spreads (Adaptation from [76]) .....	42
Figure 3-2 Plasticity chart for data used in model calibration .....	46
Figure 3-3 CUI triaxial results for representative set of data used for model calibration .....	48
Figure 3-5 Post - peak strain softening model where $s_{up}$ = peak undrained shear strength, $s_{ur}$ = remoulded undrained shear strength, $\gamma_p$ = strain at peak stress, $\gamma_r$ = strain at remoulded shear strength, a and b = model parameters .....	50
Figure 3-6 Correlation between model parameter 'a' and $s_{up}$ .....	51
Figure 3-7 Post - peak parameters in the strain softening curve .....	54
Figure 3-8 Laboratory shear data (scatter points) along with model prediction (dotted lines) for selected clays of data used for model calibration .....	56
Figure 3-9 Correlation between $L_R$ and predicted $\gamma_r$ .....	58
Figure 3-10 Predicted $\gamma_r$ of validation data fitted with the established correlation between $L_R$ and $\gamma_r$ .....	60
Figure 3-11 Predicted post - peak strength degradation according to the proposed model for landslide sites outside the initial dataset (Field retrogression distances are shown adjacent to each curve) .....	61
Figure 4-1 Triaxial equipment from Wille Geotechnick used for sample testing .....	76
Figure 4-2 Desbiens and Albanel study area with sampling locations and borehole locations of FVT .....	80
Figure 4-3 (a) Grain size distributions of samples from Desbiens and Albanel sites (b) Variations of Atterberg limits and natural water content with depth in Desbiens samples .....	81
Figure 4-4 (a) Plasticity chart and (b) activity of Desbiens and Albanel clays .....	82
Figure 4-5 Variation of salinity with depth for Desbiens clays .....	83
Figure 4-6 XRD spectra of (a) and (b) whole sample and; (c) and (d) clay fractions of sample in Desbiens and Albanel clays respectively .....	84
Figure 4-7 SEM images of (a) Desbiens clay with a band length of 10 $\mu\text{m}$ , (b) Desbiens clay with a band length of 1 $\mu\text{m}$ , (c) Albanel clay with a band length of 2 $\mu\text{m}$ , (d) Albanel clay with a band length of 1 $\mu\text{m}$ , (e) Remoulded Desbiens clay with a band length of 1 $\mu\text{m}$ .....	86
Figure 4-8 Energy Dispersive Spectrometry results of (a) Desbiens and (b) Albanel clays .....	87

Figure 4-9 (a) Deviatoric stresses and (b) excess pore water pressures, and (c) stress paths of CUI tests carried out in this study.....	89
Figure 4-10 Variations of horizontal effective stress ( $\sigma'_3$ ) with vertical effective stress ( $\sigma'_1$ ) in CUK0 tests of this study.....	90
Figure 4-11 (a) Stress - strain behaviour and (b) stress paths of CUK0 tests .....	92
Figure 4-12 : Peak and residual stress states of Desbiens and Albanel clays from CUI and CUK0 tests.....	92
Figure 4-13 Best fit lines from which Mohr-Coulomb parameters are determined for (a) Desbiens and (b) Albanel samples from both CUI and CUK0 tests .....	93
Figure 4-14 $A_f$ - OCR relations for Desbiens and Albanel in comparison with other Eastern Canadian clays. ....	94
Figure 4-15 FVT results showing variations of (a) $s_{upFVT}$ and (b) $s_{urFVT}$ with depth for Desbiens clays and (c) $s_{upFVT}$ and (d) $s_{urFVT}$ with depth for Albanel clays along with average values at each 2 m depth.....	96
Figure 4-16 CPT profiles at a Desbiens site showing variation of (a) $q_t$ , (b) $u_2$ , (c) $Q_{tn}$ and (d) $B_q$ with depth .....	97
Figure 4-17 CPT profiles at an Albanel site showing variations of (a) $q_t$ , (b) $f_s$ , (c) $u_2$ , (d) $Q_{tn}$ , (e) $F_r$ , (f) $I_c$ and (g) $B_q$ with depth.....	98
Figure 4-18 Soil behaviour type chart according to [131] for Albanel clays.....	99
Figure 4-19 Estimated $N_{kt}$ values for (a) peak and (b) remoulded strengths at Desbiens site and (c) peak and (d) remoulded strengths at Albanel site.....	101
Figure 4-20 Peak undrained strength profiles in (a) Desbiens and (b) Albanel clays from field (CPT and FVT) and laboratory (FCT and CUI triaxial) tests .....	102
Figure 4-21 Remoulded undrained strength profiles in (a) Desbiens and (b) Albanel clays based on field FVT and laboratory FCT and LVT tests .....	103
Figure 4-22 Variation of sensitivity with depth in Desbiens and Albanel clays based on FVT and CPT results of this study.....	104
Figure 4-23 Remoulded undrained strengths of Desbiens and Albanel clays based on FCT and FVT results of this study and comparisons with empirical correlations .....	104
Figure 5-1 Stress-strain behaviour of clays as a function of overconsolidation.....	113
Figure 5-2 Geological history of the Lac-Saint-Jean (modified from Nutz et al. 2015). ....	115
Figure 5-3 Aerial photograph from 1960 showing almost no scars near Saint Jerome but small scars towards the west. ....	116
Figure 5-4 Aerial photographs from (a) 1972, (b) 1991 and (c) 2000 showing landslide scars from 1946, 1953, 1964, 1983 as well as small scars along the shore. ....	118
Figure 5-5 A 2013 LiDAR image showing landslide scars in the Desbiens region.....	118
Figure 5-6 LiDAR image from 2013 showing the landslide scar in the Albanel area .....	119
Figure 5-7 LiDAR from 2013 showing contour lines and possible start of pre-failure topography .....	120
Figure 5-8 DTM of Desbiens from which pre-failure topography was developed in LeapFrog Geo software .....	122
Figure 5-9 DTM of Albanel from which the pre-failure topography was developed in LeapFrog Geo software .....	124
Figure 5-10 Examples of few sections extracted from the LiDAR image of Albanel in LeapFrog Geo .....	125
Figure 5-11 Models used for stability analysis of (a) Desbiens and (b) Albanel sites .....	126
Figure 5-12 Model for (a) Desbiens and (b) Albanel in Slide 2 D with initial $c'$ and $\phi'$ used for analysis.....	128
Figure 5-13 Slope stability analysis showing marginally stable Desbiens slope in Slide 2D .....	129
Figure 5-14 Slope stability analysis showing marginally stable Albanel slope in Slide 2D.....	130
Figure 5-15 Finite element modelling results of (a) Desbiens and (b) Albanel in RS2 software.....	132
Figure 5-16 LiDAR image of Albanel showing landslide debris at foot of the scar.....	132
Figure 5-17 Predicted strain softening curve until remoulded state of Desbiens and Albanel for the determination of remoulding energy.....	134

## LIST OF SYMBOLS

$a$	coefficient of exponential strain softening model dependent	$G$	secant shear modulus
$A$	activity	$G_s$	specific gravity
$A_f$	Skempton's pore pressure parameter at failure	$\gamma$	shear strain of the soil
$b$	coefficient of exponential strain softening model dependent	$\gamma^p$	plastic strain in post - peak region
$B_q$	excess pore pressure ratio in CPT	$\gamma_{95}$	shear strain corresponding to a strength reduction of 95% of ( $s_{up}-s_{ur}$ )
$B_{St}$	brittleness for sensitive clays	$\gamma_p$	shear strain at peak shear strength of the soil
$c'$	effective cohesion	$\gamma_r$	shear strain at remoulded shear strength of the soil
$c'_p$	effective cohesion at peak state	$\gamma_{res}$	shear strain at residual state of the soil
$c'_r$	effective cohesion at residual state	$\gamma_s$	unit weight of the soil
$\bar{\delta}$	nominal displacement of the shear band	$\gamma_{yx}$	shear strain in X direction of a soil element below a slope
$\Delta\sigma_f$	deviatoric stress at failure	$\gamma_{xy}$	shear strain in Y direction of a soil element below a slope
$\Delta\sigma_i$	initial deviatoric stress	$H$	height of the clay slope
$\Delta u$	excess porewater pressure	$H_f$	height of the slumped remoulded clay in a quickness test
$\Delta u_f$	porewater pressure at failure	$H_o$	initial height of the cylinder for a quickness test
$\dot{\epsilon}$	axial strain rate	$I_B$	brittleness index
$\epsilon_a$	axial strain	$I_c$	soil behaviour type index
$\epsilon_f$	axial strain at failure	$I_L$	Liquid limit
$\epsilon_r$	radial strain	$I_p$	plasticity index
$\epsilon_{vol}$	volumetric strain	$I_r$	remoulding index
$\epsilon_x$	axial strain along X direction on a soil element below a slope	$K_0$	coefficient of lateral earth pressure at rest
$\epsilon_y$	axial strain along Y direction on a soil element below a slope	$L_R$	retrogression distance
$E_F$	frictional energy	$\lambda$	shape factor
$E_K$	kinetic energy	$n$	stress normalization exponent
$E_N$	normalized remoulding energy	$N_C$	stability number
$E_P$	potential energy	$N_{kt}$	cone factor
$E_R$	remoulding energy	$p'$	effective mean stress
$\phi'$	effective friction angle	$P_a$	atmospheric pressure
$\phi'_p$	effective friction angle at peak state	$q$	deviatoric stress
$\phi'_r$	effective friction angle at residual state	$q'$	effective deviatoric stress
$F_r$	friction ratio	$Q$	quickness
$f_s$	sleeve friction	$q_t$	corrected cone tip resistance

$Q_{tn}$	normalized cone tip resistance parameter	$\tau_{ff}$	shear stress along the failure plane of a soil element below a slope
$r_u$	excess pore pressure ratio in a triaxial test	$\tau_p$	peak shear strength
$\sigma'_1$	effective vertical stress at the end of $K_0$ consolidation	$\tau_r$	residual shear strength
$\sigma'_{1m}$	major principal stress	$\tau_{yx}$	shear stress along X direction of a soil element below a slope
$\sigma'_3$	effective horizontal stress at the end of $K_0$ consolidation	$\tau_{xy}$	shear stress along Y direction of a soil element below a slope
$\sigma'_{3c}$	confining pressure	$T_{tot}$	total corrected torque
$\sigma'_{3m}$	minor principal stress	$u_2$	Pore pressure behind the shoulder in a CPT
$\sigma_{ff}$	normal stress along the failure plane of a soil element below a slope	$\omega_L$	liquid limit
$\sigma_n$	normal stress	$\omega_P$	plastic limit
$\sigma'_n$	effective normal stress	$w_N$	natural water content
$\sigma'_p$	preconsolidation pressure		
$\sigma_v$	total vertical stress		
$\sigma'_v$	effective vertical stress on a soil element below a slope		
$\sigma'_x$	effective stress along X direction on a soil element below a slope		
$\sigma'_y$	effective stress along Y direction		
$S$	softening modulus/index		
$S_t$	sensitivity		
$s_u$	undrained shear strength of the soil		
$s_{uCPT}$	undrained shear strength from cone penetration test		
$s_{uFCT}$	undrained shear strength from fall cone test		
$s_{uFVT}$	undrained shear strength from field vane test		
$s_{up}$	undrained shear strength of intact soil		
$s_{upFVT}$	undrained shear strength of intact soil from field vane tests		
$s_{ur}$	undrained shear strength of remoulded soil		
$s_{urFCT}$	undrained shear strength of remoulded soil from fall cone test		
$s_{urFVT}$	undrained shear strength of remoulded soil from field vane test		
$s_{urLVT}$	undrained shear strength of remoulded soil from laboratory vane test		
$s_{ux}$	undrained shear strength of partially remoulded soil		
$\theta$	angle of inclination of a plane within a soil element below a slope		

## LIST OF ABBREVIATIONS

ASTM	American Society of Testing Materials	LVDT	Linear Variable Differential Transformer
BP	Before present	MC	Mohr-Coulomb
CF	Clay fraction	MPM	Material Point Method
CGS	Canadian Geotechnical Society	MTQ	Ministère des Transports et de la Mobilité Durable du Québec
CPT	Cone Penetration Test	MTMDET	Ministère des Transports, de la Mobilité durable et de l'Électrification des transports
CUI	Isotropically Consolidated Undrained	NGF	Norsk Geoteknisk Forening
CUK0	K <sub>0</sub> Consolidated Undrained	OCR	Overconsolidation ratio
DSS	Direct Simple Shear	SBT	Soil Behaviour Type
EFVST	Electric Field Vane Shear Test	SEM	Scanning Electron Microscopy
FCT	Fall Cone Test	SJV	Saint Jean Vianney
FVT	Field Vane Test	SLSJ	Saguenay-Lac-Saint-Jean
GWT	Ground Water Table	SPF	Smoothed Particle Hydrodynamics
LDfEM	Large Deformation Finite Element Method	VPC	Volume Pressure Control
LiDAR	Light Detection and Ranging	XRD	X-ray Diffraction
LSJ	Lac-Saint-Jean		



## **DEDICATION**

*To Acha and Amma,  
For always urging me to scale great heights*

## ACKNOWLEDGMENTS

I am deeply grateful to all the individuals whose support, guidance, and encouragement have been pivotal in the completion of my PhD thesis.

First and foremost, my heartfelt thanks go to my supervisor, Dr. Ali Saeidi, for his unfaltering belief in my abilities. His support and encouragement throughout my Ph.D. journey were instrumental in enabling me to pursue forward. Dr. Saeidi's patience and kindness helped me to carry out this huge task with enthusiasm and vigour.

I am also profoundly appreciative of my co-supervisor, Dr. Abouzar Sadrekarimi, for his sharp knowledge and strong guidance. His proficiency and contribution has been crucial in solving several complexities of this research and has helped me to approach every avenue of my research with critical thinking.

A special thank you to my mentor, Dr. Rama Vara Prasad Chavali, for guiding me through the right path and imparting in me the fundamentals of writing and approaching research articles. He has always made time even during his busy schedules that I deeply appreciate and cherish.

I am deeply indebted to the laboratory technicians at Université du Québec à Chicoutimi (UQAC), especially Ms. Maryse Doucet and Mr. David Noel for guiding me through experimental investigations associated with this project including sample recovery and instrumentation. My fellow team members at UQAC, members of our research group - R2Eau especially Dr. Julien Walter, Yan Levesque and other colleagues have been extremely supportive and I truly acknowledge their presence in my time of need. My gratitude extends especially towards my team mates especially Zinan, Vineeth and Mahsa who have gone out of their way to reach out and lend a helping hand.

I could not have completed this journey without the support of my loving husband, Aaron who has always encouraged me to think forward and trusted my capabilities even when I faltered. The unconditional love and understanding of my parents, brother and mother-in-law will always be the foundation of my confidence to take up this journey. My family is my strength and no words could encompass the gratitude I have for them. Lastly, my heartfelt thanks goes to all my friends especially Jyotsna, Pooja, Sreelekshmi, Rony, Namitha, Sharook, Mohan, Jaya, Sreedevi, Silpa, Arun, David and Sanal who have been my steadfast support system and has helped me through the emotional challenges of my Ph.D. journey.

I sincerely appreciate each of you for your invaluable contributions to my academic and personal development. Your belief in me have been essential to this remarkable journey. Thank you for being such an integral part of it.

## CHAPTER 1

### INTRODUCTION

#### 1.1 GENERAL

Sensitive clays underlie extensive regions of the Northern hemisphere, including Canada, Sweden, Norway, Finland, Russia, as well as Northwestern America. These clays formed due to isostatic depression and post-glacial rebound followed by the leaching of marine sediments [1]. In Eastern Canada, the post glaciation period brought about the melting of the ice caps to a reduced profile followed by glacial erosion of the Canadian Shield abundant in rock flour. This enabled rock flour rich streams to flow into the marine limits. Subsequently, the rising sea level as well as the crust exposed the marine sediments to weathering. Rains and other fresh water sources leached out these clay sediments resulting in the formation of sensitive clays [2]. Clays are considered sensitive when they are susceptible to strain softening. This susceptibility of clays to undergo strength loss is often quantified by the sensitivity ( $S_t$ ) which is the ratio of shear strength of undisturbed soil to that of remoulded soil [3]. Highly sensitive clays with low remoulded shear strength, defined as less than 0.5 kPa and 0.4 kPa in Norway and Sweden, respectively, are referred to as quick clays [4]; [5]. In Canada, quick clays are defined based on sensitivity, according to the modified fourth edition of the Canadian Foundation Engineering Manual, where clays with sensitivities of 16 or above are termed quick [6].

A major hazard posed by sensitive clays are the retrogressive landslides, often leading to loss of life and property. Some of the examples of landslides in sensitive clays of Quebec are Saint Jean Vianney landslide in 1971 [7], slope failures associated with Saguenay earthquake in 1988 [8], St. Jude landslide in 2010 [9] and the landslide at Saint-Luc-de-Vincennes in 2016 [10]. Following initial failure, these landslides typically exhibit multiple retrogressive failures with significant post failure movements. Owing to the severity and the complexity involved in understanding and assessing them, several pragmatic approaches – both experimental and numerical are under way. One such approach is the analysis of these clays from the point of view of remoulding process and post-failure movements [11]. Remoulding in sensitive clays is the result of continuous strength degradation due to the destruction of its fabric [12]. The strain energy required for remoulding is termed the “remoulding energy.” It is often quantified in terms of the energy consumed to bring the soil from an intact state to a remoulded state which is represented as area under the stress-strain curve during strain softening [13].

Strain softening refers to the decrease in strength past the peak (intact) strength, into the post - peak regime during shear deformation. This reduction in strength could be due to a destruction in soil fabric thereby lowering their Mohr Coulomb (MC) parameters in overconsolidated clays [14]. It can also be due to an increase in shear induced pore water pressure leading to a reduction in effective stresses, a phenomenon more common in sensitive clays of contractive nature [15]; [16]; [17]. Natural processes like heavy rainfall and melting of snow; and human activities like vibration and heavy loading, can cause an increase in pore water pressure leading to a reduction in shear stresses in soil. One significant struggle in the laboratory analysis of strain softening in sensitive clays is that it requires large displacements/strains for the soil in its intact state to reach a completely remoulded state, where retrogressive failures are likely. This poses to be a difficult task due to the laboratory limits of strain. However, researchers have approached this problem by simplifying it using a linear strain softening model [13]; [18] or using models that maintain the non-linearity supported by several parametric studies and sensitivity analyses on well-studied landslides [19]. The severity of retrogressive failure depends on the amount of softening in the soil which is in turn dependant on the various geotechnical properties of the soil.

Geotechnical studies on sensitive clays have brought forward several interesting aspects about their physical and mechanical properties in the last two decades. In Eastern Canada, sensitive clay deposits occur primarily on three sedimentary basins - Champlain, Laflamme and Goldthwait Sea basins. Based on depositional conditions and extent of marine invasions, the geotechnical properties of Eastern Canadian clays vary significantly among the different sedimentary basins [20]. Sediments from the Laflamme basin are often found to be overconsolidated with lower water contents and higher percentages of silt and sand in comparison to those of Champlain and Goldthwaite basins [21]. This is attributed to the marine invasion being more recent in the Laflamme sea with significant erosion of the Canadian Shield supplying huge quantities of rock flour in the sediments. During the last glaciation period, the Laflamme sea was divided into two sub-basins – the Saguenay lowlands and the Lac-Saint-Jean (LSJ). A very distinguishing feature of the sediments in the LSJ is its extremely low salinity compared to the Champlain clays and other Laflamme clays of the Saguenay Fjord. The LSJ basin has a significant source of fresh water from the melting of continental inlands and glaciers and is primarily connected to the sea through the Saguenay River and the Saguenay Fjord. Thus, although the existing sediments in the LSJ region are of marine origin, there is a significant influx of freshwater, creating a

lacustrine environment unlike the marine environment in the Saguenay Fjord region. Accordingly, the geological history of the Laflamme sea shaped its present state which may be somewhat different from other Eastern Canadian clays.

A major application of geotechnical characterization study in clays is its use towards analysis of clay slopes and stability studies. Strain softening in sensitive clays extend to large deformations, which typically cannot be determined experimentally. This could sometime create difficulties with numerical modelling especially with regard to the choice of model parameters. Currently, the multiple retrogressive failure involving large deformation strains and strain softening is modelled using advanced techniques such as BIFURC, MPM (Material Point Method), LDFEM (Large deformation finite element modelling) and SPH (Smoothed Particle Hydrodynamics) [18]; [22]; [23]; [24]. However, these retrogressive failures are often triggered by a small scar or an initial slide which initiates at the toe of the slope due to a long term erosion. Slope stability analysis using limit equilibrium method or finite element analysis can be used for an initial estimation of safety as well as assess the possibility of it progressing to a retrogressive failure later [25].

Analysis of landslides in sensitive clays requires several tools and interpretation of various aspects of sensitive clays. Detailed geotechnical investigations coupled with appropriate strain softening models aid to analyse these failures with more precision. Moreover, interpreting the likelihood of a retrogressive failure using a first slide analysis is critical. These are the key factors that are primarily explored in this study.

## **1.2 PROBLEM STATEMENT**

The sensitive clay landslides in Canada are mostly devastating because of the significant retrogression it undergoes. The vulnerability is extremely prominent in the province of Quebec, in which 89% of the population lives in the marine limits of Champlain, Laflamme and Goldthwaite seas. The frequency of occurrence of landslides is most predominant during spring season (May – June), when the ice and snow trapped in the voids of the soil starts to melt leaving behind air voids in the soil [26]. The most pronounced and extensive slope failures have occurred in the Champlain basin and several experimental and numerical modelling studies on sensitive clays are based on this region [27]; [23]. In contrast, the Laflamme basin suffers occasional slope failures, some more destructive than others. However, studies in this region are limited if not non-existent. Hence, the following problems are addressed in this study:

- There are several existing criteria for retrogression in sensitive clays. As opposed to these isolated criteria based on individual parameters such as slope geometry [28], physical properties like Liquidity Index [29], Liquid Limit [11] or remoulded shear strength [30]; [31] mechanical properties like brittleness index for sensitive clays [32] or quickness [33], remoulding energy and remoulding index encompass the effect of several parameters together. With reference to a slope, remoulding energy represents the total work involved in the disintegration of that part of the slope involved in remoulding into a soil debris. Since remoulding energy is often expressed as the derivative of potential energy of the slope, the parameters that make up the potential energy (eg: topographical parameters like slope height) and kinetic energy (eg: rate of strain softening determined by overconsolidation ratio) of the slope affects it the most. This way, remoulding energy is able to represent the effect of several parameters together.
- An accurate model that can depict the complete stress–strain behaviour of sensitive clays in the post-peak regime of the stress - strain curve is essential in the estimation of remoulding energy. In the case of sensitive clay landslides, shear induced pore pressures at the failure surface and stress history of the soil have significant impact on its strength degradation and this should be reflected in the model used for analysis. Thus, a model that can capture the appropriate strain softening behaviour in sensitive clays, supplemented by its actual field behaviour, would aid in a comprehensive understanding of both remoulding and retrogression.
- Existing criteria on retrogressive landslides that take into consideration physical and mechanical properties of the clay like Liquidity Index ( $I_L$ ) and remoulded shear strength ( $s_{ur}$ ) [29]; [30]; [31], liquid limit, remoulding index and remoulding energy [11] are based on inspections on properties mainly pertaining to Champlain clays. The liquid limits of clays from the Laflamme Sea basin have been shown to be lower than the Champlain clays [20] and the  $I_L$ - $s_{ur}$  relationship established by [30] and [31] seem to underpredict the high  $s_{ur}$  of Laflamme clays [34]. Numerical modelling and theoretical analysis of sensitive clays often rely on assumptions of properties based on a range of values typically available in the literature [13]. Thus, neglecting site specific data and criteria while predicting retrogression could lead to erroneous judgements. This is explored primarily through Laflamme clays of the Lac-Saint-Jean (LSJ) in this study.

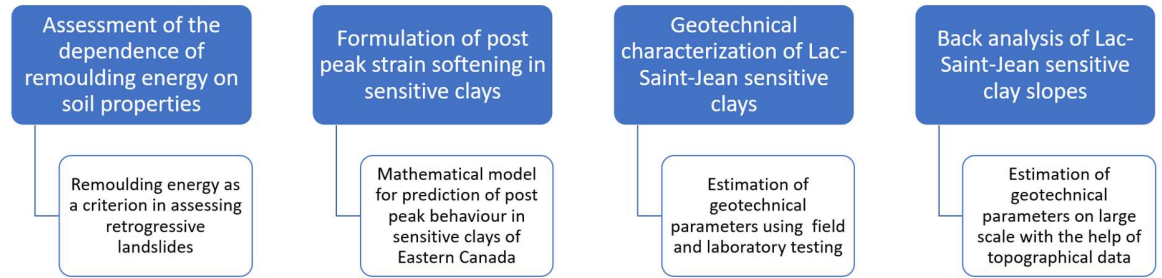
### **1.3 RESEARCH OBJECTIVES**

The general objective of the thesis is determine the geotechnical characteristics of sensitive clays of the Lac-Saint-Jean with the objective of use in the prediction of retrogressive landslides. In order to achieve this objective, the following specific objectives are accomplished.

1. Assessment of remoulding energy as a criterion for the analysis of retrogressive landslides and its dependence on geotechnical parameters in sensitive clays of Eastern Canada through comparative studies.
2. Development of a mathematical model for prediction of post - peak strain softening behaviour in sensitive clays of Eastern Canada.
3. Assessment of geotechnical parameters of sensitive clays of Lac-Saint-Jean in laboratory scale and large scale using experimental results and back analysis of slope stability.

### **1.4 METHODOLOGY**

The assessment of retrogressive landslides involves a good estimation of accurate post - peak strain softening behaviour, detailed geotechnical characterization of the clays as well as a reasonable understanding of the stability of clay slopes and the topography of the site. The following methodology has been proposed for analysing the of retrogressive landslides in sensitive clays of Laflamme basin based on geotechnical characteristics of the soil. A flowchart of the various steps involved in the methodology and the realization of each of the objectives is shown below:



#### 1.4.1 Assessment of the dependence of remoulding energy on soil properties

Any clay slope possess a certain amount of energy which maybe called its potential energy, that is dependent on the slope height (H) and density of the soil [11]. When a sensitive clay slope fails, the source of energy for remoulding comes from this potential energy. A part of the potential energy is also used in post failure movements/ retrogression. Since the total potential energy of a slope is constant, a higher or lower remoulding energy signifies a subsequent lower or higher kinetic energy and in turn the extent of retrogressive movements post-failure. Hence, the remoulding energy proves to be a significant factor upon which a criteria for retrogression could be based on and has been used for the same in the past according to several methods [11]; [35]; [36]; [13]; [37]. A study is conducted to assess the application of existing methods to determine the remoulding energy of Eastern Canadian sensitive clays, particularly the linear approximation proposed by [13]. A detailed methodology and subsequent results are discussed in Chapter 2 of this thesis.

#### 1.4.2 Formulation of post - peak strain softening behaviour of sensitive clays

Remoulding in sensitive clays is due to post - peak strain softening in sensitive clays. This reduction in shear strength with increasing shear deformations continues upto large deformations where the remoulded state is typically attained. This is often beyond the laboratory limits of shear strain (Figure 1-1). Existing models that are in use to capture this strain softening behaviour either simplifies it using a linear variation of shear strength with increasing shear strains beyond the peak strength [13]; [18], which is not the actual soil behaviour or make use of assumptions for the strains at such large deformations for which prior studies and assessments on the post-peak strain softening behaviour of the clay is generally essential. This offers a limitation in the analysis of new or unexplored landslides in particular at regions where limited experimental and numerical modelling



studies have been conducted (eg: Laflamme clays). Moreover, the strain softening in sensitive clays is highly dependent on its stress history and mechanical behaviour under effective vertical stresses. In order to accommodate these factors, a non-linear strain-softening model is proposed that captures strain softening through triaxial testing. This ensures that the in-situ stress states, drainage and effect of field phenomena (eg- overconsolidation, stress history etc) of the soil are replicated for accuracy. The methodology for the development of the model including its validation is explained in detail in Chapter 3 of this thesis.

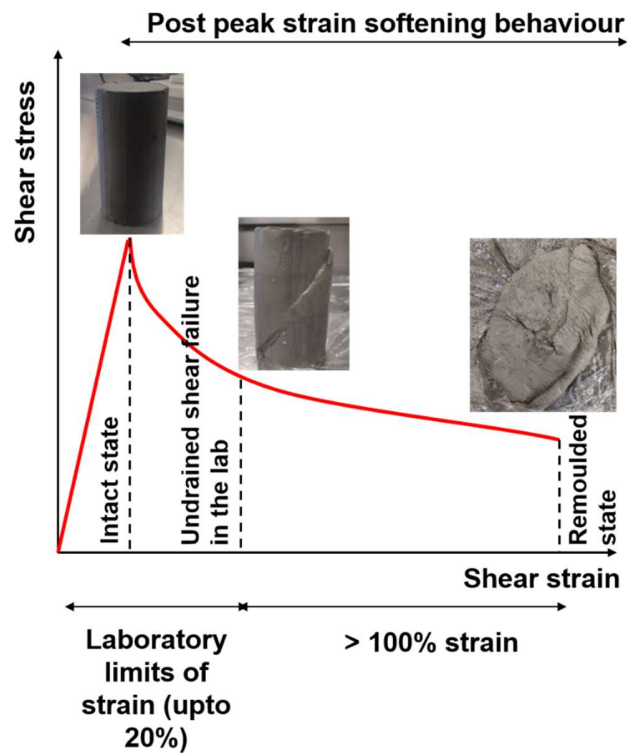


Figure 1-1 Post - peak strain softening behaviour in sensitive clays

### 1.4.3 Geotechnical characterization of sensitive clays

In the prediction of post - peak behaviour of sensitive clays and other landslide hazard studies, an appropriate model for strain softening should be supported by a detailed geotechnical characterization of the region under study. Previous characterisation studies to develop criteria for landslide hazard assessment often consider the properties of Champlain clays to represent Eastern Canadian sensitive clays as a whole. However, these could be misleading as geotechnical parameters from various sedimentary basins are significantly affected

by geology. Laflamme clays of Canada exhibit properties different to other Eastern Canadian sensitive clays as they are the result of a recent marine invasion. As such, the post - peak behaviour of Laflamme clays is accompanied with a detailed geotechnical characterization for two Laflamme clay sites - Desbiens and Albanel, surrounding the LSJ basin which can throw light on the unique mechanical behaviour of the clays of this region. In addition to basic physical properties, experimental investigations including Scanning Electron Microscopy, and isotropic and  $K_0$  triaxial compression tests have been carried out. A detailed account of the different tests used for the geotechnical characterization including a meticulous discussion of the subsequent results is provided in Chapter 4 of this thesis.

#### **1.4.4 Evaluation of geotechnical parameters for sensitive clay slopes on large scale**

Retrogressive slope failures are often initiated by a small erosive scar or an initial slide that takes place due to active stream erosion along a slope adjacent to a lake or increase in shear stresses due to heavy rainfall or snow melt leaving the slopes marginally stable for further retrogressive failure to take place [25]. The initiation of slope failure and slope stability analysis in Laflamme clays is explored through limit equilibrium and finite element analysis of Desbiens and Albanel clay slopes in Slide 2D and RS2 respectively. LiDAR data and aerial photographs are used for obtaining the topography of the slopes over the years. The DTMs from LiDAR images are imported into LeapFrog Geo to obtain the respective cross sections for stability analysis. The scale effect on Mohr-Coulomb parameters determined from the laboratory when applied to large clay slopes is analysed using back analysis. Furthermore, these slopes are analysed based on an energy criterion. Since the geometry of the slope determines its potential energy and in turn the energy available for remoulding, a threshold energy that could cause strength degradation of the clay and possible retrogressive failure is assessed by application of the developed strain softening model to monotonic stress-strain curves determined through triaxial tests. This threshold energy which is the remoulding energy, is obtained as area under the stress-strain curves. This comprehensive methodology of analysing a sensitive clay slope for possible retrogressive failure by incorporation of accurate geotechnical parameters, appropriate strain softening model and numerical tools is discussed in detail in Chapter 5.

### **1.5 ORIGINALITY**

The failure in sensitive clay slopes is highly dependant on seasonal changes as well as changes in topography. Hence, their analysis often becomes complex due to several unpredictable factors. This study aims to throw light on the importance of geotechnical characterisation studies, a good interpretation of the geological history and use of topographical data to minimise uncertainties in the determination of geotechnical parameters for stability analysis in sensitive clays. Although hazard assessment studies in sensitive clays are being extensively carried out by researchers, the study area chosen in this thesis has not been explored much in spite of past landslide occurrences. The following outlines the main contributions of the thesis.

- A non-linear strain softening model that uses experimental data in the form of triaxial tests is proposed which helps minimise uncertainties as well as is applicable to sensitive clays where significant data on its post - peak behaviour is not available. The advantage of the triaxial test in terms of obtaining a well-rounded understanding of the behaviour of the clay maybe exploited. The strain softening model also gives a good understanding of the large deformation strains and can be incorporated towards numerical modelling tools.
- Among existing criteria for retrogression, an energy criterion in terms of remoulding energy forms a useful tool in understanding the strength of the clay and potential for post failure movements. The strong dependance of remoulding energy with stress history is highlighted by application to Eastern Canadian clays.
- Studies on Laflamme clays of Eastern Canada are quite limited inspite of several landslide occurrences in this region. A comprehensive geotechnical characterization study of the Laflamme clays from the LSJ is conducted. Along with a detailed analysis of the physical, chemical and mechanical behaviour of the clays, the main differences in its properties with the more commonly studied Champlain clays are also highlighted. This helps to have a deeper understanding of the behaviour of clays in this region which is later expanded to slope stability analysis to determine these parameters on a large scale.

## **1.6 THESIS OUTLINE**

The outcome of this thesis includes four manuscripts and they are presented separately in Chapters 2 to 5. The general structure of the articles comprises the Abstract, Introduction, Methodology, Discussion, and Conclusions.

CHAPTER 1 describes the overall structure of the thesis by explaining the statement of the problems, the objectives of the thesis, the methodology used to achieve the general and sub objectives, and the originality and novelty of the thesis.

CHAPTER 2 presents a detailed literature review of existing criteria used to analyse retrogressive landslides with a focus on remoulding energy and its dependence on various geotechnical parameters.

CHAPTER 3 proposes an exponential non-linear strain softening model to accurately depict the post - peak behaviour of sensitive clays by using the stress - strain curves in a triaxial test and the validation of the model using field observations of post failure movements.

CHAPTER 4 presents a detailed geotechnical characterization study of Laflamme clays from LSJ – Desbiens and Albanel. This includes grain size distribution, water content and Atterberg limits, salinity, chemical composition, microstructural investigations, stress states and undrained shear strength along with a comprehensive comparison of these properties with respect to those of Champlain clays.

CHAPTER 5 presents a slope stability analysis using Rocscience including initiation of failure in sensitive clay slopes of Desbiens and Albanel by making use of topographical data from LiDAR and aerial photographs followed by an energy criterion for retrogressive failure.

CHAPTER 6 presents the most important outcomes of the present work and the recommendations for future research.

## CHAPTER 2

### **Article 1: Remoulding energy as a criterion in assessing retrogressive landslides in sensitive clays – A review and its applicability to Eastern Canada**

Sarah Jacob<sup>1</sup>, Rama Vara Prasad Chavali<sup>2</sup>, Ali Saeidi<sup>3</sup>, Abouzar Saderkarimi<sup>4</sup>

<sup>1</sup>**Corresponding author:** Doctoral student, Department of Applied Science, Université du Québec à Chicoutimi, Quebec, Canada

<sup>2</sup>Post doctoral researcher, Department of Applied Science, Université du Québec à Chicoutimi, Quebec, Canada

<sup>3</sup>Professor, Department of Applied Science, Université du Québec à Chicoutimi, Quebec, Canada

<sup>4</sup>Associate Professor, Department of civil and environmental engineering, Western University, Ontario, Canada

Published, Natural Hazards, Volume 118, July 10 2023

#### **Credit authorship contribution statement**

**Sarah Jacob:** Conceptualization, Data curation, Formal analysis, Resources, Writing – original draft, Writing – review and editing. **Ali Saeidi:** Supervision, Methodology, Resources, Writing – review and editing. **Abouzar Sadrekarimi:** Supervision, Writing – review and editing. **Rama Vara Prasad Chavali:** Writing – review and editing.

#### **Declaration of competing interests**

The authors declare the following financial interests/personal relationships which may be considered as potential competing interests: Ali Saeidi reports financial support was provided by Natural Sciences and Engineering Research Council of Canada (Grant ID: NSERC- 950- 232724). Ali Saeidi reports financial support was provided by Hydro Quebec (Grant ID: RDCPJ 521771–17). If there are other authors, they declare that they have no known competing financial interests or personal relationships that could have appeared to influence the work reported in this paper.

## 2.1 ABSTRACT

Sensitive clays are heavily vulnerable to disturbance making them highly susceptible to landslides. The Eastern Canadian region of Quebec and Ontario have large deposits of such sensitive clays which pose a serious threat to life and property. The cause of these land movements and various criteria for assessing their instability are compared and assessed in this review paper based on the remoulding energy and the remoulding index, along with other in-situ and mechanical properties of the soil. The energy distribution within a slope at the time of failure is used to link the remoulding energy to the nature of the material, making it an ideal tool for landslide risk assessment. A comparison of several existing methods for the determination of remoulding energy is made to understand the suitability of each method in future research. The applicability of these methods to Eastern Canadian soils are also verified. The post - peak behaviour of sensitive clays and its influence on remoulding energy is analysed and the estimation of remoulding energy through a linear post - peak approach is examined. The paper highlights the importance of remoulding energy and its accurate determination through the best fit stress-strain curve to understand retrogressive landslides in sensitive clays.

**Keywords:** sensitive clays, retrogressive landslides, remoulding energy, strain softening.

## 2.2 INTRODUCTION

Sensitive clays underly large areas of the Northern hemisphere including Canada, Sweden, Norway, Finland, Russia, as well as Northwestern regions of America. Their existence is due to isostatic depression and post-glacial rebound followed by the leaching of sea sediments [1]. Clays are considered sensitive when they are susceptible to strain softening. The susceptibility of clays to undergo strength loss is often quantified by the sensitivity ( $S_i$ ) which is the ratio of shear strength of the undisturbed soil to that of the remoulded soil [3]. Highly sensitive clays with very low remoulded shear strength,  $s_{ur}$  (defined as less than 0.5 kPa and 0.4 kPa in Norway and Sweden respectively) are referred to as quick clays [4] [5]. In Canada, this is defined based on sensitivity according to the modified fourth edition of the Canadian Foundation Engineering Manual, where clays with sensitivities of 16 or above are termed quick clay [6]. A major hazard posed by sensitive clays are the retrogressive landslides, often leading to loss of life and property.

Landslides in sensitive clays have often been described in the past to be initiated from a small circular slide followed by several slides leading to a large retrogressive landslide [40]; [41] or due to shear bands along a nearly horizontal failure surface within a clay slope [42]; [43]; [44]. However, years of rigorous research on landslides in sensitive clays by researchers has yielded a wider perspective of landslide types and mechanisms [44]; [32]. Some examples of landslides in sensitive clays of Quebec include retrogressive slope failures that occurred at Saint Jean Vianney in 1971 [7], St. Jude in 2010 [9] and Saint-Luc-de-Vincennes in 2016 [10].

The retrogressive nature of landslides in sensitive clays has led to the analysis of these clays from the point of view of post failure movements and remoulding process. Remoulding in sensitive clays is the result of continuous strength degradation due to the destruction of its fabric [12]. The strain energy required for remoulding is termed the “remoulding energy.” It is also referred to as the “disintegration energy,” “degradation energy” or simply “strain energy” [45]; [11]; [13]. An accurate depiction of the complete stress-strain behavior in the post-peak regime is essential in its estimation. There are several criteria in the analysis of retrogression in sensitive clays. As opposed to these isolated criteria based on only individual parameters such as slope geometry [28], physical properties like liquidity index [29], liquid limit [11] or remoulded shear strength [30]; [31], mechanical properties like brittleness index for sensitive clays [32] or quickness [33], remoulding energy and remoulding index encompass the effect of several parameters together. It takes into consideration undrained shear strength, brittleness as well as slope geometry in its estimation. The importance of representing strength degradation during slope failures in terms of remoulding index is also highlighted by [46] and [47] as evidences suggest that the undrained shear strength at the end of retrogression may not always correspond to the completely remoulded shear strength. The objective of this review paper is to present remoulding energy and remoulding index as important criteria in the analysis of retrogressive landslides along with other physical and mechanical properties of the clay. Firstly, the mechanism of landslides in sensitive clays of Eastern Canada are thoroughly examined to get insights to establish a criterion for landslide assessment. Subsequently, the study highlighted the concept of remoulding energy and explored various methods to quantify it. Following that, a parametric study is conducted to investigate the relationships between remoulding energy and geotechnical properties such as liquidity index, plasticity index and preconsolidation pressure. Finally, this review paper concluded with a comprehensive analysis and discussion on future quantification of remoulding energy for sensitive clays of Eastern Canada.

## 2.3 MECHANISM OF LANDSLIDES IN SENSITIVE CLAYS

Most of the landslides of Eastern Canada seem to take place during the wet times of the year (mostly spring) indicating the important role played by water [40]. It has been often reported that infiltration due to rain or snow or the presence of a nearby water course can be one of the major reasons that trigger retrogressive landslides in sensitive clays. Sensitive clay layers are often found to occur in nature as sandwiched between an upper dry crust and a lower till layer or fissured bed rock [48]. Sensitive clay slopes of today have emerged over years of fluvial erosion where the rivers cut through these clay deposits to form valleys. As erosion by rivers or streams through the marine deposits and the subsequent valley formation progress over time, a critical position is reached wherein the pore water pressure tries to flow upwards but is restricted due to the relatively lower permeability of the clay layer. This leads to a high pore water pressure at a relatively low overburden stress and a subsequent reduction in effective stress. This can give rise to a low shear strength in the slope that can lead to large flowslides and subsequent retrogression [48]; [49]. Examples of similar cases include the Saint Jean Vianney landslide of 1971 where partial flooding due to surface runoff was experienced about 3-4 days before the occurrence of the landslide [7]. Investigations of the 1994 St Monique landslide attributed the presence of high porewater pressure and upward seepage conditions to the presence of the Nicolet River, only 650 m west to the landslide site [50]. Piezocone measurements on the more recent St. Jude landslide that occurred in 2010 indicated upward seepage near the toe of the slope with high artesian pressures [9]. Although 10% of the landslides take place due to human activities like excavations at the toe of the slope, blasting, overloading the crest of the slope by fill work and pile driving, the remaining 90% are all caused by natural mechanisms as the majority of these slopes have their origin near the banks of water courses which constantly cut into the marine deposits at the toe of the slope [26].

According to the Varnes classification of landslide types and their update by [51], the majority of retrogressive landslides in Quebec can be classified as flow slides or lateral spreads. The failure mechanism of flowslides is quite clear and well narrated in the literature [41]; [11]. As illustrated in Figure 2-1, in a retrogressive flowslide, an initial rotational failure surface causes the soil to flow and slide out of the crater, leaving an unstable backscarp. An unstable backscarp in this context maybe referred to a condition where the soil undergoes significant loss of shear strength and moves out of the crater leaving behind a high slope that



may not be relied upon as a counterbalance to support the remaining slope [41]; [11]. This will cause the occurrence of another failure surface where more soil slides and flows out of the initial crater. This cycle is repeated with multiple failure surfaces until a stable backscarp is formed. An interesting physical model using a geotechnical centrifuge has been shown by [46] which models this exact behavior. In the field, the remoulded clay completely flows out of the crater and can travel long distances depending on its potential energy as well as the geological conditions of the site [51]; [44].

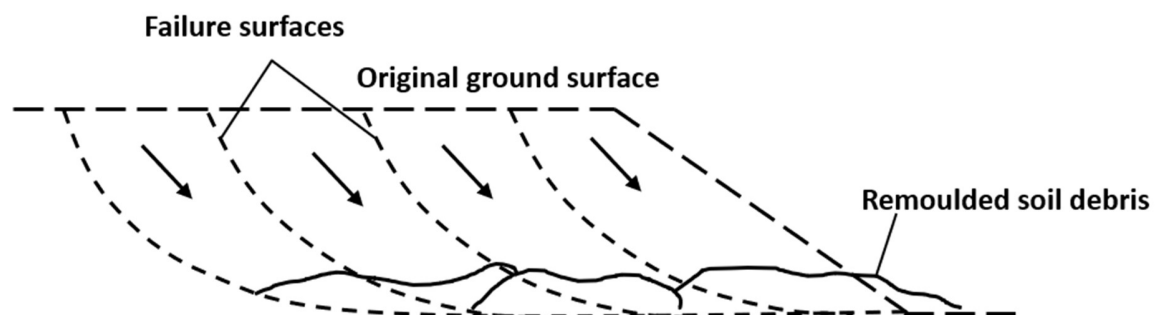


Figure 2-1 Mechanism of flowslides with rotational failure surfaces (adapted from [52] )

Lateral spreads on the other hand are characterized by a ribbed appearance of pointed soil structures (horsts) and flat-topped strips of land with the vegetation more or less intact (grabens) as shown in Figure 2-2. In a spread, failure occurs as a result of the propagation of a sub-horizontal failure surface, more specifically called a shear band/shear zone which develops near the toe of the slope dislocating the soil mass above the shear band into horsts and grabens that subsides in the underlying remoulded soil debris [51]; [44]. It is observed that there are cases where a combination of the two mechanisms of flow slides and spreads also occur. Initially, the flow slide may occur leaving behind an unstable backscarp, creating conditions for a spread to occur. The resulting landslide will have characteristics of both a flow slide and a spread [26]; [9]; [10]. Sometimes a retrogressive slip follows an episodic nature where multiple slip surfaces are formed over years rather than a single event like the Mud Creek landslide in Ottawa [47].

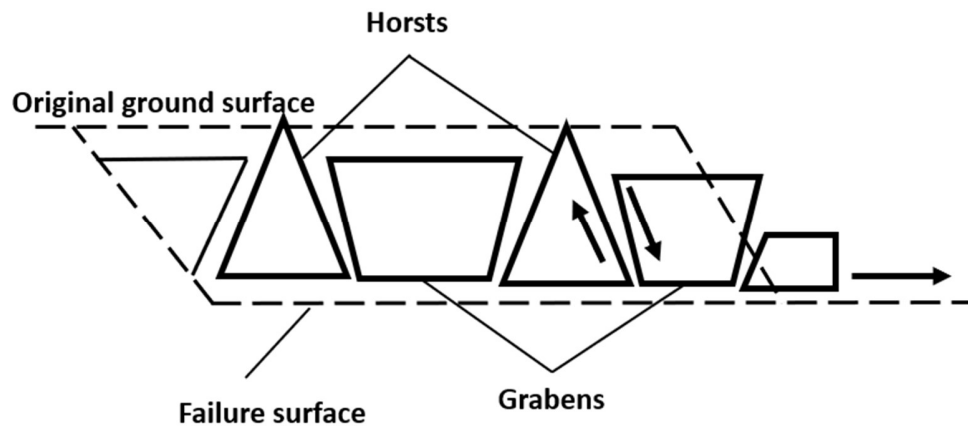


Figure 2-2 Mechanism of spreads in which the failure surface is almost horizontal forming horsts and grabens (adapted from [52])

Flow slides are more retrogressive in nature than spreads as the remoulded soil debris flows from the point of occurrence of the landslide [26]. Often times this results in the soil debris resembling a bottle neck shape [44]. The distinctive horsts and graben formation in a spread failure make them stand out from flowslides. The mechanism of the formation of horsts and graben dates back to the finding of [42] from the Skötkörp landslide in western Sweden that underwent a translatory motion. Later, several studies on the mechanism of spread failures led to the idea of a lateral spreading of a failure surface progressing upwards leading to a horst and graben formation with the remoulded soil being squeezed out due to tension cracks between the horsts and grabens [53]; [42]; [43]. In recent times, a progressive failure analysis related to large landslides in sensitive clay has been proposed, wherein the complete failure surface is formed prior to a slope's subsidence and the propagation of a shear band takes place along this failure surface [15]; [44]; [32]. As the shear band propagates, the shear stress along the failure surface at each point increases to the peak shear strength and then drops to the residual strength. The propagation of shear band ultimately leads to the global failure of the slope when horizontal forces reach active or passive failure conditions [44]. A small disturbance, in the form of erosion or human activity, can trigger the subsidence and the movement of the slope creating the effect of an apparent retrogression [54].

The realization of these land movements is often difficult due to the complex flow behavior, accurate interpretation of post failure movements and strength loss at large deformations. However, computational

techniques and numerical modelling efforts to analyse these behaviors have been evolving over the past decade especially for spread failures. Advanced modelling techniques such as BIFURC, MPM (Material Point Method), LDFEM (Large deformation finite element modelling) and SPH (Smoothed Particle Hydrodynamics) [18]; [22]; [23]; [24] have been successful in generating accurate landslide mechanisms and post-failure movements in Eastern Canada and Norway. The recent work by [24] using a fully coupled hydromechanical approach was also able to capture the development of excess pore water pressure during retrogressive flowslides, attributed to the change in permeability under large deformations. The various modelling techniques highlight the influences of sensitivity, remoulded shear strength, slope geometry, brittleness and large deformation strains in characterizing these movements.

## 2.4 EXISTING CRITERIA FOR RETROGRESSION IN SENSITIVE CLAYS

Early studies on strength loss and failure bring to light certain mechanical properties such as the brittleness index ( $I_B$ ), remoulding energy ( $E_R$ ) and remoulding index ( $I_r$ ) which characterize strength degradation and remoulding behavior of soils. The inherent properties of a soil including shear strength, stability number ( $N_c$ ) and quickness ( $Q$ ) also play important roles in assessing retrogression. These definitions are briefly summarized in the following paragraphs.

[55] introduced  $I_B$  to characterize strength loss under drained conditions from the peak to the residual shear strength while using the conventional methods of slope stability analysis for progressive failures:

$$I_B = \frac{\tau_p - \tau_{res}}{\tau_p} \quad (2-1)$$

where,  $\tau_p$  = peak shear strength,  $\tau_r$  = residual shear strength, both under drained conditions. According to [32]'s concept of progressive failure, the rupture surface/weak layer is already formed over years of strength degradation and essentially is a drained phenomenon. Through a fracture mechanics analysis, they claim that the strain or displacement along the shear band is an equally important factor in comparison to the “residual” strength in the assessment of brittleness. As [55]'s equation for  $I_B$  fails to represent this, [32] put forth a new brittleness parameter for sensitive clays ( $B_{st}$ ) in terms of nominal deformation localized in the shear band, which at any given time is a fraction of the large deformation. This incorporates strain softening behavior of sensitive clays as well (Equation 2-2).  $B_{st}$  represents the ease in which strength loss is achieved from the peak to the

remoulded shear strength and is essentially different from the original brittleness parameter developed by [55]. For sensitive clays,  $B_{St}$  is nearly equal to one.

$$B_{St} = \frac{1}{125\bar{\delta}} \quad (2-2)$$

where  $\bar{\delta}$  is the nominal deformation of the shear band.

One may think sensitivity to be a relevant parameter in the assessment of retrogression in sensitive clays, however, unless the remoulded shear strength is same, there appears to be no direct relationship between sensitivity and retrogression distance [28]. [43] proposed that rather than the exact ratio of strength loss from peak to residual, the ease with which this strength loss is achieved is more relevant in assessing retrogression.

$N_c$  is a dimensionless parameter used to evaluate the slope stability of cohesive soils and is defined as  $\gamma_s H / s_{up}$  where  $\gamma_s$  is the unit weight of the soil,  $H$  is the height of the slope and  $s_{up}$  is the undrained shear strength of the intact soil. [28] found that when  $N_c$  was more than 6, plastic flow was likely to occur causing flow slides in sensitive clays. They also observed that the retrogression distance increased parabolically with increasing  $N_c$ . However, [26] later suggested that [28]'s relation showed a scatter in the case of landslides in Quebec and were invalid. [46] explains this due to the non-inclusion of additional constraints in the form of slope angle, shear strength at the end of retrogression, geomorphology of the sites and treating flow slides and spreads separately, which would give rise to more refined correlations for retrogression.

Preliminary investigations in the field of retrogressive slides in sensitive clays by [11] show that the remoulding index and the remoulding energy can provide important information on the behaviour of remoulded soils. Remoulding energy signifies the strain energy stored in a clay material to completely disintegrate its structure into a semi fluid state and the extent of remoulding is indicated by the remoulding index. According to [11], for retrogression to happen in a flowslide two conditions must be met – the initial slide should leave an unstable backscarp and the clay must be remoulded enough to flow out of the crater. They introduced a normalized remoulding energy ( $E_N$ ) by normalizing remoulding energy by the limit state energy which is the energy involved in reaching the peak strength condition in a soil specimen. Subsequently, Tavenas et al., (1983) defined remoulding index as follows:

$$I_r = \frac{s_{up} - s_{ux}}{s_{up} - s_{ur}} * 100 \quad (2-3)$$

where,  $s_{up}$  = undrained shear strength of intact specimen,  $s_{ux}$  = undrained shear strength of partly remoulded clay and  $s_{ur}$  = undrained shear strength of remoulded soil. They further proposed that  $I_r > 70\%$  and  $E_N < 40$  were required for heavy retrogression to take place.

[29], from their observations of Champlain Sea deposits, proposed that clays with liquidity index ( $I_L$ )  $> 1.2$  could remould and undergo retrogressive landslides of more than 100 m in distance. Certain correlations between remoulded shear strength ( $s_{ur}$ ) and liquidity index ( $I_L$ ) were also proposed by [30] and [31] for Eastern Canadian clays. These include  $s_{ur} = (I_L - 0.21)^{-2}$  by [30] and  $s_{ur} = (335.87/I_L)^{2.44}$  by [31] where  $s_{ur}$  is in kPa. These equations correspond to  $s_{ur}$  as low as 1 kPa at  $I_L = 1.2$ . However, [11] provided contradictory evidences to [29] criterion ( $I_L > 1.2$ ) by proposing that heavy retrogression in certain slopes in Eastern Canada were not observed even when  $I_L$  was more than 1.2. They also proposed that when liquid limit ( $\omega_L$ ) was less than 40%, heavy retrogression could be observed for Eastern Canadian sensitive clays. [11] explained this as the loss of interparticle bonding among clay particles at  $\omega_L < 40\%$ , making the clay very brittle and easily remouldable. Researches also show that low Atterberg limit values are typical of sensitive clays owing to their reduced salt content due to leaching [41]; [56]; [2].

[33] proposed a quickness test to evaluate the potential of a sensitive clay to undergo flow sliding by assessing the slump of a sensitive clay sample formed upon lifting a cylinder filled with remoulded clay as shown in Figure 2-3. According to [33], quickness is defined as the ratio of the difference in height of the cylinder and the slumped remoulded clay to the height of the cylinder, i.e.  $Q = (H_o - H_f)/H_o$ . In the case of Norwegian quick clays, quickness ( $Q$ ) has been related to  $s_{ur}$  as  $Q = 15s_{ur}^{-0.7}$ . [33] further observed that when  $s_{ur} < 1$  kPa and  $Q > 15\%$ , flow slides and retrogressions were likely to occur.

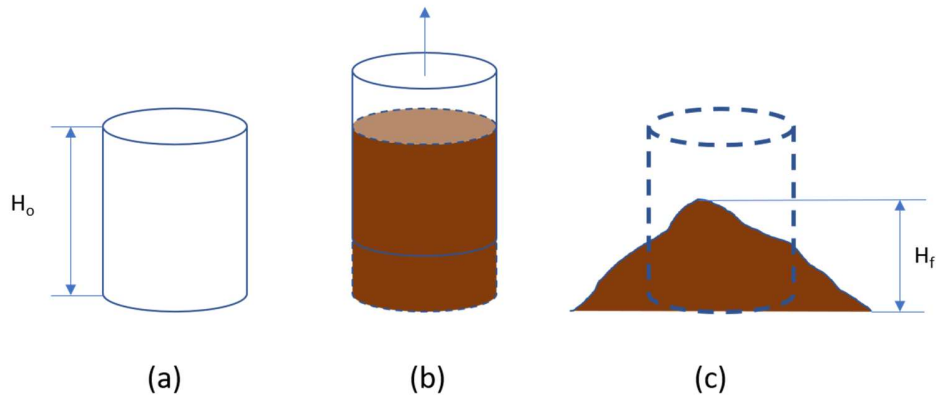


Figure 2-3 Illustration of quickness test: (a) empty cylinder into which clay is poured (b) cylinder is slowly lifted upwards (c) remoulded clay slumps (adapted from [57])

Post-failure movements in sensitive clays or the extent of retrogression may be assessed in terms of two parameters – retrogression distance and run out distance, measured respectively from crest to crest and toe to toe of the initial and retrogressed slide. Empirical relations to measure these parameters have come into picture in terms of stability number [28], volume of soil debris [36] and remoulding energy [13]. Certain statistical methods have also been used in Norway which were applied to landslides in Quebec by [58] but were found not to predict worst case scenarios. The use of these indirect methods do not always yield accurate results as these encompass only one or two parameters whereas retrogression could be aided/obstructed by several geological factors such as watercourses, presence of valley, depth of slope and etc [59]. Assessment of remoulding through cone penetration test results of Mud Creek landslide in Ottawa by [47] indicated that the soil debris that retrogressed suffered only 50% remoulding. Similar findings were observed by [46] through a physical model of retrogression where a strength degradation of 56 to 80% was observed at the end of retrogression. Thus, the degree of remoulding seems to strongly influence the extent of retrogression and further energy-based studies are warranted.

## 2.5 REMOULDING ENERGY AS A PARAMETER FOR RETROGRESSIVE LANDSLIDES

### 2.5.1 Energy balance in post failure movements

A slope failure occurs typically in four stages: 1) a pre-failure stage where the soil is intact and possesses sufficient undrained shear strength, 2) a failure stage when the initial slide or shear band propagates depending

on the failure mechanism, 3) a post-failure stage when the soil remoulds and undergoes retrogression, and possibly 4) a reactivation stage where the slope slides over a pre-existing failure surface [45]. The post-failure stage where most of the retrogression happens is an important stage in hazard and risk assessment and its behaviour depends on the energy distribution at the failure stage.

[11] suggested that the only source of energy available for remoulding a clay is the potential energy of the sliding mass. The distribution of this potential energy into remoulding energy coupled with the nature of the material determines the extent of retrogression in sensitive clays. During the occurrence of a landslide, just before the failure, the external and the resisting forces of the slope are in equilibrium and the slope has a certain potential energy. According to [11], as the failure progresses, the soil mass moves and the potential energy ( $E_P$ ) is distributed into a remoulding energy ( $E_R$ ), a kinetic energy ( $E_K$ ) and a frictional energy ( $E_F$ ) according to Figure 2-4. The remoulding energy determines the amount of remoulding and disintegration that the soil mass undergoes whereas the kinetic energy accelerates the soil debris and the frictional energy controls the movement of the soil mass along the failure surface [45]; [60]. The total potential energy is the summation of the above energy components as below:

$$E_P = E_R + E_K + E_F \quad (2-4)$$

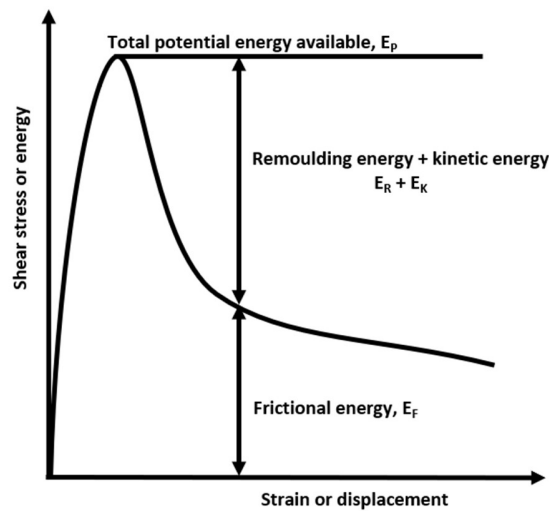


Figure 2-4 Distribution of post-failure potential energy (adapted from [61])

The distribution of potential energy into the three different forms mentioned above depends on the material type. For a purely ductile material as illustrated in Figure 2-5a, the potential energy is entirely spent as frictional energy and soil movement is very small. However, for a very brittle material (Figure 2-5b) the kinetic and the remoulding energies are very high indicating heavy remoulding and retrogression [45]. Since sensitive clays are brittle materials, the latter energy distribution represents their behaviour. The frictional energy of quick clays is often too small or negligible due to their high brittleness.

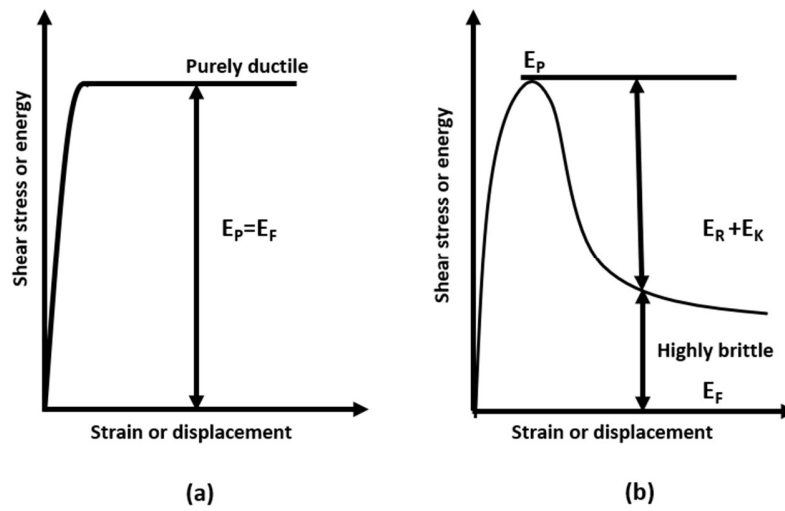


Figure 2-5 Energy distribution for (a) purely ductile material and (b) highly brittle material

[13] proposed the distribution of available potential energy for sensitive clays as follows:

$$E_p = E_R + E_{KF} \quad (2-5)$$

where,  $E_{KF}$  is energy involved in a slide movement i.e., kinetic + frictional energies. Since the total potential energy available at the time of failure is constant, a slope with a lower remoulding energy and higher kinetic energy can be easily remoulded and the remoulded debris can travel larger distances. [32] also suggested that large retrogressive landslides occur at a higher remoulding index and a lower remoulding energy.

## 2.5.2 Existing methods for determining remoulding energy



[11] were one of the forerunners that suggested the use of remoulding energy for characterizing the flow slide potential and the speed at which a clay remoulds using four techniques based on seven samples of Eastern Canadian sensitive clays (Figure 2-6) as summarized below:

- a) Free fall of a cylindrical specimen placed on an inclined board from various heights on a rigid surface.
- b) Impact from an aluminum ram, from various heights, on a cylindrical specimen placed on a rigid block.
- c) Extrusion of soil through a cylindrical mould with a conical opening of various diameters.
- d) Shearing in a simple shear box.

[11] worked out the remoulding energy in each of the above scenarios as the energy required to remould the sample at the end of each test. Certain assessments were also made by evaluating the size and the shape of the specimen after each test. Furthermore, they used the Swedish fall cone test to measure the undrained shear strength of the remoulded sample after each test. The process of remoulding starts once the soil exceeds its peak shear strength. Hence, the energy obtained through experimental investigation was divided by the strain energy at the limit state or the peak stress which was assumed as  $0.013\sigma'_p$  for Champlain Sea clays according to [62], where  $\sigma'_p$  is the preconsolidation pressure. Thus, the normalized energy per unit volume ( $E_N$ ) maybe written as:

$$E_N = \frac{\text{Energy per unit volume}}{0.013\sigma'_p} \quad (2-6)$$

For each of the test scenarios shown in Figure 2-6, [11] plotted  $E_N$  versus  $I_r$ . It was observed that for the same remoulding energy, different samples exhibited different remoulding indices indicating that the degree of remoulding undergone by each sample, even at the same remoulding energy, was different depending upon their physical properties which most likely represents their depositional characteristics and minerology.

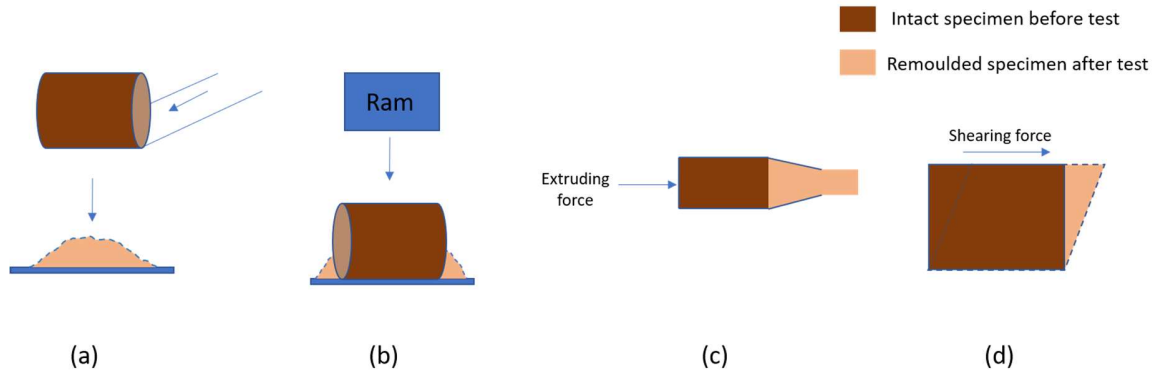


Figure 2-6 Experimental investigations of remoulding by Tavenas et al., (1983) (a) Free fall test, (b) Impact test, (c) Extrusion test, and (d) Shearing test (adapted from [63])

The fundamental experimental data by [11] were later incorporated to develop empirical relationships to determine remoulding energy. [45] showed that the remoulding energy was directly proportional to the in-situ undrained shear strength ( $s_{up}$ ) and plasticity index ( $I_p$ ). They proposed the following empirical equation for remoulding energy,  $E_R = 12.5s_{up}I_p$  at a remoulding index of 75%. Another empirical equation was proposed by [36] where  $I_R = 14.9(E_R/s_u I_p)^{0.69}$ . For complete remoulding ( $I_R = 100\%$ ),  $E_R = 16s_{up}I_p$  is obtained from this correlation.

An analytical approach was developed by [13] for determining the remoulding energy as the area under a simplified stress-strain curve with linear post-peak strength behaviour.

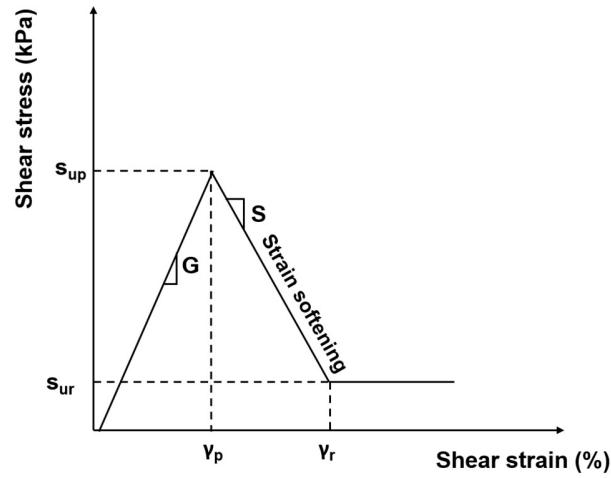


Figure 2-7 Ideal shear stress - shear strain curve used to calculate remoulding energy (adapted from [64])

The following equation was subsequently proposed by [13] for calculating the remoulding energy ( $E_R$ ) based on the simplified stress-strain curve of Figure 2-7:

$$E_R = s_{ur}\gamma_r + \frac{1}{2} (s_t - s_{ur})^2 \left( \frac{1}{G} + \frac{1}{S} \right) \quad (2-7)$$

where,  $\gamma_r$  = residual/remoulded strain,  $G$  = secant shear modulus,  $S$  = softening modulus (i.e., slope of the strain-softening segment of the stress-strain curve).

Later, [37] used the electric field vane shear test (EFVST) to measure remoulding energy for Norwegian clays at a strain rate of 0.2° per minute, where shear strength measurements were carried out from the total corrected torque ( $T_{tot}$ ) until the vane completed a rotation of 360°. The remoulded shear strength was measured after 25 revolutions of the vane. Based on the results of EFVST, [37] observed that the shear resistance after a vane rotation ( $\theta$ ) of 90° remained more-or-less unchanged and they reported it as due to the drainage of excess pore water pressure which was considered to be a limitation of the experiment. Thus, remoulding energy was calculated by linear extrapolation of the curve beyond a vane rotation of 90° (Figure 2-8). Despite its limitations, the remoulded energy obtained from an EFVST test is found to be consistent with those reported by [45] and [13].

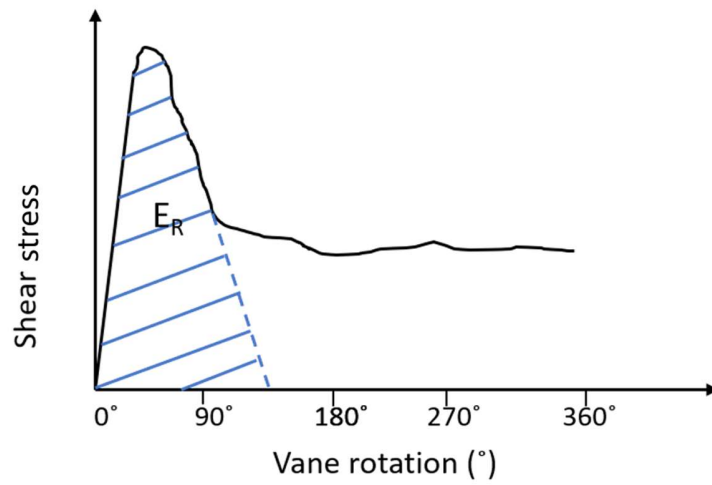


Figure 2-8 Shear stress - rotation curve according to [65]

## 2.6 DETERMINATION OF REMOULDING ENERGY FOR SENSITIVE CLAYS OF EASTERN CANADA

A study was conducted to assess the application of existing methods to determine the remoulding energy of Eastern Canadian sensitive clays, particularly the linear approximation proposed by [13]. This study has been carried out based on the information obtained from 12 Eastern Canadian sensitive clay sites as given in Table 2-1. The data represent soil characteristics at a particular depth. Undrained shear strength values were obtained through standard field vane tests (FVT).

Table 2-1 Properties of Eastern Canadian sensitive clays

Site	Sample depth (m)	I <sub>p</sub> (%)	I <sub>L</sub>	S <sub>upFVT</sub> (kPa)	S <sub>urFVT</sub> (kPa)	S <sub>t</sub>	Source
Saint – Leon	4.8	45	1.1	30	1.1	27	[11]
Louiseville	6	45	1.1	39	1.3	30	[11]
Saint - Hilaire	5.6	35	2.3	35	0.8	44	[11]
Saint – Thuribe	6	20	1.6	55	0.4	137	[11]
Mascouche	9	30	1.2	135	1.3	104	[11]
Saint – Alban	6.6	19	2.4	21	0.2	105	[11]
Saint – Jean Vianney	30	13	1.1	320	1.2	260	[11]
Saint Monique	13.45	35	1.25	40	0.7	57	[66]
Saint Jude	22.1	36	2	47.3	0.3	158	[9]
James Bay	12	10	2	18	0.09	200	[67]
Casselman	22.39	10	1.1	85	1.5	57	[68]
Saint Barnabé	23.31	10	2	77	1.8	43	[69]

Table 2-2 Properties of Norwegian sensitive clays from [13]

Site	$I_p$ (%)	$I_L$	$s_{upFVT}$ (kPa)	$S_t$
Leistad	6	1.5	16.5	110
Hekseberg	4	2.4	25	100
Vibstad	17	0.2	32	8
Borgen	20	1.2	70	100
Lyngen	12	1.5	17.5	50
Byneset	4.8	3.8	14.4	120
Kattmarka	8	2.9	15.12	63
Fredrikstad	20	1	15	30
Rissa	6	2.2	24	100
Baastad	8	1.8	18.55	35
Selnes	7	2.3	35	100
Skjelstadmarka	10	1.6	39.84	48
Furre	6	1.3	17	85
Drammen	11	1.1	10	4
Lodalen	17.1	0.8	51	3
Bekkelaget	9	2.4	26	130
Ullensaker	6.7	1.9	14.7	42
Verdalen	5	2.2	60	300

The remoulding energy is calculated using Equation 2-7 which fits a linear segment to the post-peak stress-strain behaviour of a soil. The equation requires several parameters which are often not readily available from field or laboratory investigations alone and warrants the need of certain assumptions. A critical parameter in this equation is the strain at remoulded strength ( $\gamma_r$ ). The accurate determination of  $\gamma_r$  in the laboratory is difficult because of the limited shear strain range of most conventional laboratory strength tests. Hence some of the parameters in Equation 2-7 were determined through correlations and assumptions based on laboratory

and field investigations conducted on Eastern Canadian sensitive clays from various literature [66]; [9]; [67]; [68]; [69].

Direct simple shear (DSS) tests conducted on high-quality Eastern Canadian clay samples are sheared up to peak strains of 1 - 5% [66]; [9]; [67]; [68]; [69] Based on these laboratory investigations, strain at peak strength ( $\gamma_p$ ) and secant shear modulus ( $G$ ) are assumed to be 4% and  $25c_u$ , respectively. In order to obtain the strain at remoulded strength ( $\gamma_r$ ), the DSS curves were extrapolated by an exponential curve fitting approach up to the remoulded shear strength and an average value of 200% was obtained for Eastern Canadian sensitive clays (Figure 2-9). Numerical modelling of the post-peak behavior of Eastern Canadian sensitive clays also yielded  $\gamma_r = 100 - 200\%$  [9]; [22].

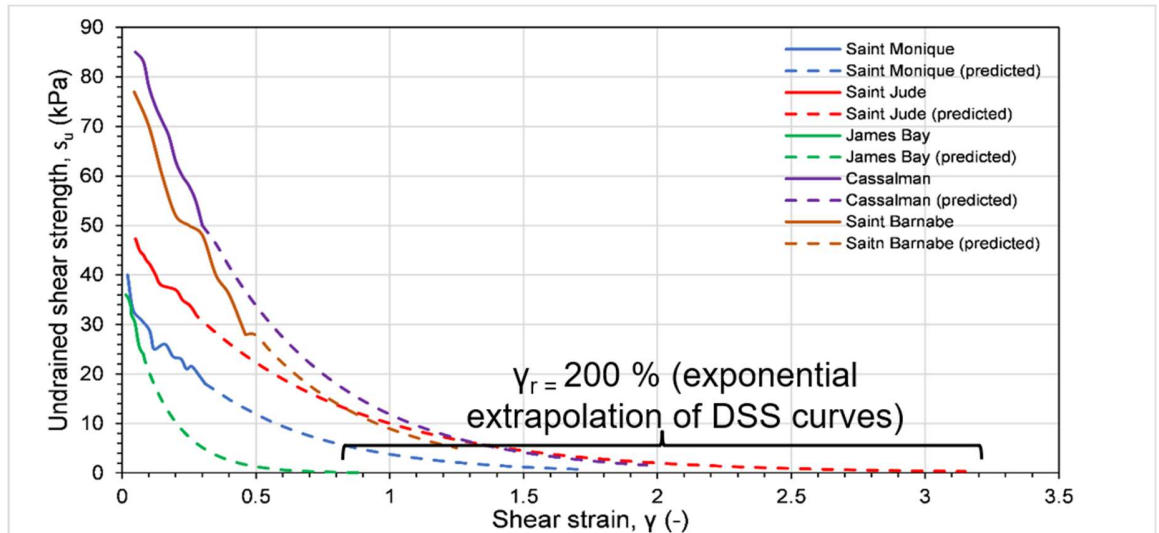
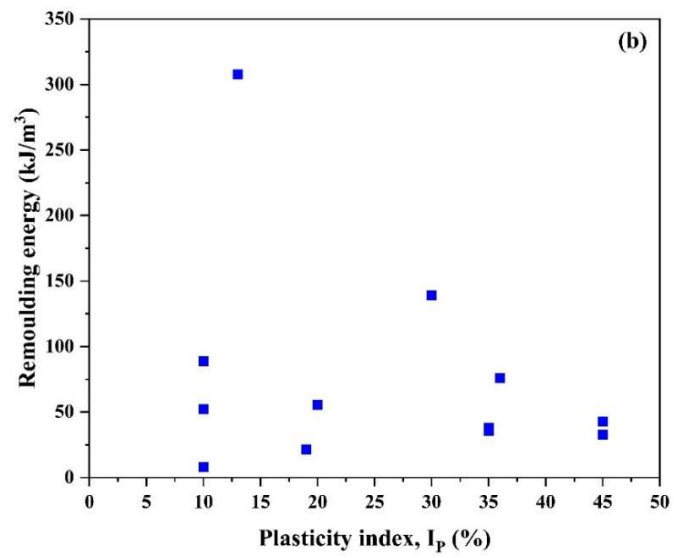
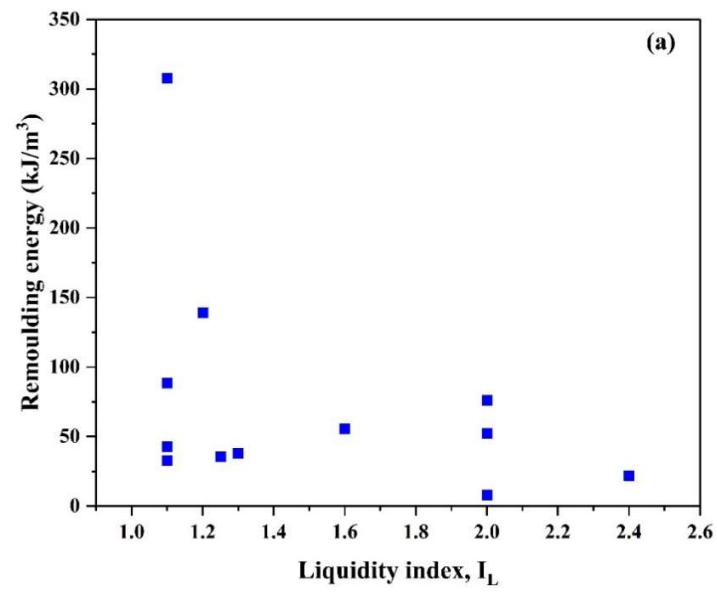


Figure 2-9 Exponential extrapolation of DSS curves until remoulded shear strength to obtain  $\gamma_r$

The remoulding energy per unit volume estimated from Equation 2-7 for Eastern Canadian clays is in the range of 20-310 kJ/m<sup>3</sup>. The results in Figure 2-9 indicate a certain amount of scatter which primarily resulted from the assumptions made in the estimation of various parameters in Equation 2-7 as well as the differences in sampling methods – 20 cm in diameter tube sampler in St Leon, Louisville, Saint Hilaire, Saint Thuribe, Mascouche and Saint Alban; 70 mm in diameter thin-walled tube sampler in Saint Monique, Saint Jude, Casselman and Saint Barnabé and block samples in Saint Jean Vianney and James Bay. Similar studies conducted by [13] on Norwegian sensitive clays, yielded remoulding energies per unit volume of 20 - 160

$\text{kJ/m}^3$ . Here, the strain at peak shear stress ( $\gamma_p$ ), shear modulus ( $G$ ) and strain at remoulded shear strength ( $\gamma_r$ ) were respectively considered as 0.5%, 150 times peak shear stress, and 300% according to previous Norwegian database [13]





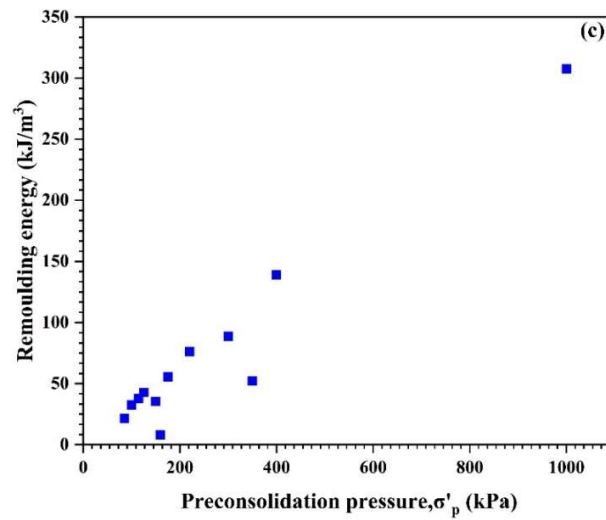


Figure 2-10 Variations of remoulding energy for Eastern Canadian clays with (a) liquidity index, (b) plasticity index and (c) preconsolidation pressure

The value of remoulding energy primarily depends on the undrained shear strength and the ease of strength degradation or the softening undergone by the soil. Figure 2-10 shows that the remoulding energy has a positive correlation with the preconsolidation pressure ( $\sigma'_p$ ) and no correlation with  $I_L$  and  $I_p$ . This means that the factor that primarily affects remoulding energy is the stress history of the soil and physical parameters have very low to no dependence on the remoulding energy. Figure 2-11 compares the remoulding energies of Eastern Canadian (this study) and Norwegian [13] clays and further shows the poor correlation of physical properties with remoulding energy even for Norwegian clays. On average, remoulding energies of Eastern Canadian and Norwegian clays seem to be more or less in the same range. The Norwegian clay data used for comparison are taken from [13] and are shown in Table 2-2.

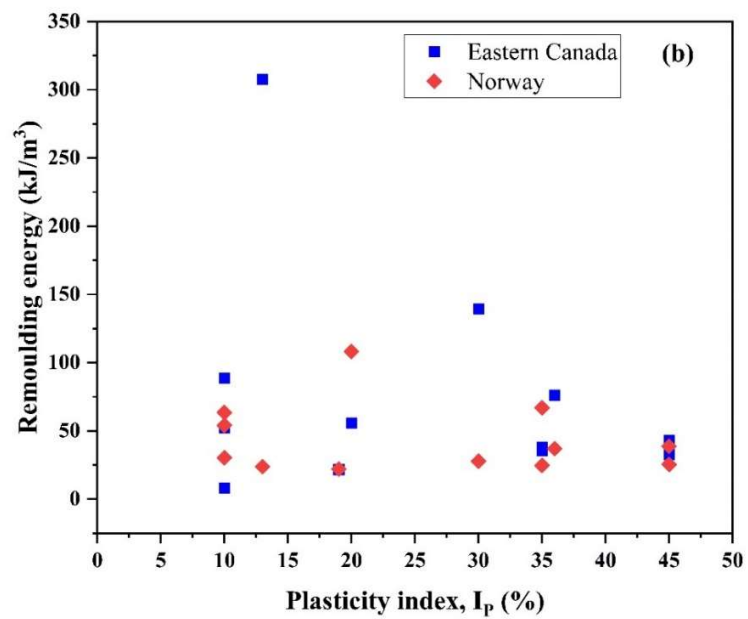
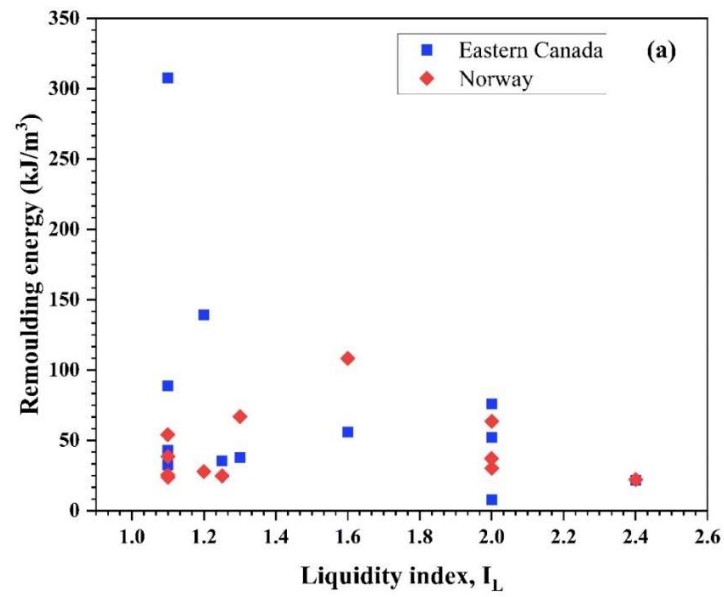


Figure 2-11 Comparison of remoulding energy of Eastern Canadian and Norwegian clays and their dependence on (a) liquidity index and (b) plasticity index

As mentioned earlier, [13] considered a linear post-peak behavior in their estimation of remoulding energy. It is however apparent that the actual post - peak behavior is non-linear even though this is quite difficult to portray. Here, an attempt was made to estimate the remoulding energy by an exponential prediction of the non-linear strain softening curve. Data from five of the sites in Table 2-1 (Saint Monique, Saint Jude, James Bay, Casselman, Saint Barnabé) were used for this estimation. The DSS test results seem to fit well with an exponential variation and hence this simple extrapolation was carried out to obtain the complete non-linear post-peak behavior curve (Figure 2-12). In the analysis of post-peak behavior of large retrogressive landslides, it is often noticed that strength degradation at end of retrogression does not always correspond to 100% remoulding in the field [47]. Thus, energy at each level of remoulding indicated by the remoulding index,  $I_r$  (Equation 2-3) would be a much better representation. Remoulding energy at each degree of remoulding is presented in Figure 2-13 and these curves are obtained from the stress-strain curves of Figure 2-12. Due to the brittle nature of sensitive clays, energy degradation close to complete remoulding (taken as 80% in this study) could happen quite soon and the variations are almost linear as shown in Figure 2-13. As suggested by [47], strength degradations beyond this may not always take place in the field. Also,  $s_{ur}$  for these clays is about 1.5 – 0.1 kPa (as reported by the corresponding literatures) and the accurate measurements of such low strengths could also be difficult. Hence the practical effect of remoulding energy corresponding to exactly 100% remoulding should be further analysed with sophisticated numerical computations.

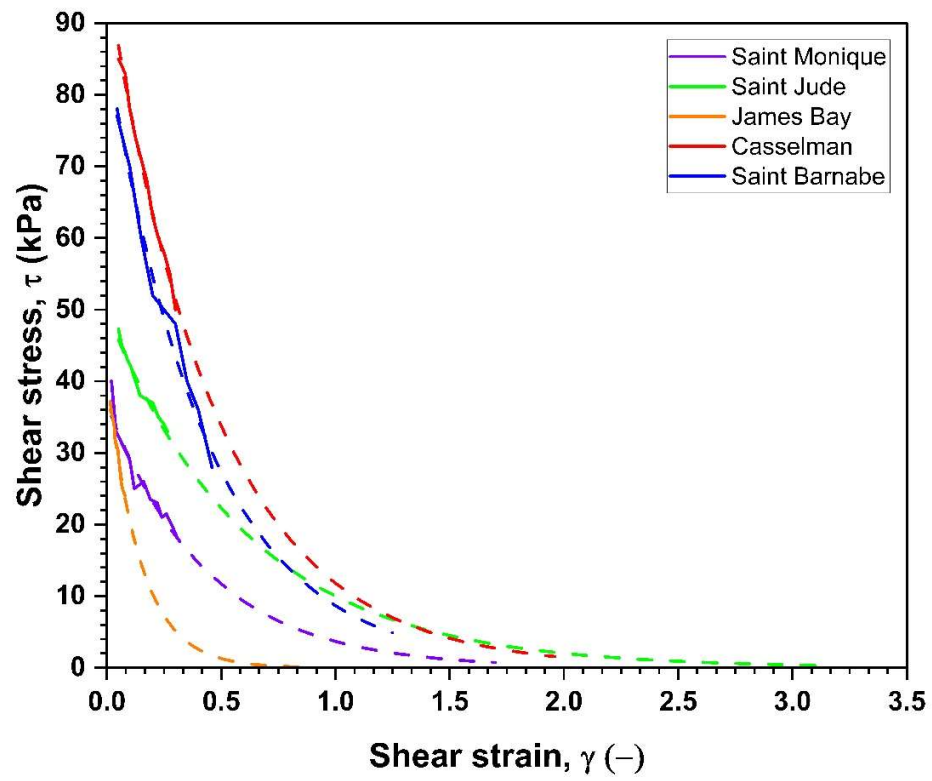


Figure 2-12 Post-peak strain softening curves from DSS results of selected Eastern Canadian sites (solid lines represent the laboratory data and dashed lines show the exponential extrapolations)

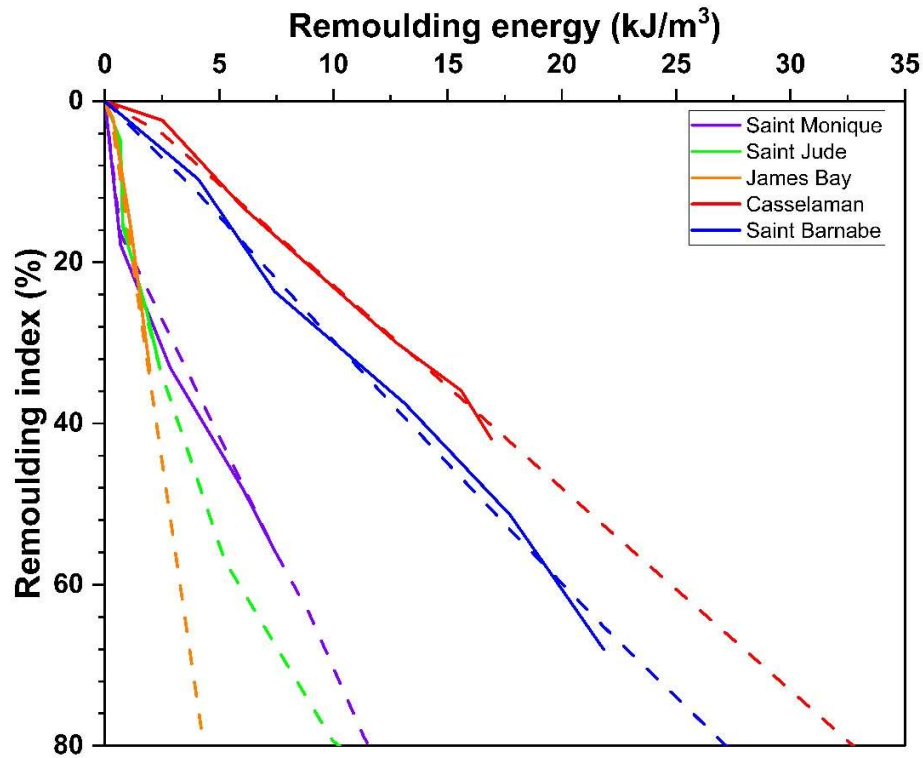


Figure 2-13 Remoulding energy at various degrees of remoulding index obtained from DSS results (solid lines represent the laboratory data and dashed lines show the exponential extrapolations).

## 2.7 DISCUSSIONS

The occurrence of disastrous landslides in sensitive clay slopes of certain Northern countries, especially in Eastern Canadian region, has been studied extensively over decades in various literature [11]; [70]; [32]; [3]. Natural processes like erosion or climate change can cause reduction in mean stress and an increase in shear stress under drained loading. These seemingly stable slopes can undergo remoulding through sudden loading in the form of loss of resisting forces (e.g., toe erosion near marine slopes, excavation), increase in driving forces (e.g., construction of embankment) or increase in pore pressure (e.g., heavy rainfall, melting of snow, vibration, rapid loading), followed by retrogressive landslides depending on soil conditions and morphology. In the analysis of retrogressive landslides, the advantage of material properties such as quickness, brittleness index, remoulding index and remoulding energy is that they directly represent the nature of a sensitive clay material, whereas other criteria based on post failure movements are mostly empirical and hence require site

specific data. However, since the determination of liquid limit, liquidity index, plasticity index and remoulded shear strength are relatively straightforward and reliable, criteria based on these parameters are widely accepted and used. Retrogression is quantified in terms of retrogression distance and runout distance. Although there are specific soil parameters that affect the amount of retrogression, an energy dissipation approach in the form of remoulding energy seems to accurately encompass strain softening and the severity of strength loss. An empirical relation in this very context has been given by [13] and confirms that a lower remoulding energy is associated with more retrogression.

The linear approximation made by [13] in forming Equation 2-7 provides a simplified and adequate methodology to determine remoulding energy. However, a clear analysis of the observations made in this paper indicates that it is the post-peak behaviour which impacts the remoulding energy, and the rate of strain softening coupled with strain at residual/remoulded state is a critical parameter in this regard. In this context, the impact of secant shear modulus ( $G$ ) on the remoulding energy is found to be inconsequential. In Equation 2-7, keeping all other parameters the same, a change in  $G$  (even an increase of 5 times) does not produce any significant changes in remoulding energy. An observation is that, as the peak strength is mobilized at small strains, the area under the stress-strain curve up to the peak strength constitutes a relatively insignificant part of the remoulding energy and as a result variation in secant shear modulus ( $G$ ) has little effect on the remoulding energy. Furthermore, Figures 2-10 and 2-11 predominantly show the poor correlation of remoulding energy with physical properties such as the Atterberg limits and the importance of stress history in the determination of remoulding energy. Past empirical correlations and studies for remoulding energy which show its positive correlation with plasticity index [45]; [36]; [13] should be used with caution as they alone may not provide accurate assessments of remoulding energy. Considerations of post-peak parameters at large deformations and the ease with which this state is arrived at based on a non - linear stress-strain behavior is specifically important for the estimation of remoulding energy. Upon observation of Figures 2-12 and 2-13 it is noticed that the variation of remoulding energy with remoulding index is almost linear and this slope is dependent on the softening of the corresponding stress-strain curves.

Overconsolidated clays under undrained shear exhibit strain-softening behaviour and sometimes with much pronounced strain softening at low confining stresses [44]; [71]; [56]. It is well understood that Norwegian

sensitive clays are only slightly overconsolidated in comparison to Eastern Canadian sensitive clays [13]; [3] and hence may exhibit lower brittleness and higher remoulding strains in comparison to Eastern Canadian clays. As a result, a linear post - peak behaviour may correlate well with the actual non-linear post - peak behaviour. However, in the case of Eastern Canadian sensitive clays, a linear approximation overestimates the remoulding energy due to the pronounced strain softening it undergoes at low confining stresses. This could be corrected through experimental investigations on site specific samples and considering the non-linear strain-softening behaviour of sensitive clays. Moreover, material properties like brittleness index could provide better physical dimensions to develop an equation for remoulding energy considering their relevance in the process of remoulding.

Researchers are still struggling to understand the extend of retrogression and the reactivation of landslides in sensitive clays in terms of time. These landslides are very unpredictable as to whether they continue to be active or not. The Saint Jean Vianney landslide in Saguenay in 1971 was said to have started from the crater of a larger landslide which occurred 500 years ago [7]. The Beattie mine in Quebec, where a landslide occurred in 1943, witnessed a shallow slide in 1937 before the occurrence of the landslide and even continued to have large slides until 1946 [72]. The Mink Creek landslide which occurred in Terrace, British Columbia in 1994 was also not the first movement in this area with two other landslides in 1962 and several prehistoric flowslides in this area [73]. Thus, the susceptibility of an area to disastrous landslides does not end with a single event or even several events over the course of few years. This creates further uncertainty in post-landslide operations including restoration and rehabilitation. These uncertainties may be reduced through detailed soil investigations which can add more precision to the estimation of remoulding energy and the constitutive and numerical models for landslide prediction.

Based on the aforesaid observations, the authors believe that there is limited experimental data after Tavenas' study and there is a need to continue research on the post-peak behaviour of Eastern Canadian sensitive clays with site specific data to determine remoulding energy and its correlations with other post-peak parameters.



## 2.8 CONCLUSIONS AND SUMMARY

This review paper provided a comprehensive overview of different types and failure mechanisms of sensitive clay landslides in Eastern Canadian region and evaluated various criteria for their assessment. Among existing criteria, remoulding energy and remoulding index were found to assess post-failure landslide movements with more precision. However, the expansion of these concepts towards detailed assessment of retrogressive landslides in sensitive clays was found to have received less attention in spite of their potential. Some of the key findings of the present study are as follows:

- Critical evaluation of various studies indicated that post - peak stress - strain behavior of strain-softening soils has significant influence on the accurate quantification of remoulding energy and possibly on post-failure landslide mechanisms.
- In the case of Eastern Canadian clays, the determination of remoulding energy based on a non-linear post-peak stress-strain behavior may reduce inconsistencies shown by existing approaches.
- Preliminary comparison of results highlighted that the remoulding energy of Eastern Canadian and Norwegian quick clays appears to be controlled by stress history instead of physical parameters. Existing studies which indicate otherwise should be used with caution.
- Post-failure movements in retrogressive landslides are significantly dependent on energy dissipation during slope failures which in turn depends on the inherent material behavior (brittle or ductile).
- There is a huge need to accurately determine the non-linear post-peak stress-strain behavior of sensitive clays, reproducing in-situ conditions through experimental studies, considering its significance in assessing post-failure landslide movements, and the authors plan to explore this gap in future research.

### Funding

This research was partially funded by the Natural Sciences and Engineering Research Council of Canada (NSERC) and Hydro-Quebec under project funding no. RDCPJ 521771 – 17.

## CHAPTER 3

### Article 2: An exponential model for strain softening behaviour of sensitive clays

Sarah Jacob<sup>1</sup>, Ali Saeidi<sup>2</sup>, Rama Vara Prasad Chavali<sup>3</sup>, Abouzar Saderkarimi<sup>4</sup>

<sup>1</sup>**Corresponding author:** Doctoral student, Department of Applied Science, Université du Québec à Chicoutimi, Quebec, Canada

<sup>2</sup> Professor, Department of Applied Science, Université du Québec à Chicoutimi, Quebec, Canada

<sup>3</sup> Post doctoral researcher, Department of Applied Science, Université du Québec à Chicoutimi, Quebec, Canada  
Present address – Assistant Professor, Department of Civil Engineering, Velagapudi Ramakrishna Siddhartha Engineering College, Vijayawada, India

<sup>4</sup> Associate Professor, Department of civil and environmental engineering, Western University, Ontario, Canada

Submitted to a journal

#### Credit authorship contribution statement

**Sarah Jacob:** Conceptualization, Data curation, Formal analysis, Resources, Writing – original draft, Writing – review and editing. **Ali Saeidi:** Supervision, Methodology, Resources, Writing – review and editing. **Abouzar Sadrekarimi:** Supervision, Writing – review and editing. **Rama Vara Prasad Chavali:** Writing – review and editing.

#### Declaration of competing interests

The authors declare the following financial interests/personal relationships which may be considered as potential competing interests: Ali Saeidi reports financial support was provided by Natural Sciences and Engineering Research Council of Canada (Grant ID: NSERC- 950- 232724). Ali Saeidi reports financial support was provided by Hydro Quebec (Grant ID: RDCPJ 521771–17). If there are other authors, they declare that they have no known competing financial interests or personal relationships that could have appeared to influence the work reported in this paper.

### 3.1 ABSTRACT

Strain softening in sensitive clays is a major cause of retrogressive landslides. The assessment of post failure movements like retrogression or run out in such landslides requires detailed data regarding the post - peak parameters, especially in terms of stress and strain at remoulded state. The limitations concerning experimental studies in this regard is well known which has often led to the use of mathematical and analytical models in assessing strain softening. Here, an exponential model to predict strain softening is proposed by making use of triaxial testing data. The model is developed through a series of triaxial testing results collected from ten different sites in Eastern Canada. The developed softening equation is governed by the peak undrained shear strength, sensitivity of the clay, ease of strength reduction from the peak to the remoulded state and the strain at remoulded strength. The main advantage is that a quick and reasonable evaluation of the softening behaviour of the sensitive clay maybe carried out through experimental studies. The prediction of strain at remoulded state is an important outcome of this study and is consistent with field data. Keeping in mind the effect of geological and topographical factors in the estimation of post failure movements in retrogressive landslides, an attempt has been made to conduct a preliminary assessment of the retrogression distance through the strain at remoulded state.

**Keywords:** sensitive clays, strain softening, triaxial test, retrogressive landslides, post failure movement

### 3.2 INTRODUCTION

#### 3.2.1 Background

Landslides in sensitive clays of Eastern Canada and Scandinavia suffer substantial retrogressive failure, mostly involving the displacement of several million cubic meters of remoulded soil debris [43]; [58]. An illustration of this type of failure in sensitive clay landslides (flowslides and spreads) is shown in Figure 3-1. The extent of failure is represented in terms of retrogression distance ( $L_R$ ), which is measured from the crest of the original slope to that of the post failure slope. The ratio of  $L_R$  to the height of the clay slope ( $H$ ) is often used to assess the range of hazard with  $L_R/H > 2$  being a good indication of “large retrogressive landslide” [74]. An inventory of retrogressive landslides in Quebec from 1840 to 2012 conducted by Ministère des Transports du Québec have shown an average  $L_R$  of 225 and 145 m for flowslides and spreads respectively [26]. The

realization of these land movements is often difficult due to sample disturbance, complex flow behavior, accurate interpretation of post failure movements and strength loss at large deformations. However, computational techniques and numerical modelling efforts to analyse these behaviors have been evolving over the past decade. Advanced modelling techniques such as BIFURC, MPM (Material Point Method), LDFEM (Large deformation finite element modelling), SPFEM (Smooth particle finite element modelling) and SPH (Smoothed Particle Hydrodynamics) [18]; [22]; [75]; [23]; [24] have been successful in generating landslide mechanisms and post-failure movements in Eastern Canada and Norway. Additionally, a physical model using a geotechnical centrifuge has been used by [46] to study retrogressive failure in Eastern Canadian clays.

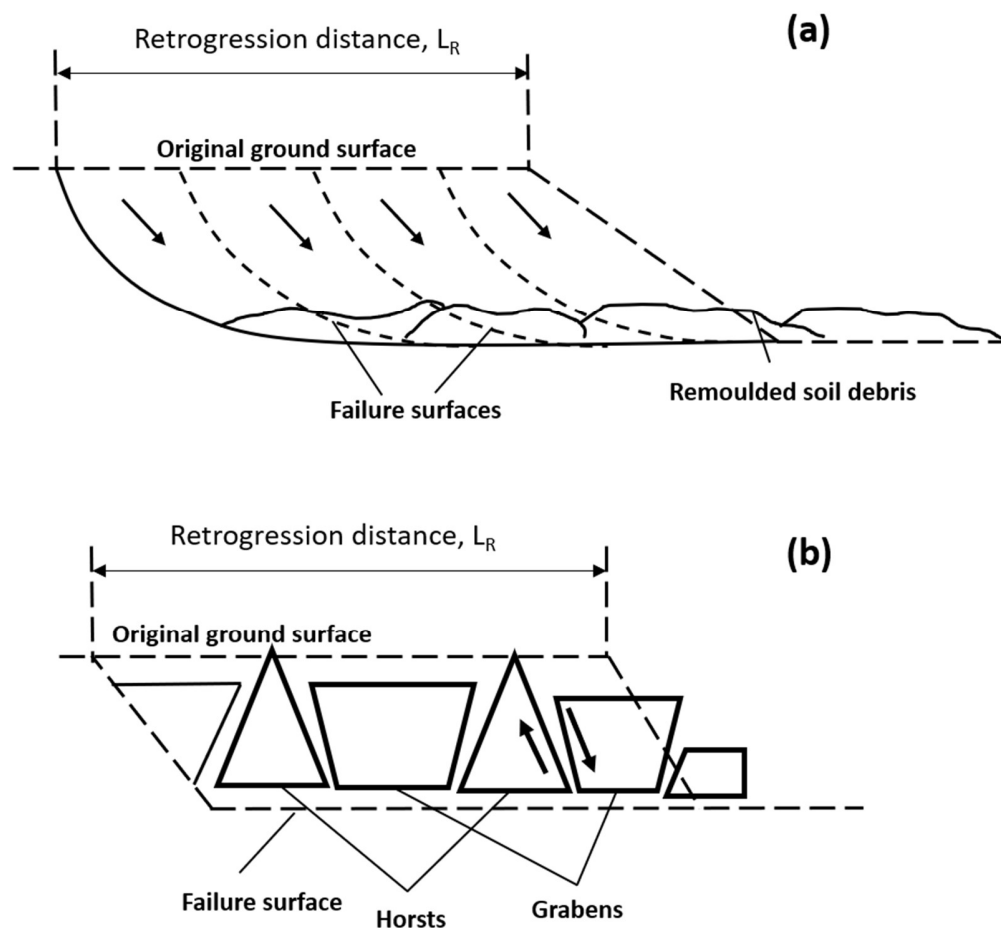


Figure 3-1 Retrogressive failure morphology in (a) flowslides and (b) spreads (Adaptation from [76])

The occurrence of sensitive clay landslides is primarily due to strain-softening and formation of shear bands. Strain softening generally refers to the decrease in strength past the peak (intact) strength, into the post - peak regime during shear failure. [14] attributed the decrease in strength to a reduction in the friction angle and cohesive strength when analysing long term slope stability in overconsolidated clays. On the other hand, [41] credited the decrease of shear strength in quick clays to the shear induced pore pressure during undrained loading. Natural processes like heavy rainfall and melting of snow; and human activities leading to vibration and heavy loading can cause an increase in pore water pressure leading to a reduction in shear stresses in soil. This has been confirmed by various authors including [15], [16], [17], [77] and [2]. Hence, the possibility of retrogressive failure in sensitive clays largely depends on the amount of softening that is likely to take place during failure.

### 3.2.2 Existing studies on strain softening in sensitive clays

The post - peak strength degradation approaches the remoulded state over large displacements/strains in sensitive clays which cannot be typically simulated using conventional laboratory tests. Owing to this limitation, certain constitutive models have come into play to predict strain softening beyond the laboratory limits of strain. [78] proposed an exponential function (Equation 3-1) inspired by [79] as a constitutive model to capture strain softening in sensitive clays.

$$s_u = s_{ur} + (s_{up} - s_{ur})e^{-3\gamma/\gamma_{95}} \quad (3-1)$$

where,  $s_u$  is the post - peak strength,  $\gamma$  is the post - peak strain,  $s_t$  is the sensitivity,  $s_{ur}$  is the remoulded shear strength and  $\gamma_{95}$  is the strain corresponding to a strength reduction of 95% of  $(s_{up}-s_{ur})$ . Similarly, a Mohr Coulomb cohesion softening model with zero friction angle for reduction in strength in the post - peak region (Equation 3-2) has also been used by researchers in numerical simulations using MPM [80]; [81] and SPFEM [75].

$$s_u = s_{ur} + (s_{up} - s_{ur})e^{-\lambda\gamma^p} \quad (3-2)$$

where  $\lambda$  is the shape factor and  $\gamma^p$  is the plastic strain in the post - peak region. It may be noticed that Equation 3-1 is essentially the same as Equation 3-2 with  $3/\gamma_{95}$  as the shape factor. The aforementioned equations which were primarily derived from [79] have become increasingly popular and several studies on sensitive clay landslides use this equation [22]. A parameter called  $\gamma_{95}$  which corresponds to strain at 95% remoulding is used in the equation and allows for the development of the complete post-peak strain softening curve up to the remoulded state. [19] used [32]'s data to calibrate the equation and determine  $\gamma_{95}$  for a set of Eastern Canadian clays previously studied by [32]. However, in the absence of such data, there is no definitive way of determining a strain corresponding to a strength reduction of 95% for any site and generalized use of it without site specific data can be erroneous [25]. In fact, the shape factors used in other studies have been chosen after several parametric studies and sensitivity analyses on the same region. Although these models are successful in predicting failure mechanisms and post failure movements, their utility is often restricted to certain regions with a good understanding of the post - peak behaviour of the clay. In the case of new and unexplored landslides, the shape factors have to be recalibrated with several simulations that can often become strenuous and difficult. Researchers also rely on an ideal linear strength degradation model in the post - peak domain for ease [13]; [18], but the actual strain softening behaviour of sensitive clay is truly non-linear. The direct utilization of experimental results to capture strain softening could reduce the aforementioned ambiguities and could provide a methodology to assess retrogressive landslides at any region of interest. Hence, a non-linear strain-softening model is proposed that captures strain softening by simulation of field conditions through triaxial testing. Several non-linear elastoplastic models in the past have relied on triaxial tests [82]; [83]; [84]; [85]. The main advantage of the proposed model is that reasonable understandings of strain at the remoulded state and post-failure landslide movements may be made by conducting only a triaxial test.

This research seeks to propose a simple non-linear mathematical model for simulating the strain-softening behavior of sensitive clays of Eastern Canada and predicting strain at the remoulded state based on triaxial testing data. In order to accomplish this, a database of triaxial tests on sensitive clays of Eastern Canada was collected from existing literature. The triaxial test data were interpreted according to the Mohr-Coulomb failure criterion. Subsequently, an exponential strain softening equation was developed, using mathematical formulations and parametric studies to predict the post-peak stress-strain behavior and the post failure movements. Finally, the validity of the developed model was evaluated through field observations.

### 3.3 DATA ACQUISITION FOR MODEL DEVELOPMENT

Sensitive clay landslides are often analysed under plane strain conditions. However, here model calibration is carried out based on triaxial tests instead of a DSS test. This is done by keeping in mind the importance of stress history of the soil in the strain softening behaviour of sensitive clays and the triaxial tests can better incorporate insitu stress states, complex stress history of sensitive clays and drainage conditions. The data for the development of the strain-softening model was obtained from ten sites spread over the Eastern Canadian region and includes sixteen high quality triaxial test results. These include clays of varying preconsolidation pressures and physical properties subjected to different test conditions. Preconsolidation pressures ( $\sigma'_p$ ) have been obtained experimentally by CRS oedometer tests. The plasticity chart shows clays ranging from high compressibility to low compressibility (Figure 3-2). Samples were obtained from various depths ranging from 4 m to 23 m. Almost all the samples were trimmed from block samples except in one case where a Laval piston sampler was used [86]. The remoulded undrained shear strengths ( $s_{ur}$ ) were estimated by field vane/fall cone tests. All the results used correspond to strain-controlled isotropically consolidated undrained (CUI) triaxial tests with pore pressure measurements. Back pressures ranging from 50 - 670 kPa were used for specimen saturation. Strain rates ( $\dot{\epsilon}$ ) covering 0.5-1.2%/h were used for shearing. The samples were tested in the overconsolidated range i.e. confining pressures,  $\sigma'_{3c} < \sigma'_p$  was applied resulting in brittle behaviors and strain-softening due to destruction of cementation bonds in these clays [71]. Failure occurred at low strains of 0.7 - 2%. Tables 3-1 and 3-2 show the details of the soil samples and testing conditions. Figure 3-3 shows the triaxial results of representative clays used in the analysis with the respective  $\sigma'_{3c}$  in brackets. Figure 3-3 does not include all data used in model calibration to prevent crowding and due to limitations with scale.

Table 3-1 Properties of data used for model calibration

Site	Depth (m)	Water content (%)	$\sigma'_p$ (kPa)	$s_{ur}$ (kPa)	Source
Arnprior	20	78.5	210	5.5	[86]
St Louis	9	69	159	0.9	[87]
St Vallier	23	60	98	8.8	[71]
Grand Baleine	-	59.5	112	4.8	[88]

Olga	4	91.5	78	5	
Saint-Jean-Vianney	-	42	940	6	[89]
Rigaud clay	9.5	47.6	180	0.3	[90]
Outardes	12	25.2	595	0.3	[91]
Ottawa clay	5	35.5	175	2.5	[92]
St Leon	9.3	75	170	1.1	[93]

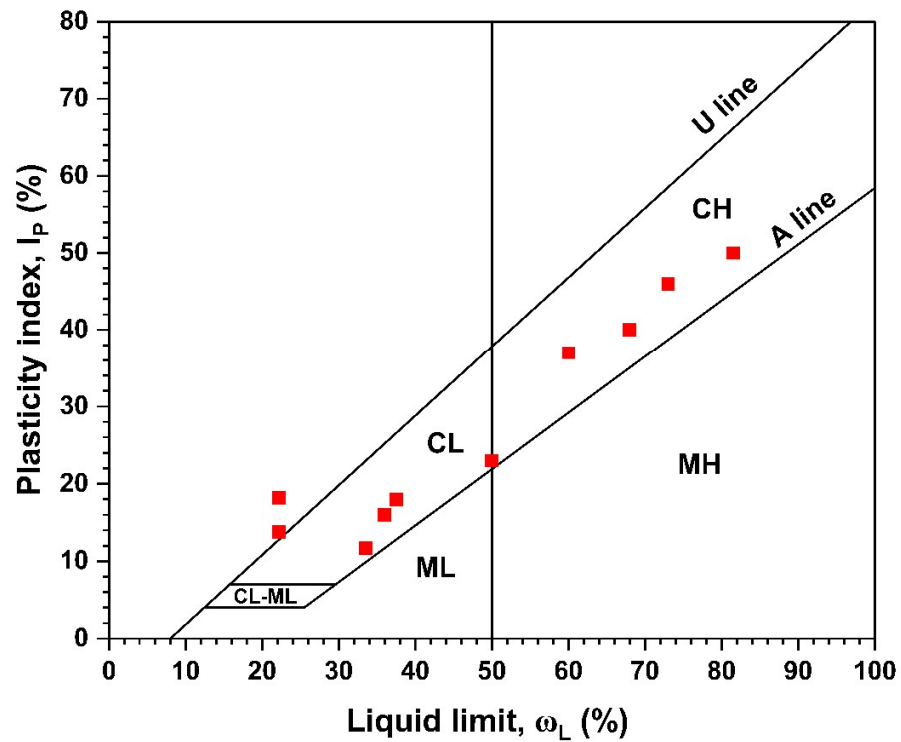


Figure 3-2 Plasticity chart for data used in model calibration

Table 3-2 Triaxial testing conditions of data used in model calibration

Site	$\sigma'_{3c}$ (kPa)	$\dot{\epsilon}$ (%/h)	Source
Arnprior	60	1	[94]



St Louis	20.7	0.5	[95]
	41.4		
	68.9		
St Vallier	20.6	0.5	[96]
	41.2		
	69.6		
Grand Baleine	45	1	[97]
Olga	17.6	0.5	
Saint-Jean-Vianney	40	1.2	[98]
Rigaud clay	50	0.5	[99]
	90		
Outardes	200	-	[100]
	400		
Ottawa clay	50	0.5	[101]
St Leon	170	-	[102]

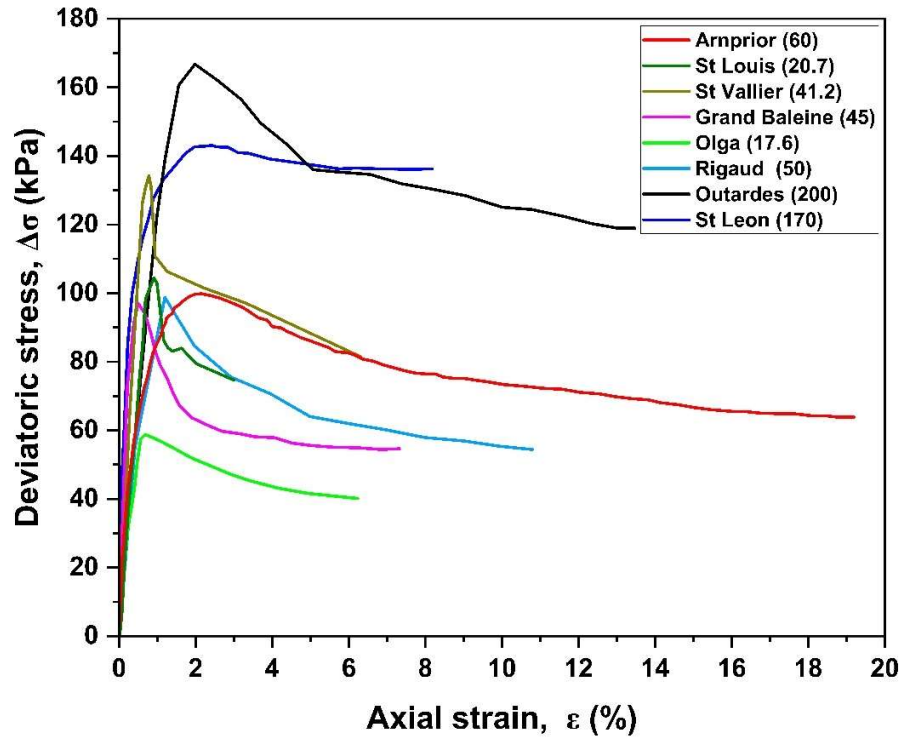


Figure 3-3 CUI triaxial results for representative set of data used for model calibration

The triaxial test results are converted to shear data by considering shear stresses and strain at the failure plane in a triaxial test as well as simple assumptions in literature i.e. shear stress is half of deviatoric stress and shear strain is 1.5 times of axial strain [67].

### 3.4 DEVELOPMENT OF THE STRAIN SOFTENING MODEL

In the analysis of strain softening in sensitive clays, it is quite clear that the variation of stress with respect to strain in the post - peak region is non-linear. The strength degradation in the post - peak region takes place somewhat rapidly initially and once the maximum curvature of the softening curve is attained the rate of strength degradation with strain becomes slower as it approaches the remoulded state. Several numerical models show that even after strength degradation reaches the remoulded state, shear deformations continue until large deformations with negligible decrease in strength [15]; [19]. However, this point of final strain is not important

as the process of remoulding is completed at the remoulded state and the kinetics and post-failure landslide movements would have already been initiated. Extension of the proposed model towards analysis of post failure movements and determination of remoulding energy would also be more accurate by utilisation of the strain at a point where most of the strength degradation is complete. Thus, the proposed model is used to evaluate the value of strain when remoulding is completed, referred to as  $\gamma_r$  in this study. This is carried out by considering an exponential strength degradation from the peak to the remoulded states. The shear displacements in the post - peak region are localised in the shear band, however the experimental estimation of shear band thickness and the corresponding shear strains are very difficult and still quite uncertain [16]; [17]; [19]. Hence accumulated shear strain based on laboratory strain data is considered.

By observation of laboratory data and existing literatures, the pre-peak part of the curve undergoes elastic linear deformations with increasing stresses and the slope of the curve maybe represented as the shear modulus (G). Figure 3-5 shows the variation of shear stress with respect to shear strain in the post - peak region according to the following equation:

$$s_u = ae^{-b\gamma} \quad (3-7)$$

where,  $s_u$ = undrained shear strength and  $\gamma$  = plastic shear strain

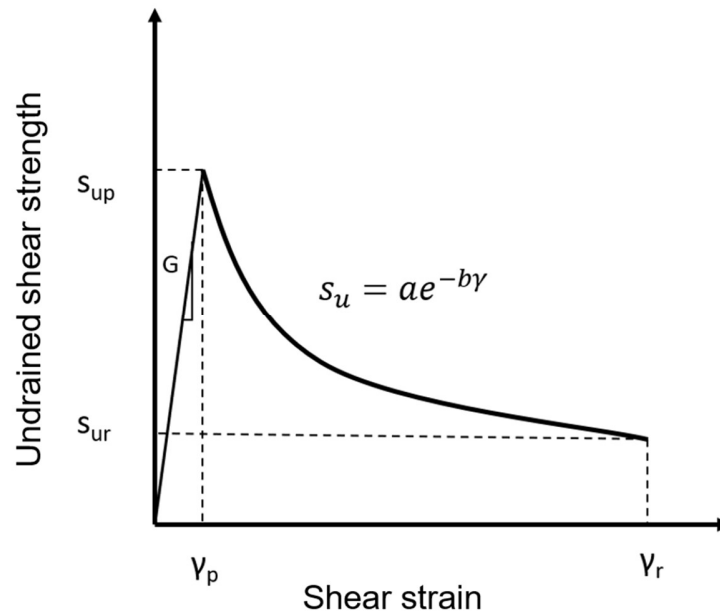


Figure 3-4 Post - peak strain softening model where  $s_{up}$  = peak undrained shear strength,  $s_{ur}$  = remoulded undrained shear strength,  $\gamma_p$  = strain at peak stress,  $\gamma_r$  = strain at remoulded shear strength, a and b = model parameters

Some of the key features of this curve are as follows:

- The coefficient 'a' only depends on the peak undrained shear strength ( $s_{up}$ ) and for a specific curve, its subsequent increase or decrease, increases or decreases the peak of the curve.
- The coefficient 'b' is the shape factor that primarily depends on the softening of the curve and hence is dependant on the ease of strength degradation of the sample. For a specific curve, an increase in 'b' would indicate pronounced softening and very brittle soils and vice versa.
- A higher 'b' and pronounced softening gives a lower  $\gamma_r$  value, meaning brittle soils undergo less shear displacement.

These coefficients determine the peak and the curvature of the strain softening curve and hence are the main model parameters in the prediction of  $\gamma_r$ . The following section shows the determination of these parameters based on interdependence and mathematical formulations.

As mentioned earlier, it was observed that changes in parameter 'a' seem to affect the peak of the curve or  $s_{up}$ . Hence, a correlation was carried out between 'a' obtained via exponential curve fitting and  $s_{up}$ . Figure 6 shows that all the data lies close to the  $a = s_{up}$  line, therefore the following assumption may be deduced:

$$a = s_{up} \quad (3-8)$$

Thus, the model parameter 'a' for all the data is considered as  $s_{up}$  itself.

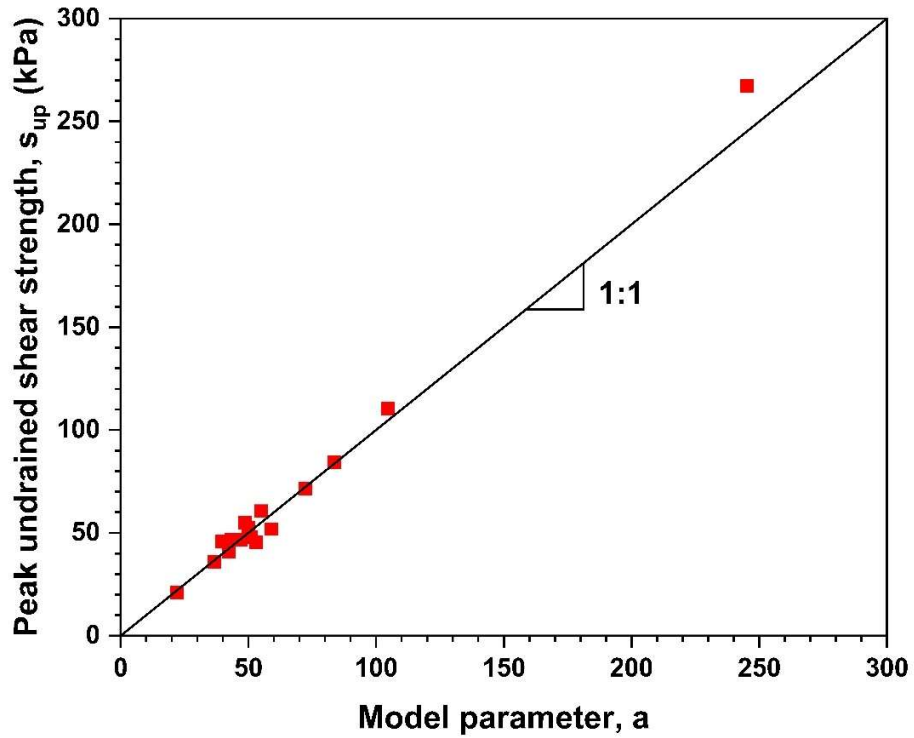


Figure 3-5 Correlation between model parameter 'a' and  $s_{up}$

The parameter 'b' is a bit more complex as it is dependant on the softening of the curve. Softening maybe defined as the rate of decrease of shear strength with respect to strain in the post - peak region and maybe represented by a parameter called softening index. Since the curve is non-linear, the softening index varies at each point in the post - peak region and cannot be defined as a constant for the entire curve. Let us consider 'S' as the softening index. Hence:

$$S = \frac{d}{d\gamma}(s_u) \quad (3-9a)$$

$$= \frac{d}{d\gamma}(ae^{-b\gamma}) \quad (3-9b)$$

$$= -abe^{-b\gamma} \quad (3-9c)$$

$$S = -bs_u \quad (3-10)$$

Thus, it is clear that the softening index varies linearly with the undrained shear strength at each subsequent point of the post - peak curve according to 'b'. However, the authors observed no correlation between 'b' and any physical/ mechanical parameter like water content, Atterberg limits,  $s_{up}$ , sensitivity and  $\dot{\epsilon}$ . Hence, 'b' was estimated using certain mathematical assumptions.

At the peak and remoulded states, Equation (3-7) may be written as below:

$$s_{up} = ae^{-b\gamma_p} \quad (3-11a)$$

$$s_{ur} = ae^{-b\gamma_r} \quad (3-11b)$$

where  $\gamma_p$  and  $\gamma_r$  are the strains at peak and remoulded states, respectively.

Dividing (3-11a) and (3-11b), we get,

$$\frac{s_{up}}{s_{ur}} = e^{-b(\gamma_p - \gamma_r)} \quad (11c)$$

Sensitivity ( $S_t$ ) is the ratio of  $s_{up}$  to  $s_{ur}$ . Therefore,

$$S_t = e^{-b(\gamma_p - \gamma_r)} \quad (3-11d)$$

From this, 'b' maybe written as,

$$b = \frac{\ln(S_t)}{\gamma_r - \gamma_p} \quad (3-11e)$$

The strain at the peak stress ( $\gamma_p$ ) can be expressed in terms of the secant shear modulus ( $G$ ) as,

$$\gamma_p = \frac{s_{up}}{G} \quad (3-11f)$$

Substituting in (3-11e),

$$b = \frac{G \ln(S_t)}{\gamma_r G - s_{up}} \quad (11g)$$

To simplify further,

$$b = \frac{G \ln(S_t)}{\gamma_r \frac{s_{up}}{\gamma_p} - s_{up}} \quad (3-11h)$$

$$= \frac{G \ln(S_t)}{s_{up}(\frac{\gamma_r}{\gamma_p} - 1)} \quad (3-11i)$$

The strain at peak stress is very small, in the range of 0.5-2%. However, numerical analysis of sensitive clay landslides in Eastern Canada have often assumed strains of 55-120% in the post - peak region [44]; [22].

(Hence,  $\frac{\gamma_r}{\gamma_p} \gg 1$  and  $(\frac{\gamma_r}{\gamma_p} - 1)$  can be replaced by  $\frac{\gamma_r}{\gamma_p}$ . Thus, equation (3-11i) maybe further simplified as,

$$b = \frac{\ln(S_t)}{\gamma_p \frac{\gamma_r}{\gamma_p}} \quad (3-11j)$$

$$b = \frac{\ln(S_t)}{\gamma_r} \quad (3-12)$$

Substituting (3-8) and (3-12) in Equation (3-5), the strain softening model for sensitive clays upto  $\gamma_r$  could be defined by Equation (3-13). It maybe noticed that the equation primarily depends on the peak undrained shear strength, soil sensitivity, and  $\gamma_r$ .

$$s_u = s_{up} e^{-\frac{\ln(S_t)}{\gamma_r} \gamma} \quad (3-13)$$

An approximation for  $\gamma_r$  can be obtained through the proposed stress – strain model and the laboratory post - peak curve. The post - peak curve, up to the residual state (denoted by  $s_{ures}$  and  $\gamma_{res}$ ), obtained in the laboratory through triaxial tests depicts the actual stress-strain behavior of the soil and its involvement in the estimation of  $\gamma_r$  is important. This helps to incorporate the true softening behavior in the estimation of  $\gamma_r$  (Figure 3-7).

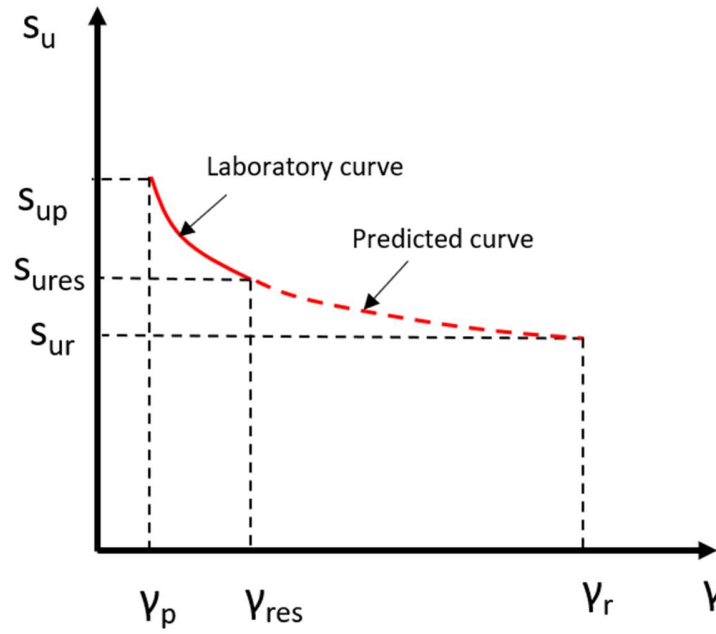


Figure 3-6 Post - peak parameters in the strain softening curve

Applying natural log to both sides of Equation (3-13), we get,

$$\ln(s_u) = \ln(s_{up}) - \frac{\ln(S_t)\gamma}{\gamma_r} \quad (3-14a)$$

Solving for  $\gamma_r$ , we get,

$$\gamma_r = \frac{\gamma \ln(S_t)}{\ln\left(\frac{s_{up}}{s_u}\right)} \quad (3-14b)$$

Here,  $s_u$  and  $\gamma$  could stand for any point of the post - peak region of the laboratory curve. However, the residual state would signify the maximum possible level of post - peak behavior achievable through conventional laboratory tests and would provide a more accurate value of  $\gamma_r$ . Equation (3-14b) would then be,



$$\gamma_r = \frac{\gamma_{res} \ln(S_t)}{\ln\left(\frac{S_{up}}{S_{ures}}\right)} \quad (3-15)$$

Table 3-3 Model parameters for the strain softening equation applied to data for calibration

Site	a	b	r <sup>2</sup>	γ <sub>r</sub> (calculated)
Arnprior (60)	36.08	2.37	0.925	0.794
St Louis (20.7)	41	9.45	0.638	0.404
St Louis (41.4)	45.63	10.34	0.915	0.38
St Louis (68.9)	51.84	11.84	0.865	0.342
St Vallier (20.6)	46.79	9.68	0.736	0.172
St Vallier (41.2)	52.69	6.61	0.746	0.271
St Vallier (69.6)	60.63	6.82	0.692	0.283
Grand Baliene (45)	45.81	5.74	0.735	0.393
Olga (17.6)	20.94	2.1	0.978	0.683
Rigaud clay (50)	46.68	3.78	0.868	1.335
Rigaud clay (90)	54.88	4.85	0.801	1.073
Outardes (200)	83.37	1.833	0.882	3.362
Ottawa – Heron Road (50)	47.79	2.74	0.994	1.076
St Leon (170)	71.53	0.91	0.962	12

In the following section, the stress-strain model is applied to the data for model calibration (Figure 3-8). The results for ‘a’ and ‘b’ parameters and the  $\gamma_r$  obtained from this dataset based on the calculations above are shown in Table 3. The model predictions are made through the following steps:

- i. From the laboratory test results, the residual stress-strain point is noted and an estimation of  $\gamma_r$  is made using Equation (3-15).
- ii. The parameter ‘b’ is obtained from Equation (3-12) using the  $\gamma_r$  obtained in the previous step. Furthermore, parameter ‘a’ is also obtained from the peak undrained shear strength (Equation 3-8).

- iii. In this way, the model parameters 'a' and 'b' are used to generate the strain softening model from the laboratory data according to Equation (3-13).

The model seems to capture the laboratory range of stress-strain data well and the prediction is extended according to Equation (3-13) up to the remoulded strain determined based on Equation (3-15). As mentioned before, pronounced softening leads to a lower  $\gamma_r$ , meaning that a lower shear displacement is required to reach a remoulded state. It can be observed that the data shows an array of curves with varying softening behaviors. A range of  $\gamma_r$  from 20% to 1200% can be seen. These differences emerge from differences in clay sensitivities and the range of available data in the post - peak domain. They also depend on the amount of strength degradation undergone by the samples from the peak to the post-peak region as well as the rate with which this degradation is achieved.

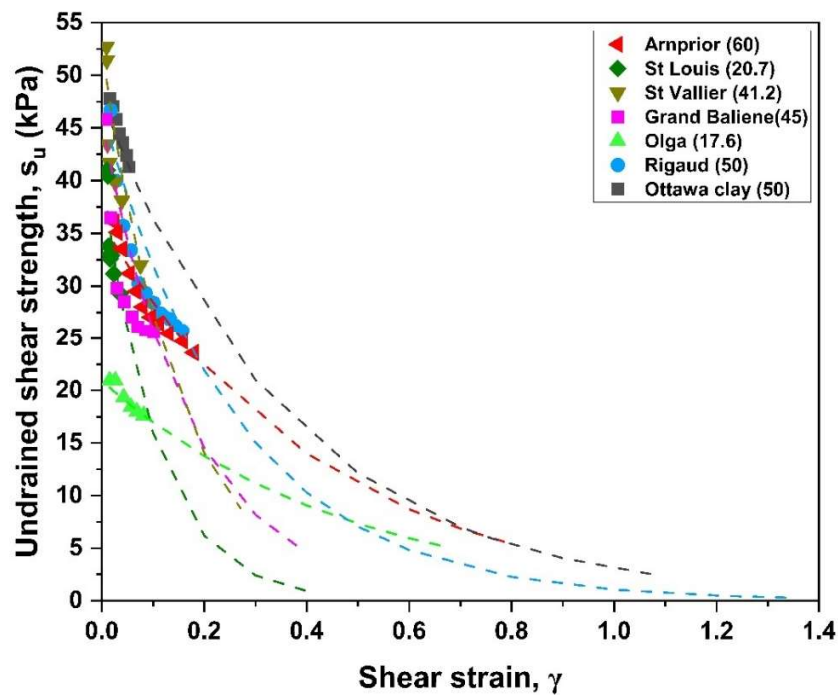


Figure 3-7 Laboratory shear data (scatter points) along with model prediction (dotted lines) for selected clays of data used for model calibration

### 3.5 VALIDATION OF PREDICTED REMOULDED STRAIN BY FIELD DATA

#### 3.5.1 Establishing a correlation between $L_R$ and predicted $\gamma_r$

Post failure movements like  $L_R$  is often used to assess the extent of damage caused by retrogressive landslides and is also one of the primary aims of modelling these landslides. The proposed model and the predicted  $\gamma_r$  could be a useful tool in the analysis of these movements. While numerical modelling using complex computational techniques are progressing in that direction, here an attempt has been made to apply the proposed simpler model to few landslide data and confirm its validity with respect to field data.  $L_R$  in the field are usually obtained based on observations of field sliding geometries, landslide scars, eyewitness accounts, aerial images, and LiDAR data. These often involve exploratory site investigations, huge amount of data and experience. As such, the data regarding post failure movements are usually available for slope failures with significant impact where further analysis was required. In the present study, this information was available in the literature for four landslide locations of the initial data used for model calibration which includes Saint Jean Vianney landslide 1971, Rigaud landslide 1978, St Louis (Yamasaka) landslide 1945 and the 1963 landslide in Ottawa-Gatineau region. The field  $L_R$  data was used to obtain a power law correlation with the corresponding  $\gamma_r$  predicted by the developed model. The correlation shows that a brittle soil reaching the remoulded state sooner or at a smaller shear displacement undergoes more retrogression (Figure 3-9). This in line with existing theories about remoulding energy, which is often represented as the area under the stress-strain curve, that brittle soils can be easily remoulded requiring lesser energy and undergo more retrogression due to the increased kinetics [35]; [36]; [13].

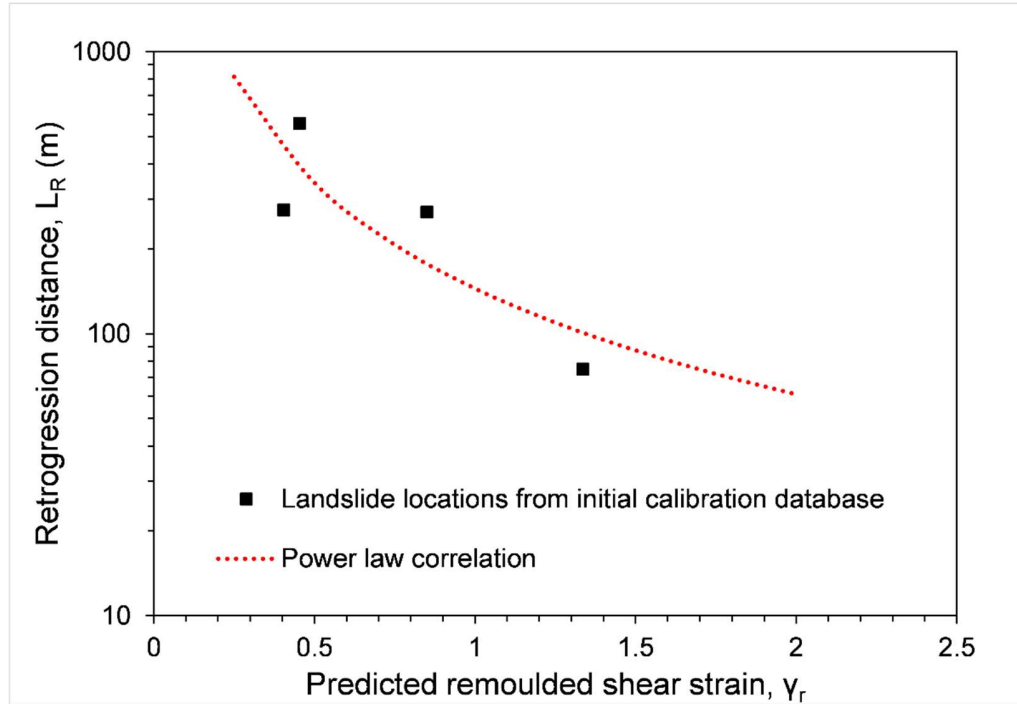


Figure 3-8 Correlation between  $L_R$  and predicted  $\gamma_r$

### 3.5.2 Validation of predicted $\gamma_r$ by other landslide data

The accuracy of the correlation shown in Figure 3-9 is further validated by considering three landslide locations outside of the initial data for model development which include – St Jude landslide 2010 [9], St Luc-de-Vincennes landslide 1986 [68] and Desbiens landslide 1983 [28]. The triaxial results for these sites were also obtained from the literature and the proposed model was applied to predict  $\gamma_r$ . Accordingly, the post - peak curves up to  $\gamma_r$  for the validation data and the corresponding field  $L_R$  (shown adjacent to the curves) are shown in Figure 3-11. The predicted  $\gamma_r$  of the validation data and the field  $L_R$  shows good agreement with the relation established in Figure 3-9 (Figure 3-10). Figure 3-11 shows that heavy retrogression is associated with pronounced strain softening and lesser  $\gamma_r$ ; e.g.: - Desbiens, which has the most pronounced softening, has the lowest  $\gamma_r$  and highest retrogression. The data regarding landslide type and retrogression distances used in this analysis are shown in Table 3-4. Although a good correlation between  $L_R$  and predicted  $\gamma_r$  has been established an equation for  $L_R$  is not yet proposed as it should be kept in mind that the prediction of post failure movements is severely affected by topography and geomorphology of a slide [59], explained in detail in the next section.

Furthermore, since this study makes use of experimental results on a laboratory scale, a possible scaling factor has to be considered before it can be mathematically utilized for post failure movements in the field. As such, these avenues need to be further explored with more data before strong conclusions can be made. There are existing research works that rely on empirical equations based on stability number [28] and slope geometry [103]; [32] for the prediction of  $L_R$ . Hazard mapping and statistical studies (eg – MTMDET method in Quebec and NIFS method in Norway) are also being used for its estimation [58]. Although most of these methodologies give a safe estimation of  $L_R$ , a worst-case scenario could not be predicted [26]; [58]. Hence, a site-specific constitutive model where the post - peak parameters (predicted  $\gamma_r$ ) can be easily incorporated in numerical simulations could reduce such uncertainties. Since the model proposed in this study is based on experimental results, it could be a close representation of field conditions.

Table 3-4 Landslide data used in the application of the proposed model

Name	Type	$L_R$ (m)	H (m)	$L_R/H$	Source	Data used
Saint Jean Vianney 1971	Flowslide	557.8	38	15	[28]	Landslide locations from data used for model calibration
Rigaud 1978	Spread	75	7.5	10	[103]	
St Louis (Yamasaka) 1945	Flowslide	275	18	15	[28]	
Ottawa-Gatineau 1963	Flowslide	270	-	-	[28]	
St Jude 2010	Spread	80	22	4	[9]	Landslide locations used for validation
St Luc du Vincennes 1986	Flowslide + Spread	150	18	8	[68]	
Desbiens 1983	Flowslide	304.8	4	22	[28]	

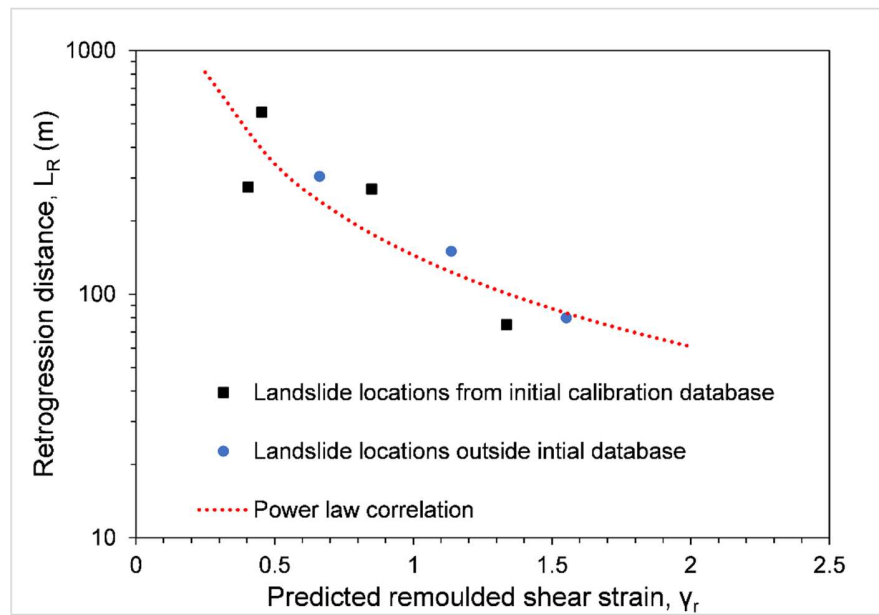


Figure 3-9 Predicted  $\gamma_r$  of validation data fitted with the established correlation between  $L_R$  and  $\gamma_r$

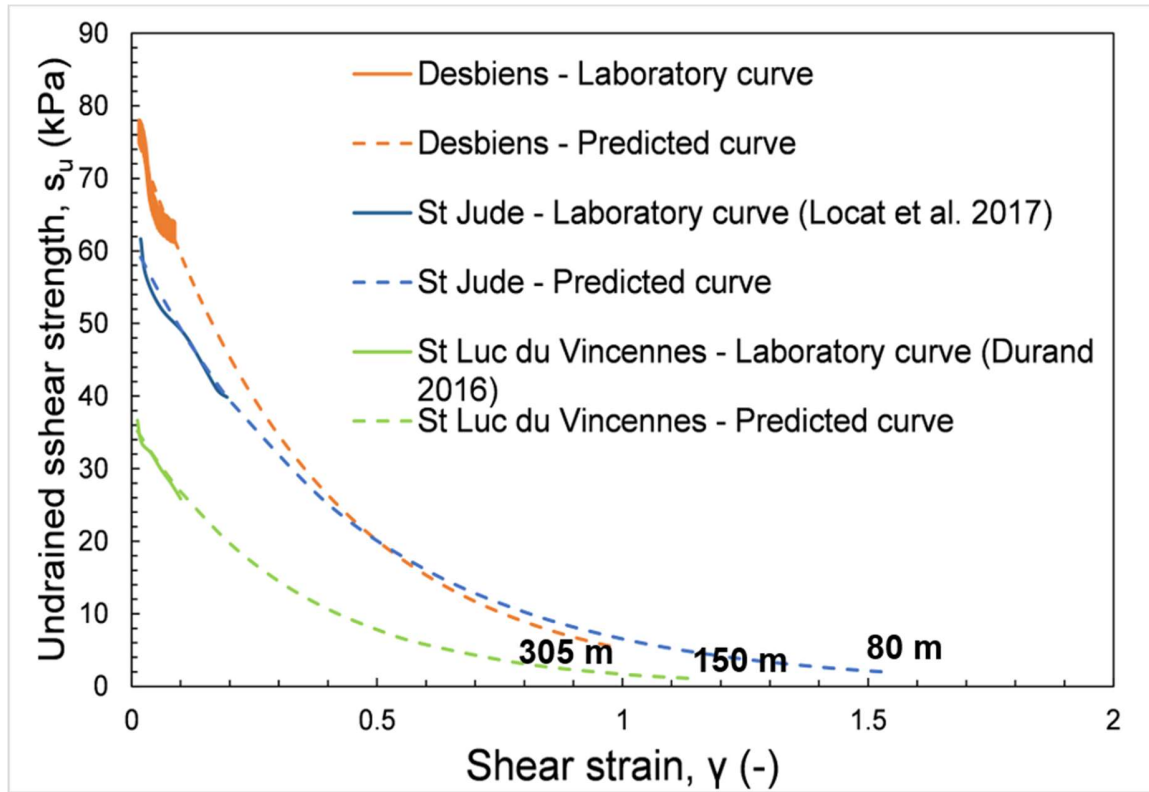


Figure 3-10 Predicted post - peak strength degradation according to the proposed model for landslide sites outside the initial dataset (Field retrogression distances are shown adjacent to each curve)

### 3.5.3 Effect of topography on $L_R$

According to [59], a higher potential energy due to larger slope height, restriction of movement due to the presence of trees and increased mobility due to water bodies are some factors that control post failure movements. Certain topographical features like a shallow bedrock, changes in soil stratigraphy and the presence of an old landslide scar or a ravine are some other features of influence [66]. Hence a small discussion on the geological conditions of the landslide sites used in this study is warranted for better understanding. A more detailed outline of geological conditions and failure involved in each of the landslide cases used in this study is provided in Table 3-5. The more retrogressive nature of flowslides is evident from the higher  $L_R/H$  ratio in Table 4. The kinetics of retrogression depends on the total potential energy of a slope i.e. slope height. Although a higher slope is not always indicative of heavy retrogression, it can provide conditions favourable for an unsupported backscarp leading to multiple retrogressive failures [11]. However, this analysis could be restricted

to flowslides as the underlying conditions for a spread failure are still not fully understood. In several cases, the topography of the bed rock representing a valley and the presence of sand pockets seem to have led to conditions favourable for leaching and strength loss such as in St Louis, Desbiens, and St Jude landslides (Table 3-5). The Saint Jean Vianney landslide was also enabled by hydrostatic pressures in the Petit Bras Valley where the debris from the initial slide was accumulated [7]. However, in the case of St Jude landslide, the accumulation of debris in the Salvali river seems to have not aided in further retrogression [9]. This was probably because the failure was a spread type slide with intact vegetation on the grabens offering resistance from further flow. Thus, these external factors should be considered in the numerical or the analytical models for assessing retrogression.

Table 3-5 Outline of geological conditions at each landslide location

Landslide location	Stratigraphy	Topographical and geological conditions	Failure plane and type of failure	Groundwater conditions	Source
Saint Jean Vianney 1971	21-30 m of marine sensitive clay with sand pockets and a deep layer of undisturbed clay that overlies the bedrock at 60 m depth.	Bounded by Petite Bras valley on the Northeast side and the scar of an ancient landslide on the Southwest side.  Surrounded by grazing lands, woods and swamps.  Initial slide slowed due to accumulation of trees and other vegetation in the	Flowslide where failure plane occurred within the scar of an ancient landslide at 22.5 m from the ground surface.	Melting of snow and heavy rainfall on days prior to the event led to partial flooding of the lower terrain of the SJV	[7]



		debris that blocked the Petite Bras valley leading to hydrostatic pressure buildup which aided in destruction of dam and further retrogression.			
Rigaud 1978	40 m of dark grey colour silty clay with lenses of fine sand followed by till. Clay layer has three zones – top 9 m of weathered crust, 9 – 23m of an intermediate zone of high sensitivity (35-80) and a third lower sensitivity layer from 23-40 m.	Limited retrogression due to the obstruction provided by a narrow, wooded ravine.	Retrogressive failure by spreading mechanism triggered by pile driving. Almost horizontal and abnormally deep failure surface at 17 – 19 m from the ground.	Piezometer readings indicated a strong downward flow possibly due to a permeable layer at deep depths and the water level of the Rigaud river. GWT at a depth of 2 m from the top of the slope	[103], [90], [104]

				behind the landslide.	
St Louis (Yamasaka) 1945	Homogeneous clay deposit of grey colour with thin dark grey bands spaced at 2.5 cm in the first 15.2 m depth. Highly stratified silty clay in the next 6.1 m and dense silt turning sand in the next 21.3 m until bedrock.	Presence of a valley in the bedrock.  Bedrock rises to the surface 11-16 km Southwest of Saint Louis and on the East, clay deposit rises before it dips into River Richelieu 16.1 km away.	Flowslide followed by the debris having a typical bottleneck shape	Piezocone installations show downward water gradient in the upper parts of the slope and an upper gradient in the bottom of the slope.	[105], [87]
Ottawa-Gatineau 1963	Homogeneous blue-grey marine clay with black mottling without any banding	Several visible landslide scars from past landslides could be observed.	Retrogressive flowslide	Piezometers revealed only slight downward flow.  Failure surface was at the elevation of Ottawa river.	[92]

St Jude 2010	Intact soil above bedrock categorised into five zones – unit A of top 3.8 m dense grey-brown sandy crust, unit B of 22.2 m intact grey sensitive clay, unit C of 5 m thick silty clay of lower sensitivity, unit D of 6 m very stiff grey-brown clayey silt and finally the bedrock	Original slope had an inclination of 12-20° occurring in a preglacial valley below the Salvali river.  Southern part of the landslide involved debris of a previous old landslide that occurred before 1931.  Evidences of active river erosion near the toe of the slope.  Debris completely blocked the Salvali river and moved over to the opposite bank, however the river did not aid in any further retrogression.	Spread failure with distinct horsts and grabens formation and vegetation intact on the grabens.  The failure surface was horizontal for about 115 m at a depth of 2.5 m below the Salvali river bed. It later rises to an elevation of 14 m before reaching the backscarp of the landslide.	Piezocone installations show a downward flow near the crest of the slope and upward flow near the toe of the slope with high artesian pressure conditions.	[9]
St Luc du Vincennes 1986	Sandy crust of 4 m thick followed by gray silty clay	Original slope had an inclination varying from 20° for the first	Combination of spread failure and flowslide.	Only a period of low precipitation (25 mm) in the	[68], [10]

	from 5 - 23 m depth	11 m followed by 6° for the next 8.5 m.  Small rotational slides on days prior to the event was observed.	Horizontal failure surface at a depth of 20.2 – 20.4 m depth.	days prior to the event.  Piezocone readings showed level of water table at 1 m below the ground surface.	
Desbiens 1983	2 m thick sandy crust and brownish clay at 9.1 – 12 m depth which turns grey at greater depth. Highly stratified with silt and sand.	The topography consists of a plateau which dips into the lake.  Presence of a valley in the bedrock.  Region scarred with several backscarps of previous landslides.	Retrogressive flowslide where the failure surface was at the level of the Lac-Saint-Jean.  Typical bottleneck shape of retrogressive flowslide was not observed.	Piezocone installations show downward water gradient in the upper parts of the slope and an upper gradient in the bottom of the slope.	[105], [106], [58]

### 3.6 DISCUSSIONS

The proposed strain softening equation strongly depends on the peak undrained shear strength and sensitivity. The mobilized undrained shear strength of soft clays has been proved to have poor correlations with

certain physical parameters like plasticity index and significant dependence on the consolidation stresses by [107] and [108] using regression models for Scandinavian clays and Eastern Canadian clays respectively. Under this context, the influence of physical parameters like Atterberg limits on the strain softening behavior could be lesser in comparison to the stress history of the soil and consolidation stresses experienced in the field. In the present study,  $\sigma'_{3c}$  in the triaxial tests used for model development were all less than the respective  $\sigma'_p$  which gave OCR values ranging from 1.4 to as high as 23.5 (in the case of Saint Jean Vianney). The average OCR of the test samples used in this study was 3.5. Hence, the model is valid for all tests that exhibit strain softening behaviour in the overconsolidated range of stresses for  $OCR = 1.4$  to  $23.5$ . The tests conditions should simulate the field setting such as effective vertical stress at the depth of possible slip surface, and the choice of confining stresses when analysing strain softening is of utmost importance [20].

The post - peak behavior in the strain softening model proposed in this study is strongly dependant on its model parameters 'a' and 'b'. These model parameters vary with the testing conditions, the consolidation stress history and brittleness and hence, is unique for a particular testing condition but not constant for a site. A drawback with respect to the model prediction is that it fails to capture the exact peak of the curves and predicts it 6% lower on average, in comparison to the laboratory data. This is due to the assumption that model parameter 'a' is equal to  $s_{up}$ , made in Equation (3-6). Since the general trend of softening is followed and the focus here is primarily on the prediction of  $\gamma_r$ , this limitation is insignificant for the purpose of the present study.

Progressive failure analysis requires the need for comprehensive information on the post-peak strain softening parameters along with peak undrained shear strength [17]. The aim of numerical analysis of progressive failure of spreads and flowslides is ultimately to have a better understanding of the retrogression that is likely to happen so that suitable precautions maybe undertaken. This also entails having access to accurate information regarding the post-peak strain softening behavior which is usually obtained through constitutive models. The scarcity of data regarding large displacement strains in general has forced the existing models to use assumptions with several uncertainties regarding suitability to laboratory/ field data. Furthermore, these assumptions come with an immense amount of experience regarding sensitive clay landslides and their behavior at large strains. New and unexplored landslide locations and slope failures would be difficult to assess with

existing models, in contrast to well studied landslides like the Saint Monique landslide [66]; [22]; [23]. Under these circumstances, the model parameters in the present study can be easily obtained from triaxial data.

The proposed softening model is largely based on mathematical equations and the parameter of primary concern is the post - peak parameter at the residual state, which can be easily obtained through laboratory shear tests and proves to be simple and much less complex. [109] explains that the post-peak strength is different from the fully remoulded state in that it still retains some of its stress history and is found to have a positive correlation with the preconsolidation pressure. Since the proposed model accounts for this post-peak strength in its formulation, the inherent stress history of the soil is also considered in developing the post-peak behavior. The  $\gamma_r$  obtained through the proposed model correlates well with retrogression data of some well-known landslides. However, as explained in section 3.4.3, it should be also kept in mind that the extent of retrogression is severely affected by geological factors such as changes in terrain or stratigraphy, obstruction in the path of retrogression and the surrounding topography of the slope [59]. In Figure 3-11, it is interesting to note that even though St Jude undergoes an overall heavier strength degradation in terms of the shear strength reduction from a peak of 60 kPa to remoulded strength of 1.9 kPa, it undergoes lesser retrogression of 80 m as opposed to St Luc du Vincennes with a retrogression distance of 150 m and lesser strength degradation from 30 to 1.1 kPa. Thus, the ease with which this degradation occurs determines the amount of retrogression rather than the actual brittleness of the soil. A brittleness modulus which denotes the rate of strength degradation could provide more insights into the analysis of strain softening and post failure movements and can be explored further in future. This could be determined by dividing the amount of strength reduction from the peak to the residual by the corresponding change of shear strain. On revisiting the Saint Monique landslide, it can be noted that the modeling of landslides using different approaches [18] ; [22] resulted in varying outcomes. The linear constitutive model used by [18] which estimated a large deformation strain of 55% does not capture the actual stress-strain behavior and the constitutive model used by [22] assumes a large deformation strain of 120% according to idealized simple shear tests. These technicalities regarding confining stresses used, rate of deformation or effective stress analysis governs the brittle behavior of the clay which could range from extremely brittle to ductile (non-brittle). This would also control  $\gamma_r$  and consequently the retrogression data. As such, the proposed strain softening equation serves as a tool for preliminary analysis of retrogressive landslides

and can be easily incorporated into numerical modelling of sensitive clay landslides as each parameter can be obtained from conventional laboratory tests and is much simpler and more direct.

Finally, it should be mentioned that the proposed model has been developed based on triaxial test data from Eastern Canadian sensitive clays and has been applied to analyse landslides of the Eastern Canadian region. Thus, the proposed model could only be valid for Eastern Canadian soils. More data and further calibration with respect to sensitive clays of other regions would help to improve the model for a wider application.

### 3.7 CONCLUSIONS

This paper presents a methodology to develop a non-linear strain softening model for sensitive clays of Eastern Canada based on experimental results, and its application to the assessment of post-failure retrogressive movements. The following conclusions are drawn based on the findings of this study:

- The post - peak strain softening curve follows an exponential function as significant reduction in strength with strain is observed immediately after the peak with it being relatively minute as it approaches the remoulded state.
- The proposed model makes use of the post-peak residual state parameters ( $s_{ures}$  and  $\gamma_{res}$ ) from triaxial tests for the development of the strain-softening curve.
- Post-failure movements like the retrogression distance which is a key in analysing sensitive clay landslides maybe determined by making use of the proposed constitutive model in numerical analysis.
- The peak undrained shear strength, sensitivity of the clay, stress history of the soil and the ease with which strength degradation takes place are the primary factors that affect strain softening.

#### Funding

This research was partially funded by the Natural Sciences and Engineering Research Council of Canada (NSERC) and Hydro-Quebec under project funding no. RDCPJ 521771 – 17.

## CHAPTER 4

### Article 3: Geotechnical characterization of Laflamme clays from the lac-Saint-Jean basin, Quebec

Sarah Jacob<sup>a,\*</sup>, Ali Saeidi<sup>a</sup>, Abouzar Sadrekarimi<sup>b</sup>, Rama Vara Prasad Chavali<sup>a</sup>

**\*Corresponding author:** Email address- sjacob2@etu.uqac.ca

<sup>a</sup>Department of Applied Science, Université du Québec à Chicoutimi, Quebec, Canada

<sup>b</sup>Department of Civil and Environmental Engineering, Western University, Ontario, Canada

Accepted by Engineering Geology

#### Credit authorship contribution statement

**Sarah Jacob:** Conceptualization, Data curation, Formal analysis, Resources, Experimentation, Writing – original draft, Writing – review and editing. **Ali Saeidi:** Supervision, Methodology, Resources, Writing – review and editing. **Abouzar Sadrekarimi:** Supervision, Writing – review and editing. **Rama Vara Prasad Chavali:** Writing – review and editing.

#### Declaration of competing interests

The authors declare the following financial interests/personal relationships which may be considered as potential competing interests: Ali Saeidi reports financial support was provided by Natural Sciences and Engineering Research Council of Canada (Grant ID: NSERC- 950- 232724). Ali Saeidi reports financial support was provided by Hydro Quebec (Grant ID: RDCPJ 521771–17). If there are other authors, they declare that they have no known competing financial interests or personal relationships that could have appeared to influence the work reported in this paper.



#### 4.1 ABSTRACT

The unique characteristic of sensitive clays is often attributed to their depositional and post depositional environment and sedimentation mechanism. This is further affected by geological and geoenvironmental factors that are mostly site-specific and time dependant. Since most sensitive clays of Eastern Canada are in the Champlain basin, existing studies on landslide hazard assessment often extend their properties to all Eastern Canadian sensitive clays. However, this extension could lead to erroneous judgements as geotechnical characteristics of clays from different sedimentary basins and geological settings could be different. Sensitive clays of the Laflamme basin in Eastern Canada are the product of a recent marine invasion and as such exhibit properties different than other Eastern Canadian sensitive clays. In this paper, a detailed geotechnical characterization has been carried out for two Laflamme clay sites - Desbiens and Albanel - surrounding the Lac-Saint-Jean basin, providing detailed insights on the unique mechanical behaviour of clays from this region. In addition to basic physical properties, experimental investigations including field tests measuring undrained shear strength, isotropic and  $K_0$ -consolidated triaxial compression tests, X-ray diffraction analysis and scanning electron microscopy have been carried out. The results show that, as opposed to typical Champlain clays, the Laflamme clays are highly leached and preconsolidated due to heavy preloading.

**Key words:** sensitive clays, undrained shear strength, mineralogy, stress states, overconsolidation

#### 4.2 INTRODUCTION

Saguenay-Lac-Saint-Jean (SLSJ) is a region located towards the south of Quebec, underlain by sensitive clay deposits, which is known for some disastrous landslides notably the Saint Jean Vianney landslides in 1663 and 1971 [34]. It also suffered occasional small slope failures in regions surrounding the Saguenay Fjord and the Lac-Saint-Jean (LSJ) including La Baie, Saint Monique, and Desbiens. In Eastern Canada, sensitive clay deposits occur primarily at three sedimentary basins – Champlain, Laflamme and Goldthwait - of which SLSJ is located at the Laflamme sea basin. The Laflamme sea invasion was the shorter and the most recent of the

three basins and hence the clays deposited here exhibit properties different than those in the other regions and seem to be somewhat distinct from what is typically considered as Eastern Canadian clays [20]; [34].

Landslides in sensitive clays are often assessed based on criteria that take into consideration physical and mechanical properties of a clay such as its liquidity index ( $I_L$ ) and remoulded undrained shear strength,  $s_{ur}$  [29]; [30]; [31], liquid limit, remoulding index, and remoulding energy [11]. While these have been determined for Champlain clays, the liquid limit of clays from the Laflamme Sea basin have been shown to be lower than that of the Champlain clays [20], and the  $I_L$ - $s_{ur}$  relationship established by [30] and [31] for Eastern Canadian sensitive clays seem to underpredict the high  $s_{ur}$  of Laflamme clays [34]. The SLSJ region is also known for significantly high preconsolidation pressures ( $\sigma'_p$ ) which causes the high brittleness of these clays as opposed to Champlain clays which are usually classified as normally-consolidated to lightly-overconsolidated [110]. These factors show that existing theories and criteria for retrogressive landslide assessment should be re-examined for heavily overconsolidated Laflamme clays. In the past, geotechnical characterization studies on Laflamme clays focused on Saint Jean Vianney and the Saguenay Fjord regions [7]; [89]; [34]. Whereas, the LSJ area, despite its history of past landslide activities, has received comparatively less research attention. This paper focuses on bringing forth certain geotechnical aspects pertaining to this region.

Two sites across the LSJ area – Desbiens and Albanel - are chosen to represent soil characteristics in this region. This paper further presents the geological environment of these sites followed by the sampling details, index properties, field and laboratory tests on undrained shear strengths. Mineralogical composition and microstructural investigations have been also carried out through X-ray diffraction (XRD) analyses and scanning electron microscopic (SEM) images, respectively. The mechanical behaviour of Laflamme clay is studied through a series of laboratory experiments including triaxial compression tests on isotropically and  $K_0$ -consolidated specimens. The primary aim of this study is to provide relevant characterization data representing the Laflamme clays which will provide a useful reference for future studies to analyse retrogressive landslides in this region.

#### **4.3 GEOLOGICAL ORIGIN AND SAMPLING**

The glacial retreat and marine invasion are most recent and shorter in the Laflamme Sea basin dating back to about 10,000 - 8000 years BP [20]; [111]; [21]; [34]. During the rapid glacio-isostatic rebound that followed the glacier's retreat, the first series of rocky ridges at the level of Lake Kénogami (known as the Kénogami threshold) allowed the Laflamme Sea to be divided into two sub-basins: the Haut-Saguenay lowlands sub-basin (between Cap Éternité and Kénogami thresholds), and the LSJ sub-basin west of the Kénogami threshold [112]. One of the distinguishing features of these sediments between the LSJ sub-basins and the Haut-Saguenay lowlands is their very low salinity compared to the Champlain clays and other Laflamme clay sediments of the Saguenay Fjord [21].

The present state of the Laflamme clays is a result of successive abrasion and deposition of the rocks in the Canadian Shield by the glacial retreat, leading to an abundance of rock flour in the sediments over clay minerals. The sediments of this region have been identified to be primarily of silty nature with occasional sand deposits. The LSJ basin has a significant source of fresh water from the melting of continental inlands and icebergs due to glacial calving and is primarily connected to the sea through the Saguenay River and the Saguenay Fjord. Thus, although the existing sediments in the LSJ region are of marine origin, there is a significant influx of freshwater, creating a lacustrine environment unlike the marine environment in the Saguenay Fjord region.

The stress history of a soil can have a significant effect on its shear strength and mechanical behaviour. [113] proposed that overconsolidation in Champlain clays is only an apparent preconsolidation caused by cementation agents such as hematite and magnetite. However, Laflamme clays owe their preconsolidation to other factors. For example, [21] show variations in water content, shear strength, and preconsolidation pressure with depth which indicate preloading and erosion of the overlying soils. This suggests that cementation in Laflamme clays would have been relatively recent, allowing their erosion and preconsolidation. Additionally, [34] showed that sediments of the Saguenay Fjord region were prone to bioturbation activity through which these sediments were disturbed or reworked by living organisms [114]. Bioturbated sediments were found to have increased strength and preconsolidation pressure, as well as decreased water content [115]; [116]. These evidences show the importance of the depositional environment which can produce unique physio-mechanical properties in clays from different regions across Eastern Canada.

The soil samples used in this study were collected from Desbiens and Albanel sites, two villages to the south and north of LSJ, respectively as shown in Figure 4-2. Desbiens is a site known for unstable sensitive clay slopes, some of which are still active [105]; [106]. The topography of this region represents a valley along with sand deposits at varying depths [105]. The valley structure is considered to have aided in supplying fresh water throughout the sediments leading to low salinities. Albanel is a site of a very old flowslide (about 1000 years old). The samples from both sites were collected using a high-quality tube sampler by the Ministère des Transports et de la Mobilité Durable du Québec (MTQ). The sample locations are marked as D\_SL and A\_SL and are shown in Figure 4-2. Desbiens samples were obtained from a single borehole of 3.5 - 33.3 m deep. Sand layers interbedded with silt were observed at depths of 11.5 to 17.5 m. At the Albanel site, three boreholes were drilled side by side and samples were obtained from depths of 6.0 – 7.2 m, adjacent to the scar of the old flowslide. Cylindrical samples were obtained with a diameter of 70 mm and heights of 100 to 130 mm. These samples were coated with wax and stored in a humidity chamber throughout this study. All samples were fairly uniform and greyish to dark grey in colour, typical of sensitive clays of this region, and with small traces of sand. Visual observations revealed that the Desbiens samples were looser and softer than those from Albanel.

#### **4.4 SAMPLE PREPARATION AND TESTING METHODOLOGY**

##### **4.4.1 Physical properties and microstructural investigations**

Properties such as grain size distribution [117], water content [118], Atterberg limits [119] and specific gravity [120] of the clay samples from both sites were measured in accordance with the American Society for Testing and Materials (ASTM) standards. In addition to these index tests, the salinity, chemical composition, and microstructure of the clay samples were also determined. Salinity of soil samples was determined by preparing a mixture of air-dried soil and deionised water at a ratio of 1:5 (20 g of air-dried soil and 100 mL of deionised water). The soil suspension was then mixed thoroughly using a magnetic stirrer for about a minute at an interval of 30 minutes for 2 hours to dissolve all soluble salts. Another 15 minutes was allowed for the soil to settle. Soil salinity was then measured in g/L by dipping a multiparameter probe (Hanna HI 9828) into the supernatant fluid to take measurements at 25°C. The multiparameter probe provided a multitude of measurements including salinity and electrical conductivity among others. A similar technique for measuring the pore fluid salinity of clay soils was adopted by [121] and [122].

The mineralogy of the samples was determined through X-ray diffraction (XRD) analyses of powdered samples of both clays. The microstructures of intact and remoulded samples of the clay were visualized using a Hitachi SU8230 Regulus Ultra High - Resolution Field Emission SEM at Western University, Ontario. Remoulded samples were prepared according to [39] at a water content of 1.5 times their liquid limit. A 3 kV accelerating voltage was used and secondary electron images were collected. The samples were sputter coated with approximately 4 nm of iridium. Microscopic images of oven dried intact and remoulded clay samples were captured up to a magnification of 50,000 with band lengths of 10, 2 and 1  $\mu\text{m}$ .

#### **4.4.2 Laboratory element tests**

##### **4.4.2.1 Isotropically consolidated undrained tests**

The monotonic shearing behaviour of the clay samples in undrained loading was determined by performing undrained (CUI) monotonic triaxial compression tests on isotropically-consolidated specimens. The CUI tests were performed using a computer-controlled triaxial testing apparatus manufactured by Wille Geotechnik (Germany). As illustrated in Figure 4-1, this apparatus includes a 10 kN uniaxial loading frame, a 4 L triaxial cell with maximum pressure capacity of 2,000 kPa, three pressure transducers, a linear variable differential transformer (LVDT), an automatic double volume pressure control (VPC) pump with two channels and a data acquisition and control system. The cell and back pressures along with the pore water volume change are measured and controlled using the double VPC pump with a capacity of 500 mL and equipped with electrical pressure transducers that could measure pressures of up to 2,000 kPa at a resolution of 0.1 kPa. A third pressure transducer placed at the bottom of the cell measures the specimens pore pressure. The axial deviator stress is applied by the loading frame and piston on the specimen. Axial deformations are subsequently measured using an LVDT with a resolution of 0.002 mm and a measuring range of  $\pm 25$  mm. The volumetric strains of the specimen were determined using the pore volume changes measured by a channel of the VPC pump. The data acquisition and control software allowed performing a wide variety of tests and stress paths including isotropic and anisotropic triaxial tests,  $K_0$  compression tests, as well as cyclic triaxial testing.

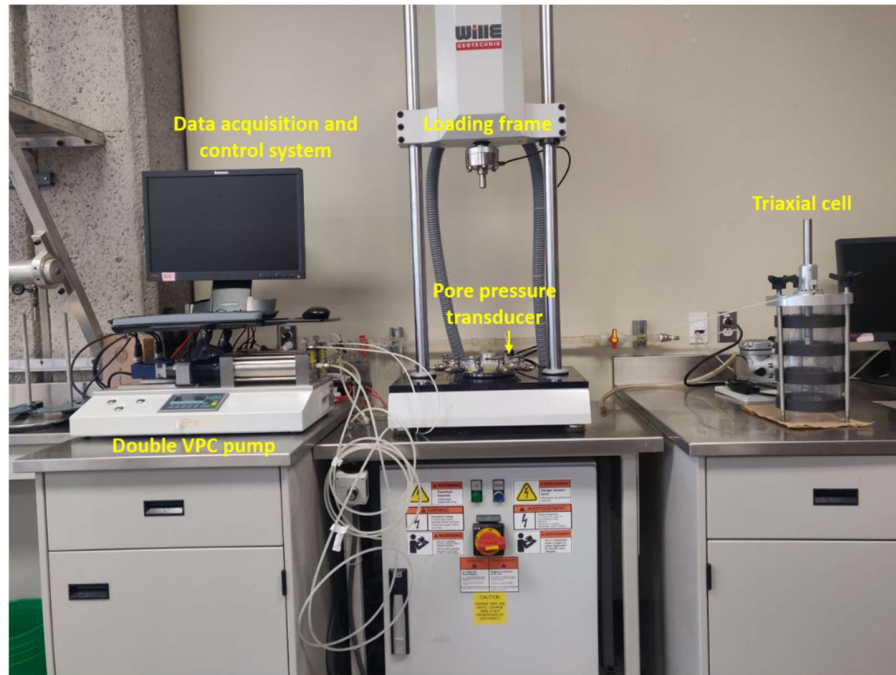


Figure 4-1 Triaxial equipment from Wille Geotechnick used for sample testing

The specimen preparation and testing procedure were carried out in accordance with the ASTM D4767 [123] standard. Cylindrical specimens of 50 mm in diameter and 100 mm high were trimmed from intact samples. Filter paper strips were placed around the specimen to improve radial drainage. The specimen was then assembled with filter papers, porous discs, latex membrane as well as a loading pad. All drainage lines were flushed until no air bubbles were observed. Specimen saturation was initially carried out by flushing the sample at a low effective confining pressure of 5 kPa for three hours. Following this, the back pressure saturation method was adopted, where the cell and the back pressures were simultaneously raised in increments until a Skempton's pore pressure ratio,  $B$ , of at least 0.96 was achieved. The low permeability of the specimen (on the order of  $10^{-10}$  m/s) required high back pressures in the range of 300-650 kPa for saturation. Sensitive clay slopes often occur in nature in the overconsolidated state owing to significant erosion [71]. As such, the samples were consolidated in the overconsolidated range of stresses. An investigation of borehole data from the database of MTQ around Desbiens and Albanel regions provided an initial estimate of the preconsolidation pressure ( $\sigma'_p$ ) to be around 280 kPa for Desbiens and 275 kPa for Albanel clays. Hence, the samples were consolidated to confining pressures lower than these values. After consolidation, samples were sheared at a

strain rate of 1%/h up to an axial strain ( $\epsilon_a$ ) of 20%. A total of 7 CUI triaxial tests were carried out – three on Desbiens and four on Albanel samples. The details of these tests are summarized in Table 4-1.

Table 4-1 Summary of the CUI triaxial tests performed in this study

Test name	$\sigma'_{3c}$ (kPa)	$\Delta\sigma_f$ (kPa)	$\epsilon_f$ (%)	$\Delta u_f$ (kPa)
D-CUI1	20	81.04	3.59	-2.2
D-CUI2	40	138.1	2.17	6.31
D-CUI3	100	168.36	1.08	19.82
A-CUI1	30	174.38	1.72	3.91
A-CUI2	46	193.52	1.69	4.78
A-CUI3	70	232.93	2.59	9.07
A-CUI4	100	238.09	2.51	14.6

where,  $\sigma'_{3c}$  = confining pressure,  $\Delta\sigma_f$  = deviatoric stress at failure,  $\epsilon_f$  = axial strain at failure,  $\Delta u_f$  = porewater pressure at failure

#### 4.4.2.2 $K_0$ compression tests

A series of triaxial compression tests (CUK0) were also conducted on anisotropically-consolidated specimens to evaluate the coefficient of earth pressure at rest ( $K_0$ ) and examine the effect of anisotropic consolidation on the shearing behavior of the clay samples. Desbiens samples from depths of 7 m and 9.5 m with overconsolidation ratios (OCR) of 7 and 11.7 respectively, and Albanel samples from a depth of 6.5 m with an OCR of 10.6 were used in these experiments. Specimens were trimmed from cylindrical tube samples and mounted in the triaxial cell. After assembling the cell, saturation was carried out by flushing and applying back pressure, as in the CUI tests. Once saturation was completed, the specimens were isotropically consolidated under a low confining stress of 15 – 30 kPa for about 16 hours. Following this, they were consolidated under a zero lateral strain condition. An initial deviatoric stress ( $\Delta\sigma_i$ ) was applied in the vertical direction on the specimen to cause small axial deformations during which the cell pressure was increased or

decreased to change volumetric strains in such a way that  $K_0$  condition was attained. This was achieved by keeping the axial ( $\varepsilon_a$ ) and volumetric ( $\varepsilon_{vol}$ ) strains of the specimen equal thereby inducing a zero-radial strain,  $\varepsilon_r = \varepsilon_a - \varepsilon_{vol}/2 = 0$ .  $\varepsilon_a$  was measured using the LVDT attached on the piston and  $\varepsilon_{vol}$  was measured using the VPC pump. A total of four CUK0 tests were carried out, the details of which are shown in Table 4-2.

Table 4-2 Summary of the CUK0 triaxial tests performed in this study

Test name	$\sigma'_3$ (kPa)	$\Delta\sigma_f$ (kPa)	$\sigma'_1$ (kPa)	$w_f$ (%)	$\Delta u_f$	$K_0$
D-CUK01	40	101.43	61	37.3	8.33	0.64
D-CUK02	24	111.22	48	51.5	2.21	0.53
A-CUK01	26	164.74	67	52.1	-1.3	0.39
A-CUK02	60	224.53	111	45.3	4.37	0.56

where,  $\sigma'_3$  = effective horizontal stress at the end of  $K_0$  consolidation,  $\sigma'_1$  = effective vertical stress at the end of  $K_0$  consolidation

#### 4.4.3 Undrained shear strength profiles

##### 4.4.3.1 Field tests

The undrained shear strength in the field at the sampling locations (D\_SL and A\_SL) was examined through cone penetration tests (CPT) carried out by MTQ. Information on field vane tests (FVT) were also obtained from 11 and 7 boreholes surrounding the sampling locations at Desbiens and Albanel sites, respectively from MTQ. The sampling location and surrounding boreholes are shown in Figure 4-2. For Desbiens, the examination of these borehole data indicated the presence of sand deposits in the top 1 to 3 m in most boreholes and sand-silt interbeds at certain depths in certain boreholes. In the case of Albanel, such sand deposits were observed upto 5 m from the ground. Undrained shear strength profiles based on the cone tip resistance ( $s_{uCPT}$ ) were obtained from the following equation commonly used in clayey soils,



$$s_u = \frac{q_t - \sigma'_v}{N_{kt}} \quad (4-1)$$

where,  $q_t$  = corrected cone tip resistance,  $\sigma'_v$  = effective vertical stress, and  $N_{kt}$  = cone factor.

$N_{kt}$  values for soft clays typically lie between 10 and 20 [124]. [125] showed that an  $N_{kt}$  value of 9.94 gave  $s_u$  which showed good agreement with FVT and triaxial results for Champlain clays. Here,  $N_{kt}$  values for Desbiens and Albanel were obtained through their correlation with  $s_u$  from the FVT results based on Equation 4-1.

#### 4.4.3.2 Laboratory tests

The undrained shear strength of the intact samples was also determined in the laboratory using fall cone test (FCT). These are denoted by  $s_{uFCT}$  in the following discussions. In the FCT tests, a 60 g cone with a 60° apex angle was pushed into an intact sample placed in the measuring cup. An average of five set of penetration values were noted for each sample and  $s_{uFCT}$  was measured based on depth of penetration. To measure the remoulded strengths, remoulded samples were prepared by hand kneading sample trimmings for about 15 minutes. The remoulded samples were then filled into the measuring cup and their strength was measured using FCT ( $s_{urFCT}$ ). The remoulded strength, denoted by  $s_{urLVT}$ , was also determined using a handheld laboratory vane (LVT) of 32 mm height and 16 mm in diameter.

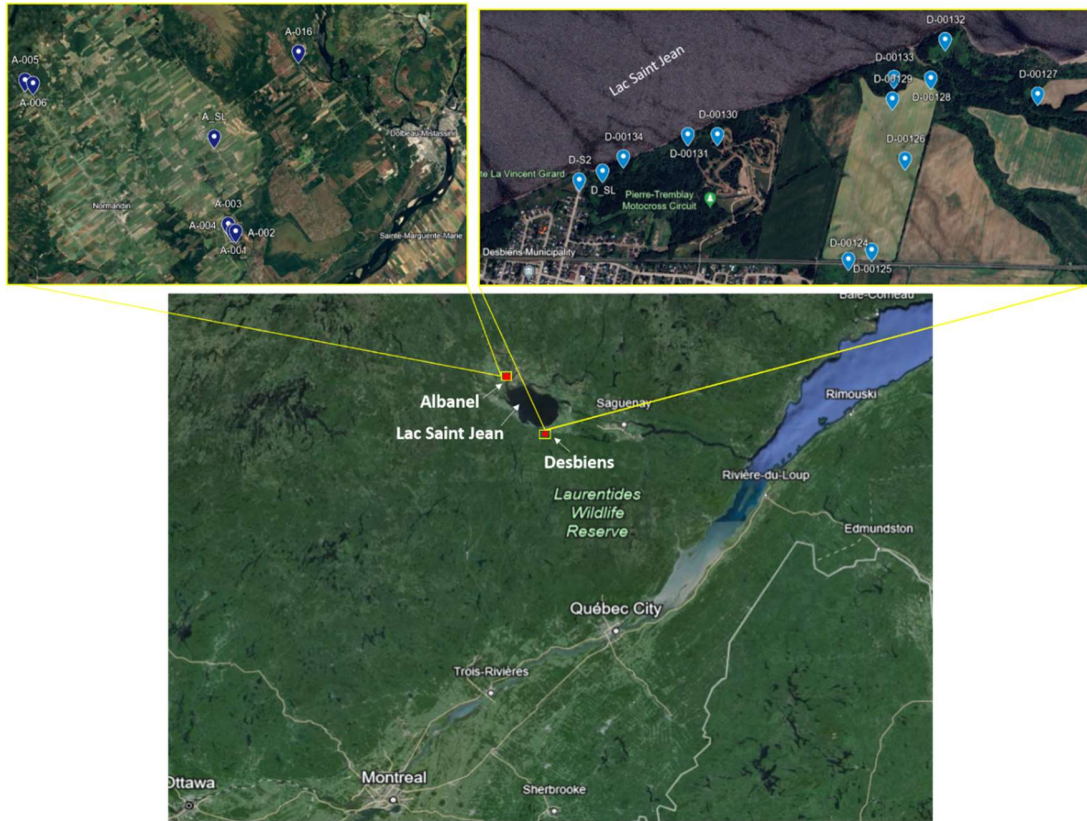


Figure 4-2 Desbiens and Albanel study area with sampling locations and borehole locations of FVT

## 4.5 EXPERIMENTAL RESULTS

### 4.5.1 Index properties

The index properties that were determined from both study areas are summarised in Table 4-3 and Figure 4-3 shows their gradation curves and Atterberg limits. As shown in in Figure 4-3a, Desbiens samples from depths of 9.5 m (D-9.5) and 13.4 m (D-13.4), and Albanel samples from all three boreholes were used to determine their grain size distributions by sedimentation and sieve analyses. Albanel samples contained a clay fraction (CF) of about 52-60%, while Desbiens samples from 9.5 m depth (i.e., D-9.5) showed a similar CF of about 52%. At the sand – silt interbed in Desbiens, labelled as D-13.4, the estimated clay fraction (CF) was about 36%. This lower percentage was due to the interbedded sand layers with fine silt and clay at this depth. This is consistent with the observations of [21] and the silty nature of clays in these regions. Other clays from the SLSJ region also showed CF of approximately 48-55% [27]; [89].

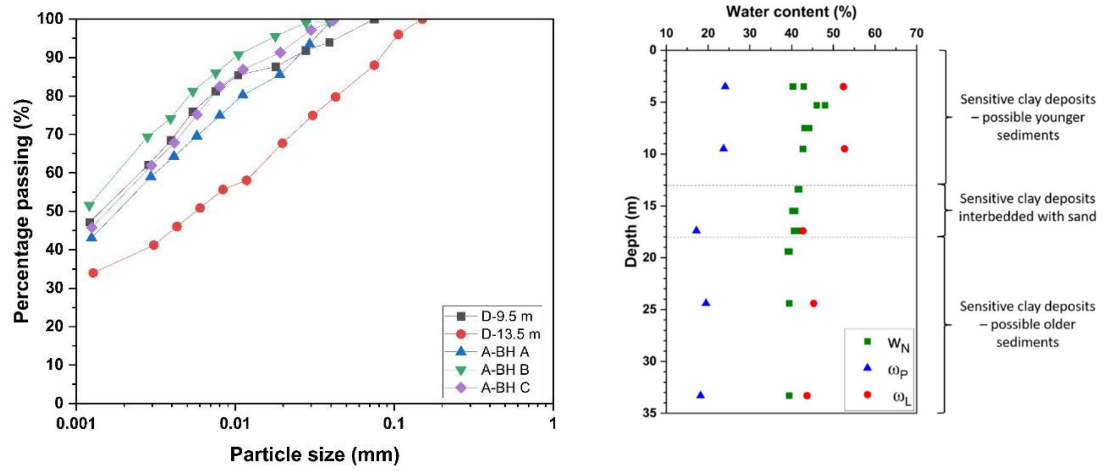
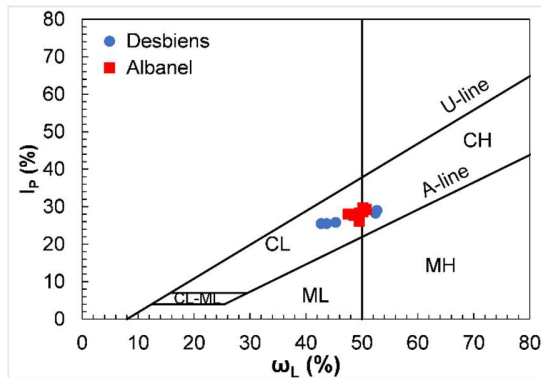


Figure 4-3 (a) Grain size distributions of samples from Desbiens and Albanel sites (b) Variations of Atterberg limits and natural water content with depth in Desbiens samples

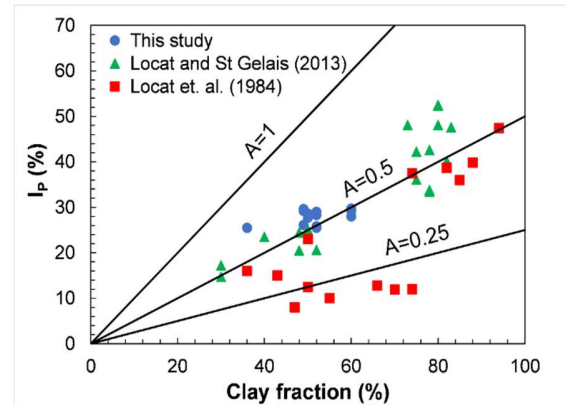
Figure 4-3b shows slight reductions of the natural water content ( $w_N$ ), liquid limit ( $\omega_L$ ), and plastic limit ( $\omega_P$ ) with depth at the Desbiens site. Atterberg limits were the lowest at the depths interbedded with sand layers (i.e., 13 – 17 m). Such variations were not observed at the Albanel samples because of their limited depth (from 6.0 to 7.2 m). According to Table 3, the Atterberg limits were generally lower than those of typical Champlain clays, likely due to the significant leaching and the silty nature of these clays. Figure 4a further indicates that clays of this region were at the border of low to high plastic clays. The activities of both clays lied in the range of 0.4 – 0.7, much like similar studies on Eastern Canadian clays carried out by [126] and [27] as compared in Figure 4-4b.

Table 4-3 Average index properties of Desbiens and Albanel clay samples

Property	Desbiens	Albanel
Specific gravity ( $G_s$ )	2.71	2.74
Clay fraction (%):		
At sand – silt interbed	36	-
In sensitive clay layer	52	52-60
$w_N$ (%)	39 – 48	41-47
$w_L$ (%)	43-53	48 – 51
$w_P$ (%)	17 – 24	19 – 21
Plasticity index, $I_P$ (%)	25 – 29	26 – 30
Liquidity index, $I_L$	0.6 – 1.0	0.7 – 0.9



(a)



(b)

Figure 4-4 (a) Plasticity chart and (b) activity of Desbiens and Albanel clays

#### 4.5.2 Chemical composition and microstructural investigations

#### 4.5.2.1 Salinity

Salinity was measured directly using a multi-parameter probe. These measurements were carried out for various depths in Desbiens clays and all three boreholes in Albanel clays. The depth-wise variation of salinity for Desbiens and Albanel clays are shown in Figure 4-5. On average, the salinities were extremely low (0.12 – 0.28 g/L) for Desbiens clays whereas it was almost non-existent in Albanel clays (average of 0.05 g/L). These indicate that the samples were highly leached. Although Champlain clays of low salinities in the range of 0.2 – 0.3 g/L exist, e. g. Olga [126] and Gatineau [27]; on an average, Champlain clays present higher salinities (in the range of 0.4-11.8 g/L) in comparison to the LSJ clays [27]. These low salinities further highlight the glaciolacustrine nature of these clays, contributing to their significant dilution and leaching.

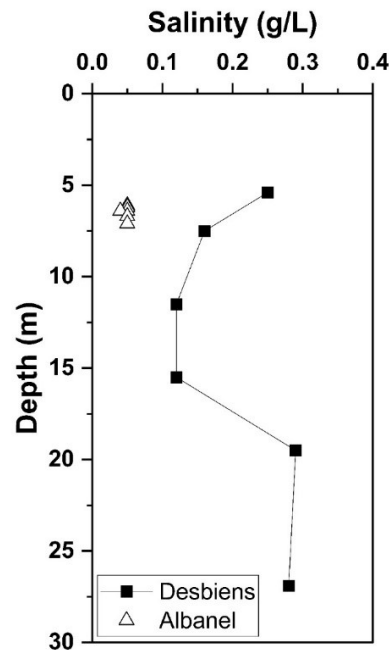
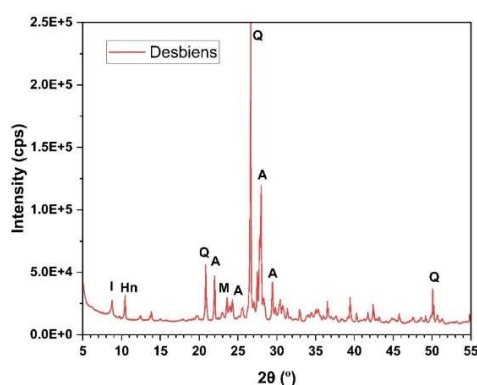


Figure 4-5 Variation of salinity with depth for Desbiens clays

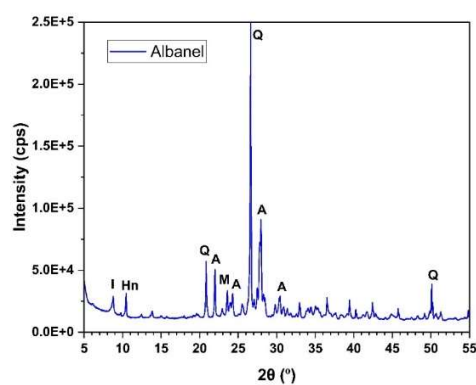
#### 4.5.2.2 X-ray Diffraction analysis

The XRD spectra of powdered whole samples and clay fractions of samples shown in Figure 4-6 were analyzed using Xpert Highscore Plus software as well as [127]. These show that the XRD spectra of both samples were extremely similar. The primary clay minerals were interpreted as illite and kaolinite

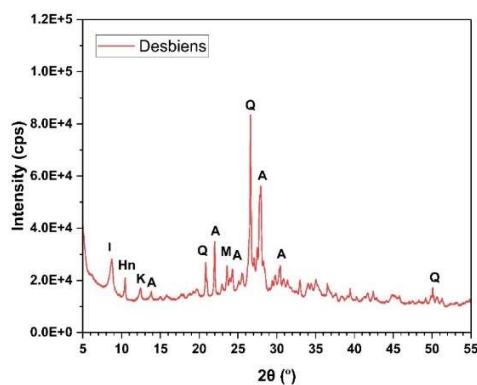
corresponding to peaks of  $8.5^\circ$  ( $\sim 10 \text{ \AA}$ ) and  $12.5^\circ$  ( $\sim 7.02 \text{ \AA}$ ). Although kaolinite peaks were not prominent in the spectra of the whole sample, these were observed in the XRD spectra of the clay fraction in Figures 4-6c and 4-6d. The samples also included quartz (Q), albite (A), microcline (M) and hornblende (Hn) minerals. Overall, the mineralogical composition of these clays is somewhat typical of Eastern Canadian sensitive clays where the primary constituent is rock flour originating from glacial grinding and erosion.



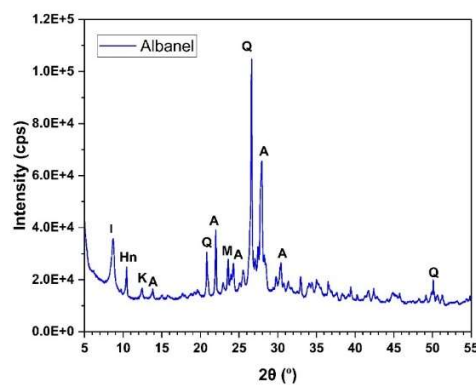
(a)



(b)



(c)

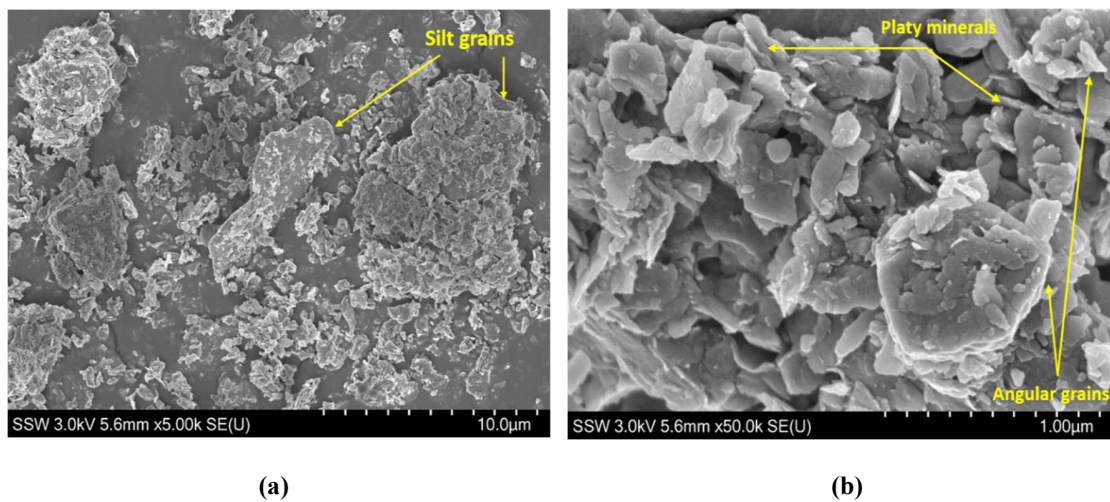


(d)

Figure 4-6 XRD spectra of (a) and (b) whole sample and; (c) and (d) clay fractions of sample in Desbiens and Albanel clays respectively

#### 4.5.2.3 Scanning Electron Microscopy

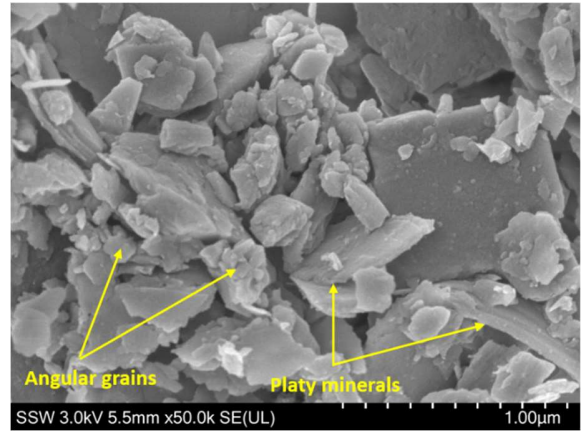
The microstructures of intact Desbiens and Albanel clays are shown in Figures 4-7 (a-d). A microstructural study conducted on Eastern Canadian clays by [128] highlighted a marked difference in the microstructure of Champlain clays of the St Lawrence lowlands and the clays from the Canadian Shield. Under this context, the microstructure of clays in this study resembles the latter with platy minerals and angular aggregates. Moreover, their fabric seems to be dispersed as opposed to the more flocculated structure of Champlain clays. Unlike the Laflamme clays, the typical microstructure of Champlain clays as well as Norwegian sensitive clays consists of silt sized particles embedded in clay aggregates with clay bridges that act as connectors between the silt aggregates [128]; [129]. As proposed by [128] it is possible that the fine minerals in these photographs were detrital in nature (i.e., fine rock flour) occurring due to the grinding of the Canadian Shield by glaciers. SEM images of remoulded specimens in Figures 4-7 (e-f) further show a destruction of the clay structure from its intact form. Figure 4-8 presents the elemental compositions of Desbiens and Albanel samples. These indicate high percentages of aluminium silicates and low amounts of sodium and calcium (2.1 – 3.5 % by weight) present in the clay samples, further confirming the significant leaching undergone by these clays. Similarly, [86] performed characterization studies on Champlain clays and found higher percentages (11 – 17% by weight) of sodium and calcium.



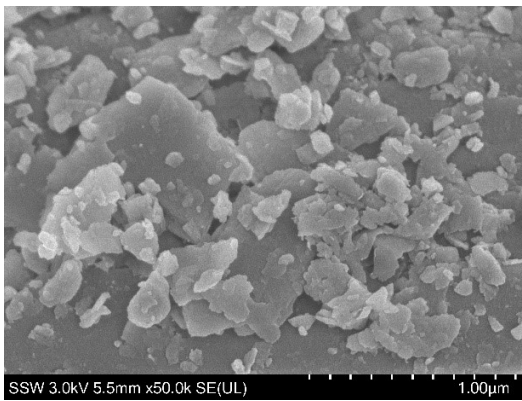




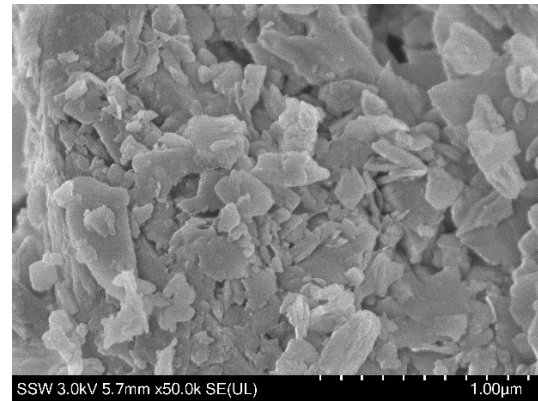
(c)



(d)



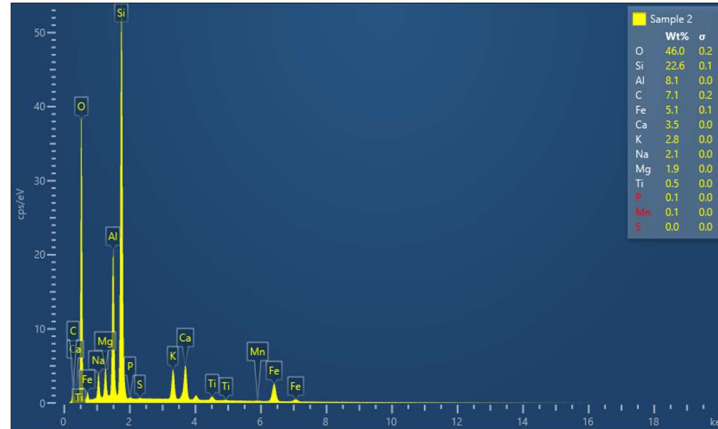
(e)



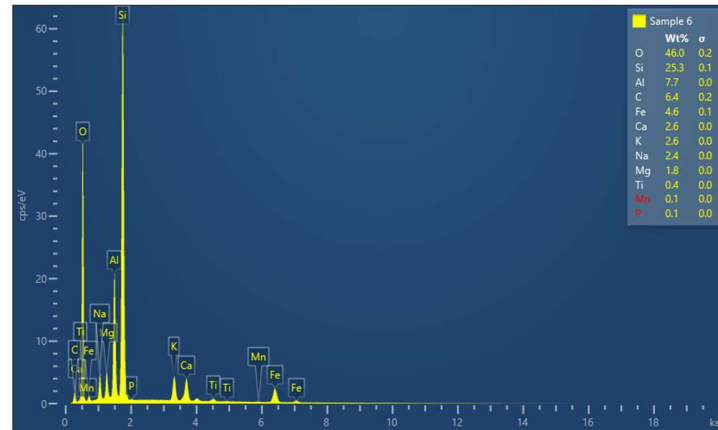
(f)

Figure 4-7 SEM images of (a) Desbiens clay with a band length of 10  $\mu\text{m}$ , (b) Desbiens clay with a band length of 1  $\mu\text{m}$ , (c) Albanel clay with a band length of 2  $\mu\text{m}$ , (d) Albanel clay with a band length of 1  $\mu\text{m}$ , (e) Remoulded Desbiens clay with a band length of 1  $\mu\text{m}$





(a)



(b)

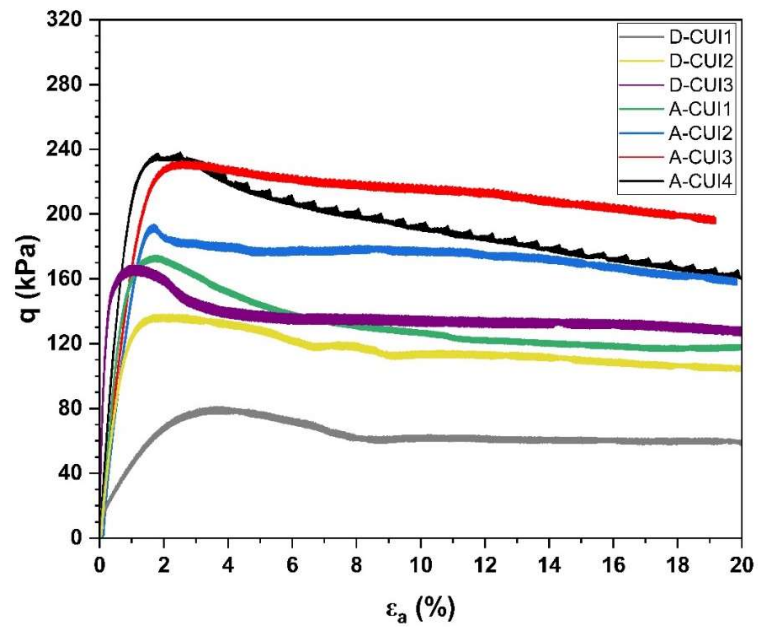
Figure 4-8 Energy Dispersive Spectrometry results of (a) Desbiens and (b) Albanel clays

#### 4.5.3 Laboratory element tests

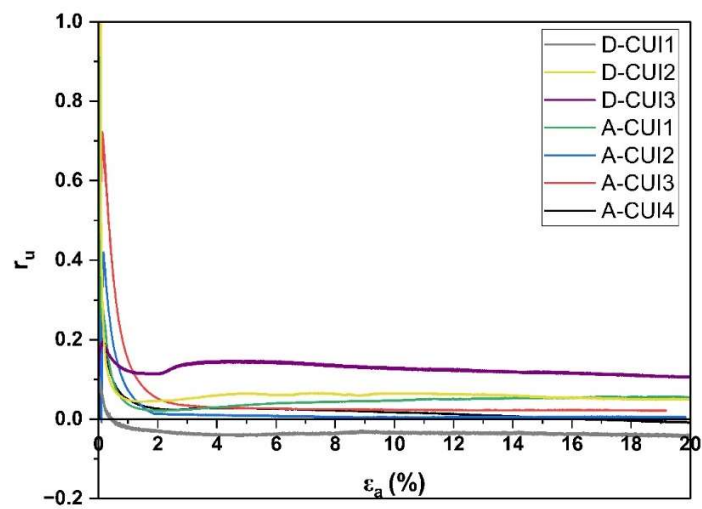
##### 4.5.3.1 Isotropically consolidated undrained tests

Undrained triaxial tests on isotropically-consolidated samples of Desbiens and Albanel clays were conducted in the overconsolidated range of stresses (i.e.,  $OCR = 2.8 - 14$ ). Typical stress-strain curves with pore pressure ( $\Delta u$ ) generation are shown in Figure 4-9(a-b). As  $\Delta u$  rose with increasing confining pressure after consolidation ( $\sigma'_{3c}$ ), it is characterized by an excess pore pressure ratio,  $r_u = \Delta u / \sigma'_{3c}$ . Failure took place at small  $\epsilon_a = 1.0 - 3.5$  %. Although both clay samples developed positive pore water pressures ( $r_u > 0$ ), these  $r_u$  were quite low in comparison to the high deviatoric stresses at failure. In fact, negative shear-induced pore water

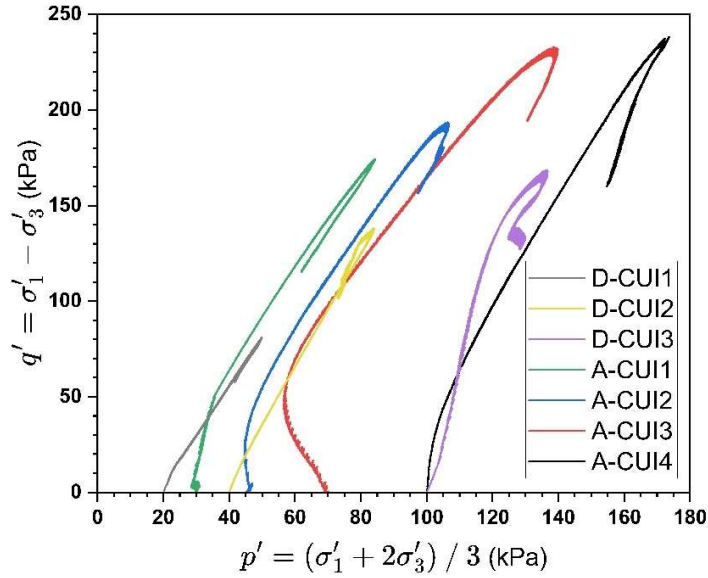
pressures ( $r_u < 0$ ) were generated in test No. D-CUI1 on Desbiens clay which was consolidated to a confining pressure of 20 kPa. According Figure 4-9b,  $r_u$  dropped to negligible values after an initial rise, possibly due to the significant overconsolidation of these clays.



(a)



(b)



(c)

Figure 4-9 (a) Deviatoric stresses and (b) excess pore water pressures, and (c) stress paths of CUI tests carried out in this study

The residual strength of the clay samples was measured from the CUI tests by shearing them up to a large  $\epsilon_a = 20\%$ . However, except in the cases of tests No. A-CUI3 and A-CUI4 on Albanel clays, visually no changes in deviatoric stress were observed beyond  $\epsilon_a$  of 10%. The residual state was thus considered at  $\epsilon_a = 20\%$  in all the samples. According to [20], overconsolidated clays of LSJ are susceptible to dilatant behaviour under low confining stresses. This was also observed by [87] while performing undrained triaxial tests on St Louis clay. The dilatant nature of the clays of this study is also evident from the stress paths of Figure 4-9c, besides their low  $r_u$  shown in Figure 4-9b.

#### 4.5.3.2 $K_0$ – consolidated triaxial tests

Figure 4-10 shows the effective principal stress paths during anisotropic consolidation of Desbiens and Albanel clay samples to attain a  $K_0$  condition. The lateral stress ratio,  $K_0 = \sigma'_3/\sigma'_1$ , was obtained through the

slope of the line connecting the final consolidation stresses to the origin. This resulted in  $K_0 = 0.53$  and  $0.64$  for Desbiens and  $0.39$  and  $0.56$  for Albanel clays.

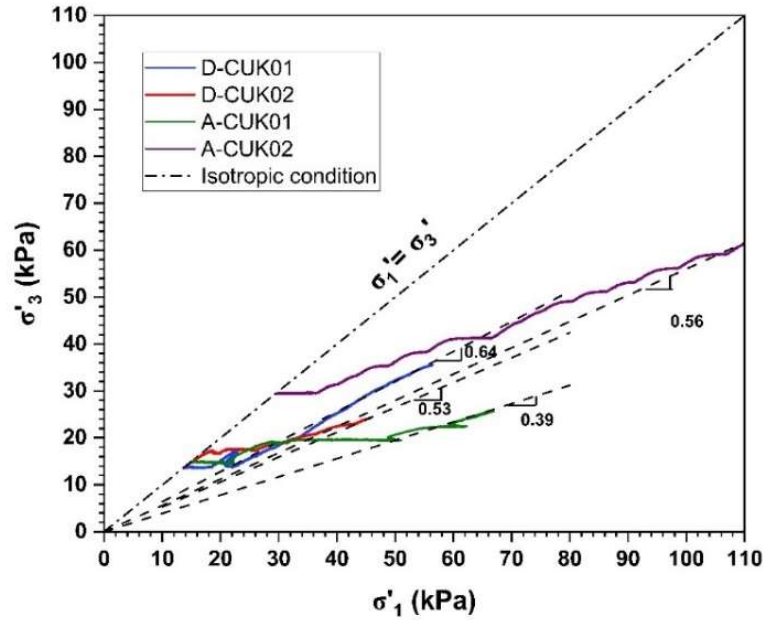
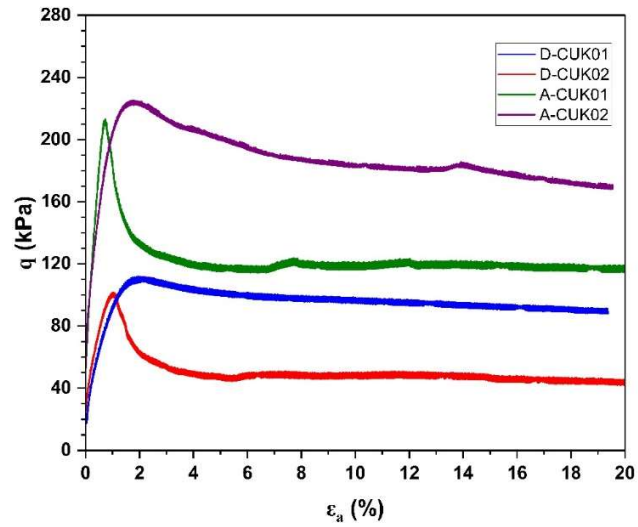


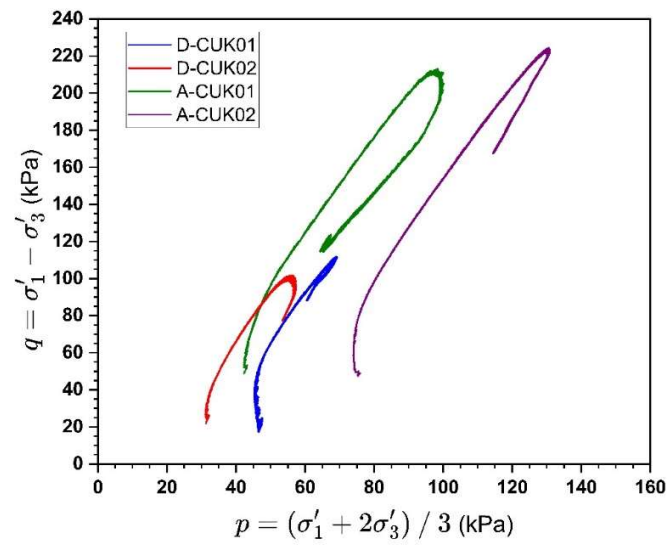
Figure 4-10 Variations of horizontal effective stress ( $\sigma'_3$ ) with vertical effective stress ( $\sigma'_1$ ) in CUK0 tests of this study

The stress-strain behaviour and the stress paths of the CUK0 tests are further shown in Figure 4-11. According to these figures, the samples exhibited strong strain-hardening behaviour which was followed by strain-softening and undrained strength reduction possibly due to the destruction of the clay's fabric. As shown in Figure 4-12, the peak and residual stress states from both CUI and CUK0 tests are plotted together to develop the failure envelope of the clays corresponding to these states. It is noticed that the failure envelope is curved, particularly at low confining stresses. This is attributed to the overconsolidated nature of the clay at low  $\sigma'_{3c}$  and moving from overconsolidated to normally consolidated condition with increasing  $\sigma'_{3c}$  [87]; [109]. Due to this curvature, the best fit lines were used to obtain Mohr-Coulomb (MC) strength parameters, i.e., cohesion intercept ( $c'$ ) and effective friction angle ( $\phi'$ ) as shown in Figure 4-13 and Table 4-4. The cohesion softening from peak to residual state in both clays occurred in Albanel because of destruction of the overconsolidated structure of these clays. Albanel samples also exhibited higher undrained shear strengths as seen from the stress-strain curves in Figure 4-9a and the higher stress states in Figure 4-12. Although both clays have similar water

content, plasticity and fines percentage, the difference in the depositional environment could contribute to the higher strength in Albanel clays. Some Desbiens samples tested are from the upper strata consisting of younger sediments (see Figure 4-3b) by virtue of which they could be less overconsolidated in comparison to the Albanel clays.



(a)



(b)

Figure 4-11 (a) Stress - strain behaviour and (b) stress paths of CUK0 tests

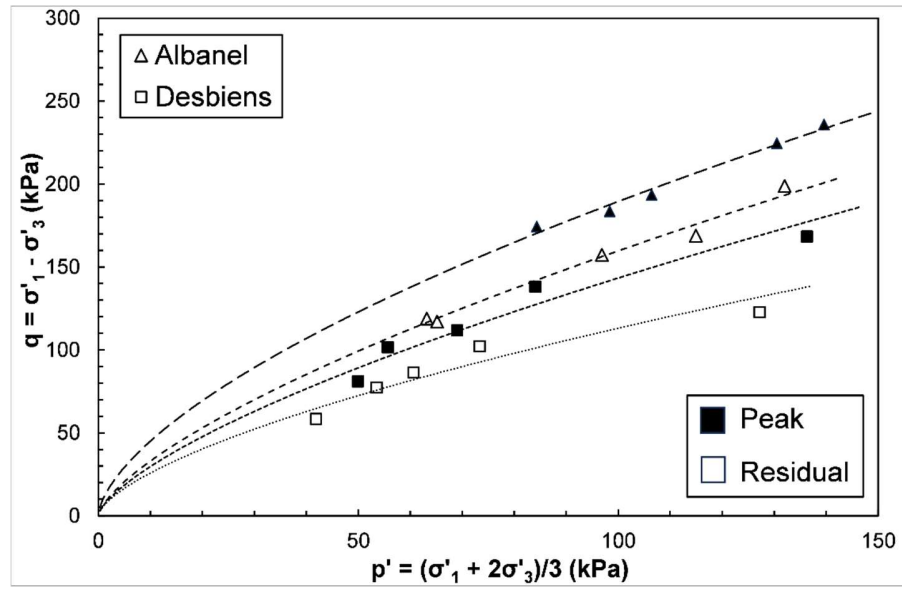
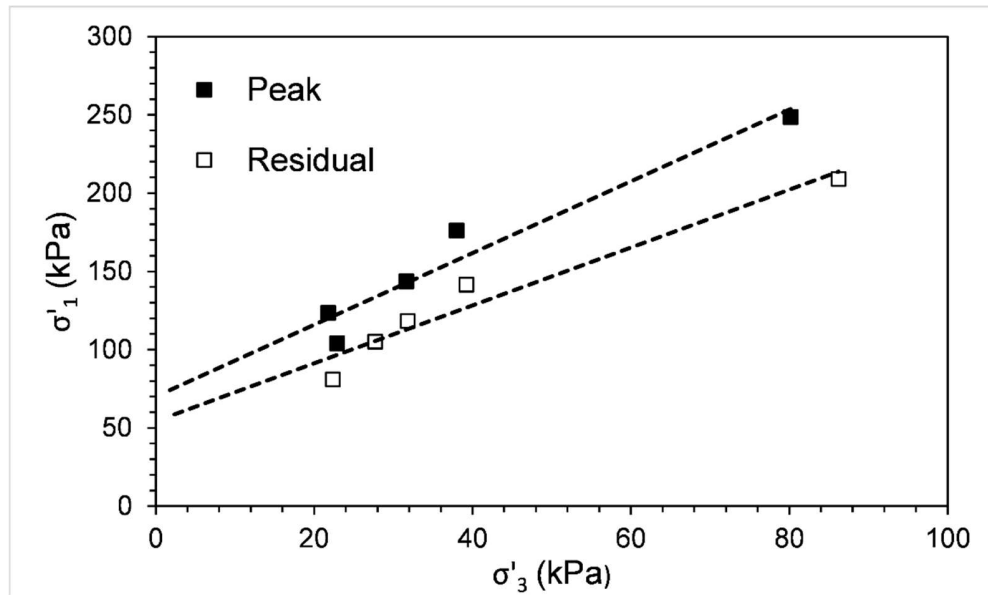
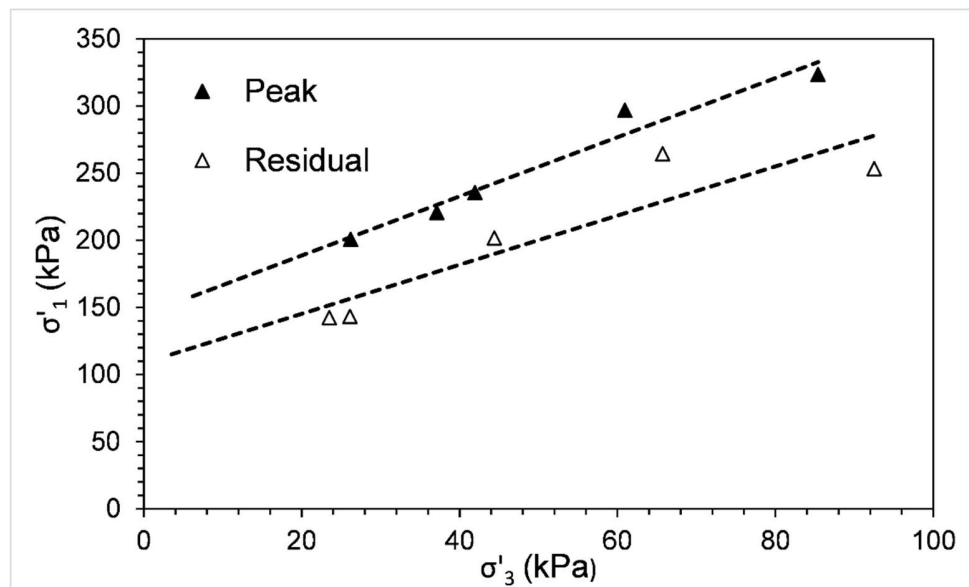


Figure 4-12 : Peak and residual stress states of Desbiens and Albanel clays from CUI and CUK0 tests



(a)



(b)

Figure 4-13 Best fit lines from which Mohr-Coulomb parameters are determined for (a) Desbiens and (b) Albanel samples from both CUI and CUK0 tests

Table 4-4 Mohr-Coulomb strength parameters

Clay	$c_p'$ (kPa)	$\phi_p'$ (°)	$c_r'$ (kPa)	$\phi_r'$ (°)
Desbiens	20.3	18.3	19.9	17.3
Albanel	35.3	28.8	22	28.3

where  $c_p'$  and  $c_r'$  are effective cohesion at peak and residual states, respectively;  $\phi_p'$  and  $\phi_r'$  are friction angles at peak and residual states, respectively.

The clays of this study are evaluated further using the Skempton's pore pressure parameter at failure,  $A_f = \Delta u_f / \Delta \sigma_f$  (Skempton 1954). The variation of  $A_f$  with OCR as shown by [130] for Weald clay is reproduced in Figure 4-14 along with some common Eastern Canadian clays as well as the results of this study. The figure shows extremely low  $A_f$ , indicating overconsolidation and dilatancy. Furthermore, the experimental data and the empirical reduction of  $A_f$  with increasing OCR suggested by [130] seem to be inapplicable to the structured sensitive clays of Figure 4-14. This is especially prominent in the case of clays from this study and Saint Jean

Vianney (SJV), both belonging to the Laflamme basin, where the high OCR does not reflect the corresponding  $A_f$  as proposed by [130].

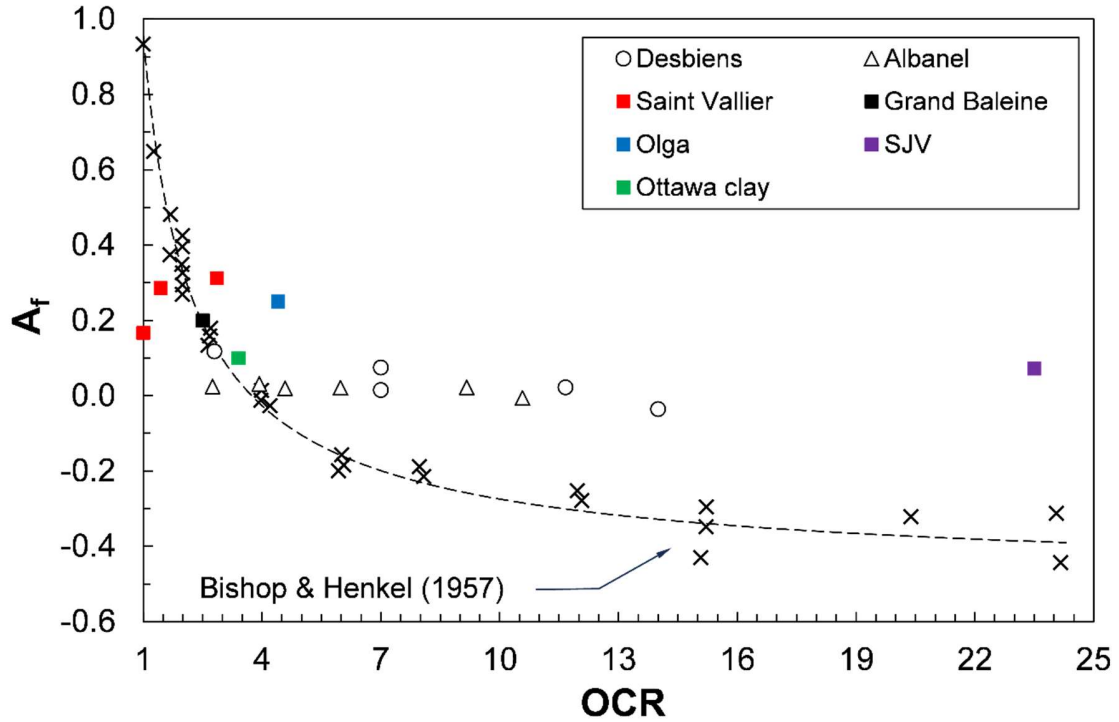
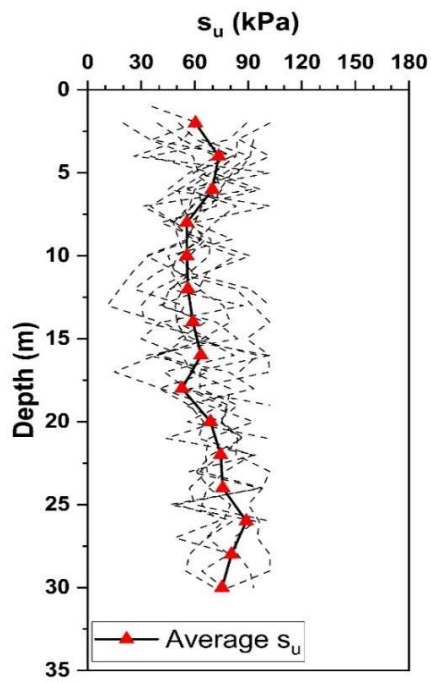


Figure 4-14  $A_f$ - OCR relations for Desbiens and Albanel in comparison with other Eastern Canadian clays

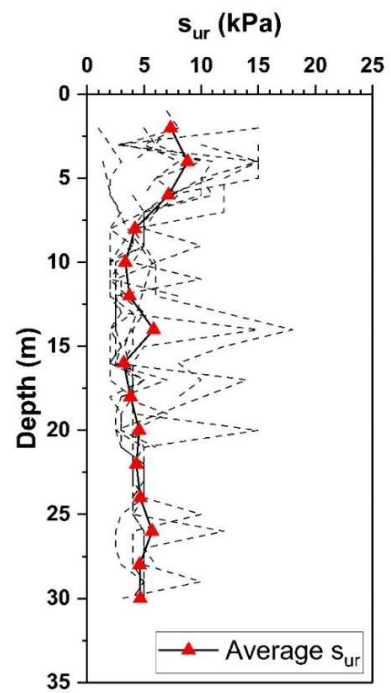
#### 4.5.4 Undrained shear strength profiles

The FVT results of the clays surrounding the sampling locations of Desbiens and Albanel (from Figure 4-2) are discussed in this section. Figure 4-15 shows the ranges of  $s_{uFVT}$  with depth for different clays (dashed lines) as well as the average values at each depth (red markers). The average peak ( $s_{upFVT}$ ) and remoulded ( $s_{urFVT}$ ) undrained strengths in different boreholes at Desbiens site ranged from 53 to 89 kPa and 3.2 to 8.8 kPa respectively as shown in Figures 4-15a and 4-15 b. A steady increase of  $s_{upFVT}$  with depth was observed in Albanel clays from 51 kPa at 4 m depth up to 143 kPa at a depth of 14 m. At 2 m depth,  $s_{upFVT}$  was 77 kPa, possibly associated with a crust layer (Figure 4-15c). The  $s_{urFVT}$  however shows scatter among the various boreholes varying from 1.3 to 11 kPa on average in Figure 4-15d.

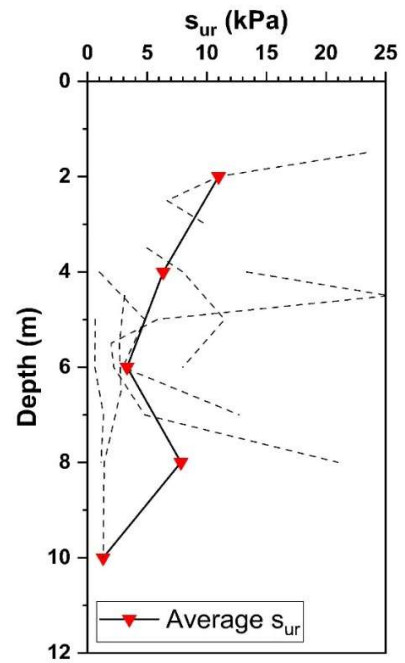
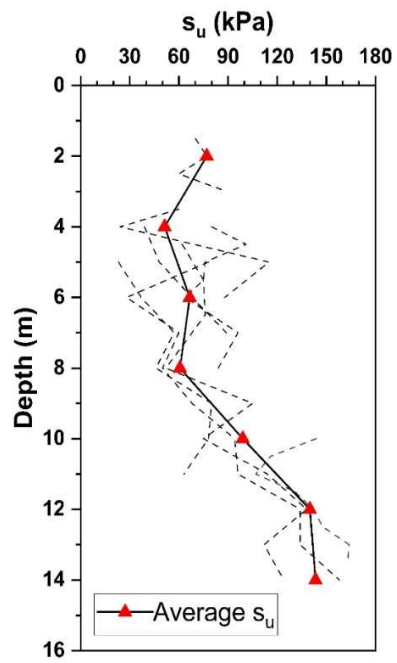




(a)



(b)



(c)

(d)

Figure 4-15 FVT results showing variations of (a)  $s_{upFVT}$  and (b)  $s_{urFVT}$  with depth for Desbiens clays and (c)  $s_{upFVT}$  and (d)  $s_{urFVT}$  with depth for Albanel clays along with average values at each 2 m depth

The CPT soundings were carried out up to depths of 25- 30 m at both sites and variation of cone tip resistance  $q_t$  (corrected for area effects and pore water pressure), and pore water pressure ( $u_2$ ) measured behind the cone shoulder are depicted with depth in Figures 4-16 and 4-17. According to Figure 4-16a,  $q_t$  in Desbiens clay showed an increasing trend with depth as well as relatively higher resistances in the sand-silt interbeds (16 – 18 m). The  $u_2$  at this depth (Figure 4-16b) was also much lower due to the interbedded sand layers. On the other hand, as seen in Figure 4-17a, in Albanel,  $q_t$  remained more or less constant down to a depth of 24 m. The high tip resistances at depths of 30 and 25 m in Desbiens and Albanel clays, respectively, suggest a till layer at these respective depths. The ground water table (GWT) at Desbiens and Albanel was at depths of 1.63 and 2.5 m from the ground level, respectively as shown in Figures 4-16b and 4-17c. The high pore pressures shown in Figures 4-16b and 4-17c and the positive excess pore pressure ratio,  $B_q$  values in Figures 4-16d and 4-17g are indicative of sensitive clays deposits. In general,  $B_q$  values ranged from 0.5 – 1 which is typical of Eastern Canadian sensitive clays [110]. [131] suggested a normalized cone tip resistance parameter ( $Q_{tn}$ ) which is obtained by applying an overburden stress normalization factor to the net tip resistance ( $q_t - \sigma_v/P_a$ ) as below:

$$Q_{tn} = \frac{q_t - \sigma_v}{P_a} \left( \frac{P_a}{\sigma'_v} \right)^n \quad (4-2)$$

where  $P_a$  = atmospheric pressure ( $\approx 100$  kPa),  $\sigma_v$  = total vertical stress,  $\sigma'_v$  = effective vertical stress,  $(P_a/\sigma'_v)^n$  is the stress normalization factor,  $n$  is the stress normalization exponent which is often considered as one for clay soils. As measurements of sleeve friction ( $f_s$ ) was available at the Albanel site (in Figure 4-17b), friction ratio ( $F_r$ ) and subsequently the soil behaviour type (SBT) index ( $I_c$ ) were calculated in Figure 4-17f according to [131]. As seen in Figure 4-17f,  $I_c$  was about 2.6 down to a depth of 4 m, below which it progressively increased to 3.4. According to [132], out of 991 CPT measurements on samples from 40 sites in Southern Quebec, silt mixtures or silty clays ( $2.6 < I_c < 2.95$ ) is the most frequent type. An  $I_c = 2.6$  often indicates the transition of soil type from sand-like to clay-like behavior [133]. This suggests that beyond 5 m depth, the soil was transitioning

into a clay-like behaviour. The samples of this study were obtained from depths of 6 - 7 m and represented a clay like behaviour as seen from previous experimental results. According to the SBT charts in Figure 4-18, the soil at Albanel site was a sensitive fine-grained clay mixed with predominantly silt mixtures and some sand mixtures. In the absence of similar data from the Desbiens sampling location, a similar soil type could be assumed for Desbiens clays as well since these clays occurred in similar geological environments and possess identical mechanical behaviours as those from Albanel.

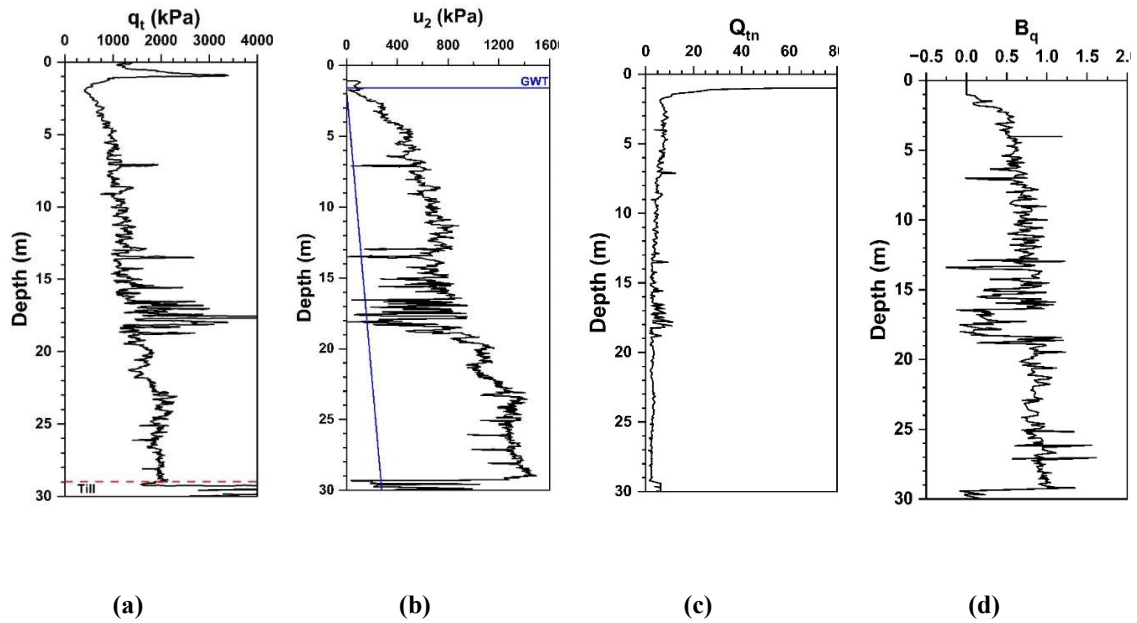


Figure 4-16 CPT profiles at a Desbiens site showing variation of (a)  $q_t$ , (b)  $u_2$ , (c)  $Q_{tn}$  and (d)  $B_q$  with depth

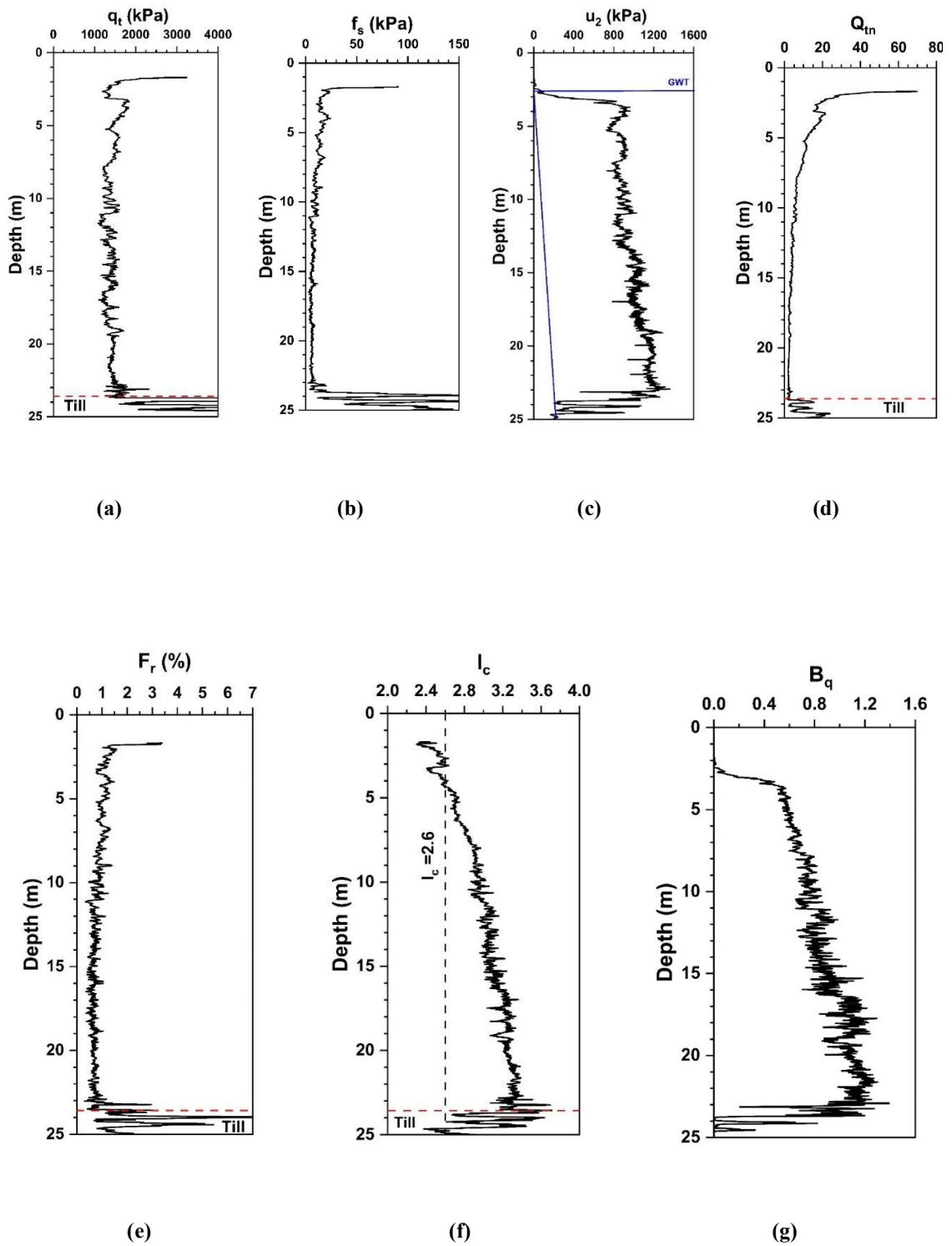


Figure 4-17 CPT profiles at an Albanel site showing variations of (a)  $q_t$ , (b)  $f_s$ , (c)  $u_2$ , (d)  $Q_{tn}$ , (e)  $F_r$ , (f)  $I_c$  and (g)  $B_q$  with depth

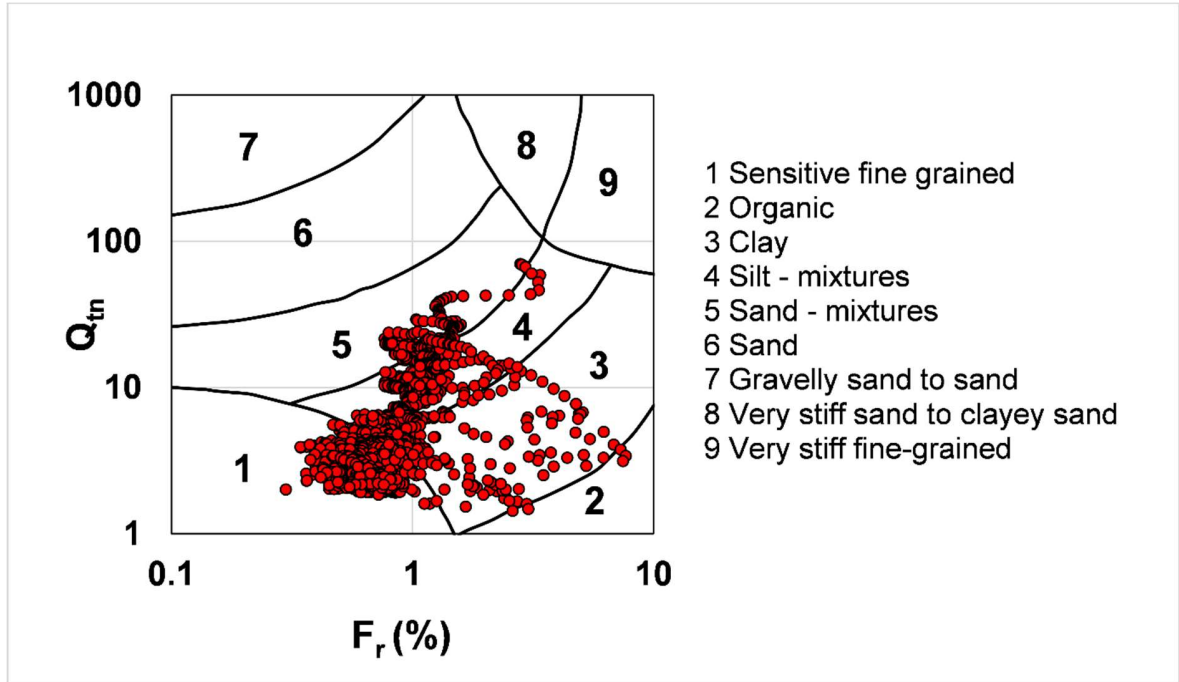
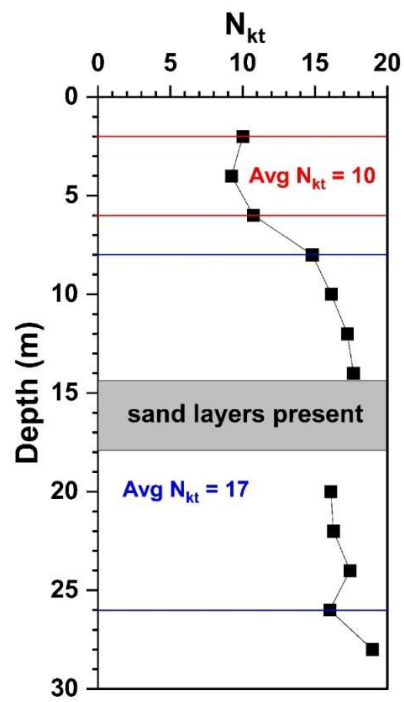
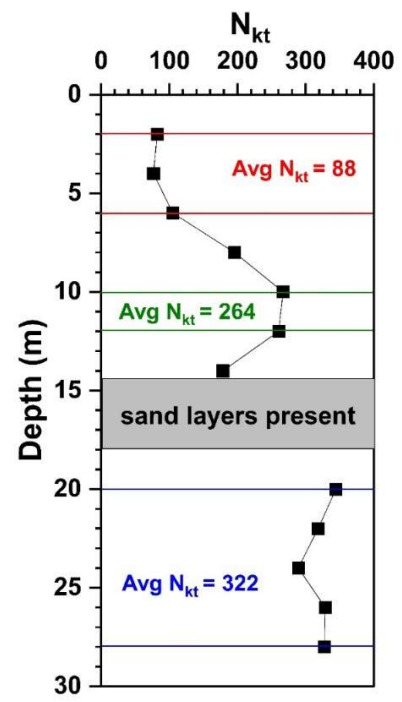


Figure 4-18 Soil behaviour type chart according to [131] for Albanel clays

The average FVT results presented in Figure 4-15 were further used to calibrate  $q_t$  profiles and determine  $N_{kt}$  values for estimating peak and remoulded undrained shear strengths,  $s_{u\text{CPT}}$  and  $s_{ur\text{CPT}}$ . The calibrated  $N_{kt}$  values for Desbiens and Albanel clays are shown in Figure 4-19. At Desbiens,  $N_{kt}$  values at depths of 11- 17 m were excluded due to their higher  $q_t$  and lower  $u_2$  in comparison to other layers suggesting interbedded sand layers. In the case of Albanel clays, boreholes surrounding the sampling location showed sand layers up to 5 m depth. Also, according to the  $I_c$  values in Figure 4-17f, there is a transition of SBT from sand-like to clay-like at about 5 m depth. As such,  $N_{kt}$  values at depths shallower than 5 m in Albanel clays were also excluded. A depth wise variation of  $N_{kt}$  was considered in determining  $s_{u\text{CPT}}$  and  $s_{ur\text{CPT}}$ . Similar  $N_{kt}$  values from certain depths were grouped together to form an average  $N_{kt}$  for those depths. According to Figures 4-19(a-b),  $N_{kt}$  values varied from 9.2 to 21.7 for peak conditions and 76.8 to 344.2 for remoulded conditions respectively in Desbiens clays. For Albanel clays,  $N_{kt}$  at peak and remoulded conditions varied from 7.4 – 15.6 and 147.9 – 892.5 respectively (Figures 4-19c and 4-19d). According to [110], most Eastern Canadian clay deposits show an average  $N_{kt} = 13.7$  for peak strength. Using the depth dependant  $N_{kt}$  values in Figure 4-19,  $s_{u\text{CPT}}$  and  $s_{ur\text{CPT}}$  profiles were determined and shown in Figures 4-20 and 4-21.



(a)



(b)

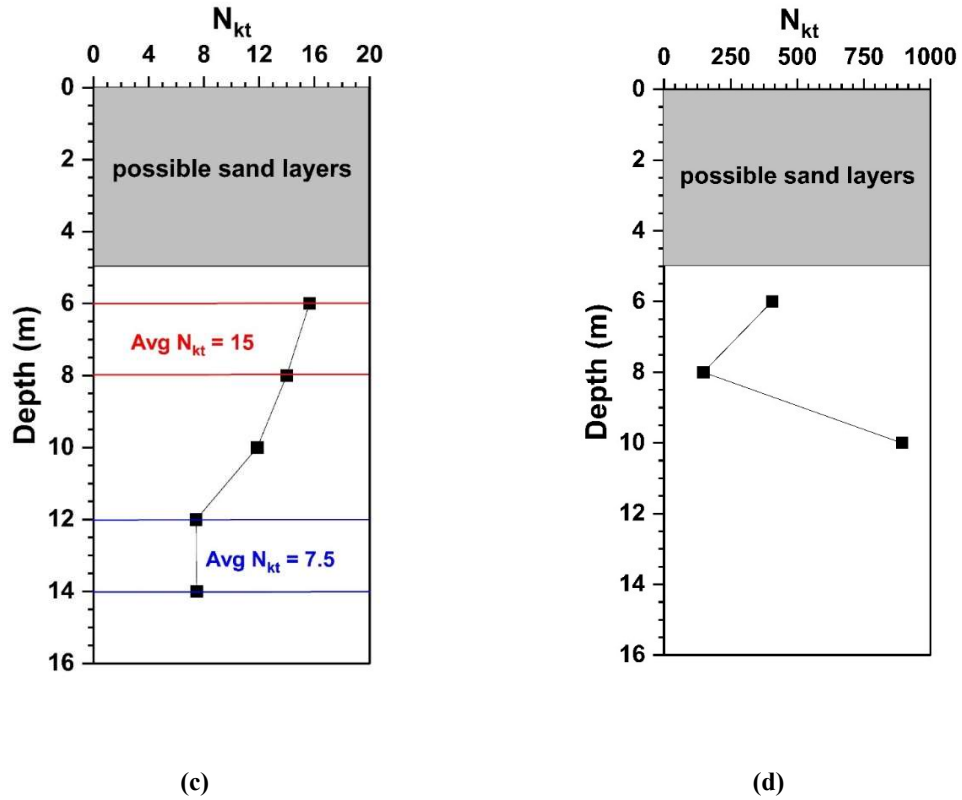


Figure 4-19 Estimated  $N_{kt}$  values for (a) peak and (b) remoulded strengths at Desbiens site and (c) peak and (d) remoulded strengths at Albanel site

As seen in Figure 4-20a, in Desbiens,  $s_{uCPT}$  rose almost linearly from 31 kPa to about 70 kPa down to a depth of 28 m, except from 15 to 19 m where significant sand layers were observed. The peak undrained strengths from the laboratory FCT and CUI triaxial tests compare favourably with the field undrained strengths obtained from the CPT measurements and FVT. In particular, those from the triaxial tests plotted with the average  $s_{uFVT}$ . At the Albanel site  $s_{uCPT}$  decreased from 97 kPa at 6 m to 71 kPa at 8 m, and then progressively increases to 163 kPa up to a depth of 14 m (in Figure 4-21a). The samples tested in the laboratory using FCT in the present study (i.e. for depths of 6 - 7 m), from all the three boreholes presented similar  $s_{uFCT}$  of 142 kPa. However, the CUI triaxial tests seem to be somewhat lower than the FCT measurements and closer to  $s_{uFVT}$ . As for the  $s_{ur}$  profiles in Figures 4-20b and 4-21b, the  $s_{urFCT}$  and  $s_{urLVT}$  measured in the laboratory for Desbiens clays ranged from 3.9 – 6.8 kPa, similar to the field FVT tests. Albanel clay samples showed an average  $s_{urFCT/LVT}$  value of 4.5 kPa while the average  $s_{urFVT}$  was 6 kPa. In general,  $s_{ur}$  measured by FCT and LVT were

similar in Albanel clays. The  $s_{urCPT}$  values seem to be in line with the FVT, FCT and LVT measurements in both Desbiens and Albanel clays. The measured peak and remoulded strengths from FCT correspond to sensitivities on the order of 19 in Desbiens and 32 in Albanel clays. Based on FVT result, sensitivities range from 7-20 in both clays depending on the depth. The results based on CPT tests are also along similar lines. Sensitivity ( $S_t$ ) values from FVT and CPT tests are shown in Figure 4-22. According to the  $I_L$ - $s_{ur}$  correlation of [30] and [31],  $s_{ur}$  for Desbiens and Albanel clays should be in the range of 2.1 - 3.3 kPa based on their  $I_L$  values (0.6 - 1). However, it has been shown by [34] that these correlations underpredict  $s_{ur}$  of Laflamme clays. This is shown in Figure 4-23, where most of the results, especially those for Albanel clays fall above the correlations.

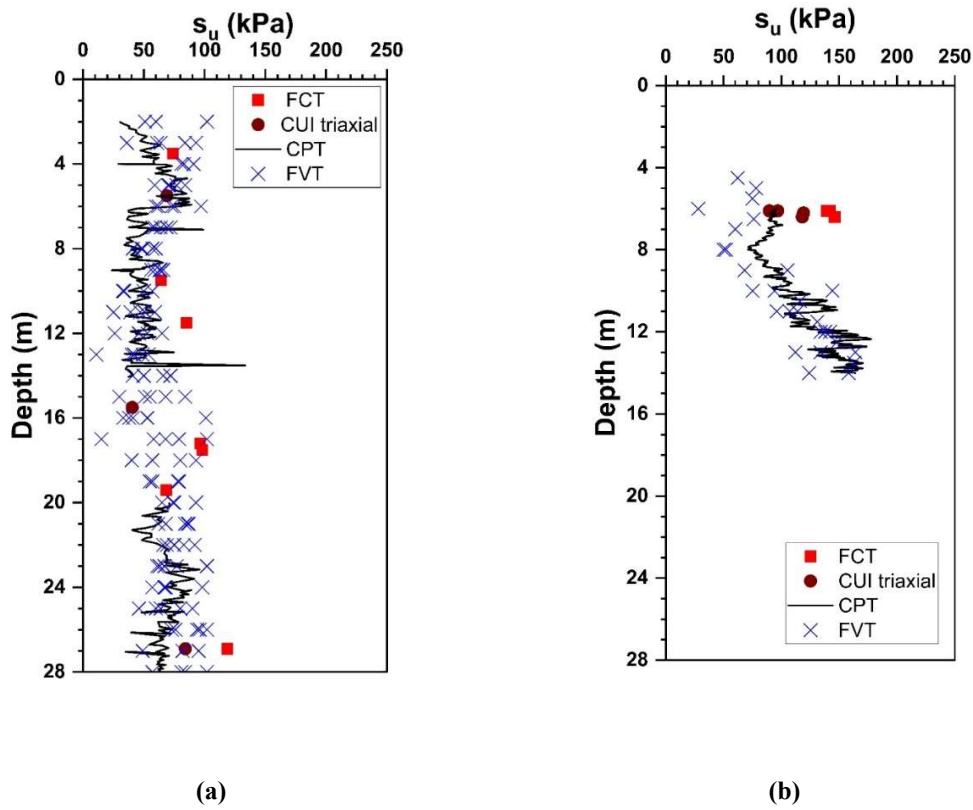
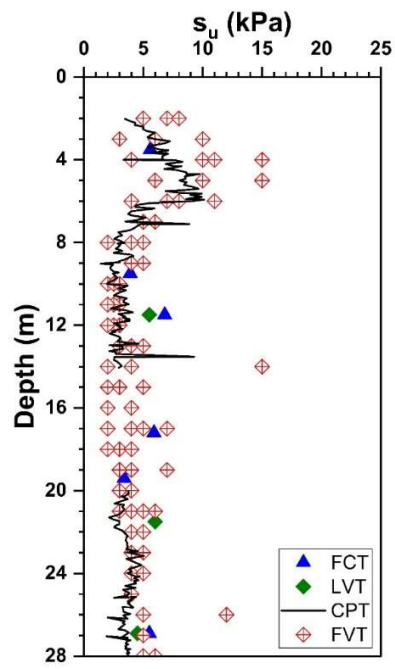
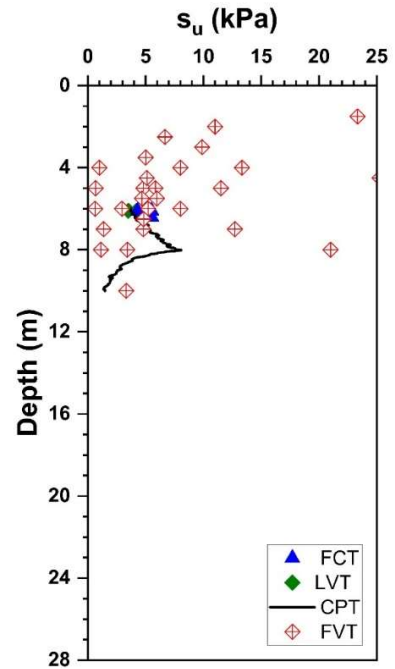


Figure 4-20 Peak undrained strength profiles in (a) Desbiens and (b) Albanel clays from field (CPT and FVT) and laboratory (FCT and CUI triaxial) tests





(a)



(b)

Figure 4-21 Remoulded undrained strength profiles in (a) Desbiens and (b) Albanel clays based on field FVT and laboratory FCT and LVT tests

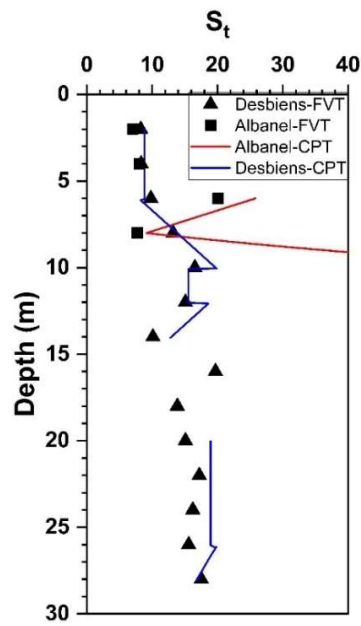


Figure 4-22 Variation of sensitivity with depth in Desbiens and Albanel clays based on FVT and CPT results of this study

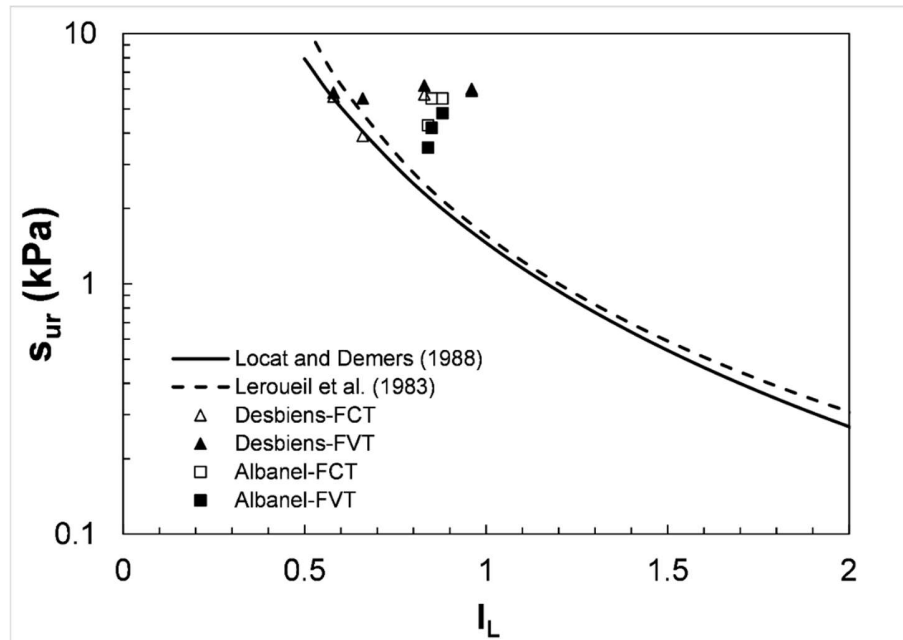


Figure 4-23 Remoulded undrained strengths of Desbiens and Albanel clays based on FCT and FVT results of this study and comparisons with empirical correlations

## 4.6 DISCUSSION

The detailed experimental results presented in this paper indicated that clays from the LSJ are different than the marine clays of Eastern Canada, especially Champlain clays, in several aspects. The unique geological history and the formation of Laflamme sea clays has definitely contributed to this. The sediments in this region are primarily sensitive clay deposits with silt and interbedded with fine sands at certain depths. However, since fine rock flour from glacial grinding was a significant source of the sediments, the sediments contain a significant amount of silt. Studies by [135] and [126] states that in most Eastern Canadian clays, the low clay mineral content does not always correlate with its high clay fraction.

The source of significant sand layers, especially at the Desbiens site could be proglacial fan sand from the last glacier retreat. In Figure 4-3b, the borehole data from Desbiens represents two distinct strata, one with higher water contents (40 - 50%) and limits up to a depth of about 13 m and a deeper layer with relative lower water content (less than 40 %) and limits. This suggests that the fine-grained sediments deposited above the interbedded sand layers at 13-17 m could be much younger. If indeed the sand layer originated following a fluvio-glacial drift, the ice margin may not have been far away, liberating a large amount of diluted melt glacial water that aided in leaching. Furthermore, these sand layers along with a unique bedrock topography representing a valley facilitated the leaching process as the presence of more permeable units favours faster groundwater flow and greater dilution [105]. The presence of such sand pockets has been observed in other Eastern Canadian regions of slope failures such as the Saint Jean Vianney [7], Rigaud [90], St Jude [9] and Saint Luc du Vincennes [10]. In short, the primary reason for heavy leaching and extremely low salinities in LSJ clays of this study is the significant source of fresh water creating a lacustrine environment as opposed to the more marine conditions in the Saguenay Fjord where salinity is still higher (in the order of 16 g/L) than Champlain clays [21]. Naturally occurring Champlain clays were found to have higher percentages (4 times that of LSJ clays) of Na and Ca [86] showing that the LSJ clays are indeed highly leached in comparison to clays of both the Saguenay Fjord and Champlain basin. This, along with the silty nature of the clays further contributed to the low Atterberg limits in comparison to typical Eastern Canadian sensitive clays of Champlain basin with  $\omega_L$  ranging from 55 – 77% and  $I_p$  from 34-52 % [27]. This leads us to reconsider the criteria for retrogressive landslides in sensitive clays proposed by [29] that retrogressive landslides occur when  $I_L > 1.2$  in

LSJ clays. The  $I_L$ - $s_{ur}$  correlations of [30] and [31], which are extensions of the said criteria were also found inapplicable to the higher  $s_{ur}$  in clays of LSJ. It is interesting to note that, Desbiens clays, although prone to retrogressive flowslides in the past, do not present very low  $s_{ur}$  as seen in Scandinavian sensitive clays or certain Champlain clays where it is considered that retrogressive flowslides occurred at  $s_{ur} \approx 1$  kPa. This means that even if the clay material does not necessarily ‘flow’, the  $s_{ur}$  needs to be only low enough for the clay to slip out of the landslide crater and leave an unsupported backscarp for a retrogressive failure to initiate [11]. The cause of retrogressive landslides in clays of LSJ with low Atterberg limits could be explained through the loss of inter particle bonding making them severely sensitive (i.e., average  $St = 19$  and  $32$  in Desbiens and Albanel clays, respectively) and susceptible to remoulding. A similar explanation was also given by [11] for sensitive clays exhibiting low liquid limits.

The mineral composition of sensitive clays is not unique and is highly dependent on the source of sediments and depositional environment. However, most sensitive clays show an abundance of quartz and plagioclase feldspar with small quantities of microcline, hornblende, dolomite and calcite among others [126]; [136]. The quantity of clay minerals is generally found to be less in these clays averaging at around 10% in the Champlain basin with lower percentages (2 - 8 %) at the Saguenay Fjord [126] with Illite and chlorite as the primary clay minerals. The LSJ clays of this study were also found to contain quartz, albite (plagioclase feldspar), microcline, hornblende, illite, and kaolinite minerals. The low percentage of clay minerals are also reflective of the low Atterberg limits further leading to its brittleness. Illite is the primary clay mineral as seen in the XRD spectra of Figure 4-6. According to Skempton, (1953), the activity of illite lies between 0.5 and 1.3, and the results of this study ( $A = 0.4 - 0.7$ ) are consistent with this range as shown in Figure 4-4b. Additionally, the stacked platy particles observed in the SEM images of Figure 4-7 resemble the structural arrangement of illite.

A comparison between highly overconsolidated clays such as London clays and soft sensitive clays by [56] highlighted their key differences in triaxial compression tests. In this context, the LSJ clays of this study behaved like an overconsolidated London clay rather than a soft structured clay. They exhibited highly dilatant behaviours as opposed to the contractive behaviour of certain soft structured clays in Figures 4-9c and 4-11b. Similar behaviour was also observed in an overconsolidated Norwegian (‘Emmerstad’) clay [77]. [14]

describes the mechanism of progressive slope failures in overconsolidated clays as an increase of mean effective stress with shearing due to dilatancy and therefore overstressing the underlying clay layers to failure. [71] observed both dilative and contractive failures in Champlain clays from Saint Vallier and Saint Louis depending on the confining stresses applied in undrained loading in a triaxial test (dilatancy at confining stress less than 5 kPa). However, such low confining stresses may not always yield accurate results in a triaxial test and samples are often tested at higher confining stress which causes a contractive behavior as seen in most Champlain clays. Nevertheless, the clays of this study were truly overconsolidated in nature that the dilatancy prevailed in the triaxial tests.

Finally, in the LSJ clays of this study, strain softening and the reduction of MC strength parameters from the peak to the residual condition were associated with the collapse of clay structure rather than effective stress reduction as little excess pore pressure was generated in these samples (see Figures 4-4 and 4-17). Accordingly, strain softening due to shear-induced pore water pressure in sensitive clays may not be generalised to all sensitive clays.

#### **4.7 CONCLUSIONS**

This paper details the unique geotechnical characteristics of clays from two sites surrounding the LSJ basin – Desbiens and Albanel, in terms of their physical, chemical and soil mechanical behaviours. These soils maybe classified as silty clays with illite as the primary clay mineral. As opposed to typical Champlain clays, clay aggregations were absent in their microstructure confirming significant quantities of rock flour. Evidences of extremely low salinities have also been presented using salinity measurements and low cation percentage in their chemical composition. Field investigations showed traces of sand and sand deposits at certain depths in both Desbiens and Albanel deposits. Undrained shear strength profiles indicated high intact and remoulded strengths. The samples when subjected to CUI and CUK0 tests exhibited strain hardening and dilatant behaviour in the overconsolidated range of stresses with very little pore water pressure generation. This was followed by undrained strength loss and strain softening. In general, when compared to Champlain clays, the Laflamme clays of the LSJ basin are highly leached clays with little clay minerals and are subjected to heavy overconsolidation and preloading leading to high intact strength. These differences become especially important towards hazard assessment studies of retrogressive landslides in the Eastern Canadian region.

**Funding**

This research was partially funded by the Natural Sciences and Engineering Research Council of Canada (NSERC) and Hydro-Quebec under project funding no. RDCPJ 521771 – 17 as well as Canada Research Chair (950-232724).

**Acknowledgement**

The authors would like to express their gratitude to their colleague at Université du Québec à Chicoutimi, Quebec, Prof. Julien Walter, for certain valuable insights that helped improve the manuscript.

**Data availability**

The data used and/or analyzed during the current study are available from the corresponding author on reasonable request

## CHAPTER 5

### Article 4: Evaluation of geotechnical parameters for sensitive clay slopes in Lac-Saint-Jean region using back analysis

Sarah Jacob<sup>a,\*</sup>, Ali Saeidi<sup>a</sup>, Abouzar Sadrekarimi<sup>b</sup>, Rama Vara Prasad Chavali<sup>a</sup>

**\*Corresponding author:** Email address- [sjacob2@etu.uqac.ca](mailto:sjacob2@etu.uqac.ca)

<sup>a</sup>Department of Applied Science, Université du Québec à Chicoutimi, Quebec, Canada

<sup>b</sup>Department of Civil and Environmental Engineering, Western University, Ontario, Canada

Draft prepared for submission to a journal

#### Credit authorship contribution statement

**Sarah Jacob:** Conceptualization, Data curation, Formal analysis, Resources, Experimentation, Writing – original draft, Writing – review and editing. **Ali Saeidi:** Supervision, Methodology, Resources, Writing – review and editing. **Abouzar Sadrekarimi:** Supervision, Writing – review and editing. **Rama Vara Prasad Chavali:** Writing – review and editing.

#### Declaration of competing interests

The authors declare the following financial interests/personal relationships which may be considered as potential competing interests: Ali Saeidi reports financial support was provided by Natural Sciences and Engineering Research Council of Canada (Grant ID: NSERC- 950- 232724). Ali Saeidi reports financial support was provided by Hydro Quebec (Grant ID: RDCPJ 521771–17). If there are other authors, they declare that they have no known competing financial interests or personal relationships that could have appeared to influence the work reported in this paper.

## 5.1 ABSTRACT

Landslides in sensitive clays are often assessed by complex numerical techniques or analytical modelling tools to estimate slope stability and possible retrogressive failures. However, these can often be tedious as it requires a good understanding of the likely failure mechanisms and detailed knowledge of complex numerical modelling techniques. Additionally, geotechnical parameters used in slope stability analysis from laboratory experiments maybe often affected by scale effect when applied to large slopes. Due to lack of data on large deformation modelling and experimental investigations, such studies are quite limited for sensitive clays of Laflamme basin in Eastern Canada, in spite of several slope failures in this region. Hence, this study focuses on slope stability studies pertaining to this region and determination of geotechnical parameters on a large scale. Although this study only shows a first slide estimate or initial failure in a possibly unstable slope, the likelihood of it turning into a retrogressive failure can be assessed and could help in deciding the need for complex modelling. Resources such as LiDAR images and aerial photographs are used to get precise topographical data for slope stability studies. Furthermore, properties of sensitive clays such as remoulding energy have been effectively used as criteria for assessing retrogressive landslides. The study shows the instability of slopes in Laflamme Sea region through a limit equilibrium analysis and finite element modelling of clay slopes. The study also highlights the importance of geological history and changing slope geometry and topography in stability of slopes.

**Keywords:** slope stability, LiDAR, numerical modelling, retrogressive landslide

## 5.2 INTRODUCTION

A major hazard associated with sensitive clays is retrogressive landslide which has significant socio-economic impacts. Most of the marine environment in which sensitive clay deposits occur, are quite populated which is one of the reasons that monitoring and assessment of landslides in sensitive clays has become important and is consequently progressing in the region of Quebec [26]. According to Natural Resources Canada (NRCan), from 1771 – 2019 there have been 239 landslides that resulted in fatalities in Quebec [138]. A large number of these slides have taken place in the spring, when there is significant water in the soil which could be



due to heavy rainfall or snow melt [26]. This aggravates fluvial erosion along the banks of sensitive clay slopes which is one of the primary reasons for the initiation of retrogressive landslides [48]. Although certain human activities like piling and machine vibrations are also known to cause such landslides, these are primarily in Norway as opposed to Eastern Canadian clays [26].

The reason for the strength loss with deformation in sensitive clays, called strain softening, maybe traced to the retreat of the Wisconsin glaciers in the last glaciation period that occurred about 18000 to 6000 years BP [111]. This exposed the flocculated marine sediments to fresh water, thereby leaching their salts, leaving behind a collapsible fabric easily susceptible to disturbances such as erosion. Although, this is the process that led to the formation of sensitive clays, the time of sediment deposition and retreat of glaciers leading to a marine invasion along with the surrounding topography has led to sensitive clays of distinguishing properties in different parts of Eastern Canada. For example, the Laflamme sea which covers the Saguenay lowlands and the Lac-Saint-Jean (LSJ) basin was a shorter and recent marine invasion allowing for preloading and later erosion of the clay sediments, leaving behind a more overconsolidated clay in comparison to the sediments of the Champlain Sea that occupies the St Lawrence lowlands [20].

Analysis of retrogressive landslides in sensitive clays requires complex modelling techniques such as BIFURC, MPM (Material Point Method), LDFEM (Large deformation finite element modelling) and SPH (Smoothed Particle Hydrodynamics) [18]; [22]; [23]; [24]. However, a first slide estimate can be done by limit equilibrium (LE) analysis or finite element modelling (FEM) to check the likelihood of a slope failure turning into a retrogressive failure with increasing disturbance [25]. In fact, numerical modelling studies focus on Champlain clays and studies in that direction among Laflamme clay slopes are quite limited. Certain studies have been carried out in Saint Jean Vianney clays, although these are mostly restricted to experimentation [89]. It has been more than 50 years since the occurrence of the notable Saint Jean Vianney landslide without any numerical modelling assessments directed towards slides of this region. Accurate landslide information, such as the in-situ geotechnical parameters that lead to failure, could be difficult to obtain experimentally in sensitive clays which are prone to sample disturbance [139]; [140]. Hence, site-scale geotechnical parameters maybe determined through back analysis from the laboratory results which is a common technique to determine soil parameters at site scale [141]; Wesley and Leelaratnam, 2001). A good understanding of the topography of the

slope, before and after failure will aid in effective back analysis [143]. Researchers often rely on LiDAR and aerial photographs to generate such data [144]; [145]. An example of one such study is the use of aerial photographs to generate elevation models for the Tessina landslide in Italy by [146]. The elevation models provided evidences of past landslide activity along with possible reactivation. Furthermore, the use of aerial photographs and digital photogrammetry in the study of evolution of landslides have also been shown by [147] in the analysis of Chin Coulee landslides in Alberta, where the photogrammetry data helped determine the kinematics of the slide. The government of Quebec has been using LiDAR survey to map landslide prone areas in Quebec from 2003 [148]. Additionally, [144] demonstrates the use of Terrestrial Laser scanning (TLS), a ground based version of the airborne LiDAR, to quantify the volume of landslide and create soil profiles using case studies from Quebec and Switzerland. Hence it could be understood that effective analysis of any landslide maybe achieved with a combination of experimental data, numerical analysis and other useful resources in the form of LiDAR data and aerial photographs.

Sometimes, numerical modelling software for landslide assessment may not be readily available in which case assessing the likelihood of retrogressive failure though a criterion maybe effective. Landslide assessment studies in sensitive clays are focused on several criteria involving geo-physical and mechanical properties such as its liquidity index ( $I_L$ ), remoulded shear strength,  $s_{ur}$  [149]; [150]; [31], liquid limit and remoulding energy [11]. Among these criteria that have been successfully used in the analysis of sensitive clay landslides, remoulding energy can encompass the effect of multiple aspects such as strain softening, slope geometry and other physical parameters of the clay as it is quantified as the area under the stress-strain curve of a sensitive clay [13]. When it comes to sensitive clays, the stress history of the soil plays an important role in its behaviour. Overconsolidated clays have a tendency to exhibit pronounced strain softening behaviour especially at low confining stresses [56]; [20]. This means that although highly overconsolidated clays have higher peak shear strengths, they also suffer from significant softening in comparison to less overconsolidated clays as seen in Figure 5-1. Thus, the area encompassed by a strain-softening curve in a shear stress-shear strain plot, quantified as remoulding energy, can largely vary depending on the type of clay and its stress history.

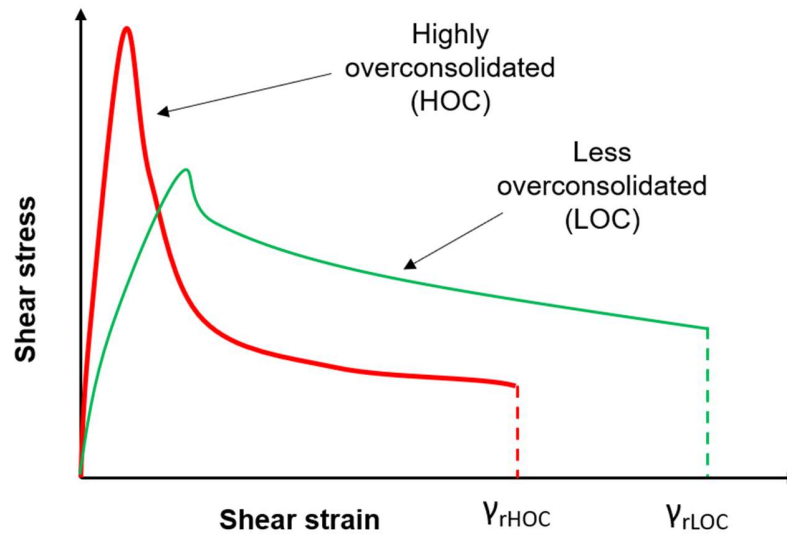


Figure 5-1 Stress-strain behaviour of clays as a function of overconsolidation

This research article analyses the stability of slopes of two regions of sensitive clay deposits surrounding the LSJ of the Laflamme basin– Desbiens and Albanel along determination of geotechnical parameters that could cause such failures on a large scale. Experimental data and resources in the form of aerial and LiDAR images have been used for analysis.

### 5.3 GEOLOGICAL BACKGROUND AND HISTORY OF LANDSLIDE IN STUDY AREA

The geological composition of the Saguenay-Lac-Saint-Jean (SLSJ) region presents a varied array of formations spanning from the Proterozoic to the Quaternary period [151]. These formations comprise of (1) A Precambrian crystalline bedrock attributed to the Grenville Province; (2) The Saguenay Graben, a significant east-west oriented topographic depression; (3) Ordovician sedimentary layers situated in low-lying areas; (4) Quaternary deposits encompassing glacial and proglacial sediments dating back to the Last Glacial Period (LGP), as well as marine, littoral, and deltaic sediments associated with the Laflamme Sea, which flooded the lowlands post the last glaciation around 11,000 to 7,000 years BP.

During the LGP, the Laurentide Ice Sheet (LIS) extensively covered the Canadian landscape, attaining thicknesses of nearly 5 kilometers [152–154]. As a dynamic mass of moving ice, the LIS facilitated the transportation of sediments, forming glacial deposits predominantly composed of diamictos (i.e., tills).

Approximately 18,000 years ago, the LIS began its retreat from southern Canada, leaving behind various glacial outwashes such as eskers, kames, and lateral moraines [155, 156]. The marine waters that retreated from the LIS invaded the Saint Jean area creating the Laflamme Gulf (Figure 5-2A). Subsequently, the isostatic depression induced by the LIS, coupled with rapid global warming and an increase in sea levels, led to a marine transgression, resulting in the intrusion of the Laflamme Gulf into the LSJ region (Figure 5-2B). This marine transgression flooded the lowlands valleys, resulting in sediment deposition reflecting deep and shallow marine environments. Following this, the post-isostatic rebound during the Holocene geological epoch triggered a marine regression, leading to the deposition of regressive sands by the retreating Laflamme Sea. As a consequence of this marine transgression and regression, the central region of the Laflamme Sea contains extensive and substantial deposits of massive or stratified clay, overlain and surrounded by sandy material along its periphery [157–159]. Clay deposits in the SLSJ area can have thicknesses of up to 30 meters [160], and can be highly susceptible to landslides. This study is focused on two regions – Desbiens and Albanel of the Laflamme basin which includes the LSJ and the Saguenay lowlands. During LGP after the glacier's retreat, the first series of rocky ridges at the level of Lake Kénogami (known as the Kénogami threshold) divided the Laflamme Sea into two sub-basins: the Haut-Saguenay lowlands sub-basin (between Cap Éternité and Kénogami thresholds), and the LSJ sub-basin west of the Kénogami threshold (Figure 5-2C). In fact, the slow emergence of the Kénogami threshold can be traced in Figure 2B setting up the marine to lacustrine transition of this water body. Finally, the Alma threshold emergence separated the paleo LSJ to its current state with a complete lacustrine environment (Figure 5-2D). Desbiens and Albanel occur on two sides of the LSJ with Desbiens being at the southern shore of the LSJ and Albanel on its north-western side and inward (Figure 5-2). A historical background on the landslides in these two regions is given in the following sections.

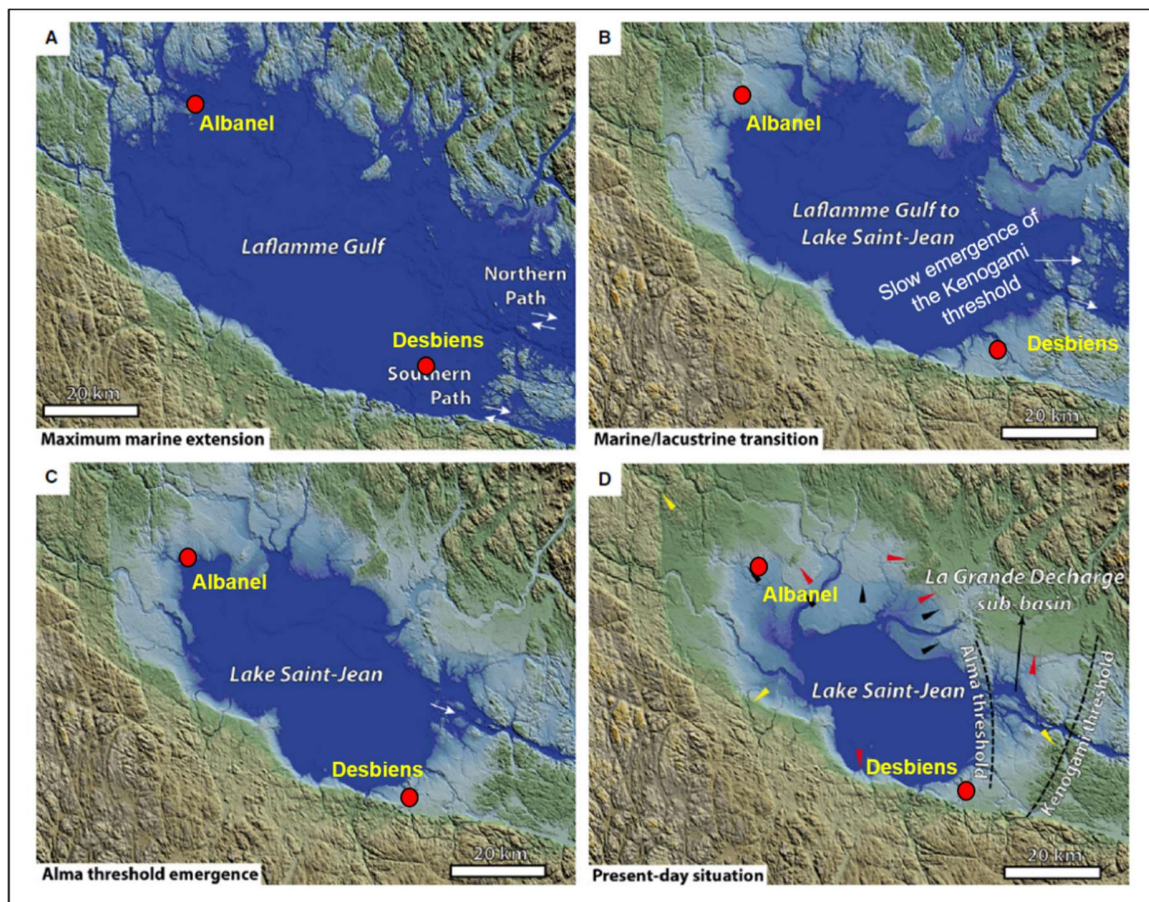


Figure 5-2 Geological history of the Lac-Saint-Jean (modified from Nutz et al. 2015).

### 5.3.1 Desbiens

Slides in this region progress from an initial slip forming a wide crater along the shore of the LSJ into multiple rotational slips at irregular frequency. The speed of retrogression is low and sometimes the slips take place months or even years apart. They predominantly occur during late fall or spring [161].

A notable slide occurred in 1962 near St Jerome, 8 km east of Desbiens. A three-storey hospital was built in saint Jerome in 1961. The parking lot and access roads to the hospital were not far from the shore. In the following spring in 1962, a slide occurred along the shore near Saint Jerome and the retrogression was about 6 m. Three other slides took place in April, August, and October of 1963. By that time the retrogressed slope had reached the access roads leading to the parking of the hospital. The main reason for the slide occurrence was the frost action, and the construction of the hospital could have had only little effect on the slope as no deep

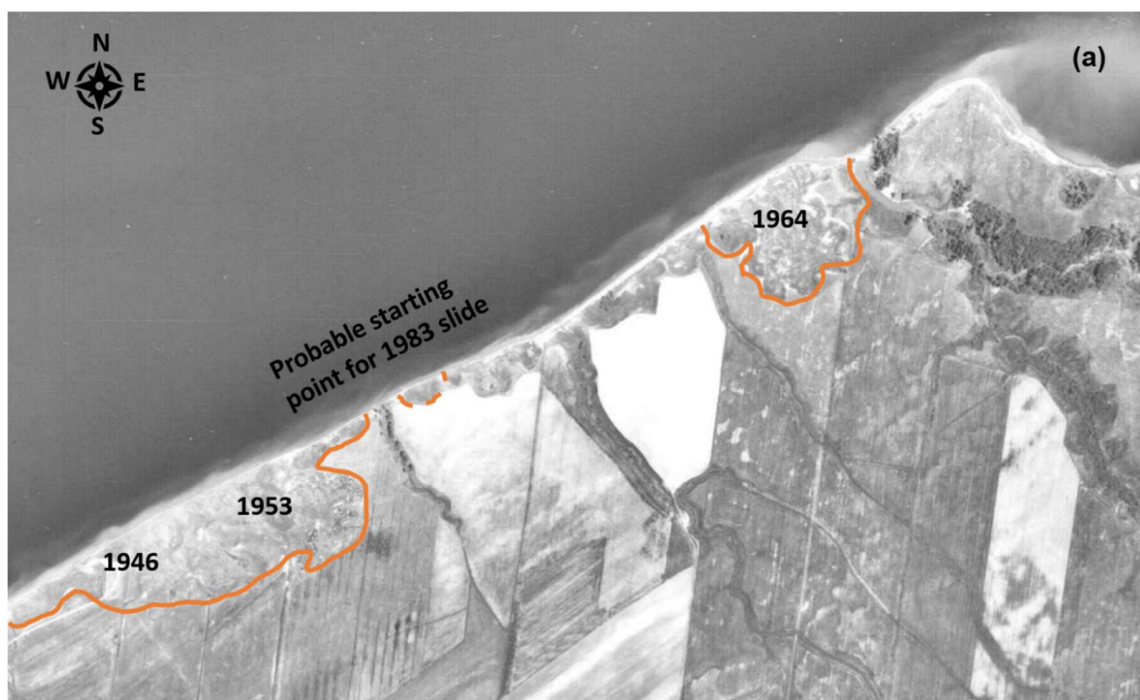
trenches were made. However, a large amount of snow was cleared from the parking areas and accumulated close to the crest of the slope which could have increased the infiltration of water during snow melt in the spring season which was aggravated further by the gentle slope of the plateau. An aerial photograph taken in 1960 (see Figure 5-3) shows that prior to this slide there were no scars in the Saint Jerome area. Nevertheless, west of the Desbiens area was already under continuous slow erosion towards the lake. Since the slide was progressing closer to the town, remedial works were carried out to ease the pressure on the toe of the slope. Trenches and drain pipes were made in the slope from the toe of the slope to the shore.



Figure 5-3 Aerial photograph from 1960 showing almost no scars near Saint Jerome but small scars towards the west.

Desbiens region has been subjected to several landslides through the years (Turmel et al. 2018). Demers et al. (2002) summarizes four landslides that took place through 1930 and 1983. The progression of these slides from 1972 to 2013 is shown in Figures 5-4 and 5-5. By the end of 2000, it can be noticed that some of these scars combined into larger scars. The aerial photograph from 2000 and LiDAR image from 2013 show almost no variation, indicating that no large landslide took place during this period. The slope stability in the Desbiens area will be analysed by considering the 1983 slide as an example. This is because a reasonable pre-failure topography may be obtained for the 1983 slide due to the availability of aerial photographs before the slide as opposed to the others.





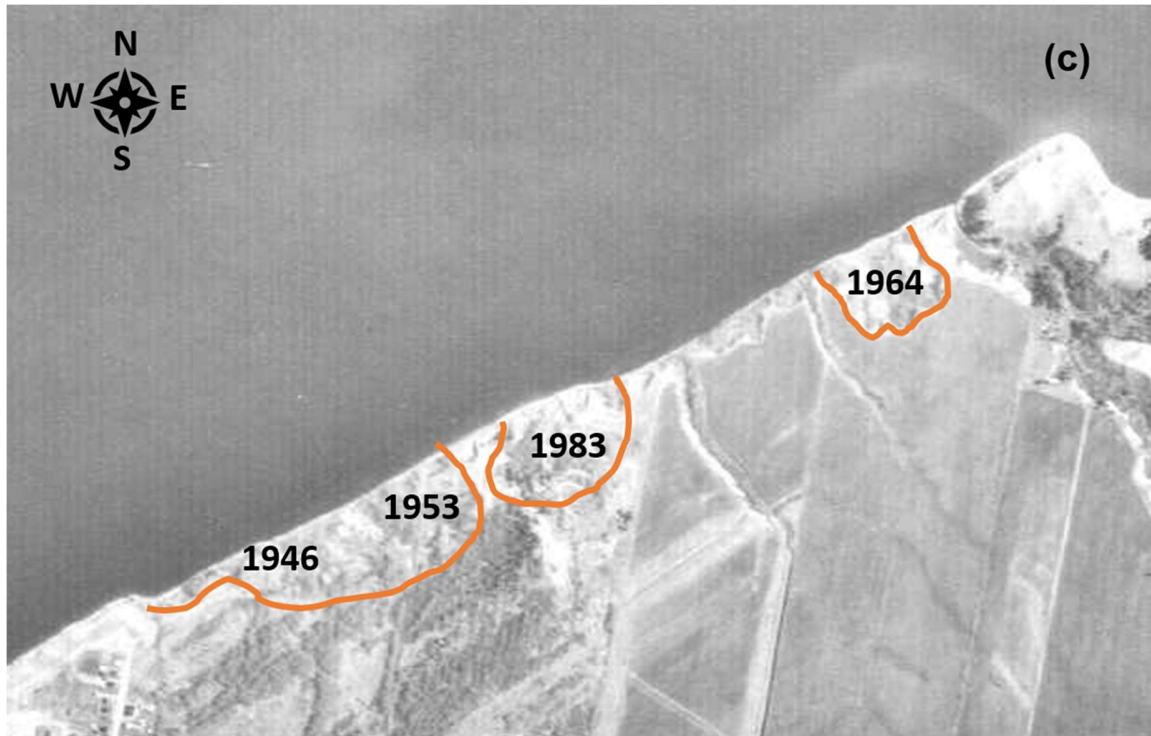


Figure 5-4 Aerial photographs from (a) 1972, (b) 1991 and (c) 2000 showing landslide scars from 1946, 1953, 1964, 1983 as well as small scars along the shore.



Figure 5-5 A 2013 LiDAR image showing landslide scars in the Desbiens region



### 5.3.2 Albanel

Albanel is the location of an old flowslide according to Ministère des Transports et de la Mobilité Durable du Québec (MTQ), although not much information is available on landslides specific to this area. However, [105] shows a map with locations of landslides in the LSJ and Saguenay areas and certain slides are identified close to Albanel. Hence, although there is evidence that this region was susceptible to landslides, it is possible that no reoccurrences have occurred in a long time. It is quite difficult to track the origin of this slide as it is believed to have occurred few thousand years ago (MTQ), although a reasonable estimate of the pre failure topography for slope stability analysis may be made based on contours from LiDAR images. The latest LiDAR image available from 2013 shows a huge landslide scar in Figure 5-6. The contour lines in Figure 5-7 passing through either side of the mouth of the scar suggested the slide topography before failure.

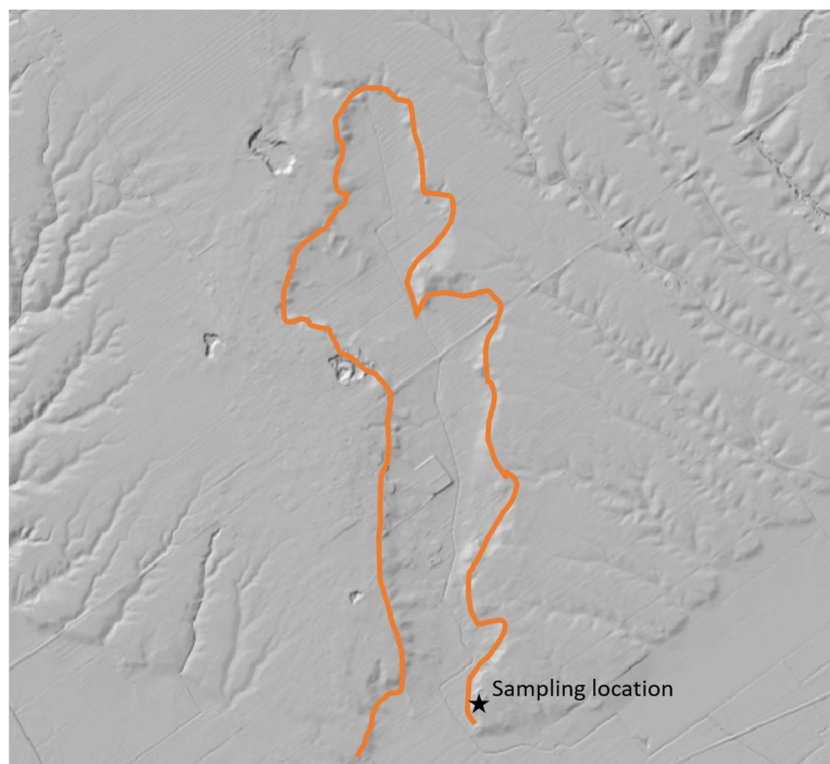


Figure 5-6 LiDAR image from 2013 showing the landslide scar in the Albanel area

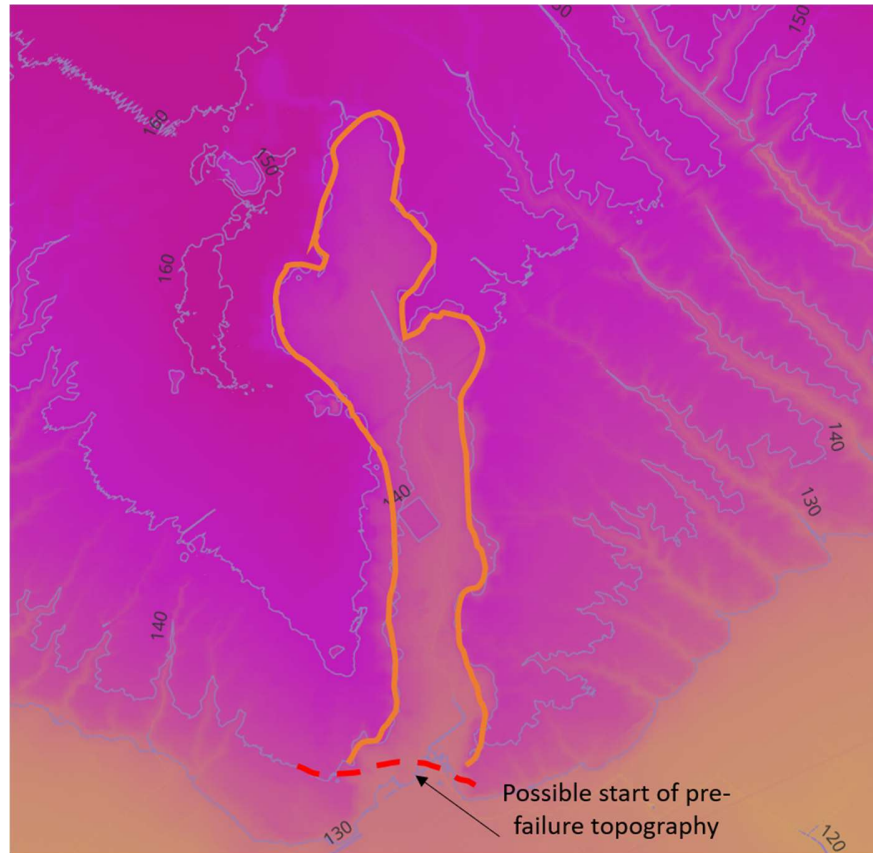


Figure 5-7 LiDAR from 2013 showing contour lines and possible start of pre-failure topography

## 5.4 METHODOLOGY

Soil sampling from the study areas was conducted by MTQ using high quality tube samplers up to a depth of 33.3 m in Desbiens. For Albanel, samples from depths of 6 to 7 m were retrieved from three adjacent boreholes. Sand layers were observed in both sampling locations in the form of interbedded sand layers within the samples. Cylindrical samples of 70 mm in diameter and 100 to 130 mm height were acquired. For the duration of the investigation, these samples were covered in wax and kept in a humidity chamber. The colour of all samples was consistent, ranging from light grey to dark grey, which is typical of sensitive clays in this area. A detailed experimental analysis and geotechnical characterization of clays from the study areas which include index properties, microstructural investigations, laboratory and field undrained shear strength measurements and stress states through triaxial tests are provided in [162]. The sampling locations are marked in Figure 5-2. Table 5-1 also summarizes several characteristics of these clays.

Table 5-1: Summary of properties of Desbiens and Albanel clays

Property	Desbiens	Albanel
Specific gravity ( $G_s$ )	2.71	2.74
Clay fraction (%):		
At sand – silt interbed	36	-
In sensitive clay layer	52	52-60
Water content, $w_N$ (%)	39 – 48	41-47
Liquid limit, $\omega_L$ (%)	43-53	48 – 51
Plastic limit, $\omega_P$ (%)	17 – 24	19 – 21
Plasticity index, $I_P$ (%)	25 – 29	26 – 30
Liquidity index, $I_L$	0.6 – 1.0	0.7 – 0.9
Salinity (g/L)	0.12-0.28	0.05
Average sensitivity ( $S_t$ )	19	32

#### 5.4.1 Prefailure topography of the study area

The progression of landslides in Desbiens area observed through aerial photographs and LiDAR images revealed that several landslides were initiated before 1950's. As such the pre-failure topography for those are difficult to obtain. However, a small erosive scar is identified in an aerial photograph taken in 1972, which is likely the incipient point of the 1983 slide in Figure 4a. To assess the initiation of landslide and its subsequent progression, the pre-failure topography prior to any scars or failures is first established. This was achieved by analyzing the LiDAR images. A digital terrain model (DTM) of the study area was developed by inputting LiDAR images into a 3D geological modelling software called LeapFrog Geo shown in Figure 8. The software allows the visualization and analysis of 2D and 3D geological models to create DTMs, cross sections, contour lines, maps and so on. There are no visible scars towards the right shore line in the DTM image in Figure 5-8

and hence can be considered as that part of the slope where prior retrogressive failures or erosive scars have not occurred. Hence, a cross section made here can provide a likely pre-failure topography for stability analysis in this region. As seen in Figure 5-8, the few cross sections considered were very similar and was utilized for further analysis.

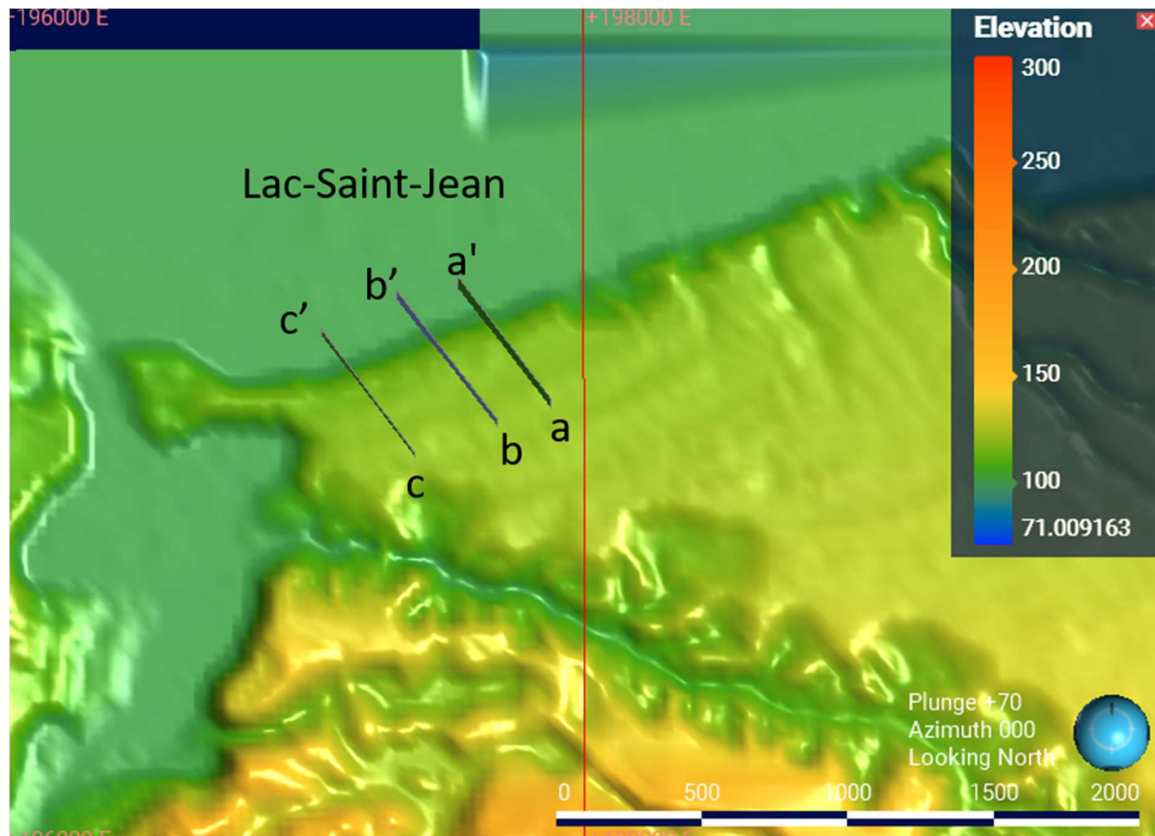


Figure 5-8 DTM of Desbiens from which pre-failure topography was developed in LeapFrog Geo software

Additionally, it has been already established that one of the main reasons for the initiation of failure in sensitive clay slopes is fluvial erosion and varying levels of water in the lake with different climatic conditions [26]. Also, since Desbiens clay slopes are located at the shore of the LSJ, the effect of ponding water at the toe of the slope cannot be ignored. As such, the level of water up to 100 m into the lake was also considered in the cross section as ponded water. The depth of the water in the lake was obtained from nautical charts of the LSJ. The generated cross section shows a slope height and angle of 15 m and 22° respectively with varying water depths from the to 100 m into the lake (1 m depth) in Figure 5-11a.

At Albanel, the age of the landslide makes it very difficult to arrive at a pre-failure topography. Nevertheless, as in the case of Desbiens, LiDAR images were used to generate a DTM. Multiple sections across (sections 1-1' to 9-9') and a section parallel to the scar (section X-X') were used to arrive at elevation points A to I that could be the points for the prefailure topography. The pre-failure topography was thus considered as if the scar in the middle was not present with slope and elevations similar to the right and left hand side of the scar. The depth of the scar is shown through some of the cross sections in Figure 5-10. The last section (section at A\_BH) signifies the section at the borehole location from which samples for experimental studies were taken. Section 1-1' in Figure 5-10 shows how the left and right end of the topography was determined to get point A in Figure 5-9. A similar approach is carried out for all the sections to arrive at points up to I. According to Ministère des Transports du Québec (MTQ), the samples that were extracted from a depth of 6 m, were from the failure plane of the ancient landslide. Hence the toe of the slope for the prefailure topography should start 6 m below the current ground elevation. The entire scar is quite long as shown in Figure 5-9, hence only the beginning of the slope i.e the first 50 m with a slope height of 6 m is considered for further stability analysis as seen in Figure 5-11b.

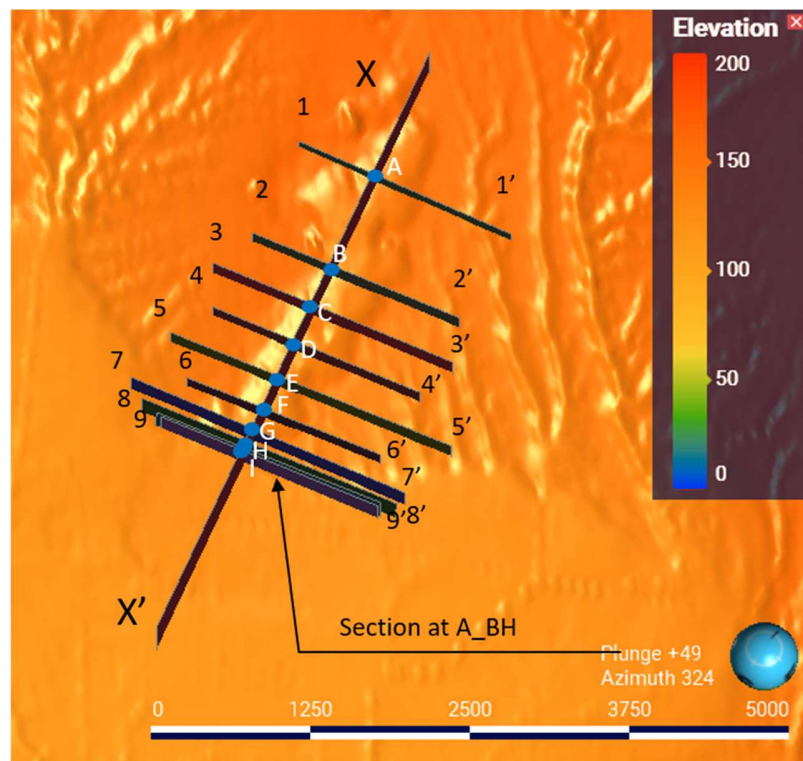
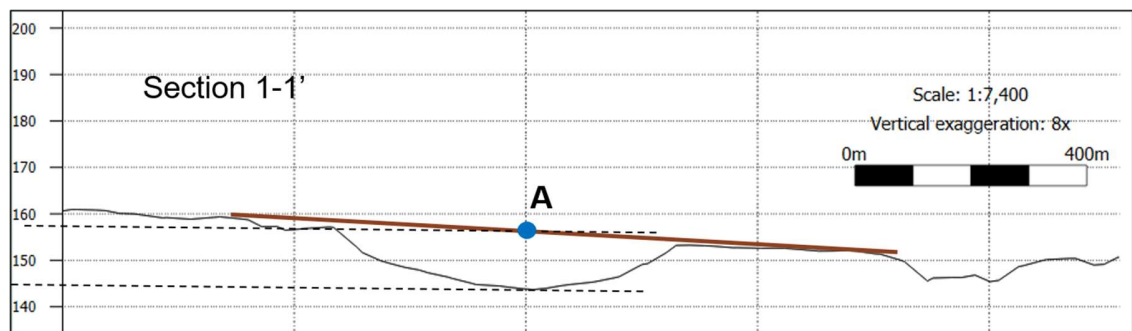


Figure 5-9 DTM of Albanel from which the pre-failure topography was developed in LeapFrog Geo software



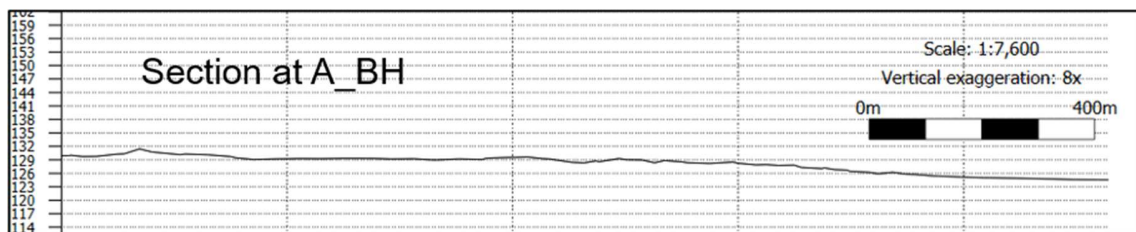
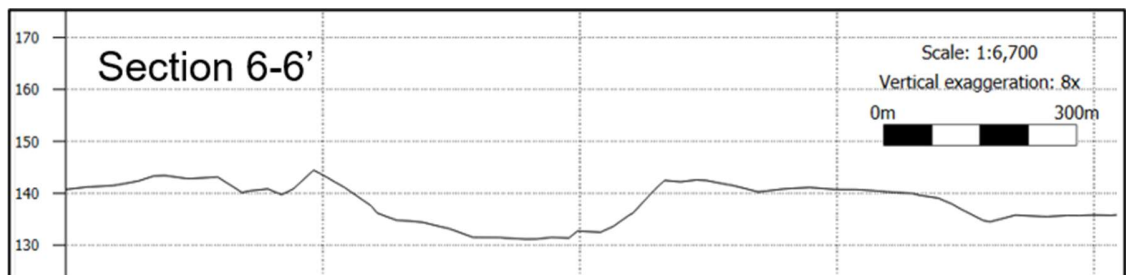
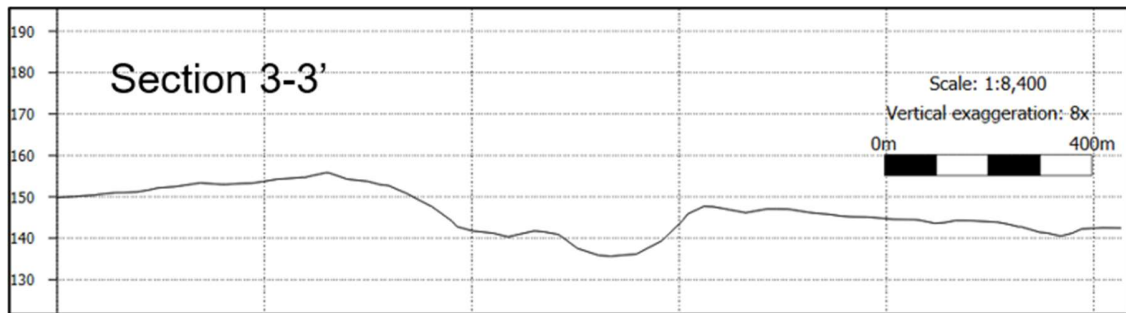
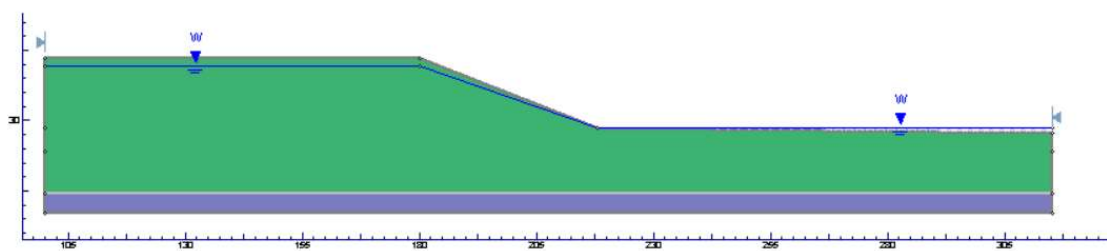
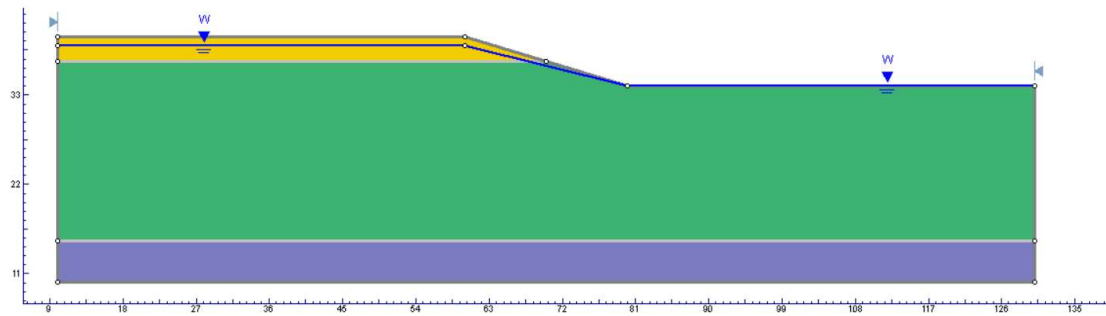


Figure 5-10 Examples of few sections extracted from the LiDAR image of Albanel in LeapFrog Geo



(a)





(b)

Figure 5-11 Models used for stability analysis of (a) Desbiens and (b) Albanel sites

#### 5.4.2 Estimation of geotechnical parameters on large scale

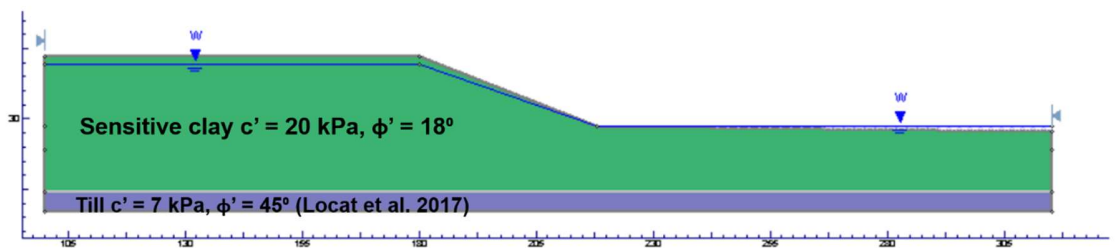
Based on geological history, the reduction in slope stability in sensitive clays of the Laflamme Sea is the result of long term fluvial erosion on the banks of water bodies with evolving topography and can be attributed as a long term phenomenon. As the slope becomes marginally stable, a sudden load in the form of loss of resisting forces (e.g. erosion, excavation), increase in driving forces (e.g. human activities such as construction) or increase in pore pressure (e.g. snowmelt and heavy rainfall) can eventually lead to the collapse of the slope under undrained loading. Although it is a common approach to study sensitive clay slopes from the perspective of a total stress approach, whatever be the triggering factor, the first slide prior to retrogressive failure of a sensitive clay slope occurs due to long term erosion and it is analysed in this chapter using an effective stress approach.[56]. The use of a total stress analysis for the first slide analysis can grossly overestimate the factor of safety and the results could be overstated [71].

The use of geotechnical parameters from tests on laboratory samples for slope stability analysis like cohesion and friction angle could have some scale effect when applied to large clay slopes. Additionally, due to sampling limitations and sample disturbances it may not be possible to conduct a comprehensive analysis of geotechnical parameters for each depth and the tests used for the determination of cohesion and friction angle for a soil may be conducted on samples from different depths. This could create a certain amount of uncertainty. Hence a back analysis method is adopted to determine geotechnical parameters on a large scale. The cohesion

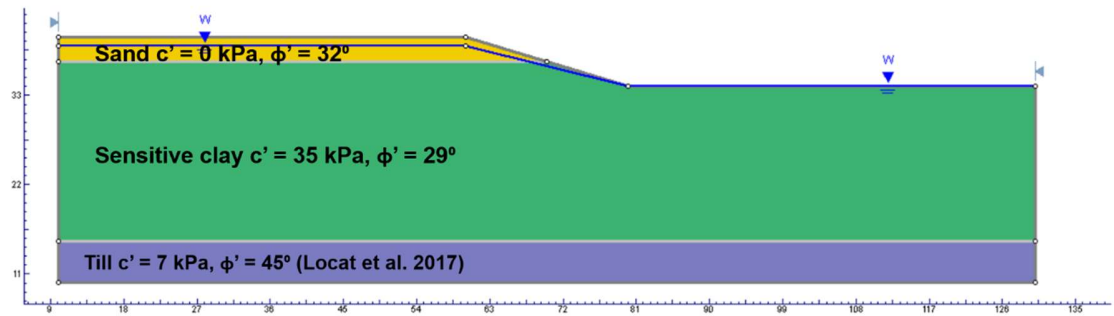


and friction angle from experimental results on Desbiens and Albanel from Chapter 4 is taken as the base values and are decreased until marginal stability i.e. Factor of Safety (FOS)  $\approx 1$  is achieved. This would be the condition from which a retrogressive failure may take place if suitable factors for such failure occurs. The analysis is carried out using limit equilibrium modelling in Slide 2D and the results are further checked in finite element modelling using RS2 software.

The Mohr-Coulomb (MC) parameters used for sensitive clay layers were obtained based on triaxial tests conducted in Chapter 4 of this thesis. For Desbiens,  $c'$  and  $\phi'$  of 20 kPa and  $18^\circ$  respectively was obtained. It may be noted that the triaxial samples used in the development of the strength envelope are obtained from varying depths within the borehole at Desbiens. A till layer was observed at 29 m. In the case of Albanel, a 3m thick layer of sand was observed from the surface as well as a till layer beyond 25 m depth. The MC parameters for the sensitive clay layer was obtained as  $c'$  of 35 kPa and  $\phi'$  of  $29^\circ$ . The MC parameters were assumed as  $c'=5$  kPa,  $\phi'=35^\circ$  for sand and  $c'=7$  kPa,  $\phi'=40^\circ$  for till layer from literature [9]. The model used in Slide 2D along with initial  $c'$  and  $\phi'$  is shown in Figure 5-12. The factor of safety (FOS) was determined by Morgenstern - Price method. The Morgenstern-Price method is a popular approach utilizing limit equilibrium method of slices to analyse stability of slopes [163]. The force and moment equilibrium equations for each slice is represented in a differential and integral form respectively which is solved further by a Newton-Raphson approach to arrive at the FOS [164]. Unlike other simpler methods of stability analysis, it can account for non-circular failure surfaces and variable pore water pressures, making it more versatile and accurate.



(a)



(b)

Figure 5-12 Model for (a) Desbiens and (b) Albanel in Slide 2 D with initial  $c'$  and  $\phi'$  used for analysis

## 5.5 RESULTS AND INTERPRETATIONS

### 5.5.1 Slope stability analysis

Stability analysis was conducted in both Slide 2 and RS2 which utilizes limit equilibrium and finite element model respectively. Ideally the FOS / strength reduction factor (SRF) obtained using both approaches should be comparable. The main advantage that RS2 has over Slide 2 is that it offers a detailed stress and deformation analysis along with SRF. The slope models of Desbiens and Albanel are interpreted using both methods and the results are discussed below.

#### 5.5.1.1 Limit equilibrium model

The slope stability analysis conducted in Slide 2 gives an understanding of the first slide and the likelihood of future retrogressive failures. In the case of Desbiens, the water table is considered to be 1 m from the surface based on CPT results. Upon observation of CPT results from Chapter 4 (Figure 4-16a), a linear variation in cone tip resistance can be seen and a significant increase in resistance from 15m. Thus the sensitive clay layer can be divided into two layers – a sensitive clay layer of lower strength upto 15 m and then a sensitive clay layer of higher strength from 15 m to the till layer at 29 m. Since it is likely that the failure plane will pass through the sensitive clay layer of lower strength, back analysis is applied to this layer. Triaxial results from Chapter 4 had shown that softening in sensitive clays of Desbiens and Albanel were primarily decided by cohesion softening and no friction softening could be observed (Table 4-4). Hence back analysis to reach

marginal stability was carried out by reducing the cohesion in the sensitive clay layer of lower strength. A FOS of 1.034 was achieved when cohesion was reduced to 14 kPa from the initial 20 kPa. The effective MC parameters for sensitive clay layer of higher strength was kept the same. The results for this analysis including the MC parameters are shown in Figure 5-13.

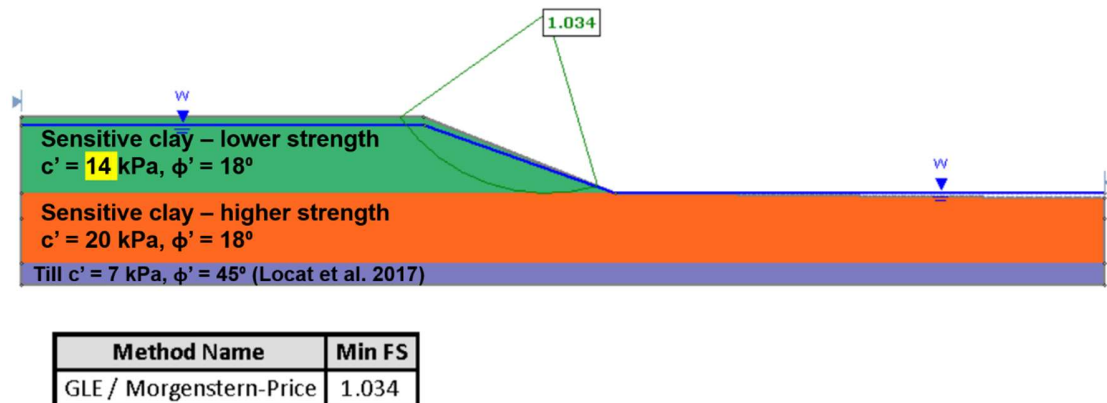
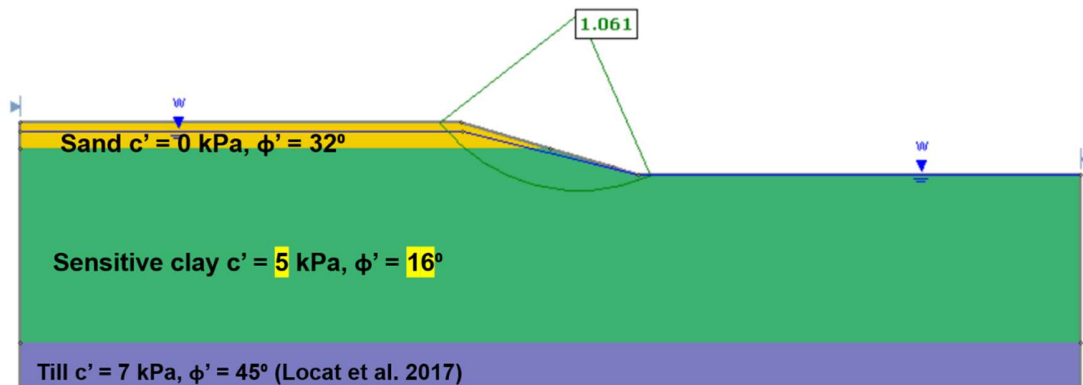


Figure 5-13 Slope stability analysis showing marginally stable Desbiens slope in Slide 2D

For Albanel, the water table is considered to be at 1.5 m from surface according to CPT data. As in the case of Desbiens, a back analysis method was adopted for Albanel to determine the MC parameters that would provide a marginally stable slope through a trial-and-error analysis of the experimentally determined MC parameters. The CPT data for Albanel shows a more or less consistent cone tip resistance with depth (Figure 4-17a) and hence a single sensitive clay layer is considered for back analysis. Here, both cohesion and friction angle had to be reduced to achieve marginal stability. This was achieved at  $c' = 5$  kPa and  $\phi' = 16^\circ$  when FOS was 1.061. . The results for this analysis including the MC parameters are shown in Figure 5-14.



Method Name	Min FS
GLE / Morgenstern-Price	1.061

Figure 5-14 Slope stability analysis showing marginally stable Albanel slope in Slide 2D

#### 5.5.1.2 Finite elemnt model

The finite element analysis uses a 2D plain strain geometry with 3000 three noded triangular elements. As in LE analysis, an effective stress analysis was carried out. Bottom and lateral boundaries were fixed in both directions. The soil is defined as an elastoplastic material with Mohr-Coulom failure criterion. The effective Mohr Coulomb parameters that caused marginal stability in limit equilibrium analysis was used again for the finite element modelling in RS2 for both Desbiens and Albanel to generate the failure plane and shear deformations. Young's Modulus for sensitive clay layer was chosen based on triaxial test results from Chapter 4 and that for sand and till was based on default values in RS2. Poisson's ratio for sensitive clay layer was chosen as 0.33 based on [25] and for sand and till from [165]. Porosity was set to 0.5. The model parameters used in the analysis for Desbiens and Albanel are shown in Table 5-2 and 5-3 respectively.

Table 5-2 Model parameters used in finite element modelling for Desbiens clay slope

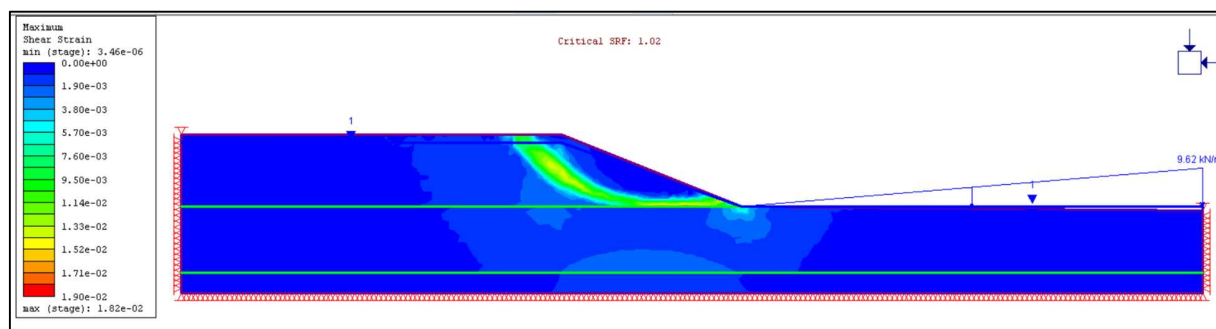
Soil layer	Young's Modulus (MPa)	Poisson's ratio
Sensitive clay of lower strength	20	0.33

Sensitive clay of higher strength	22	0.33
Till	50	0.45

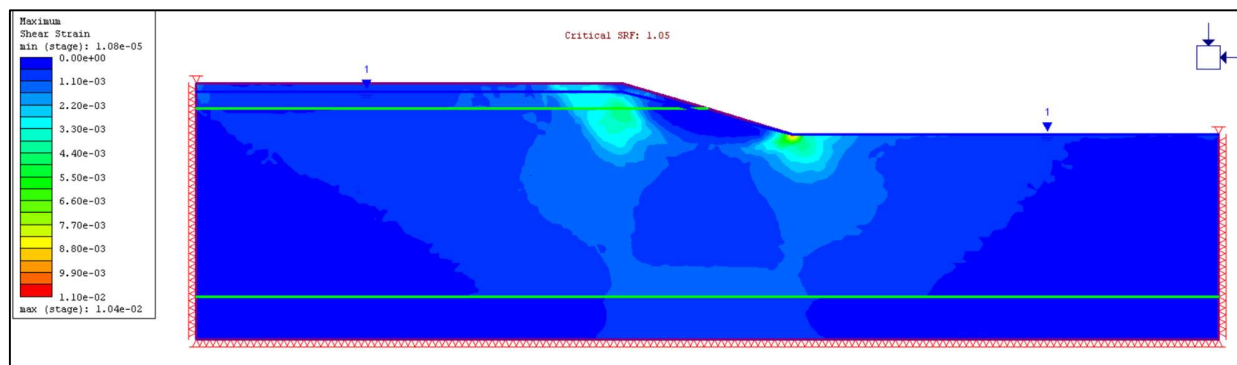
Table 5-3 Model parameters used in finite elemnt modelling for Albanel clay slope

Soil layer	Young's Modulus (MPa)	Poisson's ratio
Sand	50	0.25
Sensitive clay	20	0.33
Till	50	0.45

. The SRF obtained – 1.02 for Desbiens and 1.06 for Albanel, is found to be consistent with the results of LE analysis as seen in Figure 5-15.



(a)



(b)

Figure 5-15 Finite element modelling results of (a) Desbiens and (b) Albanel in RS2 software

### 5.5.2 Overall summary

The back analysis conducted revealed that, in the case of Desbiens, effective cohesion on large scale causing marginal stability (14 kPa) was lower than that determined in the laboratory (20 kPa). However, for Albanel both effective cohesion and friction angle had to be reduced from  $c' = 35$  kPa and  $\phi' = 29^\circ$  to  $c' = 5$  kPa and  $\phi' = 16^\circ$ . Some other observations can also be inferred from LiDAR image of Albanel in Figure 5-16. A huge landslide deposit/ debris can be observed at the foot of the ancient scar in the LiDAR image. The amount of debris seen seems to suggest that quite a lot of material was moved which could indicate that the slope was quite high. However, assumptions based on sections from current topography provided a slope height of only 6 m. This could mean that the analysis with respect to Albanel are not fully conclusive and the information at hand may not be enough to predict pre-failure topographies for scars as old as 1000 years. The topography would change drastically over the years and the shear strength parameters of the soil could have also improved. This can also be noticed by higher stress states of Albanel in comparison to Desbiens.

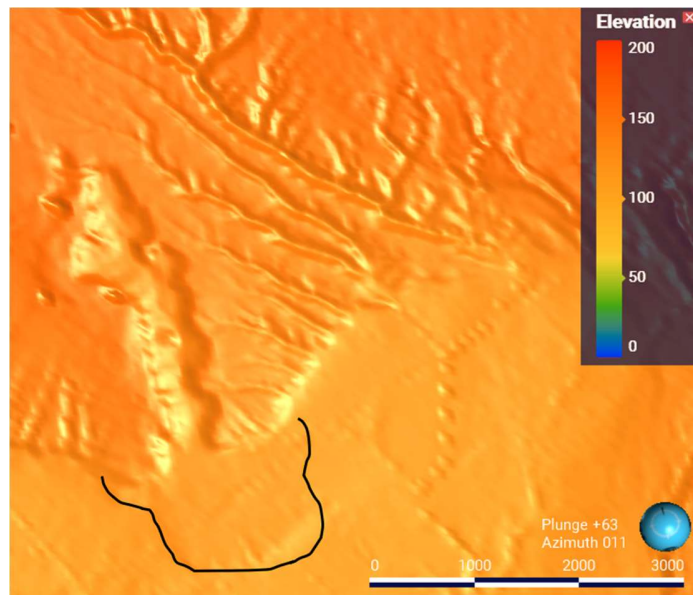


Figure 5-16 LiDAR image of Albanel showing landslide debris at foot of the scar

A more detailed analysis in terms of strain softening and remoulding energy is conducted for Desbiens and Albanel to verify possibility of retrogressive landslides. The strain softening equation developed in Chapter 3 of this thesis marked Equation 3-13 is applied to triaxial test results from Chapter 4 and the complete stress - strain curve until remoulded strength is obtained. The area under the curve can be interpreted as remoulding energy and is obtained by integrating the curve between peak and remoulded strain limits as shown in Equation 5-1.

$$E_R = \int_{\gamma_p}^{\gamma_r} s_u \quad (5-1)$$

The remoulding energies for Desbiens and Albanel was obtained as 25.62 kJ/m<sup>3</sup> and 58 kJ/m<sup>3</sup> respectively. According to [11], large retrogressive landslides are likely to take place when remoulding energy is less than 40 kJ/m<sup>3</sup>. Thus, according to the remoulding energy values obtained, retrogressive landslides are likely to take place in the case of Desbiens and may not be likely in the case of Albanel. This also indicates that it is highly likely that soils in Albanel region have improved and the topography has changed drastically since the occurrence of past landslides that more retrogressive slides are not likely to take place in this region.

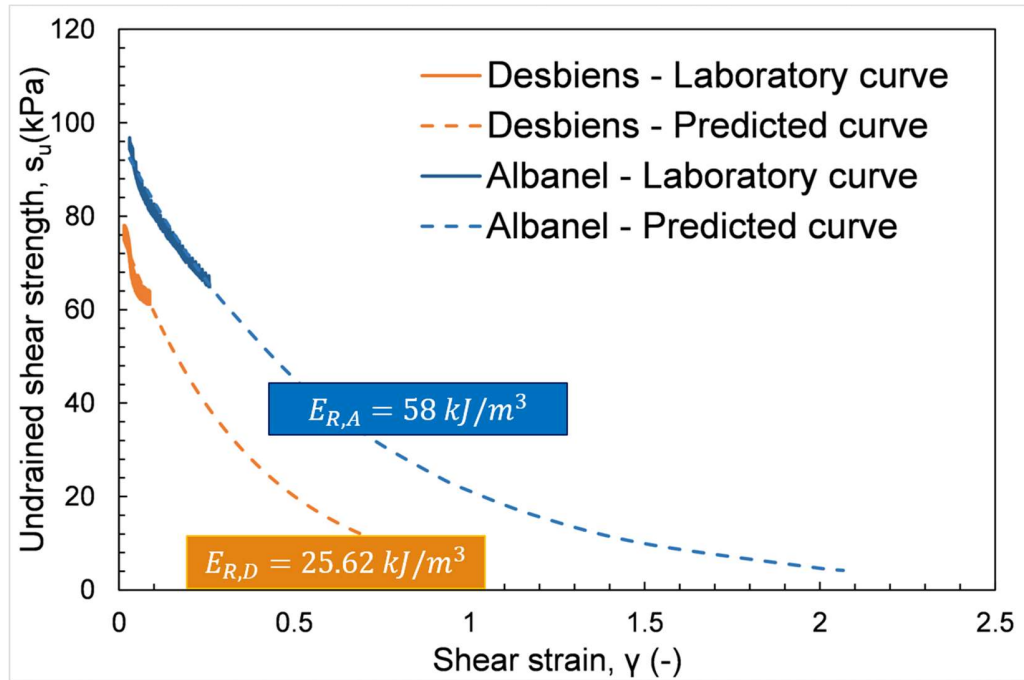


Figure 5-17 Predicted strain softening curve until remoulded state of Desbiens and Alabani for the determination of remoulding energy

This paper proposes a methodology by which analytical methods and photogrammetric tools may be used to interpret slope stability analyses in sensitive clays before conducting strenuous experimental and numerical modelling studies. LiDAR and aerial images may be used to develop topographies that can be analysed using simple LE methods for first slide estimate. Furthermore, remoulding energy determined through application of an appropriate strain softening tool can be used to check likelihood of retrogressive slides which again allows for the judgement of need for carrying out complex numerical analysis.

## 5.6 CONCLUSIONS

Slope stability in sensitive clays can be difficult to analyse and often requires complex analytical and numerical models for interpretation. In most cases, a more effective analysis is achieved through the use of multiple tools including topographical data, experimental results and numerical modelling. In this paper, a similar analysis is carried out by focussing on the clay slopes in the Laflamme basin. Likewise, a methodology may be adopted for initial assessment of slope stability and landslide progression in any region. Since complex numerical techniques are often laborious and time consuming, such initial assessments help to make



judgements in terms of the requirement of more complex analyses. Slope stability studies in Laflamme region of Eastern Canada are quite scarce, probably due to lack of sufficient detailed geotechnical investigations and assessments. This study deals with clay slopes in the Laflamme basin with a special focus on Desbiens and Albanel. Desbiens region suffers constant fluvial erosion and the area of erosive scars are not far from populated areas. Hence, this study provides an initial assessment for further complex modelling for the slopes in this region. An effective stress analysis using LE analysis and finite element modelling showed that slopes in this region could be marginally stable and can later lead to retrogressive failures. A further analysis in terms of remoulding energy as a criterion for retrogressive landslides is provided to judge the likelihood of retrogressive failures in sensitive clays. The analysis shows that Albanel clay slopes have stabilised over time and the soils have improved making them unlikely for further retrogressive slides in this region.

## CHAPTER 6

### 6.1 CONCLUSIONS

The thorough observations and analysis conducted in this study paves way to a more comprehensive understanding of landslides in sensitive clays, in particular, to the lesser investigated Laflamme Sea basin of Eastern Canada. The following primary conclusions are drawn:

- Remoulding energy was identified as an important criterion that can be utilised in the analysis of retrogressive landslides in sensitive clays and is primarily dependant on the stress history of the soil and the slope geometry as opposed to other physical parameters of the soil. This led to the understanding that sensitive clays, similar in properties, could exhibit varied strain softening behaviours depending on the stress and geological history of the clay deposit.
- An exponential strain softening model to predict strain softening in sensitive clays was developed using triaxial testing results. The proposed model allowed for the determination of remoulded strain parameter from laboratory results simulating field conditions, thereby satisfying the ambiguity with respect to large deformation strains.
- A detailed geotechnical characterization study, including physical, chemical and mechanical investigations was conducted on Laflamme clays of Eastern Canada. The study highlighted that the Laflamme clays are highly leached and more overconsolidated exhibiting dilative behaviours and higher remoulded shear strengths in comparison to Champlain clays, further calling to attention that retrogressive failures could take place even when remoulded undrained shear strengths are not extremely low, if the right conditions exist.
- Limit equilibrium analysis with real-scale slope cross sections in Laflamme region yielded marginally stable slopes which could suffer retrogressive failures if triggered. The geology of a region is shown to play a significant role in slope stability and a distinction among various sedimentary basins in Eastern Canada while analysing retrogressive failures and slope stability is necessary for precision.

## 6.2 RECOMMENDATIONS

The findings of this study present the following potential directions for future research:

- **Numerical simulations:** The proposed strain softening model maybe incorporated into computational software used in modelling sensitive clay landslides. Since the model parameters can be easily obtained through laboratory testing, the model can be utilised in the analysis of less popular and unknown landslides without significant knowledge on the large deformation parameters.
- **Dynamic parameters:** The laboratory investigations can be extended to cyclic testing to understand the dynamic parameters for Laflamme clays. Since geotechnical investigations in the Laflamme basin are very limited in general, a study focussed towards the cyclic stress – strain behaviour of the clay would provide useful information for analytical and numerical investigations on landslides in sensitive clays.
- **Region-specific criteria for retrogression:** More experimental investigations and slope stability studies can generate sufficient data to form criteria for retrogression specific to Laflamme clays, considering their significant difference in properties and behaviour with respect to Champlain clays. This could lead to a more comprehensive understanding of the various types of sensitive clays in the Eastern Canadian region.

## REFERENCES

1. Torrance, J.K.: Towards a general model of quick clay development. *Sedimentology*. 31, 595–598 (1983). <https://doi.org/10.1111/j.1365-3091.1984.tb01822.x>
2. Giles, D.P.: Quick clay behaviour in sensitive quaternary marine clays – A UK perspective. *Geological Society Engineering Geology Special Publication*. 29, 205–221 (2020). <https://doi.org/10.1144/EGSP29.7>
3. L’Heureux, J.-S., Locat, A., Leroueil, S., Demers, D., Locat, J.: Landslides in sensitive clays - From geoscience to risk management. In: *Landslides in Sensitive Clays From Geoscience to Risk Management*. pp. 1–12 (2014)
4. Norsk Geoteknisk Forening (NGF): Melding nr. 2 Symboler og definisjoner i geoteknikk (In Norwegian). (2013)
5. Karlsson, R., Hansbo, S.: *Soil Classification and Identification: Byggeforskningsradet*. (1989)
6. Canadian Geotechnical Society (CGS): *Errata – Canadian foundation engineering manual*, 4th edn. (2013)
7. TAVENAS F, CHAGNON JY, LA ROCHELLE P: Saint- Jean- Vianney landslide. Observations and eyewitnesses accounts. *Canadian Geotechnical Journal*. 8, 463–478 (1971). <https://doi.org/10.1139/t71-048>
8. Lefebvre, G., Leboeuf, D., Hornych, P., Tanguay, L.: Slope failure associated with the 1988 Saguenay earthquake, Quebec, Canada. *Canadian Geotechnical Journal*. 29, 117–130 (1992). <https://doi.org/10.1139/t92-013>
9. Locat, A., Locat, P., Demers, D., Leroueil, S., Robitaille, D., Lefebvre, G.: The saint-jude landslide of 10 May 2010, Quebec, Canada: Investigation and characterization of the landslide and its failure mechanism. *Canadian Geotechnical Journal*. 54, 1357–1374 (2017). <https://doi.org/10.1139/cgj-2017-0085>
10. Tremblay-Auger, F., Locat, A., Leroueil, S., Locat, P., Demers, D., Therrien, J., Mompin, R.: The 2016 landslide at saint-luc-de-vincennes, quebec: Geotechnical and morphological analysis of a combined flowslide and spread. *Canadian Geotechnical Journal*. 58, 295–304 (2021). <https://doi.org/10.1139/cgj-2019-0671>
11. Tavenas, F., Leroueil, S., Flon, P., Lebius, J.: Remoulding energy and risk of slide retrogression in sensitive clays p 425. *Symposium on slopes on soft clays*. (1983)
12. Skempton, A.W., Northey, R.D.: The sensitivity of clays. *Geotechnique*. 3, 30–53 (1952). <https://doi.org/10.1680/geot.1952.3.1.30>
13. Thakur, V., Degago, S.A.: Disintegration energy of sensitive clays. *Geotechnique Letters*. 3, 20–25 (2013). <https://doi.org/10.1680/geolett.12.00062>
14. Skempton, A.W.: Long-Term Stability of Clay Slopes. *Géotechnique*. 14, 77–102 (1964). <https://doi.org/10.1680/geot.1964.14.2.77>

15. Bernander, S.: Progressive landslides in long natural slopes. (2000)
16. Thakur, V.: Strain Localization in sensitive soft clays, (2007)
17. Gylland, A.S., Jostad, H.P., Nordal, S.: Experimental study of strain localization in sensitive clays. *Acta Geotech.* 9, 227–240 (2014). <https://doi.org/10.1007/s11440-013-0217-8>
18. Locat, A., Jostad, H.P., Leroueil, S.: Numerical modeling of progressive failure and its implications for spreads in sensitive clays. *Canadian Geotechnical Journal.* 50, 961–978 (2013). <https://doi.org/10.1139/cgj-2012-0390>
19. Dey, R., Hawlader, B., Phillips, R., Soga, K.: Modelling of large deformation behaviour of marine sensitive clays and its application to submarine slope stability analysis. *Canadian Geotechnical Journal.* (2016)
20. Chatillon, M.: A literature review of stability of slopes in Champlain clay. (1974)
21. Bouchard, R., Dion, D.J., Tavenas, F.: Origine de la préconsolidation des argiles du Saguenay, Québec. *Canadaian Geotechnical Journal.* 20, 315–328 (1983)
22. Tran, Q.A., Sołowski, W.: Generalized Interpolation Material Point Method modelling of large deformation problems including strain-rate effects – Application to penetration and progressive failure problems. *Comput Geotech.* 106, 249–265 (2019). <https://doi.org/10.1016/j.compgeo.2018.10.020>
23. Shan, Z., Zhang, W., Wang, D., Wang, L.: Numerical investigations of retrogressive failure in sensitive clays: revisiting 1994 Sainte-Monique slide, Quebec. *Landslides.* 18, 1327–1336 (2021). <https://doi.org/10.1007/s10346-020-01567-4>
24. Lian, Y., Bui, H.H., Nguyen, G.D., Haque, A.: An effective and stabilised (u–pl) SPH framework for large deformation and failure analysis of saturated porous media. *Comput Methods Appl Mech Eng.* 408, 1–33 (2023). <https://doi.org/10.1016/j.cma.2023.115967>
25. Urmi, Z.A., Chavali, R.V.P., Saeidi, A., Yerro, A.: Analytical and numerical assessment of the effect of erosion in sensitive clay landslide: A case study of Saint-Jude Landslide . *Geo Calgary 2022.* (2022)
26. Demers, D., Robitaille, D., Locat, P., Potvin, J.: Inventory of large landslides in sensitive clays in the province of Quebec, Canada: Preliminary analysis. In: *Landslides in Sensitive Clays From Geoscience to Risk Management.* pp. 77–89 (2014)
27. Locat, J., St-Gelais, D.: Nature of sensitive clays from Quebec. In: *Landslides in Sensitive Clays From Geoscience to Risk Management.* pp. 25–37 (2014)
28. Mitchell, R.J., Markell, A.R.: Flowsliding in Sensitive Soils. *Canadian Geotechnical Journal.* 11, 11–31 (1974). <https://doi.org/10.1139/t74-002>
29. Lebius, J., Robert, J.-M., Rissmann, P.: Reginal mapping of landslide hazard in Quebec. (1983)
30. Leroueil, S., Tavenas, F., Le Bihan, J.-P.: Propriétés caractéristiques des argiles de l’est du Canada. *Canadian Geotechnical Journal.* 20, (1983)

31. Locat, J., Demers, D.: Viscosity, yield stress, remolded strength, and liquidity index relationships for sensitive clays. *Canadian Geotechnical Journal*. 25, 799–806 (1988). <https://doi.org/10.1139/t88-088>
32. Quinn, P.E., Diederichs, M.S., Rowe, R.K., Hutchinson, D.J.: A new model for large landslides in sensitive clay using a fracture mechanics approach. *Canadian Geotechnical Journal*. 48, 1151–1162 (2011). <https://doi.org/10.1139/t11-025>
33. Thakur, V., Degago, S.A., Oset, F., Dolva, B.K., Aab  , R.: A new approach to assess the potential for flow slide in sensitive clays. *18th International Conference on Soil Mechanics and Geotechnical Engineering: Challenges and Innovations in Geotechnics, ICSMGE 2013*. 3, 2265–2268 (2013)
34. Levesque, C.L., Locat, J., Leroueil, S.: Characterisation of postglacial sediments of the Saguenay Fjord, Quebec, Canada. *Characterisation and Engineering Properties of Natural Soils*. 3–4, 2645–2677 (2007). <https://doi.org/10.1201/noe0415426916.ch27>
35. Leroueil, S., Locat, P., Picarelli, L., Lee, H., Faure, R.: Geotechnical characterization of slope movements. *Landslides*. 53–74 (1996)
36. Locat, P.: Remaniement et mobilit   des d  bris de glissements de terrain dans les argiles sensibles de l’est du Canada. *4th Canadian Conference on Geohazards*. 1971, 594 (2008)
37. Thakur, V., Gylland, A.S.: In-situ determination of disintegration energy for soft sensitive clays. *68e Conf  rence Canadienne de G  otechnique et 7e Conf  rence Canadienne sur le Perg  lisol*, 20 au 23 septembre 2015, Qu  bec, Qu  bec. (2015)
38. Tanaka, H., Hirabayashi, H., Matsuoka, T., Kaneko, H.: Use of fall cone test as measurement of shear strength for soft clay materials. *Soils and Foundations*. 52, 590–599 (2012). <https://doi.org/10.1016/j.sandf.2012.07.002>
39. Burland, J.B.: On the compressibility and shear strength of natural clays. *Geotechnique*. 40, 329–378 (1990). <https://doi.org/10.1680/geot.1990.40.3.329>
40. Eden, W.J., Mitchell, R.J.: The mechanics of landslides in Leda clay. *Canadian*. 7, 285–296 (1970)
41. Bjerrum: Stability of natural slopes in quick clays. (1955)
42. Odenstad, S.: The landslide in Skoptrop on the Lidan river. *Royal Swedish Geotechnical Institute Proceedings No. 4*. (1951)
43. Carson, M.A.: On the retrogression of landslides in sensitive muddy sediments. *Canadian Geotechnical Journal*. 14, 582–602 (1977). <https://doi.org/10.1139/t79-047>
44. Locat, A., Leroueil, S., Bernander, S., Demers, D., Jostad, H.P., Ouehb, L.: Progressive failures in eastern canadian and scandinavian sensitive clays. *Canadian Geotechnical Journal*. 48, 1696–1712 (2011). <https://doi.org/10.1139/t11-059>
45. Leroueil, S., Locat, J., Picarelli, L., Lee, H., Faure, R.: Geotechnical charectarization of slope movements, (1996)

46. Kennedy, R., Take, W.A., Siemens, G.: Geotechnical centrifuge modelling of retrogressive sensitive clay landslides. *Canadian Geotechnical Journal*. 58, 1452–1465 (2021). <https://doi.org/10.1139/cgj-2019-0677>
47. Potvin, J.J., Woeller, D., Sharp, J., Take, W.A.: Stratigraphic profiling, slip surface detection, and assessment of remolding in sensitive clay landslides using the CPT. *Canadian Geotechnical Journal*. 59, 1146–1160 (2022). <https://doi.org/10.1139/cgj-2019-0171>
48. Lafleur, J., Lefebvre, G.: Groundwater regime associated with slope stability in Champlain clay deposits. *Canadian Geotechnical Journal*. 17, 44–53 (1980). <https://doi.org/10.1139/t80-004>
49. Lefebvre, G.: Soft sensitive clays. Special Report - National Research Council, Transportation Research Board. 247, 607–619 (1996)
50. Locat, A., Leroueil, S., Jostad, H.P.: *Landslides in Sensitive Clays*. (2014)
51. Hungr, O., Leroueil, S., Picarelli, L.: The Varnes classification of landslide types, an update. *Landslides*. 11, 167–194 (2014). <https://doi.org/10.1007/s10346-013-0436-y>
52. Locat, A., Leroueil, S., Bernander, S., Demers, D., Jostad, H.P., Ouehb, L.: Progressive failures in eastern canadian and scandinavian sensitive clays. *Canadian Geotechnical Journal*. 48, 1696–1712 (2011). <https://doi.org/10.1139/t11-059>
53. Mollard, J.D., Hughes, G.T.: Earthflows in the Grondines and Trois- Rivières areas, Quebec: Discussion. *Can J Earth Sci*. 10, 324–326 (1973)
54. Quinn, P.E., Diederichs, M.S., Hutchinson, D.J., Rowe, R.K.: An Exploration of the Mechanics of Retrogressive Landslides in Sensitive Clay. *Proceedings of the 60th 729 Canadian Geotechnical Conference and 8th Joint CGS/IAH-CNC Groundwater 730 conference*, Ottawa, Ontario. 721–727 (2007)
55. Bishop, A.W.: The influence of progressive failure on the choice of the method of stability analysis. *Geotechnique*. 168–172 (1971)
56. Lefebvre, G.: Fourth Canadian Geotechnical Colloquium: Strength and slope stability in Canadian soft clay deposits. *Canadian Geotechnical Journal*. 18, 420–442 (1981). <https://doi.org/10.1139/t81-047>
57. Thakur, V., Degago, S.A., Oset, F., Dolva, B.K., Aabøe, R.: A new approach to assess the potential for flow slide in sensitive clays. *18th International Conference on Soil Mechanics and Geotechnical Engineering: Challenges and Innovations in Geotechnics, ICSMGE 2013*. 3, 2265–2268 (2013)
58. Turmel, D., Locat, J., Leroueil, S.: Empirical estimation of the retrogression and the runout distance of sensitive clay flowslides Structuration of sensitive clays View project Morphological evolution of Wabush Lake, Labrador, Canada View project. (2018)
59. Geertsema, M., L’Heureux, J.-S.: Controls on the dimensions of landslides in sensitive clays. In: *Landslides in Sensitive Clays From Geoscience to Risk Management*. pp. 105–117. Springer (2013)

60. Vaunat, J., Leroueil, S.: Analysis of post-failure slope movements within the framework of hazard and risk analysis. *Natural Hazards*. 26, 83–109 (2002). <https://doi.org/10.1023/A:1015224914845>
61. Leroueil, S., Locat, P., Picarelli, L., Lee, H., Faure, R.: Geotechnical characterization of slope movements. *Landslides*. 53–74 (1996)
62. Tavenas, F., La Rochelle, P., Roy, M., Des Rosiers, J.P., Leroueil, S.: The Use of Strain Energy as A Yield and Creep Criterion For Lightly Overconsolidated Clays. *Geotechnique*. 29, 285–303 (1979). <https://doi.org/10.1680/geot.1979.29.3.285>
63. Thakur, V., Degago, S.A., Selanpaa, J., Lansivaara, T.: Determination of remoulding energy of sensitive clays. In: *Landslides in Sensitive Clays From Research to Implementation*. pp. 97–108 (2017)
64. Thakur, V., Degago, S.A.: Disintegration energy of sensitive clays. *Geotechnique Letters*. 3, 20–25 (2013). <https://doi.org/10.1680/geolett.12.00062>
65. Thakur, V., Gylland, A.S.: In-situ determination of disintegration energy for soft sensitive clays. 68e Conférence Canadienne de Géotechnique et 7e Conférence Canadienne sur le Pergélisol, 20 au 23 septembre 2015, Québec, Québec. (2015)
66. Locat, A., Leroueil, S., Fortin, A., Demers, D., Jostad, H.P.: The 1994 landslide at Sainte-Monique, Quebec: Geotechnical investigation and application of progressive failure analysis. *Canadian Geotechnical Journal*. 52, 490–504 (2015). <https://doi.org/10.1139/cgj-2013-0344>
67. Lefebvre, G., Ladd, C.C., Pare, J.J.: Comparison of field vane and laboratory undrained shear strength in soft sensitive clays. *Vane shear testing in soils, ASTM, STP. 1014*, 233–246 (1988)
68. Durand, A.: Contribution à l'étude des étalements dans les argiles sensibles de la mer de Champlain. (2016)
69. Locat, A.: Étude d'un étalement latéral dans les argiles de l'Est du Canada et de la rupture progressive: le cas du glissement de Saint-Barnabé-Nord., (2007)
70. Locat, P., Leroueil, S., Locat, J.: ALTERATION AND MOBILITY OF LAND SLIDE DEBRIS IN SENSITIVE CLAY OF EASTERN CANADA. (2008)
71. Lefebvre, G., La Rochelle, P.: Analysis of Two Slope Failures in Cemented Champlain Clays. *Canadian Geotechnical Journal*. 11, 89–108 (1974). <https://doi.org/10.1139/t74-007>
72. Eden, W.J.: Earthflows at the Beattie Mine Quebec, Canada. *Canadian Geotechnical Journal*. 1, 104–114 (1964). <https://doi.org/10.1139/t64-004>
73. Geertsema, M., Cruden, D.M., Scwab, J.W.: A large rapid landslide in sensitive glaciomarine sediments at Mink Creel, northwestern British Columbia, Canada. *Eng Geol*. 83, 36–63 (2006)
74. Potvin, J., Thibault, C., Demers, D., Bilodeau, C.: An overview of the mapping of landslide-prone areas and risk management strategies in the province of Québec, Canada. In: *Landslides in Sensitive Clays From Geoscience to Risk Management*. pp. 331–342 (2014)



75. Jin, Y.F., Yin, Z.Y., Yuan, W.H.: Simulating retrogressive slope failure using two different smoothed particle finite element methods: A comparative study. *Eng Geol.* 279, 105870 (2020). <https://doi.org/10.1016/j.enggeo.2020.105870>
76. Kennedy, R., Take, W.A., Siemens, G.: Geotechnical centrifuge modelling of retrogressive sensitive clay landslides. *Canadian Geotechnical Journal.* 58, 1452–1465 (2021). <https://doi.org/10.1139/cgj-2019-0677>
77. Thakur, V., Jostad, H.P., Kornbrenke, H.A., Degago, S.A.: How well do we understand the undrained strain softening response in soft sensitive clays? In: *Landslides in Sensitive Clays From Geoscience to Risk Management*. pp. 291–303 (2014)
78. Dey, R., Hawlader, B., Phillips, R., Soga, K.: Modelling of large deformation behaviour of marine sensitive clays and its application to submarine slope stability analysis. *Canadian Geotechnical Journal.* (2016)
79. Einav, I., Randolph, M.F.: Combining upper bound and strain path methods for evaluating penetration resistance. *Int J Numer Methods Eng.* 63, 1991–2016 (2005). <https://doi.org/10.1002/nme.1350>
80. Soga, K., Alonso, E., Yerro, A., Kumar, K., Bandara, S., Kwan, J.S.H., Koo, R.C.H., Law, R.P.H., Yiu, J., Sze, E.H.Y., Ho, K.K.S.: Trends in large-deformation analysis of landslide mass movements with particular emphasis on the material point method. *Geotechnique.* 68, 457–458 (2018). <https://doi.org/10.1680/jgeot.16.D.004>
81. Troncone, A., Parise, A., Pugliese, L., Conte, E.: Analysis of a landslide in sensitive clays using the material point method. *Geotechnical Research.* 10, 67–77 (2023). <https://doi.org/10.1680/jgere.22.00060>
82. Lo, K.Y.: An approach to the problem of progressive failure. *Canadian Geotechnical Journal.* 9, 407–429 (1972). <https://doi.org/10.1007/BF02934131>
83. Shen, Z.: A non-linear dilatant stress -strain model for soil sand rock materials. *Hydro-Sci. Eng.* 4, 3–6 (1986)
84. Duncan, J.M., Chang, C.Y.: Non linear analysis of stress and strain in soils. *Journal of the Soil Mechanics and Foundations Division.* 96, 1629–1653 (1970)
85. Jia, M., Luo, W., Zhou, Y., Zhao, S., Zhang, Z.: A Model of Undrained Stress–Strain Curves Considering Stress Path and Strain Softening. *International Journal of Geomechanics.* 21, 1–10 (2021). [https://doi.org/10.1061/\(asce\)gm.1943-5622.0002193](https://doi.org/10.1061/(asce)gm.1943-5622.0002193)
86. Liu, J., Afroz, M., Ahmad, A.: Experimental investigation of the impact of salinity on Champlain Sea clay. *Marine Georesources and Geotechnology.* 39, 494–504 (2021). <https://doi.org/10.1080/1064119X.2020.1718811>
87. Lo, K.Y., Morin, J.P.: Strength Anisotropy and Time Effects of Two Sensitive Clays: Reply. *Canadian Geotechnical Journal.* 10, 567–569 (1973). <https://doi.org/10.1139/t73-051>
88. Lefebvre, G., Leboeuf, D.: Rate effects and cyclic loading of sensitive clays. *Journal of geotechnical Engineering.* 113, 476–489 (1987)

89. Vaid, Y.P., Kobertson, P.K., Campanella, K.G.: Strain rate behaviour of Saint-Jean-Vianney clay. *Canadian Geotechnical Journal*. 16, 34–42 (1979)
90. Burckhardt, G.: Étude en laboratoire du comportement de l'argile de Rigaud sous sollicitations monotones et cycliques, (2004)
91. Blanchette, J.D.: Étude du comportement statique et cyclique de deux argiles sensibles de l'Est du Canada, (2015)
92. Mitchell, R.J., King, R.D.: Cyclic Loading of an Ottawa Area Champlain Sea Clay. *Canadian Geotechnical Journal*. 14, 52–63 (1977). <https://doi.org/10.1139/t77-004>
93. Flon, P.: Energie de remaniement et régression des coulées d'argile, (1982)
94. Liu, J., Afroz, M., Ahmad, A.: Experimental investigation of the impact of salinity on Champlain Sea clay. *Marine Georesources and Geotechnology*. 39, 494–504 (2021). <https://doi.org/10.1080/1064119X.2020.1718811>
95. Lo, K.Y., Morin, J.P.: Strength Anisotropy and Time Effects of Two Sensitive Clays: Reply. *Canadian Geotechnical Journal*. 10, 567–569 (1973). <https://doi.org/10.1139/t73-051>
96. Lefebvre, G., La Rochelle, P.: Analysis of Two Slope Failures in Cemented Champlain Clays. *Canadian Geotechnical Journal*. 11, 89–108 (1974). <https://doi.org/10.1139/t74-007>
97. Lefebvre, G., Leboeuf, D.: Rate effects and cyclic loading of sensitive clays. *Journal of geotechnical Engineering*. 113, 476–489 (1987)
98. Vaid, Y.P., Kobertson, P.K., Campanella, K.G.: Strain rate behaviour of Saint-Jean-Vianney clay. *Canadian Geotechnical Journal*. 16, 34–42 (1979)
99. Burckhardt, G.: Étude en laboratoire du comportement de l'argile de Rigaud sous sollicitations monotones et cycliques, (2004)
100. Blanchette, J.D.: Étude du comportement statique et cyclique de deux argiles sensibles de l'Est du Canada, (2015)
101. Mitchell, R.J., King, R.D.: Cyclic Loading of an Ottawa Area Champlain Sea Clay. *Canadian Geotechnical Journal*. 14, 52–63 (1977). <https://doi.org/10.1139/t77-004>
102. Flon, P.: Energie de remaniement et régression des coulées d'argile, (1982)
103. Carson, M.A.: On the retrogression of landslides in sensitive muddy sediments; Reply. *Canadian Geotechnical Journal*. 16, 431–444 (1979). <https://doi.org/10.1139/t79-047>
104. LeBoeuf, D., Duguay-Blanchette, J., Lemelin, J.-C., Péloquin, E., Burckhardt, G.: Cyclic Softening and Failure in Sensitive Clays and Silts. 1st International Conference on Natural Hazards & Infrastructure. (2016)
105. La Rochelle, P., Chagnon, J.-Y., Lefebvre, G.: Regional geology and landslides in the marine clay deposits of eastern Canada. *Canadian Geotechnical Journal*. 7, 145–156 (1970). <https://doi.org/10.1139/t70-018>

106. Quinn, P.E.: Large Landslides in Sensitive Clay in Eastern Canada and the Associated Hazard and Risk To Linear Infrastructure. (2009)
107. D'Ignazio, M., Phoon, K.K., Tan, S.A., Lansivaara, T.T.: Correlations for undrained shear strength of soft Finnish clays. *Canadian Geotechnical Journal*. 5, 1628–1645 (2016). <https://doi.org/10.1139/cgj-2016-0686>
108. Jacob, S., Saeidi, A., Chavali, R.V.P., Sadrekarimi, A.: Assessment of the relationship between undrained shear strength and geotechnical parameters for sensitive clays of Eastern Canada. In: *Geocongress*. pp. 435–445 (2024)
109. Lefebvre, G.: Use of post peak strength in slope stability analysis.pdf, (1982)
110. Demers, D., Leroueil, S.: Evaluation of preconsolidation pressure and the overconsolidation ratio from piezocone tests of clay deposits in Quebec. *Canadian Geotechnical Journal*. 39, 174–192 (2002). <https://doi.org/10.1139/t01-071>
111. Quigley, R.M.: Geology, mineralogy, and geochemistry of Canadian soft soils: a geotechnical perspective. *Canadian Geotechnical Journal*. 17, 261–285 (1980). <https://doi.org/10.1139/t80-026>
112. Roy, J., Morin, R., Chesnaux, R., Richard, S., Pino, D.S., Rouleau, A., Noel, D.: Hydrogeological insight from geophysical water-well logging in hard rocks in the Saguenay region, Québec. In: *GeoHydro, Quebec, Canada. Proceedings Papers* (2011)
113. Torrance, J.K.: Chemistry: an essential key to understanding high sensitivity and quick clays and to addressing landslide risk. In: *Landslides in Sensitive Clays From Research to Implementation*. pp. 35–44 (2017)
114. Ben-Awuah, J., Eswaran, P.: Effect of bioturbation on reservoir rock quality of sandstones: A case from the Baram Delta, offshore Sarawak, Malaysia. *Petroleum Exploration and Development*. 42, 223–231 (2015)
115. Perret, D.: *Diagenèse mécanique précoce des sédiments fins du fjord du Saguenay*, (1995)
116. Maurice, F.: Caractéristiques géotechniques et évolution de la couche de sédiments déposée lors du déluge de 1996 dans la Baie des Ha!Ha! et le Bras Nord (Fjord du Saguenay, Québec), (2000)
117. ASTM: Standard Test Method for Particle-Size Distribution (Gradation) of Fine-Grained Soils Using the Sedimentation (Hydrometer) Analysis. ASTM Designation D7928-21e1. 1–25 (2021). <https://doi.org/10.1520/D7928-17>
118. ASTM: Standard Test Methods for Laboratory Determination of Water (Moisture) Content of Soil and Rock by Mass. ASTM Designation D2216-19. (2019)
119. ASTM: Standard Test Methods for Liquid Limit, Plastic Limit and Plasticity Index of Soils. ASTM Designation D4318-17. (2018)
120. ASTM: Standard Test Method for Specific Gravity of Soils. ASTM Designation D 854-00. (2000)

121. Liu, J., Ahmad, A.: Impact of salinity level in pore fluid on the compressibility of Champlain sea clay. In: Proceedings of the XVI Pan-American Conference on Soil Mechanics and Geotechnical Engineering (XVI PCSMGE). p. 204 (2019)
122. Gorakhki, M.R.H., Bareither, C.A.: Effects of salinity on the geotechnical characterization of fine-grained soils and mine tailings. *Geotechnical Testing Journal*. 39, 45–58 (2016). <https://doi.org/10.1520/GTJ20140283>
123. ASTM D4767-11: Standard Test Method for Consolidated Undrained Triaxial Compression Test for Cohesive Soils. ASTM International, West Conshohocken. i, 1–14 (2011)
124. Lunne, T., Robertson, P.K., Powell, J.J.M.: Cone penetration testing in geotechnical engineering. (1997)
125. Agaiby, S.S., Mayne, P.W.: Interpretation of piezocone penetration and dissipation tests in sensitive Leda clay at Gloucester test site. *Canadian Geotechnical Journal*. 55, 1781–1794 (2018)
126. Locat, J., Lefebvre, G., Ballivy, G.: Mineralogy, chemistry, and physical properties interrelationships of some sensitive clays from eastern Canada. *Canadian Geotechnical Journal*. 21, 530–540 (1984). <https://doi.org/10.1139/t84-055>
127. Mitchell, J.K., Soga, K., Wiley, J.: Fundamentals of soil behaviour. John Wiley and Sons (2005)
128. Delage, P.: A microstructure approach to the sensitivity and compressibility of some eastern Canada sensitive clays. *Geotechnique*. 60, 353–368 (2010). <https://doi.org/10.1680/geot.2010.60.5.353>
129. Lieske, W., Baille, W., Schmatz, J., Kaufhold, S., Dohrmann, R.: Characterisation of natural and remoulded Onsøy clay with focus on the influence of mica. *Eng Geol*. 295, 106378 (2021). <https://doi.org/10.1016/j.enggeo.2021.106378>
130. Bishop, A.W., Henkel, D.J.: The measurement of soil properties in the triaxial test. (1957)
131. Robertson, P.K.: Interpretation of cone penetration tests - A unified approach. *Canadian Geotechnical Journal*. 46, 1337–1355 (2009). <https://doi.org/10.1139/T09-065>
132. Salsabili, M., Saeidi, A., Rouleau, A., Nastev, M.: Development of empirical CPTu-Vs correlations for post-glacial sediments in Southern Quebec, Canada, in consideration of soil type and geological setting. *Soil Dynamics and Earthquake Engineering*. 154, 107131 (2022). <https://doi.org/10.1016/j.soildyn.2021.107131>
133. Robertson, P.K., Wride, C.E.: Evaluating cyclic liquefaction potential using the cone penetration test. *Canadian Geotechnical Journal*. 35, 442–459 (1998). <https://doi.org/10.1139/t98-017>
134. Robertson, P.K.: Interpretation of cone penetration tests - A unified approach. *Canadian Geotechnical Journal*. 46, 1337–1355 (2009). <https://doi.org/10.1139/T09-065>
135. Penner, E.: A study of sensitivity in Leda clay. *Can J Earth Sci*. 2, 425–441 (1965). <https://doi.org/10.1139/e65-037>

136. Locat, A., Locat, P., Michaud, H., Hébert, K., Leroueil, S., Demers, D.: Geotechnical characterization of the Saint-Jude clay, Quebec, Canada. *AIMS Geosci.* 5, 273–302 (2019). <https://doi.org/10.3934/geosci.2019.2.273>
137. Skempton, A.W.: The colloidal activity of clays. *Selected papers on soil mechanics.* 1, 57–61 (1953)
138. Blais-Stevens, A.: Historical landslides in Canada resulting in fatalities (1771-2018). *Geost. John's 2019, St. John's, Newfoundland and Labrador, Canada.* (2019)
139. Lefebvre, G., Poulin, C.: A new method of sampling in sensitive clay. *Canadian Geotechnical Journal.* 16, 1–8 (1979)
140. Nagaraj, B.T.S., Murthy, B.R.S., Vatsala, A., Joshi, R.C.: Analysis of compressibility of sensitive clays. *Journal of Geotechnical and Geoenvironmental Engineering.* 116, 105–118 (1990)
141. Tang, W.H., Stark, T.D., Angulo, M.: Reliability in back analysis of slope failures. *Soils and Foundations.* 39, 73–80 (1999). [https://doi.org/10.3208/sandf.39.5\\_73](https://doi.org/10.3208/sandf.39.5_73)
142. Wesley, L.D., Leelaratnam, V.: Shear strength parameters from back-analysis of single slips. *Geotechnique.* 51, 373–374 (2001). <https://doi.org/10.1680/geot.2001.51.4.373>
143. Saeidi, A., Maazallahi, V., Rouleau, A.: Assessment of slide surface and pre-slide topography using site investigation data in back analysis. *International Journal of Rock Mechanics and Mining Sciences.* 88, 29–33 (2016). <https://doi.org/10.1016/j.ijrmms.2016.07.008>
144. Jaboyedoff, M., Demers, D., Locat, J., Locat, A., Locat, P., Oppikofer, T., Robitaille, D., Turmel, D.: Use of terrestrial laser scanning for the characterization of retrogressive landslides in sensitive clay and rotational landslides in river banks. *Canadian Geotechnical Journal.* 46, 1379–1390 (2009). <https://doi.org/10.1139/T09-073>
145. Geertsema, M., Blais-Stevens, A., Kwoil, E., Menounos, B., Venditti, J.G., Grenier, A., Wiebe, K.: Sensitive clay landslide detection and characterization in and around Lakelse Lake, British Columbia, Canada. *Sediment Geol.* 364, 217–227 (2018). <https://doi.org/10.1016/j.sedgeo.2017.12.025>
146. Westen, C.J., Getahun, F.: Analyzing the evolution of the Tessina landslide using aerial photographs and digital elevation models. *Geomorphology.* 54, 77–89 (2003). [https://doi.org/10.1016/S0169-555X\(03\)00057-6](https://doi.org/10.1016/S0169-555X(03)00057-6)
147. Deane, E., Macciotta, R., Hendry, M.T., Gräpel, C., Skirrow, R.: Leveraging historical aerial photographs and digital photogrammetry techniques for landslide investigation—a practical perspective. *Landslides.* 17, 1989–1996 (2020). <https://doi.org/10.1007/s10346-020-01437-z>
148. Demers, D., Robitaille, D., Lavoie, A., Paradis, S., Fortin, A., Ouellet, D.: The Use of LiDAR Airborne Data for Retrogressive Landslides Inventory in Sensitive Clays, Québec, Canada. *Landslides in Sensitive Clays From Research to Implementation.* 279–288 (2017)
149. Lebius, J., Robert, J.-M., Rissmann, P.: Regional mapping of landslide hazard in Quebec. In: *Symposium on slopes on soft clays.* pp. 205–262 (1983)

150. Leroueil, S., Tavenas, F., Bihan, J.-P. Le: Propriétés caractéristiques des argiles de l'est du Canada. *Canadian Geotechnical Journal*. 20, 681–705 (1983). <https://doi.org/10.1139/t83-076>
151. Rouleau, A., Réal, D., Walter, J., Germaneau, Denis Tremblay, M.-L., Lambert, M.: CERM-PACES, Résultats du programme d'acquisition de connaissances sur les eaux souterraines du Saguenay-Lac-Saint-Jean. <https://constellation.uqac.ca/id/eprint/8548/>. (2013)
152. Dyke, A.S.: An outline of the deglaciation of North America with emphasis on central and northern Canada. *Quaternary Glaciations-Extent and Chronology, Part II: North America*. 2b, 373-424 (2004). [https://doi.org/10.1016/S1571-0866\(04\)80209-4](https://doi.org/10.1016/S1571-0866(04)80209-4)
153. Benn, D., Evans, D.J.A.: *Glaciers and glaciation*. Routledge, London and New York (2010)
154. Lévesque, Y., St-Onge, G., Lajeunesse, P., Desjage, P., Brouard, E.: Defining the maximum extent of the Laurentide Ice Sheet in Home Bay (eastern Arctic Canada) during the Last Glacial episode. *Boreas*. 49, 52–70 (2019). <https://doi.org/10.1111/bor.12415>
155. Margold, M., Stokes, C.R., Clark, C.D.: Ice streams in the Laurentide Ice Sheet: Identification, characteristics and comparison to modern ice sheets. *Earth Sci Rev*. 143, 117–146 (2015). <https://doi.org/10.1016/j.earscirev.2015.01.011>
156. Dyke, A.S.: An outline of the deglaciation of North America with emphasis on central and northern Canada. *Quaternary Glaciations-Extent and Chronology, Part II: North America*. 2b, 373-424 (2004). [https://doi.org/10.1016/S1571-0866\(04\)80209-4](https://doi.org/10.1016/S1571-0866(04)80209-4)
157. Lévesque, Y., Walter, J., Chesnaux, R., Dugas, S., David, N.: Electrical resistivity of saturated and unsaturated sediments in northeastern Canada. *Environ Earth Sci*. (2023). <https://doi.org/10.1007/s12665-023-10998-w>
158. Walter, J., Rouleau, A., Chesnaux, R., Lambert, M., Daigneault, R.: Characterization of general and singular features of major aquifer systems in the Saguenay-Lac-Saint-Jean region. *Canadian Water Resources Journal/Revue canadienne des ressources hydriques*. 43, 75–91 (2018). <https://doi.org/10.1080/07011784.2018.1433069>
159. Rouleau, A., Réal, D., Walter, J., Germaneau, Denis Tremblay, M.-L., Lambert, M.: CERM-PACES, Résultats du programme d'acquisition de connaissances sur les eaux souterraines du Saguenay-Lac-Saint-Jean. <https://constellation.uqac.ca/id/eprint/8548/>. (2013)
160. Lévesque, Y., Walter, J., Chesnaux, R., Dugas, S., David, N.: Electrical resistivity of saturated and unsaturated sediments in northeastern Canada. *Environ Earth Sci*. (2023). <https://doi.org/10.1007/s12665-023-10998-w>
161. La Rochelle, P., Lefebvre, G., Bilodeau, P.M.: Stabilization of a Slide in Saint-Jerome, Lac Saint-Jean. *Canadian Geotechnical Journal*. 14, 340–356 (1977). <https://doi.org/10.1139/t77-039>
162. Jacob, S., Saeidi, A., Sadrekarimi, A., Chavali, R.V.P.: Geotechnical characterization of Laflamme clays from the Lac-Saint-Jean basin, Quebec. *Eng Geol*. (2024)
163. Zhu, D.Y., Lee, C.F., Qian, Q.H., Zou, Z.S., Sun, F.: A new procedure for computing the factor of safety using the Morgenstern-Price method. *Canadian Geotechnical Journal*. 38, 882–888 (2001). <https://doi.org/10.1139/cgj-38-4-882>

164. Morgenstern, N.R., Price, V.E.: The analysis of stability of general slip surfaces. *Geotechnique*. 15, 79–93 (1965). <https://doi.org/10.1680/geot.1968.18.1.92>
165. Budhu, M. (2010). *Soil mechanics and foundations*. John Wiley and Sons.

## PUBLICATIONS

### JOURNALS

1. Jacob, S., Chavali R. V. P., Saeidi, A., Sadrekarimi A. 2023. Remoulding energy as a criterion in assessing retrogressive landslides in sensitive clays: a review and its applicability to Eastern Canada . Natural Hazards, Volume 118, 1833-1853. <https://doi.org/10.1007/s11069-023-06088-6>
2. Jacob, S., Saeidi, A., Chavali R. V. P., Sadrekarimi A. 2024. An exponential model for strain softening behaviour of sensitive clays. Under review in Geoenvironmental Disasters.
3. Jacob, S., Saeidi, A., Sadrekarimi A., Chavali R. V. P. 2024. Geotechnical characterization of Laflamme clays of the Lac-Saint-Jean basin, Quebec. Accepted by Engineering Geology.
4. Jacob, S., Saeidi, A., Sadrekarimi A., Chavali R. V. P. 2024. Stability of slopes in sensitive clays of Laflamme sea with a landslide assessment criterion. Initial draft submitted for review to the co-authors.

### CONFERENCES

1. Jacob, S., Saeidi A., Sadrekarimi, A., Chavali, R. V. P. 2024. A comparative study between sensitive clay deposits in the Laflamme and Champlain basins of Eastern Canada. In: GeoMontreal, 2024. 15<sup>th</sup> – 18<sup>th</sup> September, 2024, Montreal, Canada.
2. Jacob, S., Saeidi, A., Chavali R. V. P., Sadrekarimi A. 2024. Assessment of the relationship between undrained shear strength and geotechnical parameters for sensitive clays of Eastern Canada. In: Geo Congress 2024 .25<sup>th</sup> -28<sup>th</sup> February 2024, Vancouver, Canada.
3. Jacob, S., Chavali R. V. P., Saeidi, A. 2022. Assessment of post peak strain softening behaviour of Eastern Canadian sensitive clays. Proceedings of the 8th Canadian Conference on Geotechnique and Natural Hazards – Geohazard 2022, 12<sup>th</sup> – 15<sup>th</sup> June 2022, Quebec, Canada.



4. Jacob, S., Saeidi, A., Chavali R. V. P. 2021. Comparison of existing methods of determination of remoulding energy. In: The 74th Canadian Geotechnical Conference – Geo Niagara 2021, 26<sup>th</sup> – 29<sup>th</sup> September 2021, Niagara, Canada.
5. Jacob, S., Saeidi, A., Chavali R. V. P. 2021. Remoulding energy as a criterion in assessing cyclic failure and retrogression in sensitive clays. The 1971 Saint Jean Vianney disaster: 50 years of advancing geotechnical knowledge, 13<sup>th</sup> – 14<sup>th</sup> May 2021, Quebec, Canada.

## **APPENDIX: CONFERERENCE PUBLICATIONS**

## Comparison of existing methods of determination of remoulding energy

Sarah Jacob, Ali Saeidi & Rama Vara Prasad Chavali  
*Department of Applied Sciences – Université du Québec à  
Chicoutimi, Chicoutimi, Quebec, Canada*



### ABSTRACT

Sensitive clays are highly vulnerable to even the slightest of disturbance making them highly disastrous and detrimental. The Eastern Canadian region of Quebec and Ontario have large deposits of such sensitive clays which are susceptible to landslide occurrence. Remoulding energy and remoulding index are essential factors in determining the cyclic failure and slide retrogression in sensitive clays along with other geotechnical parameters. In particular, the remoulding energy maybe considered as a better tool to identify retrogressive landslides for risk mitigation and disaster management due to its direct association with the nature of soil as well as slide retrogression. A comparison of the few existing methods of determination of remoulding energy has been made to understand the suitability of each method for different types of sensitive clays. The remoulding energy has been compared with few important geotechnical properties like brittleness index, shear wave velocity etc., to establish some relationships or empirical equations that maybe used as a criterion for assessing the cyclic failure of sensitive clays. The results show that the analytical methods of determination of remoulding energy seem to be more representative of the process of remoulding compared to the experimental method and will be helpful in gauging retrogression in sensitive clays. The nature of the soil (brittle/ductile) coupled with the remoulding energy and remoulding index can prove to be an important criterion in the prediction of liquefaction potential and retrogressive landslides allowing us to formulate better control measures before the occurrence of such landslides.

### RÉSUMÉ

Les argiles sensibles sont très vulnérables à la moindre perturbation, ce qui les rend extrêmement désastreuses et nuisibles. La région de l'est du Canada, au Québec et en Ontario, possède d'importants dépôts d'argiles sensibles qui constituent une menace sérieuse pour la vie et la propriété. L'énergie de remoulage et l'indice de remoulage sont des facteurs essentiels pour déterminer la susceptibilité à la régression de glissement dans les argiles sensibles ainsi que d'autres propriétés in situ et mécaniques du sol. Cependant, l'énergie de remoulage peut être directement associée à la nature du sol, ce qui en fait un meilleur outil pour identifier les glissements de terrain rétrogrades pour l'atténuation des risques et la gestion des catastrophes. Une comparaison des quelques méthodes existantes de détermination de l'énergie de remoulage a été faite pour comprendre l'adéquation de chaque méthode à différents types de sols sensibles. L'énergie de remoulage étant un outil prometteur pour identifier les glissements de terrain régressifs, a été comparée à quelques propriétés importantes du sol telles que l'indice de fragilité, la vitesse de l'onde de cisaillement, etc., pour établir des relations ou des équations empiriques qui peuvent être utilisées comme critère pour évaluer le potentiel de liquéfaction des argiles. Les résultats montrent que la connaissance de l'énergie de remoulage et de l'indice de remoulage sera utile pour mesurer la rétrogression dans les argiles sensibles. Les méthodes analytiques de détermination de l'énergie de remoulage semblent être plus représentatives du processus de remoulage que la méthode expérimentale. La nature du sol (fragile / ductile) couplée à l'énergie de remoulage et à l'indice de remoulage peut s'avérer être une mesure importante dans la prédiction du potentiel de liquéfaction et des glissements de terrain rétrogressifs nous permettant de formuler de meilleures mesures de contrôle avant la survenue de tels glissements de terrain.

## 1 INTRODUCTION

The importance of the need to assess landslides in sensitive clays has been stressed upon in past literatures (Demers et al. 2014, Lefebvre et al. 1988). Large parts of northern countries of the world like Canada, Norway, Sweden, Finland, Russia and Northwestern regions of United State have huge deposits of sensitive clay. Their occurrence is due to isostatic depression and post glacial rebound followed by leaching of sea sediments (L'Heureux et al. 2016).

In the Eastern Canadian region of Quebec, almost 89% of the population lives in the marine limits of such sensitive clays. These landslides generally occur on clayey plains with mild slopes with a gradient in the range of 1% usually formed by the banks of water courses (Demers et al. 2014). They cause loss of life and property and leave such soils vulnerable to cause more destruction and havoc. Some of the examples of landslides in sensitive clays of Quebec are Saint Jean Vianney 1971 (Tavenas F. et al., 1971) as et al. 1971), slope failures associated with Saguenay earthquake 1988 (Lefebvre et al. 1992) St. Jude landslide 2010 (Locat et al. 2017) [167] and Saint-Luc-de-Vincennes 2016 (Tremblay-Auger et al. 2021)

According to Varnes classification of landslide types (1996) and its update by Hungr et al. 2014, a vast majority of landslides in Quebec may be classified as flow slides and spreads. The initiation of flow slides and spreads in Eastern Canada are similar in the sense that, both occur due to erosion at the toe of the slope which is often associated to the presence of a water course. However, the mechanism of occurrence of both landslide types is slightly different [51].

In flow slides, the soil at the toe gets remoulded due to erosion leading to the formation of an initial rotational failure surface which flows and slides out of the crater by leaving an unstable backscarp. This will cause the occurrence of another failure surface, where the soil slides and flows out of the initial crater. This cycle continues and multiple failure surfaces are formed until the backscarp is stable (Figure 1) (Hungr et al. 2014, Locat et al. 2011).

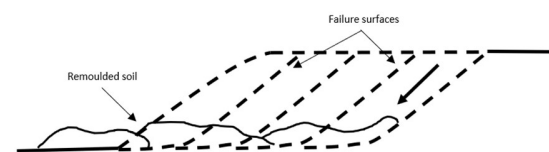


Figure 0-1. Mechanism of flow slides

Spreads, on the other hand are characterized by a ribbed appearance of pointed soil structures (horsts) and flat-topped strips of land with vegetation more or less intact (garbens) (Figure 2). In spreads, the failure is initiated by the upward progression of a shear band/ shear zone due to the erosion at the toe causing the surface above the shear zone to be spread into horsts and grabens (Hungr et al. 2014, Locat et al. 2011). The soil below the shear band undergoes remoulding and it liquefies.

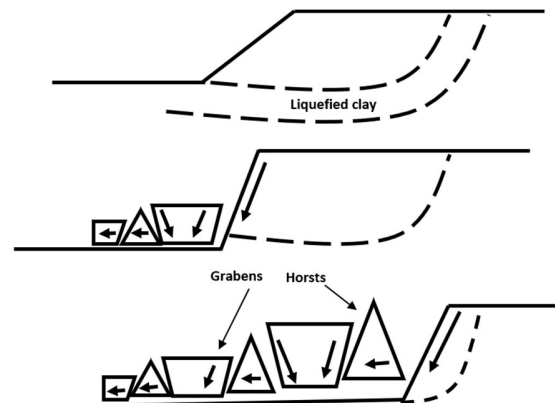


Figure 0-2 The various stages of spreads where the shear band propagates upwards disintegrating the remoulded clay into horsts and grabens

Flow slides maybe considered to be more catastrophic than spreads due to the large retrogression it undergoes in terms of travel of the remoulded soil debris. It is observed that there are cases when a combination of the two mechanisms of flow slides and spreads also occur. Initially, a disturbance may trigger a flow slide which forms multiple failure surfaces, finally leaving behind an unstable back scarp. This initiates the conditions for a spread to occur and the remoulded soil spreads into horsts and grabens. The resulting landslide will have characteristics of both flow slides and spreads (Demers et al. 2014, Locat et al. 2017, Tremblay-Auger et al. 2021).

According to Demers et al. (2014), the most common mechanism observed in Eastern Canadian soils are of flow slides.

The present paper provides an overview of retrogression in sensitive clays and remoulding energy as a criterion in assessing this retrogression. The existing approaches/criteria in the determination of remoulding energy associated with landslides have been evaluated. Lastly, a comparative study of these existing methods is carried out to understand the effectiveness of each method in perspective of future research. The author has also tried to establish certain relationships between the properties of sensitive clays and remoulding energy to recognize the significance of remoulding energy in slide retrogression.

## 2 CRITERIA FOR RETROGRESSION IN SENSITIVE CLAYS

The potential for remoulding and cyclic failure in sensitive clay landslides are governed by in – situ parameters like undrained shear strength ( $c_u$ ), remoulded shear strength ( $c_{ur}$ ), stability number ( $N_s$ ), plasticity index ( $I_p$ ), liquidity index ( $I_L$ ) and sensitivity ( $s_r$ ), although these may vary depending on site conditions and other geologic and geometric parameters. (Thakur et al. 2014).

For simplicity, the aforementioned criteria and correlations are integrated in Table 1.

Early studies by Tavenas et al. (1983) show that the remoulding index and remoulding energy are two main parameters that maybe used as a criterion to detect slide retrogression in sensitive clays along with the other in-situ parameters shown in Table 1.

The ability of the slide debris to be remoulded depends on the remoulding index. Tavenas et al. (1983) proposed that remoulding index exceeding 70% is likely to cause large retrogressions. He also observed that large retrogressions can be predicted for the samples whose normalized remoulding energy was more than 40.

Table 0-1 Various criteria for retrogression and flowslides

Criteria	Reference
<b>Stability number (<math>N_s</math>):</b>	
$N_s > 6c_u$	Mitchell et al. (1974)
$N_s < 4$ when $I_p = 10$	Leroueil et al. (1996)
$N_s < 7$ or $8$ when $I_p = 40$	
<b>Liquidity index (<math>I_L</math>):</b>	
$I_L > 1.2$	Lebius et al. (1983) Leroueil et al. (1983) Locat et al. (1988)
<b>Liquid limit (<math>w_L</math>):</b>	
$w_L < 40\%$	Tavenas et al. (1983)
<b>Remoulded shear strength (<math>c_{ur}</math>):</b>	
$c_{ur} < 1$ kPa	Lebius et al. (1983) Leroueil et al. (1983) Locat et al. (1988) Thakur et al. (2013)
<b>Sensitivity (<math>s_t</math>):</b>	
$s_t > 25$	Lebius et al. (1983)
<b>Quickness (Q):</b>	
$Q > 15\%$	Thakur et al. (2013)
<b>Brittleness index (<math>I_B</math>):</b>	
$I_B \sim 1$	Quinn et al. (2011)
<b>Remoulding index (<math>I_r</math>):</b>	
$I_r > 70\%$	Tavenas et al. (1983)
<b>Normalized remoulding energy (<math>w_N</math>):</b>	
$w_N < 40$	Tavenas et al. (1983)

### 3 REMOULDING ENERGY AS A PARAMETER FOR RETROGRESSIVE LANDSLIDES

The potential for retrogression of landslides in sensitive clays is directly dependent on the potential energy released at the onset of failure of the slope followed by distribution of that potential energy into energy used in remoulding of the soil (Tavenas et al. 1983).

#### 3.1 Energy balance in post failure movements

At the onset of failure of a landslide, the external forces that induce the failure in the slope as well as the resisting forces induced by the soil parameters will be in equilibrium. During this time, the only energy possessed by the slope is

its potential energy. As the failure progresses, this potential energy ( $E_p$ ), is the single source of energy for remoulding the soil. The potential energy gets distributed into remoulding energy ( $E_R$ ). Kinetic energy ( $E_K$ ) and frictional energy ( $E_F$ ) (Figure 3). This distribution maybe represented as Equation 1. (Leroueil S. et al. 1996, Vaunat et al. 2002).

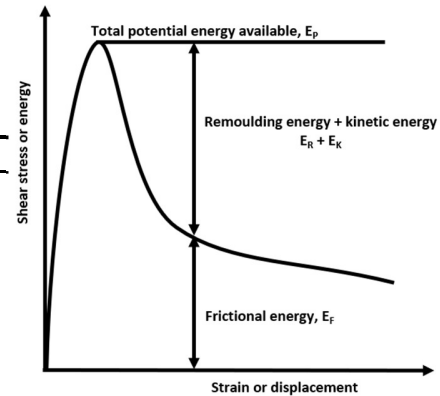


Figure 0-3 Distribution of potential energy during slope failure

$$E_p = E_R + E_K + E_F \quad [1]$$

However, it is seen that this distribution depends on the nature of the material in terms of its stiffness or brittleness. For a purely ductile material or a highly brittle material, the above distribution may vary as shown in Figure 4

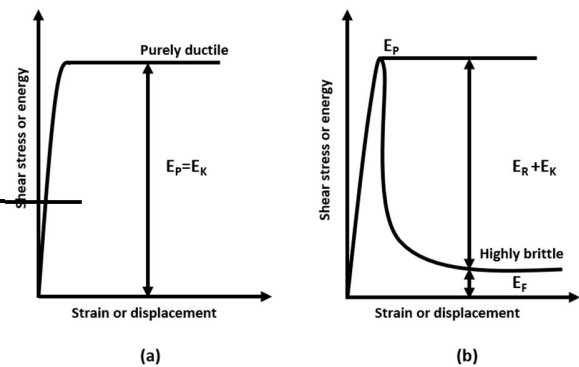


Figure 0-4 Energy distribution of (a) purely ductile material (b) highly brittle material

#### 3.2 Existing methods of determination of remoulding energy

In light of the current advancements and knowledge in the field of retrogression, many researchers have focused on remoulding energy and the energy distribution concept to

assess retrogression and cyclic failure in sensitive clays. Some methods have been developed to determine remoulding energy experimentally or empirically.

Tavneas et al. (1983), one of the fore runners in the study of remoulding energy and slide retrogression, used four techniques which he believed closely represents the field conditions at the time of failure, to determine remoulding energy of Eastern Canadian soils. They were, free fall of the sample from a known height, impact on the sample by an aluminium ram, extrusion of the sample through a conical extruder and shearing by a simple shear box. The shearing method was found to be most suitable. The energy used in each of these methods were noted and normalized with the limit state energy to obtain the remoulding energy.

Subsequently, Locat et al. (2008) used the experimental results by Tavenas et al. (1983) to form empirical relationships between remoulding index and remoulding energy along with the undrained shear strength ( $c_u$ ) and plasticity index ( $I_p$ ) (Equation 2)

$$I_r = 14.9 \left( \frac{E_R}{c_u I_p} \right)^{0.69} \quad [2]$$

They also observed that, at 100% remoulding,

$$E_R = 16c_u I_p \quad [3]$$

Thakur et al. (2013) proposed an analytical approach for the measurement of remoulding energy which he validated using Norwegian soils. Accordingly, the authors put forth that the area under the ideal stress strain curve corresponds to the remoulding energy (Figure 5). The same was calculated and is shown in Equation 4.

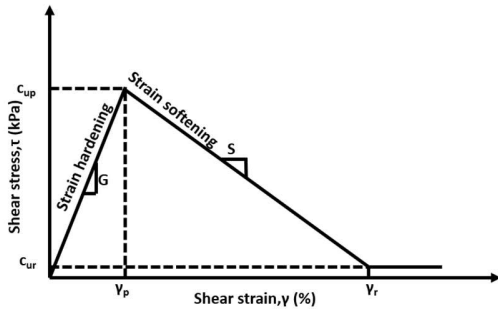


Figure 0-5 Ideal shear stress - shear strain curve (Thakur et al. 2013)

$$E_R = c_{ur} \gamma_r + \frac{1}{2} (s_t c_{ur})^2 \left( \frac{1}{G} + \frac{1}{S} \right)$$

where,

$c_{ur}$  = remoulded shear strength  
 $\gamma_r$  = residual shear strain  
 $s_t$  = sensitivity  
 $G$  = shear modulus  
 $S$  = softening modulus

In general, the remoulding energy of Eastern Canadian samples were found to be much higher than Norwegian soil samples. This is attributed to the higher over consolidation ratio of Eastern Canadian soils as a result of which they have a higher shear strength value. (Thakur et al. 2013).

Thakur et al. (2015) also introduced electric field vane shear tests to form the ideal stress strain curves for remoulding energy measurement

The present study seeks to understand the applicability of the analytical approach of Thakur et al. (2013) to other soil samples. Subsequently, a comparison was made between the remoulding energy obtained by Tavneas and the calculated remoulding energy through analytical method for the same Eastern Canadian soil samples. A small assessment of its dependence with other soil parameters have also been done.

## 4 RESULTS AND DISCUSSIONS

### 4.1 Comparison of remoulding energy determination for Eastern Canadian clays

The properties of the clay samples investigated by Tavenas et al. (1983) have been used to carry out this study along with certain assumptions. Table 2 shows the soil properties of the samples investigated by Tavneas et al. (1983) and Table 3 shows stress strain parameters developed by Quinn et al. (2011) from Tavenas' data.

Table 0-2 Properties of clay samples tested by Tavenas et al. (1983)

Site	$I_p$	$I_L$	$C_{ucone}$ (kPa)	$C_{urcone}$ (kPa)	$S_t$
Saint - Leon 4.8 m	45	1.1	30	1.1	27
Saint - Leon 9.3 m	42	1	49.5	2.1	24
Louisville 6 m	45	1.1	39	1.3	30
Saint - Hilaire	35	2.3	35	0.8	44
Saint - Thuribe 6 m	20	1.6	55	0.4	137
Saint - Thuribe 12 m	5	>4	42	<0.07	>600
Mascouche 9 m	30	1.2	135	1.3	104
Saint - Alban 6.6 m	19	2.4	21	0.2	105
Saint Jean Vianney 30 m	30	1.1	320	1.2	260

$I_p$  = plasticity index,  $I_L$  = liquidity index,  $C_{ucone}$ =undrained shear strength,  $C_{urcone}$ = remoulded shear strength and  $S_t$ = sensitivity

Table 0-3 Data obtained by Quinn et al (2011) from Tavenas' investigations

Site	$\gamma_r$	$\omega$ (m)	$I_B$
Saint - Leon 4.8 m	133.33	130	0.963
Saint - Leon 9.3 m	53.33	50	0.958
Louisville 6 m	80	65	0.967
Saint - Hilaire	80	65	0.977
Saint - Thuribe 6 m	26.67	25	0.993

Saint – Thuribe 12 m	26.67	30	0.998
Mascouche 9 m	13.33	10	0.990
Saint – Alban 6.6 m	80	65	0.990
Saint Jean Vianney 30 m	13.33	2.5	0.996

$\gamma_r$  = residual shear strain,  $\omega$  = length of end zone,  $I_B$  = brittleness index

Quinn et al. (2013) developed crude stress strain relationships by numerical methods from Tavenas' data. The length of end zone ( $\omega$ ), defined by Quinn indicated the transition between the residual stress and the next peak stress during the propagation of the shear band (Figure 6).

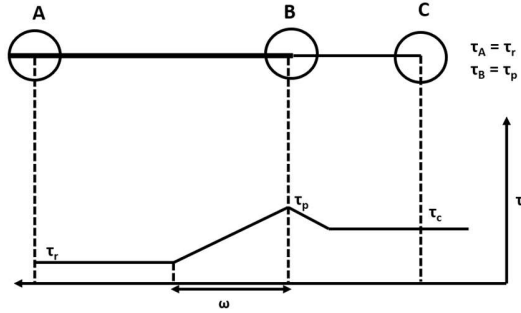


Figure 0-6 Propagation of shear band

The remoulding energy for the samples in Tables 2 and 3 are estimated by equation 4. The shear modulus ( $G$ ) is assumed to be 1.8 MPa. This value is obtained through triaxial tests conducted on sensitive clay samples of Saguenay region at Université du Québec à Chicoutimi.

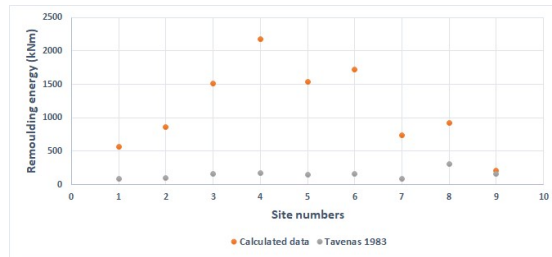


Figure 7 Comparison of remoulding energy for various sites

As is observed from Figure 7, there is an obvious disparity, as high as 80%, between the original data determined by Tavenas et al. (1983) and the calculated data in this study.

One of the reasons for this variation maybe due to overestimation of the remoulding energy values by the ideal stress – strain curve. Even though the ideal stress strain curve simplifies the determination of remoulding energy, the true behaviour of the soil is non-linear and this gives way to some over estimation in the calculation of area under the stress – strain curve. Another reason is the lack of site-specific correlations and assumptions to obtain the parameters in equation 4. Also, the ideal stress strain curve has not been validated with Eastern Canadian soils yet, so the need to incorporate other parameters may also serve as a critical factor.

## 4.2 Variation of remoulding energy with brittleness index ( $I_B$ ) and length of end zone ( $\omega$ )

Bishop (1971), defined the parameter brittleness index ( $I_B$ ) which indicates the ease with which the strength is lost from peak to post peak shear stress in a material.

$$I_B = \frac{\tau_p - \tau_r}{\tau_p}$$

[ 5]

The brittleness index is a good tool in understanding the strain softening and post failure behaviour of sensitive clays. As mentioned by Leroueil et al. (1996), the distribution of potential energy possessed by a slope at the onset of failure into remoulding energy and kinetic frictional energy depends largely on the nature of the material. A brittle material tends to have lesser remoulding energy as well as higher kinetic energy and undergoes more retrogression. Even though the materials studied by Tavenas et al. (1983) have a brittleness index close to one (Table 3), which may undergo heavy retrogression, a clear trend is observed between remoulding energy and brittleness index, where the remoulding energy decreases with increase in brittleness index (Figure 8). It may be observed that even with a small change in brittleness index (from 0.996 to 0.958), the remoulding energy varies in the order of 200 to 2000 kPa. Thus, even among fundamentally brittle materials, there is large variation in remoulding energy and in turn the retrogression they undergo. However, the basic idea that brittle materials have lesser remoulding energy stands true and the studies put forth by Tavenas et al. (1983), Leroueil et al. (1996), Thakur & Degago (2013), Quinn et al. (2011) and Thakur & Degago (2013) move in the same direction.

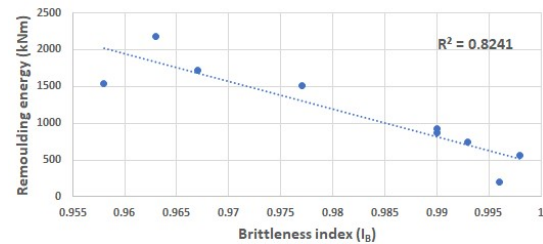


Figure 8 Variation of remoulding energy with brittleness index

Quinn et al. (2011) explains that the length of end region ( $\omega$ ) maybe closely associated to the brittleness of the material. It is observed that even though these clays are quite similar in their brittleness, their  $\omega$  values vary. Thus, even for similar clays the propagation of shear band and in turn their retrogression will vary. However, it may be interpreted that, typically clays which are more brittle, attain the residual stress rapidly resulting in a lower value of  $\omega$ . This maybe correlated to the remoulding energy as shown in Figure 9. A clay which is more brittle, can be easily remoulded and hence has a lesser remoulding energy; the shear band propagates rapidly with a lesser value of  $\omega$ .

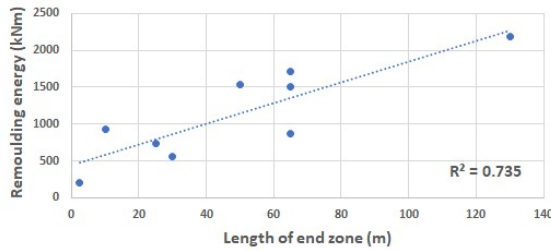


Figure 9 Variation of remoulding energy with length of end zone

Hence it may be noted that even among clays with nearly similar brittleness indices, the remoulding energy may be used to understand the difference in the degree of retrogression in such landslides.

#### 4.3 Variation of remoulding energy with shear wave velocity

The lack of an equation for shear wave velocity at the exact regions investigated by Tavenas forces us to assume the applicability of some of the simple correlations available in literatures. The simple empirical equations by Mayne et al. (1995),  $v_s = 1.75q_c^{0.627}$  and Long et al. (2010),  $v_s = 2.944q_t^{0.613}$  are used in the determination of shear wave velocity. In addition to the above two equations, a correlation for Saguenay region developed by Salsabili et al (2021) has also been used which is  $v_s = 5.565q_t^{0.487}$ .

The cone tip resistance ( $q_c$ ) and the corrected cone tip resistance ( $q_t$ ) are obtained from the modified relations by Rémai, (2013), which was originally given by Lunne et al. (1997) using the undrained shear strength ( $s_u$ ).

$$s_u = \frac{q_c - \sigma_{v0}}{N_k} \quad [6]$$

$$s_u = \frac{q_t - \sigma_{v0}}{N_{kt}} \quad [7]$$

where,  $\sigma_{v0}$  = total overburden pressure,  $N_k$  = empirical cone factor,  $N_{kt}$  = empirical cone factor for corrected cone tip resistance.

The value of  $N_k$  and  $N_{kt}$  may vary depending on the type of soil. The value of  $N_k$  for soft marine clays is considered to be 20 and that of  $N_{kt}$  is taken as 15 for clays with plasticity index value between 25% and 40% (Rémai (2013).

The shear wave velocity values obtained by empirical relationships given by Mayne et al. (1995), Long & Donohue (2010) and Salsabili et al (2021) are mostly in the range of 100 – 250 m/s, with a few exceptional cases beyond 250 m/s. Ideally, the shear wave velocity will be higher in soft soils [170] and the general tendency here is for the remoulding energy to decrease with increase in shear wave velocity. Even though a slight decreasing trend is observed in figure 10, it may not be confirmed so, due to the large scatter on the left-hand side of the graph. The author believes that sufficient data points and in situ properties provide some light in the direction of developing

a relation between remoulding energy and shear wave velocity.

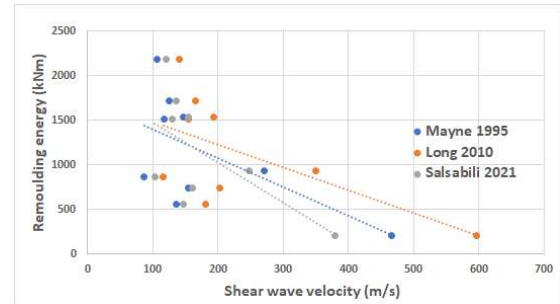


Figure 10 Variation of remoulding energy with shear wave velocity

## 5 CONCLUSIONS

The preliminary analysis on the existing methods for the determination of remoulding energy and its dependence on certain soil parameters show that the remoulding energy is a prime criterion for the analysis of retrogressive landslides. The obtained results emphasize the need to continue research on Eastern Canadian sensitive clays to determine correlations between remoulding energy and other sensitive clay characteristics.

- The accuracy of the ideal stress – strain curve in the analysis of Eastern Canadian clays have to be investigated in detail.
- Even among fundamentally brittle soils, the remoulding energy and the degree of retrogression varies.
- As the shear band propagates during slope failure, more brittle soils attain the residual stress from the peak stress at a much faster rate, in turn undergoing more remoulding and retrogression.
- The relationship between remoulding energy and shear wave velocity is yet to be studied in detail to draw strong conclusions.

## 6 ACKNOWLEDGEMENT

This research was partially funded by the Natural Sciences and Engineering Research Council of Canada (NSERC) and Hydro-Quebec under project funding no. RDCPJ 521771-17.

## 7 REFERENCES

- Bishop. 1971. Shear strength parameters for undisturbed and remoulded soil specimens, *Proc. of the Roscoe Memorial Symposium*, 3-58.
- Demers, D., Robitaille, D., Locat, P. and Potvin J. 2014. Inventory of large landslides in sensitive clay in the province of Quebec, Canada: Preliminary Analysis, *Landslides in sensitive clays – From Geoscience to Risk Management*, Springer, 77-89.



- Hungr O., Leroueil, S. and Picarelli, L. 2014. The Varnes classification of landslide types, an update, *Landslides*, 11(2): 167-194.
- Khan M. A. 2013., *Earthquake resistant structures* 1<sup>st</sup> ed, Elsevier.
- Lefebvre, G., Leboeuf, D. Hornych, P. and Tanguay, L. 1992. Slope failures associated with the 1988 Saguenay earthquake, Quebec, Canada, *Canadian geotechnical Journal*, 29(1): 117-130.
- Leroueil, S., Tavenas, F. and Bihan, J. P. 1983. Characteristic properties of Eastern Canadian clays, *Canadian Geotechnical Journal*, 20: 681-705.
- Leroueil, S., Locat, J., Vaunat, J., Picarelli, L., Lee, H. and Faure, R. 1996. Geotechnical characterization of slope movements, *Proc. of 7<sup>th</sup> International Symposium on Landslides*, 53-74.
- L'Heureux, J. S. and Long, M. 2016. Correlations between shear wave velocity and geotechnical parameters in Norwegian clays, *Proc. of the 17<sup>th</sup> Nordic Geotechnical Meeting*.
- Locat, A., Leroueil, S., Bernander, S., Demers, D., Jostad, H. P. and Ouehb, L. 2011. Progressive failures in Eastern Canadian and Scandinavian sensitive clays, *Canadian Geotechnical Journal*, 48(11): 1696-1712.
- Locat, A., Geertsema, M., Demers, D. and Locat, P. 2017. Sensitive clay landslides in Canada, *GeoOttawa*.
- Locat, J. and Demers, D. 1988. Viscosity, yield strength, remoulded strength and liquidity index relationships for sensitive clays, *Canadian Geotechnical Journal*, 25(4): 799-806.
- Locat, P., Leroueil, S. and Locat, J. 2008. Remaniement et mobilité des débris de glissements de terrain dans les argiles sensibles de l'est du Canada, *4<sup>th</sup> Canadian Conference on Geohazards*.
- Long, M. and Donohue, S. 2010. Characterization of Norwegian marine clays with combined shear wave velocity and piecone penetration test data, *Canadian Geotechnical Journal*, 47(7): 709-718.
- Mayne, P. W. and Rix, G. J. 1995. Correlations between shear wave velocity and cone tip resistance in clays, *Soils and Foundations*, 35: 107-110.
- Quinn, P. E., Diederichs, M. S., Rowe, R. K. and Hutchinson D. J. 2010. A new model for large landslides in sensitive clay using a fracture mechanics approach, *Canadian Geotechnical Journal*, 48(8): 1151-1162.
- Remai, Z. 2013. Correlations of undrained shear strength and CPT resistance, *Periodica Polytechnica Civil Engineering*, 57(1): 39-44.
- Tavenas, F., Chagnon, J. Y. and La Rochelle, P. 1971. Saint – Jean - Vianney landslide: Observations and eye witness accounts, *Canadian Geotechnical Journal*, 8(3): 463-478.
- Tavenas, F., Flon, P., Leroueil S. and Lebius, J. 1983. Remoulding energy and slide retrogression in sensitive clays, *Proc. of Symposium on Slopes on Soft Clays*, 423-454.
- Thakur, V. and Degago, S. A. 2013. Disintegration energy of sensitive clays, *Geotechnique letters*, 3: 20-25.
- Thakur, V., Degago, S. A., Oset, F., Dolva B. K. and Aabøe, R. 2013. A new approach to assess the potential for flowslides in sensitive clays, *18<sup>th</sup> International Conference on Soil Mechanics and geotechnical Engineering: Challenges and innovations in Geotechnics, ICSMGE*, 3: 2265-2268.
- Thakur, V. and Degago, S. A. 2014. Characterization of post failure movements of landslides in soft sensitive clays, *Landslides in sensitive clays – From Geoscience to Risk Management*, 91-101.
- Thakur, V. and Gylland, A. S. 2015. In-situ determination of disintegration energy for soft sensitive clays, *68<sup>e</sup> Conférence Canadienne de Géotechnique et 7<sup>e</sup> Conférence Canadienne Sur Le Pergélisol, Québec*.
- Tremblay-Auger, F., Locat, A., Leroueil, S., Locat P., Demers D., Therrien J. and Mompin, R. 2021. The 2016 landslide at Saint – Luc – de – Vincennes, Québec: Geotechnical and morphological analysis of a combined flow slide and spread, *Canadian Geotechnical Journal*, 58(2): 295-304.
- Vaunat, J and Leroueil, S. 2002. Analysis of post failure slope movements within the framework of hazard and risk analysis, *Natural Hazards*, 26(1): 83-109.

## Assessment of post-peak strain softening behaviour of Eastern Canadian sensitive clays

Sarah Jacob, Rama Vara Prasad Chavali & Ali Saeidi

*Department of Applied Sciences – Université du Québec à Chicoutimi,  
Chicoutimi, Quebec, Canada*

Abouzar Sadrekarimi

*Department of Civil Engineering – University of Western Ontario, London,  
Ontario, Canada*



### ABSTRACT

The post-peak behaviour of sensitive clays is rather complex unlike other soils due to their continuous strength loss at large strains. Typical laboratory investigations cannot truly simulate the actual field conditions during a sensitive clay landslide due to the difficulty in the replication of shear mechanisms as well as imposing such high strains in the soil samples. Although attempts have been made in the past to model this strength degradation, the extent of its applicability to Eastern Canadian soils, especially to Laflamme Sea clays, is not clear. The present study aims to do a preliminary analysis of the post failure strain softening behaviour in sensitive clays of Desbiens, up to the remoulded state of the soil through a compression testing machine combined with hand kneading of the sample. The post peak strength degradation curve has been developed which can be an important advantage in the evaluation of remoulding energy and assessment of landslide risk.

### RÉSUMÉ

Le comportement post-pic des argiles sensibles est plutôt complexe contrairement à d'autres sols en raison de leur perte continue de résistance aux grandes déformations. Les enquêtes de laboratoire typiques ne peuvent pas vraiment simuler les conditions réelles sur le terrain lors d'un glissement de terrain d'argile sensible en raison de la difficulté de répliquer les mécanismes de cisaillement ainsi que d'imposer des contraintes aussi élevées dans les échantillons de sol. Bien que des tentatives aient été faites dans le passé pour modéliser cette dégradation de la résistance, l'étendue de son applicabilité aux sols de l'Est canadien, en particulier aux argiles de la mer de Laflamme, n'est pas claire. La présente étude vise à faire une analyse préliminaire du comportement de relâchement rupture des argiles sensibles de Desbiens, jusqu'à l'état remanié du sol à l'aide d'une machine d'essai de compression combinée à un malaxage manuel de l'échantillon. La courbe de dégradation de la résistance post-pic a été développée, ce qui peut être un avantage important dans l'évaluation de l'énergie de remaniement et l'évaluation du risque de glissement de terrain.

## 1 INTRODUCTION

The post-failure movements in sensitive clays are often understood poorly due to difficulty in modelling large deformation strain softening behaviour, inadequate tools to model the quick clay flow pattern, limitations in the existing experimental setups and the rigour in minimizing sample disturbances (Thakur et al. 2014). However, the severity of the problems posed by these clay movements makes it inevitable to do a comprehensive study to minimize it. As such, many simplified methods have been suggested in the literature as useful tools in this domain (Tavenas et al. 1983; Leroueil et al. 1983; Locat 2008; Thakur & Degago 2013; Dey et al. 2016). Within this frame of reference, remoulding energy is an important criterion to predict strain softening and retrogression (Jacob et al. 2021).

In simple terms, remoulding energy is the strain energy required to remould a soil specimen and hence is often quantified as the area under the stress-strain curve (Thakur and Degago 2013). The post-peak stress – strain curve shows the strength degradation of the soil specimen with increasing strains until it is completely remoulded. It is crucial to incorporate the entire post-peak stress-strain curve up to the point of complete remoulding to accurately quantify remoulding energy. The integration of the post-peak curve gives the remoulding energy which is a primary criterion in assessing retrogressive landslides (Jacob et al. 2021).

The post-peak strength of a soil and its behaviour in this state of stress are key criteria to predict strain softening and remoulding of soil. According to Lefebvre (1983), the post-peak strength is the strength mobilized in the soil, in both drained and undrained conditions, after it has reached failure at a given effective stress. Hence, it is different from the residual as well as the remoulded state of the soil. However, at the post-peak state, the soil still retains some of its stress history. Generally, in clays, a post-peak strength reduction is observed under increased loading due to strain softening. Under normal circumstances, this behaviour could be easily analyzed in the laboratory using conventional tests such as direct shear or the triaxial tests where the soil can be sheared up to 10-15 % shear strain. In the case of sensitive clays, a complexity arises due to a continuous strength loss even at a large strain ( $> 30\%$ ). As such, it becomes difficult to assess this behaviour with conventional laboratory tests available and demands the use of some unconventional methods to obtain the best possible results. Although there are methods to obtain the remoulded shear strength of soils, the difficulty arises in discovering the corresponding remoulded strain. This is the biggest challenge that most researchers face in the prediction of geohazards in sensitive clays

ASTM D4646 and 2501-110 CAN/BNQ as well as some literature propose certain remoulding methods which have been successful for many sensitive clays (Tavenas et al. 1983; Thakur & Gylland 2015; Tanaka et al. 2012; Boukpeti et al. 2012, Rasmussen 2012). Remoulding the soil by uniaxial pressing was first proposed by Ladanyi et al. (1968) where the soil sample was subjected to various strains and the remoulded strength at each strain was measured using the vane shear test. In the present study, this method has been altered slightly for better accuracy.

The sensitive clay used in the present study was collected from Desbiens, a village in Quebec. Desbiens is located to the south of Lac Saint-Jean, occupied by the former Laflamme Sea. The region is known to have stratified sand deposits and the piezometric levels here infer the presence of a valley in the bedrock. The combined effect of these two phenomena leads to an increase in leaching which results in a decrease of shear strength and an increase of sensitivity in this area (Rochelle et al. 1970). Sensitive clay slopes of this region are unstable and some are even active (Rochelle et al. 1970; Quinn et al. 2009).

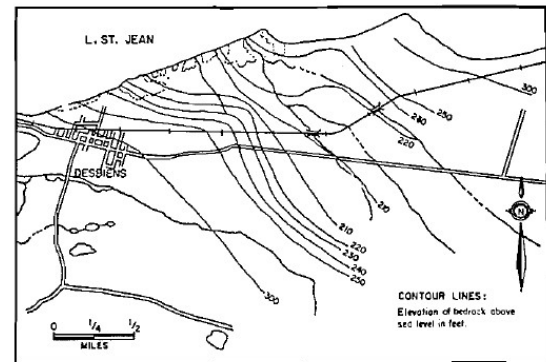


Figure 1. Bedrock Topography of Desbiens (Rochelle et al. 1970) © Canadian Science Publishing or its licensors

## 2 METHODOLOGY

Remoulding by uniaxial pressing is advantageous over other methods of remoulding as we are aware of the strain at which strength loss takes place. As discussed earlier, measurement of strain is close to impossible otherwise, making the post-peak strain softening analysis further difficult. Although this is an indirect method to develop the post-peak stress-strain curve, the results may be seen as a preliminary step to develop a more sophisticated experimental setup for the current study. The following sections explain the characterization of the soil sample used and the testing procedure adopted which closely follows that of Ladanyi et al. (1968).

### 2.1 Basic properties of the soil specimen

Clay samples were obtained from the Desbiens landslide area in Quebec. The samples used in this study were extracted from a depth of 9.5 to 17.5 m. The soil was observed to be mostly clayey with very few sand layers below 13 m depth. The basic properties of the soil obtained as an average from the samples of depth 9.5 to 17.5 m are enumerated in Table 1. The undrained and remoulded shear strength of the sample was measured using the fall cone test. All the properties have been estimated as per ASTM standards.

Table 1. Properties of soil under study

Properties	Value
------------	-------

Water content (%)	42.7
Liquid limit (%)	62.7
Plastic limit (%)	23.7
Specific gravity	2.71
Clay fraction (%)	32
Activity	1.2
Undrained shear strength (kPa)	11.2
Remoulded shear strength (kPa)	0.9
Sensitivity	12

The soil falls under the category of highly plastic clay in the plasticity chart (CH). The XRD analysis of soil indicated the presence of quartz, microcline, albite, calcite and ferropargasite minerals.

## 2.2 Testing procedure

The post-peak soil strength behaviour was investigated by Ladanayi et al. (1968) by compressing soil samples between two parallel platens and measuring the remoulded shear strength using vane shear test at the end of each compression. This procedure was adopted to measure remoulded shear strengths corresponding to axial strains of up to 200%. A similar testing procedure was adopted in the present study as well.

A total of four soil samples were used in the entire testing procedure to obtain the complete post-peak behaviour for Desbiens clay. The first sample was used to measure the intact shear strength of the soil using fall cone test. The strain corresponding to the peak strength was taken as 2% according to an unconsolidated undrained triaxial test conducted on one of the samples. The three other samples were used to measure the remoulded strength of samples at axial strains of 20, 50 and 90% by uniaxial pressing. The sample trimmings were used to determine the completely remoulded strength of the soil by hand kneading.

For uniaxial pressing, all the samples were trimmed to a diameter of 35 mm and a height of 70 mm. The samples were loaded between two plates in a uniaxial compression testing machine to pre-determined strains of 20, 50 and 90% at a strain rate of 1% per minute. This would induce deformations of 14, 35 and 63 mm respectively in the sample. Two filter papers were placed at the top and bottom of the specimen to ensure a uniform contact with the plates of the machine. At the end of each test the disturbed samples were taken out of the machine and carefully placed inside the fall cone cup in layers to measure the undrained shear strength by fall cone apparatus. Figure 3 shows an intact sample and the several samples which were compressed to different strains of 20, 50 and 90%.

In order to obtain the remoulded shear strength, the samples were hand kneaded for complete remoulding. The trimmings of samples were used for hand kneading. According to 2501-110 CAN/BNQ procedure, in order to completely remould a sample, the unused sample trimmings should be kneaded thoroughly in a bowl until its consistency is homogenous (Rasmussen 2012). The Desbiens samples were kneaded for 15 minutes after which they were wrapped in sufficient amount of cellophane to

preserve their water content and to prevent air entrapment. The sample was observed to be completely disturbed with an appearance close to that of a liquid mass (Figure 4). Later, the sample was transferred in layers to the fall cone cup to avoid air bubbles and the remoulded shear strength was measured using a fall cone apparatus.

The methodology adopted in this study follows closely to that of Ladanayi et al. (1968). However, the authors did not reuse the samples for higher strains as in the case of Ladanayi et al. (1968). This is because the continuous manipulation of the same soil specimen could lead to a scatter in the data. Hence this was not followed and a new soil specimen was used for each test for better accuracy. The test was not continued beyond a strain level of 90% for the same reason and the remoulded shear strength was measured by hand kneading followed by a fall cone test. The stress-strain curve was extrapolated from the strain of 90% to the point of complete remoulding by curve fitting.



Figure 2. A sample placed inside the uniaxial compression testing machine

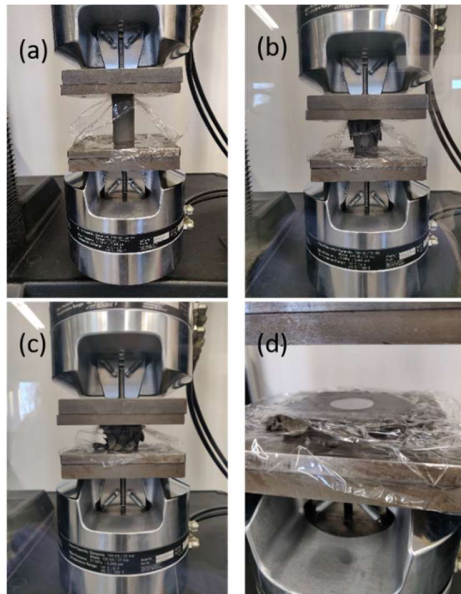


Figure 3. (a) Before compression, (b), (c), and (d) Soil samples compressed to 20, 50 and 90% strains, respectively

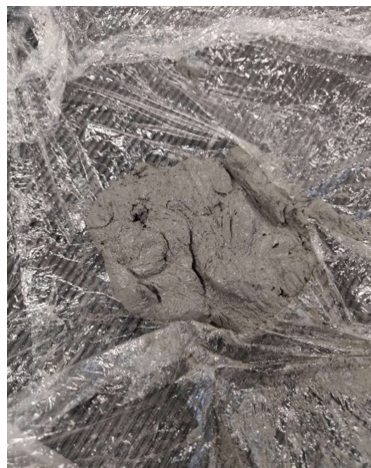


Figure 4. A completely remoulded sample after hand kneading

### 3 RESULTS AND DISCUSSION

The post-peak stress-strain curve for Desbiens soil was obtained up to 90% strain. The initial intact shear strength was measured as 11.2 kPa. After hand kneading for 15 minutes, the remoulded shear strength of the sample dropped to 0.9 kPa which presents a sensitivity of about 12.

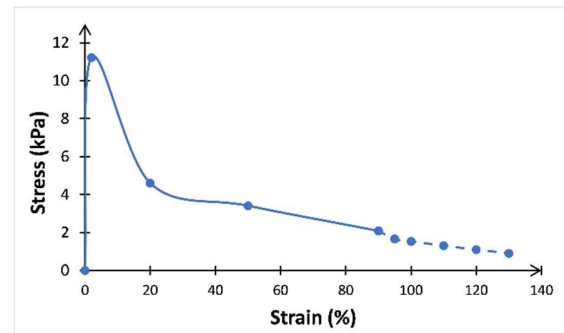


Figure 5. Complete stress – strain curve for Desbiens sample

The complete post-peak curve beyond 90% strain up to the remoulded shear strength of 0.9 kPa was obtained by curve fitting (Figure 5). This yielded a strain of 130 % corresponding to the remoulded shear strength. The strength degradation prediction is indicated in Figure 5 by dotted lines.

#### 3.1 Remoulding energy from post-peak curve

The remoulding energy is an important parameter that helps in quantifying the strain softening and post-peak strength degradation in soils. The literature suggests few existing methods to determine remoulding energy based on experimental (Tavenas et al. 1983, Thakur & Gylland 2015), empirical (Leroueil et al. 1996; Locat 2008) and analytical (Thakur & Degago 2013) methods. A comparison of various methods for determining remoulding energy by Jacob et al. (2021) highlights the importance of a non-linear approach to estimate remoulding energy as opposed to a linear stress-strain curve that seems to highly overestimate the remoulding energy. The current method employs the non-linear approach and does not overestimate the remoulding energy and hence can be used with reasonable accuracy.

The remoulding energy per unit volume is calculated from the area under the shear stress-strain curve in Figure 5 as 415.15 kJ/m<sup>3</sup>. The Eastern Canadian clays investigated by Tavenas et al. (1983) have a majority of sites with remoulding energies ranging from 350 to 400 kJ/m<sup>3</sup> as well. Figure 6 shows the remoulding energy of Desbiens samples along with other Eastern Canadian clays. According to this figure, the remoulding energy for Desbiens samples is in line with other sensitive clay samples of the same region investigated previously.

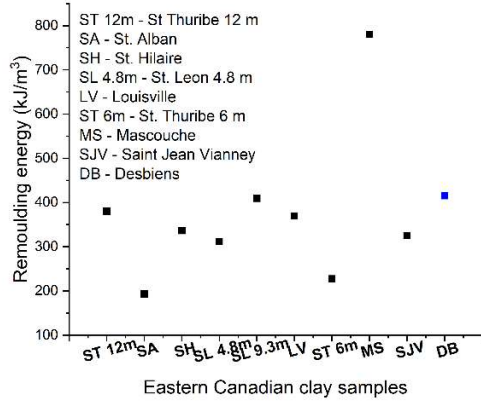


Figure 6. Comparison of remoulding energy for Desbiens clay (blue dot) with other Eastern Canadian clay samples (red dots)

The remoulding index ( $I_r$ ) is a property closely associated with remoulding energy which indicates the degree of remoulding that a soil specimen undergoes. It is defined by Tavenas et al. (1983) as follows:

$$I_r = \frac{c_u - c_{ux}}{c_u - c_{ur}} * 100 \quad (1)$$

where,  $c_u$  = undrained shear strength of the soil specimen,  $c_{ux}$  = strength of a partially remoulded soil specimen, and  $c_{ur}$  = remoulded shear strength of the soil specimen.

The remoulding indices and the corresponding remoulding energies at each point of strength reduction was obtained from the stress-strain curve of Figure 5. This is represented in Figure 8. Similar to Tavenas et al. (1983), the remoulding energy is also expressed as normalized remoulding energy ( $W_N$ ) using the limit state energy as shown in Equation (2). The remoulding of the soil begins once the peak state is achieved and the energy up to the peak state or the limit state is called the limit state energy as represented in Figure 7. Here, the limit state energy is obtained as area of the stress-strain curve up to the peak strength in Figure 5.

$$W_N = \frac{\text{Remoulding energy}}{\text{Limit state energy}} \quad (2)$$

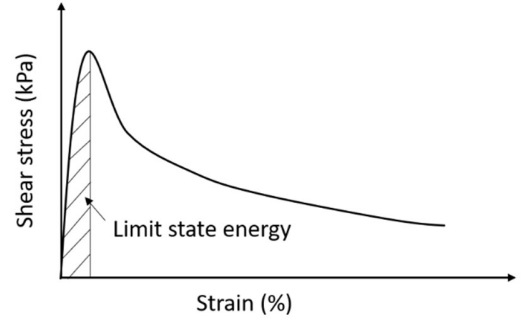


Figure 7. Representation of limit state energy

The normalized remoulding energy – remoulding index curve for a Desbiens soil sample is shown in Figure 9. In contrast to similar curves from Tavenas et al. (1983), the slope of the curve is very gradual, which indicates that the Desbiens soil requires more energy for remoulding in comparison to other Eastern Canadian clays. In other words, the Desbiens clay sample takes an appreciable amount of energy to become remoulded. A steeper slope would indicate lesser energy to remould the sample.

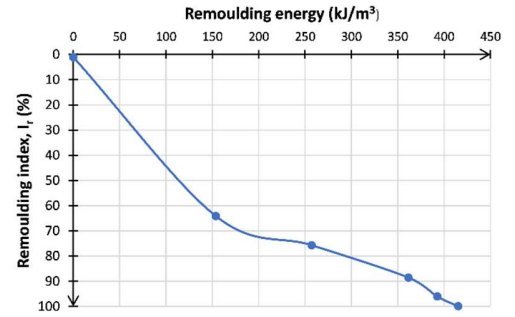


Figure 8. Remoulding energy – remoulding index curve for a Desbiens clay sample

According to Tavenas et al. (1983), large retrogressions are possible when  $I_r > 70\%$  and  $W_N < 40$ . This is represented by the area of the curve below the dotted line in Figure 9.

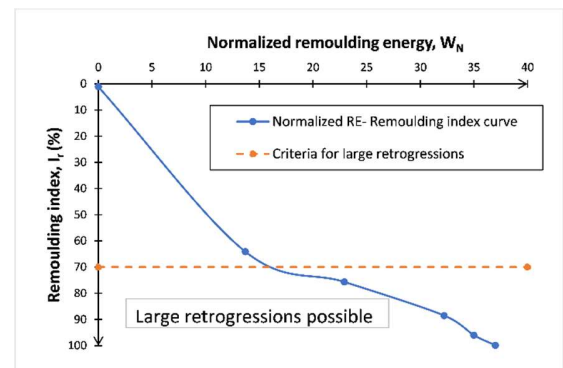




Figure 9. Normalized Remoulding energy – remoulding index curve for a Desbiens sample indicating criterion for large retrogressions

The remoulding energy is also compared with an empirical equation for remoulding energy corresponding to 75% of the remoulding index proposed by Leroueil et al. (1996) based on Tavenas's data. This is enumerated in Figure 10 which shows a larger amount of remoulding energy for the Desbiens clay sample than the empirical correlation. Further testing and data from this region could throw more light on this.

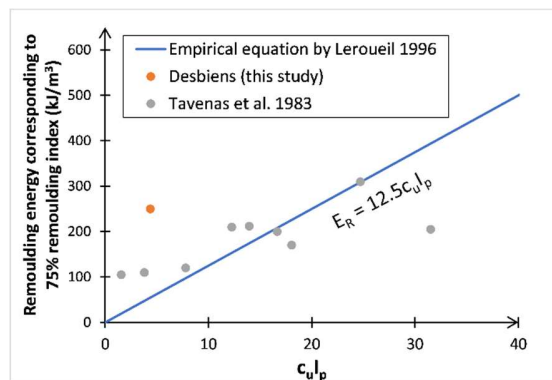


Figure 10. Comparison of remoulding energy with empirical equation by Leroueil et al. (1996)

The importance of remoulded shear strength in comparison to sensitivity as a criterion to predict retrogression is also evident from this study. As suggested by Carson (1979), the rate at which the strength is lost from the peak to the remoulded state is more important than the exact value of sensitivity. Here the sensitivity is 12, however, the strength loss from the peak to the remoulded state is significant where the remoulded shear strength value drops rapidly to 0.9 kPa. Hence a clay's extreme sensitivity and ability to undergo retrogression may not be assessed solely by the value of sensitivity.

Uniaxial pressing is an adequate method of understanding the post-peak behaviour of sensitive clays which is otherwise quite difficult to interpret experimentally. The complete stress-strain curve which includes the peak, post-peak and remoulded stress-strain parameters of the soil is difficult to predict from conventional laboratory shearing experiments.

### 3.2 Limitations of the method

The methodology is promising and helps in the assessment of the post-peak behaviour of soils to a great extent. However, there is room for improvement and certain limitations that should be kept in mind. The compression of soil leads to the formation of multiple failure surfaces which might overlap during the process of loading. This may lead to non-uniform straining of the soil specimen. Secondly, all the tests were carried out at a strain rate of

1%/minute. Therefore, at higher strains (e.g., 90%), the quick condition of an undrained shear would not be properly maintained. It would have been ideal to increase the strain rate at higher strains to ensure undrained conditions. Lastly, when the sample is transferred from the uniaxial machine to the fall cone cup, there is a small amount of energy used which is not accounted for in the analysis. However, this could be considered negligible.

This method should be primarily viewed as part of a preliminary investigation to develop a more sophisticated methodology for determination of remoulding energy. Nevertheless, it is simple to perform and useful in understanding the post-peak strength reduction in sensitive clays and to assess remoulding energy to an extent.

## 4 CONCLUSIONS

The uniaxial pressing method originally developed by Ladanyi et al. (1968) to assess the post-peak behaviour of soils in undrained shear was used with slight modifications to analyze the post-peak strength degradation of Eastern Canadian sensitive clays of Desbiens. The following conclusions may be drawn from this study

- The complete stress-strain curve for sensitive clays of Desbiens have been developed by uniaxial pressing along with curve fitting.
- The post-peak strength reduction is quantified by the area under the stress-strain curve which is the remoulding energy
- The remoulding energy for sensitive clays of Desbiens is comparable to other sensitive clays of Eastern Canada
- Along with sensitivity, the value of remoulded shear strength and the ease with which this strength loss is achieved is also important from the point of view of retrogression in sensitive clays.
- The uniaxial pressing method is a simple and adequate method to conduct preliminary analysis on post-peak behaviour of sensitive clays.

## 5 ACKNOWLEDGEMENT

This research was partially funded by the Natural Sciences and Engineering Research Council of Canada (NSERC) and Hydro-Quebec under project funding no. RDCPJ 521771-17.

## 6 REFERENCES

- ASTM Standard D 2216-10, "Standard Test Method for Laboratory Determination of Water (Moisture) Content of Soil and Rock by Mass", ASTM International, West Conshohocken, 2019.
- ASTM Standard D 4318-17, "Standard Test Methods for Liquid Limit, Plastic Limit and Plasticity Index of Soils", ASTM International, West Conshohocken, 2018.
- ASTM Standard D 854-02, "Standard Test Methods for Specific Gravity of Soil Solids by Water Pycnometer", ASTM International, West Conshohocken, 2017.

- ASTM Standard D 7928-16, "Standard Test Method for Particle Size Distribution (Gradation) of Fine-Grained Soils Using the Sedimentation (Hydrometer) Analysis", ASTM International, West Conshohocken, 2017.
- Boukpeti, N., White, D. J., Randolph, M. F., & Low, H. E. (2012). Strength of fine-grained soils at the solid–fluid transition. *Géotechnique*, 62(3), 213-226.
- CAN/BNQ (2006), "Soils – Determination of Undrained Shear Strength and Determination of Sensitivity of Cohesive Soils Using the Fall Cone Penetrometer", *National Standards of Canada*, CAN/BNQ 2501-110/2006.
- Carson, M.A., 1979. On the retrogression of landslides in sensitive muddy sediments
- Dey R., Hawlader B., Philips R. and Soga K. 2016. Modelling of large deformation behaviour of marine sensitive clays and its application to submarine slope stability analysis, *Canadian Geotechnical Journal*, 53(7): 1138-1155.
- Jacob, S., Saeidi, A., Chavali, R. V. P. 2021. Comparison of existing methods of remoulding energy, *Proceedings of the 74<sup>th</sup> Canadian Geotechnical Conference and 14<sup>th</sup> Joint CGS/IAH-CNC Groundwater Conference*, Niagara Falls, Ontario, Canada.
- Ladanyi, B., Morin, J. P., Pelchat, C. 1968. Post peak behaviour of sensitive clays in undrained shear, *Canadian Geotechnical Journal*.
- Lefebvre, G. 1983. Use of post peak strength in slope stability analysis, *Swedish Geotechnical Institute*, Report no. 17, Linköping.
- Leroueil, S., Tavenas, F. and Bihan, J. P. 1983. Characteristic properties of Eastern Canadian clays, *Canadian Geotechnical Journal*, 20: 681-705
- Leroueil, S., Locat, J., Vaunat, J., Picarelli, L., Lee, H. and Faure, R. 1996. Geotechnical characterization of slope movements, *Proc. of 7<sup>th</sup> International Symposium on Landslides*, 53-74.
- Locat, P., Leroueil, S. and Locat, J. 2008. Remaniement et mobilité des débris de glissements de terrain dans les argiles sensibles de l'est du Canada, *4<sup>th</sup> Canadian Conference on Geohazards*.
- Quinn, P. E. 2009. Large landslides in sensitive clay in eastern Canada and the associated hazard and risk to linear infrastructure (Vol. 71, No. 11).
- Rasmussen, K. K. 2012. An investigation of monotonic and cyclic behaviour of Leda clay.
- Rochelle, P. La, J. Y. Chagnon, and G. Lefebvre. 1970. Regional geology and landslides in the marine clay deposits of eastern Canada. *Canadian Geotechnical Journal* 7, no. 2 :145-156.
- Tanaka, H., Hirabayashi, H., Matsuoka, T., & Kaneko, H. (2012). Use of fall cone test as measurement of shear strength for soft clay materials. *Soils and Foundations*, 52(4), 590-599.
- Tavenas, F., Flon, P., Leroueil S. and Lebius, J. 1983. Remoulding energy and slide retrogression in sensitive clays, *Proc. of Symposium on Slopes on Soft Clays*, 423-454.
- Thakur, V. and Degago, S. A. 2013. Disintegration energy of sensitive clays, *Geotechnique letters*, 3: 20-25.
- Thakur, V. and Gylland, A. S. 2015. In-situ determination of disintegration energy for soft sensitive clays, *68e Conférence Canadienne de Géotechnique et 7e Conférence Canadienne Sur Le Pergélisol, Québec*.



# **Assessment of the relationship between undrained shear strength and geotechnical parameters for sensitive clays of Eastern Canada**

**Sarah Jacob,<sup>1</sup> Ali Saeidi, Ph.D., P.Eng.,<sup>2</sup> Rama Vara Prasad Chavali, Ph.D.,<sup>3</sup> and Abouzar Sadrekarimi, Ph.D., P.Eng.<sup>4</sup>**

<sup>1</sup> Université du Québec à Chicoutimi, Department of Applied Sciences, 555 Bd de l'Université, Chicoutimi, QC, Canada G7H 2B1; E-mail: sjacob2@etu.uqac.ca

<sup>2</sup> Université du Québec à Chicoutimi, Department of Applied Sciences, 555 Bd de l'Université, Chicoutimi, QC, Canada G7H 2B1; E-mail: asaiedi@uqac.ca

<sup>3</sup> Velagapudi Ramakrishna Siddhartha Engineering College, Department of Civil Engineering, Kanuru, Vijayawada, 520007, India; E-mail: rvprasad@vrsiddhartha.ac.in

<sup>4</sup> Western University, Department of Civil and Environmental Engineering, 3010D Spencer Engineering Building, London, Ontario, Canada N6A 5B8; E-mail: asadrek@uwo.ca

## **ABSTRACT**

Eastern Canadian clays are characterized by high sensitivity and compressibility and warrants the need for an appropriate estimation of the undrained shear strength for a safe geotechnical design. A multivariate geotechnical database consisting of natural water content, Atterberg limits, undrained shear strength, effective vertical stress, preconsolidation pressure and over consolidation ratio from 49 sites in Eastern Canada is compiled from literatures for this purpose. The primary objective of this study is to analyse the dependence of undrained shear strength on the aforementioned parameters and propose a correlation that satisfies practical conditions through regression analysis. Bias and uncertainties of existing empirical correlations are assessed. A comparative study is also made with sensitive clays of Norway and Sweden. The results show the poor correlation of Eastern Canadian clays with index parameters and their strong dependence on the stress history of the soil.

## **INTRODUCTION**

Eastern Canadian clays are characterized by high undrained shear strength ( $s_u$ ) and preconsolidation pressure due to their geological origin and depositional environment. They are predominantly composed of clays from three sedimentary basins – Champlain, Laflamme and Goldthwait sea basins (Demers et al. 2014). Certain sensitive clay deposits also occur on the North East of Quebec along the shore of the Hudson Bay. In comparison to Scandinavian clays, Eastern Canadian clays are cemented and have high preconsolidation pressures (Torrance 2017).

The most commonly adopted field test for  $s_u$  measurement in Canada is the field vane test (FVT). Cone penetration tests are also useful in determining  $s_u$  profiles in the field and to identify weak layers. In the laboratory, fall cone test (FCT) is popular due to its simplicity and results close to FVT. More precise assessment of  $s_u$  can be made through direct shear and triaxial tests. High sensitivity and sample disturbance often lead to the use of empirical equations for determination of  $s_u$ , based on different soil parameters like Atterberg limits (Hansbo 1957; Mesri 1975) or stress history (Jamiolkowski et al. 1985; Windisch and Young

1990; Ching and Phoon 2012a; D'Ignazio et al. 2016). Use of empirical equations should be carried out with caution and be accompanied by good knowledge about the original database from which such relations are calibrated. As the cause of high  $s_u$  in sensitive clays is not always attributed to their inherent characteristics and more to their depositional condition, existing  $s_u$  correlations dependant on physical characteristics should be reconsidered. A multivariate transformation model based on sensitivity analysis is adopted here to evaluate the dependence of  $s_u$  in sensitive clays of Eastern Canada to their physical properties.

## ANALYSIS OF MULTIVARIATE DATABASE

The database used for analysis involves 231 sensitive clay samples from 49 sites in Eastern Canada. Scandinavian clays from Sweden and Norway were also compiled to compare the differences in correlations between Eastern Canadian and Scandinavian clays. 153 sensitive clay samples from 53 sites in Norway and 126 sensitive clay samples from 13 sites in Sweden have been used for comparison. The data used have been collected from several literatures. Multivariate information based on seven parameters –  $s_u$  from FVT/FCT, effective vertical stress ( $\sigma'_v$ ), preconsolidation pressure ( $\sigma'_p$ ), natural water content ( $w_N$ ), liquid limit ( $\omega_L$ ), plastic limit ( $\omega_P$ ) and sensitivity ( $S_t$ ) are collected for Eastern Canada, Norway and Sweden. The plasticity charts in Figure 1(a) shows an overview of the clay types in our database. Swedish clays appear to be more compressible than Eastern Canadian and Norwegian clays with high liquid limits.

A general characteristic of sensitive clays is their high water contents, often close to their liquid limit. This is due to their high void ratios arising from a flocculated structure due to marine deposition (Giles 2020). Figure 1 (b) indicates that in most cases the natural water content is more than the liquid limit which explains the low remoulded shear strength upon disturbance of a sensitive clay. Figure 2 shows the variation of  $s_u/\sigma'_v$  with overconsolidation ratio (OCR) according to the stress history and normalized soil engineering properties (SHANSEP) framework by Ladd and Foot (1974). Eastern Canadian clays have high undrained shear strengths in comparison to the Scandinavian clays and some of them exhibit extremely high preconsolidation pressures. However, for  $s_u/\sigma'_v > 1.2$ , the increasing trend between  $s_u/\sigma'_v$  and OCR are not followed. This is because in most Eastern Canadian sensitive clays, the high undrained shear strength is a result of cementation rather than preloading and preconsolidation (Torrance 2017).

The most realistic values of  $s_u$  are often obtained from conventional laboratory shear tests like direct simple shear and triaxial tests. However, FVT/FCT is performed at much higher strain rates and result in higher values of  $s_u$ . Thus,  $s_u$  from FVT/FCT is converted to shear strength mobilized during a slope failure ( $s_{u,mob}$ ) using a correction factor  $\mu$  proposed by Larsson et al. (1984) based on  $\omega_L$  of the soil as per Eq. 1. According to Larsson et. al. (1984), this correction maybe most accurate for normally consolidated to slightly overconsolidated clays and in cases of  $\mu > 1.2$ , further investigation is required. However, Larsson et al. (2007) further proposed a modified  $\mu$  for clays with  $OCR > 1.3$  according to Eq. 2.

$$\mu = \left( \frac{0.43}{\omega_L} \right)^{0.45} \geq 0.5 \quad (1)$$

$$\mu = \left( \frac{0.43}{\omega_L} \right)^{0.45} \left( \frac{OCR}{1.3} \right)^{-0.15} \quad (2)$$

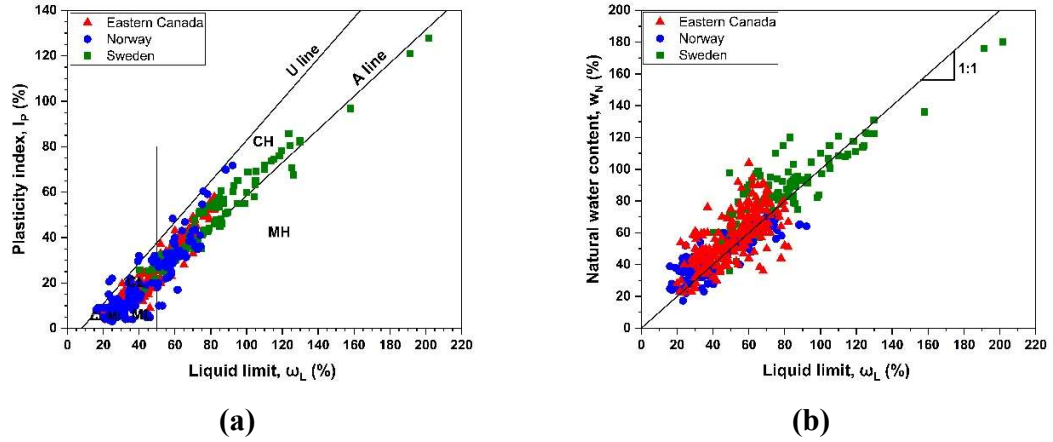


Figure 0-7. (a) Plasticity chart (b) Liquid limit vs water content

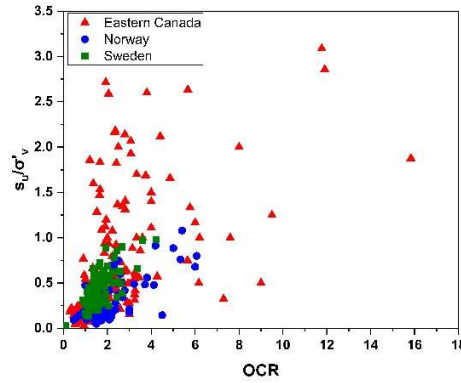


Figure 2.  $s_u/\sigma'_v$  vs OCR for the clays collected in this study

After applying the corrections based on  $\omega_L$  and OCR, 6 and 21 data points of Eastern Canada and Norway respectively were found to still show  $\mu > 1.2$ . Hence, before further analyses, these points were discarded. Thus, the final database for Eastern Canada and Norway included 225 and 132 datapoints, respectively. All datapoints for Swedish clays were carried forward for analysis.

For this study, analysis of ten dimensionless parameters derived from the seven basic parameters mentioned above was carried out. These ten parameters were –  $s_u$  normalised by  $\sigma'_p$  ( $s_u/\sigma'_p$ ),  $s_{u,mob}$  normalised by  $\sigma'_v$  ( $s_{u,mob}/\sigma'_v$ ),  $s_{u,mob}$  normalised by  $\sigma'_p$  ( $s_{u,mob}/\sigma'_p$ ),  $\omega_N$ ,  $\omega_L$ ,  $\omega_P$ , plasticity index ( $I_p$ ), liquidity index ( $I_L$ ) and  $S_t$ . The nomenclature for the final database were given according to Ching and Phoon (2014) as soil type/number of parameters of interest/number of data points i.e. EC/10/225, N/10/132, S/10/126 for Eastern Canada, Norway and Sweden respectively. In the case of Sweden, the information on sensitivity was available only for 33 data points. Thus, the analysis involving  $S_t$  and remoulded undrained shear strength ( $s_{ur}$ ) for Swedish clays were conducted for a smaller database named – S/10/33. The basic statistics of the ten dimensionless parameters, which include the number of

datapoints (n), mean value, maximum and minimum values and the coefficient of variance (COV) are shown in Tables 1, 2, and 3.

**Table 0-4. Basic statistics of dimensionless parameters of EC/10/225**

Variable	n	Mean	Maximum	Minimum	COV
$S_u / \sigma'_p$	225	0.29	1.55	0.03	0.747
$S_{u,mob} / \sigma'_v$	225	0.55	3.16	0.03	1.073
$S_{u,mob} / \sigma'_p$	225	0.28	1.73	0.03	0.82
OCR	225	2.19	29	0.3	1.221
$\omega_L$ (%)	225	50.96	82	21.5	0.282
$\omega_P$ (%)	225	23.61	37	13	0.181
$w_N$ (%)	225	56.42	104	23	0.28
$I_P$ (%)	225	27.26	58	3.6	0.452
$I_L$	225	1.41	7.6	0.14	0.631
$S_t$	225	69.1	559	2	1.413

**Table 0-5. Basic statistics of dimensionless parameters of N/10/132**

Variable	n	Mean	Maximum	Minimum	COV
$S_u / \sigma'_p$	132	0.18	0.47	0.03	0.354
$S_{u,mob} / \sigma'_v$	132	0.29	1.01	0.04	0.286
$S_{u,mob} / \sigma'_p$	132	0.17	0.45	0.03	0.347
OCR	132	1.75	6.07	0.49	1.751
$\omega_L$ (%)	132	47.86	92.2	22.8	0.338
$\omega_P$ (%)	132	25.32	48	8	0.312
$w_N$ (%)	132	49.22	73	23	0.242
$I_P$ (%)	132	22.83	71.8	3	0.666
$I_L$	132	1.44	7.33	0.2	0.708
$S_t$	132	56.6	350	2.3	1.198

**Table 0-6. Basic statistics of dimensionless parameters of S/10/126 and S/10/33**

Variable	n	Mean	Maximum	Minimum	COV
$S_u / \sigma'_p$	126	0.26	0.49	0.12	0.296
$S_{u,mob} / \sigma'_v$	126	0.31	0.81	0.03	0.367
$S_{u,mob} / \sigma'_p$	126	0.2	0.359	0.105	0.217
OCR	126	1.55	4.21	0.12	0.351
$\omega_L$ (%)	126	77.79	201.8	35	0.355
$\omega_P$ (%)	126	31.95	73.9	14.7	0.297
$w_N$ (%)	126	85.61	180.1	36	0.273
$I_P$ (%)	126	45.84	127.9	11.2	0.428
$I_L$	126	1.26	2.77	0.41	0.298
$S_t$	33	17.44	32	7	0.379

## COMPARISON TO EXISTING TRANSFORMATION MODELS

A comparative analysis among the three databases used in this study based on existing transformation models was carried out to check their consistency. The various transformation

models for  $s_u$  in the literature were grouped into two categories based on the principal dependent parameter: group 1 comprising of relationships between  $s_u$  and Atterberg limits and group 2 comprising of  $s_u$  with stress history. These are summarized in Table 4.

**Table 0-7. Transformation models grouped according to primary dependent parameter ( $P_a$  = atmospheric pressure)**

	Relationship	Literature	Transformation model
Group 1	$S_t$ - $I_L$	Bjerrum (1954)	$S_t = 0.8^{I_L}$
		Ching and Phoon (2012a)	$S_t = 20.726I_L^{1.91}$
	$s_u/\sigma'_p$ - $\omega_L$	Hansbo (1957)	$s_{umob}/\sigma'_v = 0.45\omega_L$
	$s_{ur}/P_a$ - $I_L$	Garneau and LeBihan (1977)	$s_{ur}/P_a = 0.0126/(I_L - 0.2)^2$
		Wroth and Wood (1978)	$s_{ur}/P_a = 1.7^{-4.6I_L}$
		Leroueil et. al. (1983)	$s_{ur}/P_a = 0.00987/(I_L - 0.2)^2$
		Locat and Demers (1988)	$s_{ur}/P_a = 0.0144I_L^{-2.44}$
		Jeong et. al. (2009)	$s_{ur}/P_a = 0.0088I_L^{-3.4}$
Group 2	$s_{u,mob}/\sigma'_p$ - $I_p$	Mesri (1975)	$s_{umob}/\sigma'_p = 0.22$
	$s_{u,mob}/\sigma'_v$ - OCR	Jamiolkowski et. al. (1985)	$s_{umob}/\sigma'_v = 0.23OCR^{0.8}$
		Windisch and Young (1990)	$s_{umob}/\sigma'_v = 0.27OCR$
	$s_{u,mob}/\sigma'_v$ - OCR- $S_t$	Ching and Phoon (2012a)	$s_{umob}/\sigma'_v = 0.229OCR^{0.823}S_t^{0.121}$

It should be noted that different transformation models have been generated from analysis on different regions and soil types. Most correlations are obtained based on regression analysis.  $S_t$  -  $I_L$  relationship by Bjerrum (1954) is based on Norwegian clays.  $s_u/\sigma'_p$  -  $\omega_L$  relationship of Hansbo (1957) is formulated based on correlations from fall cone tests on Swedish clays where most of them were marine clays composed primarily of Illite with sensitivity values close to 10. Several Norwegian clays also agreed with this correlation. The transformation models of Garneau and LeBihan (1977), Leroueil et al. (1983) and Locat and Demers (1988) are based on  $s_u$  from fall cone tests on Eastern Canadian clays, predominantly Champlain Sea clays. Unlike other correlations based on regression analysis, the transformation model of Wroth and Wood (1978) is based on theoretical assumptions on plastic limit of the clay combined with critical state soil mechanics. According to them, this relation is most accurate for overconsolidated clays with water contents close to their plastic limit. The relationship proposed by Ching and Phoon (2012a) is based on a multivariate normal distribution of a global database comprised of structured clays from several countries like Canada, USA, Sweden, Japan, Thailand, Brazil and India. Similarly, Jeong et al. (2009) proposed a  $s_u$  -  $I_L$  relationship based on rheological studies on sensitive clays of different mineralogical origin and rheological characteristics. Transformation models of group 2 involving stress history of the soil are primarily based on the SHANSEP framework, proposed by Ladd and Foot (1974), which describes the variation of  $s_u$  with OCR as follows:

$$s_u/\sigma'_v = s(OCR)^m \quad (3)$$

where  $S$  is  $s_u/\sigma'_v$  at normal consolidation and  $m$  is the SHANSEP intercept based on soil type. The transformation models of Mesri (1975), Jamiolkowski et al. (1985) and Windisch and Young (1990) are based on this concept with different values for the SHANSEP constants ( $S$  and  $m$ ) based on regression analysis.

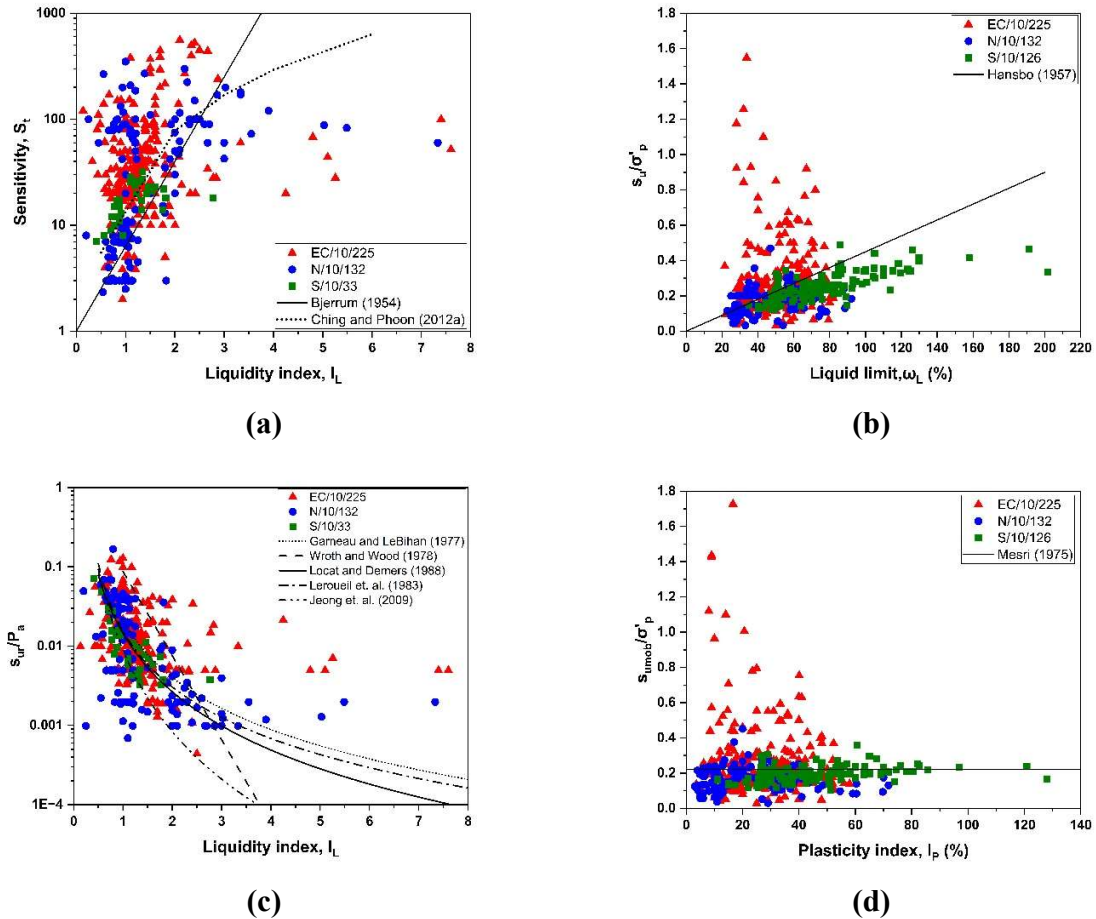


**Figure 3. Transformation models for (a)  $S_t$ - $I_L$  (b)  $s_u/\sigma'_p$ - $\omega_L$  (c)  $s_{ur}/P_a$ - $I_L$  (d)  $s_{u,mob}/\sigma'_p$ - $I_p$**

Figures 3(a-d) compare databases based on transformation models of group 1.  $S_t$  -  $I_L$  relationship in Figure 3(a) shows a reasonable fit to the databases up to  $I_L = 3$  for Bjerrum (1954) as well as Ching and Phoon (2012a). Beyond  $I_L$  of 3, the datapoints seem to deviate for both correlations.  $I_L > 3$  is observed only for Norwegian and Eastern Canadian clays. A similar observation is made in the case of  $s_{ur}/P_a$ - $I_L$  models of Figure 3(c). This is probably because a high  $I_L$  indicates extremely low  $s_{ur}$  similar to a liquid and such values are often not measurable by FVT/FCT, e.g.: - In Figure 3 (c), according to the given correlations,  $I_L > 1.3$  would give  $s_{ur} < 0.1$  kPa which is almost impossible to measure. The reported  $s_{ur}$  values indicate a limit of strength at remoulded conditions where the clay is considered quick (0.5 kPa for Norwegian clays according to NGF (2013)).  $s_u$  does not seem to correlate well with  $\omega_L$  and  $I_p$  for Eastern Canadian and Norwegian clays according to Figures 3(b) and 3(d). As Hansbo (1957)'s relation is primarily based on Swedish clays, they seem to have a good correlation although it forms an upper bound for the database. The independence of  $s_u$  of plasticity index as shown by Mesri (1975) is valid for all three databases as shown in Figure 3(d).

Figure 4 shows the dependence of  $s_u$  on stress history. As previously established by Ladd and Foot (1974),  $s_u$  shows a strong correlation with OCR and correlations of Jamiolkowski et al. (1985) and Windisch and Young (1990) in Figure 4 seem to form a reasonable fit to Norwegian and Swedish clays. However, Eastern Canadian clays present high undrained shear strengths with  $s_{u,mob}/\sigma'_v > 1.2$  and a large degree of scatter, deviating from the empirical trends. As stated earlier, the majority of Champlain Sea clays were normally consolidated to slightly overconsolidated and their high  $s_{u,mob}/\sigma'_v$  is a result of cementation rather than preconsolidation (Torrance 2017).

## BIAS AND UNCERTAINTIES

In a model prediction, the ratio of the actual value to the predicted value indicates model accuracy. Bias factor denoted as 'b' and variance denoted as 'δ' are the sample mean and COV of this ratio. A perfectly accurate model would have equal actual and predicted values, resulting in  $b = 1$ . Consequently,  $b > 1$  and  $b < 1$  indicate an underestimated and an overestimated prediction, respectively.  $\delta$  denotes data scatter with the model being truly deterministic at  $\delta = 0$  and increasingly uncertain with higher  $\delta$  values (D'Ignazio et al. 2016).  $b$  and  $\delta$  are used to calibrate the existing transformation models based on EC/10/225 data and the results are shown in Table 5. According to the  $b$  and  $\delta$  values of Table 5 and Figures 3 and 4, the majority of the existing transformation models were unable to predict the high undrained shear strengths of Eastern Canadian clays. The model by Windisch and Young (1990) seems to best fit Eastern Canadian clays with  $b = 1.03$ . In fact, parameters such as liquid limit and plasticity index have no correlation with  $s_u$  (Figures 3b and 3d). Models involving OCR and some involving  $I_L$  are relatively less biased. Ching and Phoon (2012a)'s model has  $b = 0.84$  but the power of  $S_t$  is rather low and hence the major dependence comes from OCR itself. Thus, a refined transformation model for  $s_u$  by considering OCR,  $w_N$  and  $I_L$  is sought after removal of outliers.

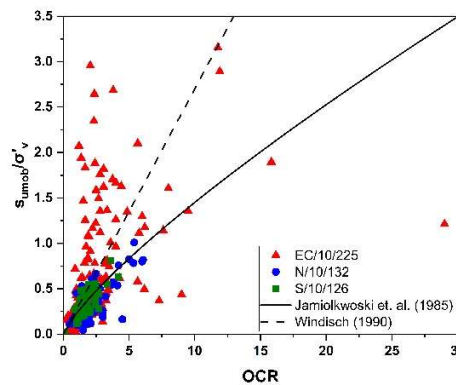


**Figure 4. Transformation models for  $s_{u,mob}/\sigma'_v$  -OCR**

## REMOVAL OF OUTLIERS

In order to provide a more refined database for correlating  $s_u$  with geotechnical parameters such as OCR,  $w_N$  and  $I_L$ , certain outliers were identified in the EC/10/225 based on the physical and mechanical properties of the soil and certain statistical analyses.

- Sensitive clay layers occur below a top layer of dry crust which is usually composed of alluvial sand or weathered clayey silt exposed to the environment with a higher undrained shear strength (Lefebvre 1996). This is usually the top 1 - 2 m from the ground surface. Thus, data

points that occur at depths < 2m were removed from further analysis. This accounted for 17 points in the database.

- Datapoints with  $I_L > 3$  were found to deviate from existing correlations as these corresponded to  $s_{ur}$  too low to be measured experimentally or in the field. Thus, these points were also removed. This accounted for 7 points in the database.
- Based on the statistical criteria for 95% confidence level of  $s_{u,mob}/\sigma'_v$ , datapoints with  $s_{u,mob}/\sigma'_v > \text{mean} + 2\sigma$ , where  $\sigma$  is the standard deviation, were also removed accounting for 14 data points.

This constituted a total of 38 datapoints from EC/10/225 i.e. 17% of the total database. The new database that will be used for further analysis was thus renamed as EC/4/187 by considering the four parameters –  $s_{u,mob}/\sigma'_v$ ,  $w_N$ ,  $I_L$  and OCR.

**Table 0-8. Calibration results for EC/10/225 for existing transformation models**

Literature	Transformation model	b	$\delta$
Bjerrum (1954)	$S_t = 0.8^{I_L}$	6.61	1.55
Ching and Phoon (2012a)	$S_t = 20.726I_L^{1.91}$	3.45	4.98
Hansbo (1957)	$s_{u,mob}/\sigma'_v = 0.45\omega_L$	1.39	0.75
Garneau and LeBihan (1977)	$s_{ur}/P_a = 0.0126/(I_L - 0.2)^2$	1.87	1.73
Wroth and Wood (1978)	$s_{ur}/P_a = 1.7^{-4.6I_L}$	1.37	0.22
Leroeuil et. al. (1983)	$s_{ur}/P_a = 0.00987/(I_L - 0.2)^2$	2.5	1.67
Locat and Demers (1988)	$s_{ur}/P_a = 0.0144I_L^{-2.44}$	3.06	2.07
Jeong et. al. (2009)	$s_{ur}/P_a = 0.0088I_L^{-3.4}$	13.76	4.18
Mesri (1975)	$s_{u,mob}/\sigma'_p = 0.22$	1.26	0.82
Jamiolkowski et. al. (1985)	$s_{u,mob}/\sigma'_v = 0.23OCR^{0.8}$	1.33	0.84
Windisch and Young (1990)	$s_{u,mob}/\sigma'_v = 0.27OCR$	1.03	0.82
Ching and Phoon (2012a)	$s_{u,mob}/\sigma'_v = 0.229OCR^{0.823}S_t^{0.121}$	0.84	0.78

#### ANALYSIS OF NEW DATABASE - EC/4/187

A multiple linear regression analysis was carried out to determine the dependence of  $s_{u,mob}$  on OCR and index parameters based on the following multivariate function (F):

$$F = f(s_{u,mob}/\sigma'_v, OCR, Y_i) \quad (4)$$

where  $Y_i = \{Y_1 = I_L, Y_2 = w_N\}$ . Linear regression analysis gave the following functions for  $I_L$  and  $w_N$ :

$$s_{u,mob}/\sigma'_v = 0.104 + 0.021I_L + 0.137OCR \quad (5)$$

$$s_{u,mob}/\sigma'_v = 0.248 - 0.0019w_N + 0.134OCR \quad (6)$$

It can be noticed that the coefficients of  $w_N$  and  $I_L$  are negligibly small to cause any significant changes in the determination of  $s_{u,mob}$ . Thus, it can be assumed that for Eastern Canadian sensitive clays,  $s_{u,mob}$  does not correlate well with any index parameters and it is only dependent on the stress history (OCR) of the soil. Thus, a power function (Eq. 7) as proposed by Ladd and Foot (1957) was used to find the correlation of  $s_{u,mob}$  with OCR using regression analysis (Fig. 5). The coefficients obtained are in line



with previous studies of D'Ignazio et al. (2016), Jamiolkowski et al. (1985) and Mesri (1975) for Scandinavian clays. Thus, existing  $s_u$  correlations based on index properties should be used with caution although correlations based on stress history applicable for Scandinavian clays maybe applicable to Eastern Canada as well. However, Eastern Canadian clays with high undrained shear strength ratios should be further analyzed as preconsolidation may not always be the reason for their high shear strengths.

$$s_{u,mob}/\sigma'_v = 0.212OCR^{0.85} \quad (7)$$

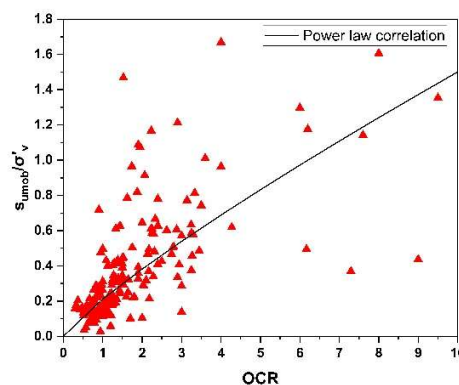


**Figure 5. Power law correlation for  $s_{u,mob}$  with OCR based on the new database**

## CONCLUSIONS

This study focused on the assessment of existing correlations of undrained shear strength with geotechnical parameters such as overconsolidation ratio, Atterberg limits, liquidity index, plasticity index, and water content for sensitive clays of Eastern Canada. The study showed poor correlations of  $s_u$  with index parameters and their strong correlation with OCR. Eastern Canadian clays with  $I_L > 1.3$  do not align with existing correlations due to their extremely low  $s_{ur}$  which is often difficult to measure. High undrained shear strengths of Eastern Canadian clays may not always correlate to their high preconsolidation and could be the result of cementation. Thus,  $s_u$  for such clays should be determined with caution even when using OCR correlations.

## REFERENCES

- Bjerrum (1954). "Geotechnical properties of Norwegian marine clays". *Geotechnique*, 4(2),49-69.
- Ching, J. and Phoon, K. K. (2012a). "Modelling parameters of structured clays as a multivariate normal distribution". *Canadian Geotechnical Journal*, 49(5), 522-545.
- Ching, J. and Phoon, K. K. (2014). "Transformations and correlations among some clay parameters – the global database". *Canadian Geotechnical Journal*, 51(6), 663-685.
- Demers D, Robitaille D, Locat P, Potvin J (2014) Inventory of large landslides in sensitive clay in the province of Quebec, Canada: preliminary analysis. *Landslides in sensitive clays from geoscience to risk management*. Springer, Dordrecht, pp 77–89

- D'Ignazio, M., Phoon, K. K., Tan, S. A., and Lansivara, T. T. (2016). "Correlations for undrained shear strengths of Finnish soft clays". *Canadian Geotechnical Journal*, 53(10), 1628-1645.
- Garneau, R. and LeBihan, J. P. (1977). "Estimation of some properties of Champlain clays with the Swedish fall cone". *Canadian Geotechnical Journal*, 14(4), 571-581.
- Giles, D. P. (2020). "Quick clay behavior in sensitive Quaternary marine clays – A UK perspective". *Engineering Geology Special Publications*, 29(1), 205-221.
- Hansbo, S. (1957). "A new approach to the determination of the shear strength of clay by the fall cone test". *Royal Swedish Geotechnical Institute*.
- Jeong, S. W., Leroueil, S. and Locat, J. (2009). "Applicability of power law for describing the rheology of soils of different origins and characteristics". *Canadian Geotechnical Journal*, 46(9), 1011-1023.
- Jamolkowski, M., Ladd, C. C., Germain, J. T., and Lancellotta, R. (1985). "New developments in field and laboratory testing of soils". *Proc. 11<sup>th</sup> International Conference on Soil Mechanics and Foundation Engineering*, San Francisco, Vol. 1, pp. 57-153.
- Ladd, C. C. and Foot, R. (1974). "New design procedure for stability of soft clays". *Journal of the Geotechnical Engineering Division*, ASCE, 100(7), 763-786.
- Larsson, R., Bergdahl, U., and Eriksson, L. (1984). "Evaluation of shear strength in cohesive soils with special references to Swedish practice and experience". *Statens geotekniska institut*.
- Larsson, R., Salfors, G., Bengtsson, P. E., Alen, C., Berdahl, U. and Eriksson, L. (2007). "Information 3: Shear strength evaluation in cohesive soil", *Statens geotekniska institut*. \
- Lefebvre, G. (1996). Soft sensitive clays. *Landslides - Investigation and Mitigation - Transport Research Board Special Report*, 247, 607-619.
- Leroueil, S., Tavenas, F. and Le Bihan, J.P. (1983). Propriétés caractéristiques des argiles de l'est du Canada. *Canadian Geotechnical Journal* 20(4), 681-705.
- Locat, J., and Demers, D. (1988). Viscosity, yield stress, remolded strength, and liquidity index relationships for sensitive clays. *Canadian Geotechnical Journal* 25(4), 799-806.
- Mesri, G. (1975). "Discussion on new design procedure for stability of soft clays". *Journal of Geotechnical Engineering Division*. ASCE, 101(4), 409-412.
- Norsk Geoteknisk Forening (2013). Melding nr. 2 Symboler og definisjoner i geoteknikk. (In Norwegian).
- Torrance, J. K. (2017). "Chemistry: an essential key to understanding high sensitivity and quick clays and to addressing landslide risks". *Landslides in sensitive clays: From research to implementation*, 35-44.
- Windisch, E. J., and Young, R. N. (1990). "A statistical evaluation of some engineering properties of Eastern Canadian clays". *Canadian Geotechnical Journal*, 27(3), 373-386.
- Wroth, C. P. and Wood, D. M. (1978). "The correlation of index properties with some basic engineering properties of soil". *Canadian Geotechnical Journal*, 15(2), 137-145.

# A comparative study between sensitive clay deposits in the Laflamme and Champlain basins of Eastern Canada



Sarah Jacob & Ali Saeidi

*Department of Applied Sciences – Université du Québec à Chicoutimi, Chicoutimi, Quebec, Canada*

Abouzar Sadrekarimi

*Department of Civil and Environmental Engineering – Western University, London, Ontario, Canada*

Rama Vara Prasad Chavali

*Department of Civil Engineering - Velagapudi Ramakrishna Siddhartha Engineering College, Kanuru, Vijayawada, India.*

## ABSTRACT

Depositional and post – depositional sedimentation environment highly affects the characteristics of sensitive clays. Among Eastern Canadian sensitive clays, Laflamme clays are the result of a recent marine invasion and as such exhibit properties different than clays from other basins, especially in terms of preconsolidation. These differences in properties is an important factor to be considered in retrogressive landslide hazard assessment. The data used in this study are part of a detailed geotechnical investigation on two sites - Desbiens and Albanel. The results show that, as opposed to typical Champlain clays, the Laflamme clays are overconsolidated due to heavy preloading. These have also led to higher shear strengths in these clays. Hence, the consideration of a regional context in the analysis of retrogressive landslides could help in a more accurate judgement regarding the initiation, mechanism, and reactivation of such landslides.

## RÉSUMÉ

L'environnement de sédimentation dépositionnel et post-dépositionnel affecte fortement les caractéristiques des argiles sensibles. Parmi les argiles sensibles de l'est du Canada, les argiles de Laflamme sont le résultat d'une récente invasion marine et présentent donc des propriétés différentes de celles des argiles des autres bassins, notamment en termes de préconsolidation. Ces différences de propriétés sont un facteur important à prendre en compte dans l'évaluation des risques de glissements de terrain rétrogrades. Les données utilisées dans cette étude font partie d'une enquête géotechnique détaillée sur deux sites - Desbiens et Albanel. Les résultats montrent que, contrairement aux argiles typiques du Champlain, les argiles de Laflamme sont surconsolidées en raison d'une précharge importante. Cela a également conduit à des résistances au cisaillement plus élevées dans ces argiles. Ainsi, la prise en compte d'un contexte régional dans l'analyse des glissements de terrain rétrogrades pourrait aider à un jugement plus précis concernant l'initiation, le mécanisme et la réactivation de tels glissements de terrain.

## 8 INTRODUCTION

Sensitive clay deposits occur extensively across Nordic countries like Canada, Sweden, Norway etc. In Eastern Canada, they may be seen along three main sedimentary basins – Champlain, Laflamme and Goldthwait, the extent of which is shown in Figure 1. The most pronounced and extensive slope failures have occurred in the Champlain basin and several experimental and numerical modelling studies on sensitive clays are focused here (Locat and St Gelais 2014; Shan et al. 2021). Additionally, the Laflamme basin suffers occasional slope failures, some more destructive than others. However, if such failures do happen, existing criteria on hazard assessment in sensitive clays, which are primarily based on Champlain clays, may not always be suitable for Laflamme clays. This is because basic properties such as liquidity index ( $I_L$ ) and remoulded shear strength ( $s_{ur}$ ) on which the above-mentioned criteria are based on, are quite different among Laflamme and Champlain clays due to different geological settings and depositional environments. The liquid limit of clays from the Laflamme Sea basin have been shown to be lower than that of the Champlain clays (Chatillon 1974), and the  $I_L$ - $s_{ur}$  relationship established by Leroueil et al. (1983) and Locat and Demers (1988) for Eastern Canadian sensitive clays seem to underpredict the high  $s_{ur}$  of Laflamme clays (Levesque et al. 2007).

For the analysis of sensitive clay landslides, a good understanding of the influence of various geological and geoenvironmental factors on soil properties is warranted. In the present paper these differences are highlighted through an experimental study on Laflamme clays and a comparison to Champlain clays based on certain physical, chemical and mechanical properties.

## 9 GEOLOGY

The glacial retreat and marine invasion were shortest and most recent in the Laflamme basin making the deposits here overconsolidated in comparison to the Champlain clays (Quigley 1980). Although Eastern Canadian sensitive clays are generally considered overconsolidated, Torrance (2017) proposed that overconsolidation in Champlain clays is only an apparent preconsolidation caused by cementation agents such as hematite and

magnetite. However, evidences of decreased water content and increased shear strength with depth (Bouchard et al. 1983), as well as bioturbation activities (Levesque et al. 2007) have been shown in literature indicating heavy preconsolidation and preloading in Laflamme clays. Any cementation in Laflamme clays, if present, would have been relatively recent allowing for their preconsolidation. The present state of Laflamme clays is a result of successive abrasion and deposition of sediments from the Canadian Shield by the glacial retreat, leading to an abundance of rock flour in the sediments over clay minerals. The sediments of this region have been identified to be primarily of silty nature with occasional sand deposits

During the last glaciation period and isostatic rebound, the Laflamme sea was divided into two sub-basins – the Saguenay lowlands and the Lac-Saint-Jean (LSJ). A very distinguishing feature of the sediments in the LSJ is its extremely low salinity compared to the Champlain clays and other Laflamme clays of the Saguenay Fjord. The LSJ basin has a significant source of fresh water from the melting of continental inlands and glaciers and is primarily connected to the sea through the Saguenay River and the Saguenay Fjord. Thus, although the existing sediments in the LSJ region are of marine origin, there is a significant influx of freshwater, creating a lacustrine environment unlike the marine environment in the Saguenay Fjord region. These further change the behaviour of LSJ clays in comparison to Champlain clays, especially in terms of Atterberg limits. Furthermore, heavy overconsolidation in these clays leads to higher undrained shear strengths. Accordingly, the geological history of the Laflamme sea shaped its present state which may be somewhat different from other Eastern Canadian clays.

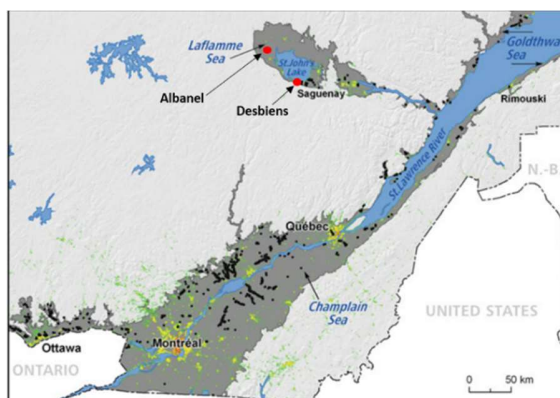


Figure 1. Extent of different sedimentary basins in Eastern Canada (from Demers et al. 2014).

## 10 METHODOLOGY

The soil samples used for analysis were collected from Desbiens and Alabanel, two villages to the south and north of LSJ, respectively as shown in Figure 1. Desbiens is a site known for unstable sensitive clay slopes, some of which are still active (Quinn 2009). The topography of this region represents a valley along with sand deposits at varying depths (Rochelle et al. 1970). This is considered to have aided in supplying fresh water throughout the sediments leading to low salinities. Alabanel is a site of a very old flowslide (about 1000 years old). The samples from both sites were collected using a high-quality tube sampler by the Ministère des Transports et de la Mobilité Durable du Québec (MTQ). Desbiens samples were obtained from a single borehole of 3.5 - 33.3 m deep. Sand layers interbedded with silt were observed at depths of 11.5 to 17.5 m. At the Alabanel site, three boreholes were drilled side by side and samples were obtained from depths of 6.0 – 7.2 m, adjacent to the scar of the old flowslide. Cylindrical samples were obtained with a diameter of 70 mm and heights of 100 to 130 mm. These samples were coated with wax and stored in a humidity chamber throughout this study. All samples were fairly uniform and greyish to dark grey in colour, typical of sensitive clays of this region, and with small traces of sand. Physical properties, chemical composition, microstructure and mechanical behaviour of the samples are explored through a series of experimental investigations and the results are compared with those of some common Eastern Canadian clays to highlight the key differences.

### 10.1 Physical properties

Properties such as grain size distribution (ASTM D7928-21), water content (ASTM D2216-19), Atterberg limits (ASTM D4318-17) and specific gravity (ASTM D854-00) of the clay samples from both sites were measured in accordance with the American Society for Testing and Materials (ASTM) standards. The index properties that were obtained from both study areas are summarized in Table 1.

Table 1. Summary of index properties of Desbiens and Alabanel clays

Property	Desbiens	Albanel
Specific gravity, $G_s$	2.71	2.74
Clay fraction (%)		
At sand-silt interbed	36	-
In sensitive clay layer	52	52-60
Water content, $w_N$ (%)	39-48	41-47
Liquid limit, $\omega_L$ (%)	43-53	48-51
Plastic limit, $\omega_P$ (%)	17-24	19-21
Plasticity index, $I_P$ (%)	25-29	26-30
Liquidity index, $I_L$	0.6-1	0.7-0.9

## 10.2 Chemical composition and microstructure

Salinity, chemical composition, and microstructure of the clay samples were also determined. Salinity of soil samples was determined by dipping a multiparameter probe (Hanna HI 9828) into a mixture of air-dried soil and deionised water at a ratio of 1:5 (20 g of air-dried soil and 100 mL of deionised water). Before taking the reading, the soil suspension was mixed thoroughly using a magnetic stirrer for about a minute at an interval of 30 minutes for 2 hours to dissolve all soluble salts. Another 15 minutes was allowed for the soil to settle. Soil salinity was then measured in g/L at 25°C. A similar methodology for measuring the pore fluid salinity of clay soils was adopted by Liu et al. (2019).

The microstructure of intact clay samples were visualized using a Hitachi SU8230 Regulus Ultra High - Resolution Field Emission SEM at Western University, Ontario. A 3 kV accelerating voltage was used and secondary electron images were collected. The samples were sputter coated with approximately 4 nm of iridium. Microscopic images of oven dried intact clay samples were captured up to a magnification of 50,000 with band lengths of 1  $\mu\text{m}$ .

## 10.3 Undrained strength and stress states

### 10.3.1 Monotonic shearing behaviour

The monotonic shearing behaviour of the clay samples in undrained loading was determined by performing undrained (CUI) triaxial compression tests on isotropically-consolidated specimens. The CUI tests were performed using an automated triaxial testing apparatus manufactured by Wille Geotechnik (Germany). The apparatus includes a 10 kN uniaxial loading frame, a 4 L triaxial cell with maximum pressure capacity of 2,000 kPa, three pressure transducers, a linear variable differential transformer (LVDT), an automatic double volume pressure control (VPC) pump with two channels and a data acquisition and control system (Figure 2). The cell and back pressures along with the pore water volume change are measured and controlled using the double VPC pump and the third pressure transducer placed at the bottom of the cell measures the specimens pore pressure. The axial deviator stress is applied by the loading frame and piston on the specimen.

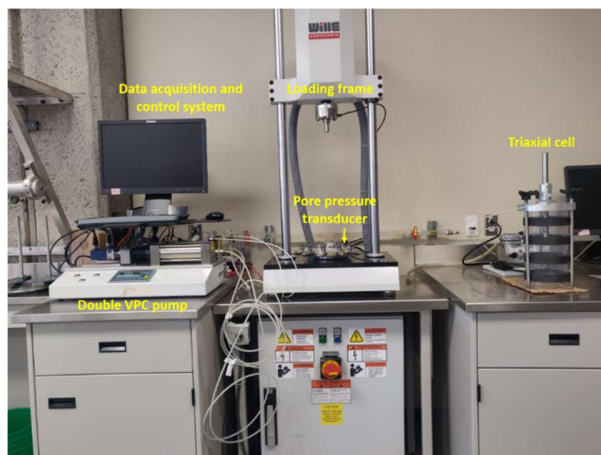


Figure 2. Triaxial testing apparatus used for CUI tests

The specimen preparation and testing procedure were carried out in accordance with the ASTM D4767 (ASTM, 2011) standard. Cylindrical specimens of 50 mm in diameter and 100 mm high were trimmed from intact samples. The specimen was assembled with porous discs and latex membranes after placing filter paper strips around the sample to facilitate radial drainage. All drainage lines were flushed until no air bubbles were observed. Specimen saturation was carried out by flushing the sample at a low effective confining pressure of 5 kPa for three hours followed by the back pressure saturation method. Skempton's pore pressure ratio,  $B$ , of at least 0.96 was achieved. Back pressures as high as 300-650 kPa were required for saturation due to the low permeability of the specimen (on the order of  $10^{-10}$  m/s). Sensitive clay slopes often occur in nature in the overconsolidated state owing to significant erosion (Lefebvre and La Rochelle 1974). As such, the samples were consolidated in the overconsolidated range of stresses. An investigation of borehole data from the database of MTQ around Desbiens and Albanel regions provided an initial estimate of the preconsolidation pressure ( $\sigma'_p$ ) to be around 280 kPa for Desbiens and 275 kPa for Albanel clays. Hence, the samples were consolidated to confining pressures lower than these values. After consolidation, samples were sheared at a strain rate of 1%/hr up to an axial strain of 20%. A total of 7 CUI triaxial tests were carried out – three on Desbiens and four on Albanel samples. The details of these tests are summarized in Table 2.

Table 2. Summary of CUI triaxial tests on Desbiens and Albanel clays

Test name	$\sigma'_{3c}$ (kPa)	$\Delta\sigma_f$ (kPa)	$\epsilon_f$ (%)	$\Delta u_f$ (kPa)
D-CUI1	20	81.04	3.59	-2.2
D-CUI 2	40	138.1	2.17	6.31
D-CUI3	100	168.36	1.08	19.82
A-CUI1	30	174.38	1.72	3.91
A-CUI2	46	193.52	1.69	4.78
A-CUI3	70	232.93	2.59	9.07
A-CUI4	100	238.09	2.51	14.6

where,  $\sigma'_{3c}$  = confining pressure,  $\Delta\sigma_f$  = deviatoric stress at failure,  $\epsilon_f$  = axial strain at failure,  $\Delta u_f$  = porewater pressure at failure

### 10.3.2 Remoulded shear strength

The remoulded undrained shear strength of the samples was determined in the laboratory using fall cone (FCT) and laboratory vane (LVT) tests. The remoulded samples were prepared by hand kneading sample trimmings for about 15 minutes. In the FCT tests, a 60 g cone with a 60° apex angle was pushed into the remoulded sample placed in the measuring cup to measure the strength. For LVT tests, a handheld vane of 32 mm high and 16 mm in diameter was used for measuring strength.

## 11 RESULTS AND DISCUSSIONS

### 11.1 Physical properties

As shown in Table 1, Desbiens samples from sand-silt interbed (depth = 13.4 m) and sensitive clay layer (depth = 9.5 m); and Albanel samples from all three boreholes were used to determine their grain size distributions by sedimentation and sieve analyses. Albanel samples contained a clay fraction (CF) of about 52-60%, while Desbiens samples from 9.5 m depth had a similar CF of about 52%. At the sand – silt interbed in Desbiens, the estimated clay fraction (CF) was about 36%. This lower percentage was due to the interbedded sand layers with fine silt and clay at this depth. This is consistent with the observations of Bouchard et. al. (1983) and the silty nature of clays in the Laflamme region. Champlain clays, however, are known to have higher CFs. Eleven out of fourteen Champlain clays studied by Locat and St Gelais (2014) showed CF in the range of 70-80%.

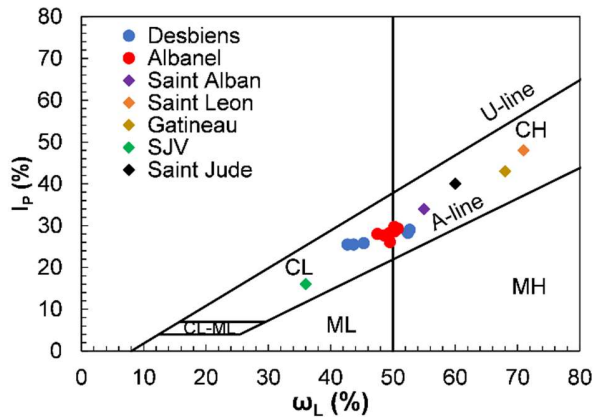


Figure 3. Plasticity chart showing Champlain and Laflamme clays

Furthermore, Atterberg limits of some common Eastern Canadian clays obtained from literature (Locat et al. 2019; Locat and St Gelais 2014; Vaid et al. 1978) have been plotted along with Desbiens and Albanel clays in the plasticity chart shown in Figure 3. Most clays plotted are Champlain clays except for Saint Jean Vianney (SJV) which belongs to the Laflamme basin. It may be noticed that the higher CF in Champlain clays classifies them as clays of high plasticity (CH). Additionally, the clays tested for this study (Desbiens and Albanel) plot at the border of low to high plastic clays, with a slight inclination towards being low plastic (CL). It may be noticed that SJV clays, also from the Laflamme basin, plot as CL further highlighting a difference in clay type between Laflamme and Champlain clays. In Champlain clays, the liquid limits were higher and the water content was closer to liquid limit due to cementation. However, in Laflamme clays, the preconsolidation and preloading lowered the water content and the corresponding limits rendering it less plastic than the Champlain clays. This leads us to reconsider the criteria for retrogressive landslides in sensitive clays proposed by Lebius et al. (1983) that retrogressive landslides occur when  $I_L > 1.2$ , in Laflamme clays.

#### 11.2 Chemical composition and microstructure

As mentioned earlier, the salinity of LSJ clays is quite unique in comparison to other Eastern Canadian clays. This is demonstrated by salinity measurements carried out at various depths in Desbiens clays and all three boreholes in Albanel clays. On average, the salinities were extremely low (0.12 – 0.28 g/L) for Desbiens clays whereas it was almost non-existent in Albanel clays (average of 0.05 g/L). These indicate that the samples were highly leached. Although Champlain clays of low salinities in the range of 0.2 – 0.3 g/L exist, e. g. Gatineau; on average, Champlain clays present higher salinities (in the range of 0.4-11.8 g/L) in comparison to the LSJ clays (Locat and St Gelais 2014).

The microstructure of Desbiens and Albanel clays are shown in Figure 4. Certain differences in the microstructure of Champlain and Laflamme clays were highlighted by Delage (2010). The typical microstructure of Champlain clays consists of silt sized particles embedded in clay aggregates with clay bridges that act as connectors between the silt aggregates (Delage 2010). Delage (2010) shows this with examples of Saint Marcel and Saint Guillaume of the Champlain basin with CF and  $I_P$  of 81% and 35%, respectively. However, these could not be observed in the relatively low plastic clays of this study. It is not just the plasticity or the fines content that contributes to the difference in microstructure. Delage (2010) further presents the microstructure of Saint Thiribe clays of the Champlain basin with a much lower CF (about 30%) where the slit grains are embedded in clay aggregates in the microstructure, much like other Champlain clays. In contrast, the clays of this study consisted of platy minerals and angular aggregates with no clay bridges/aggregations. Moreover, their fabric seems to be dispersed as opposed to the more flocculated structure of Champlain clays. Thus, along with physical parameters, the depositional environment contributes significantly to the microstructure of sensitive clays.



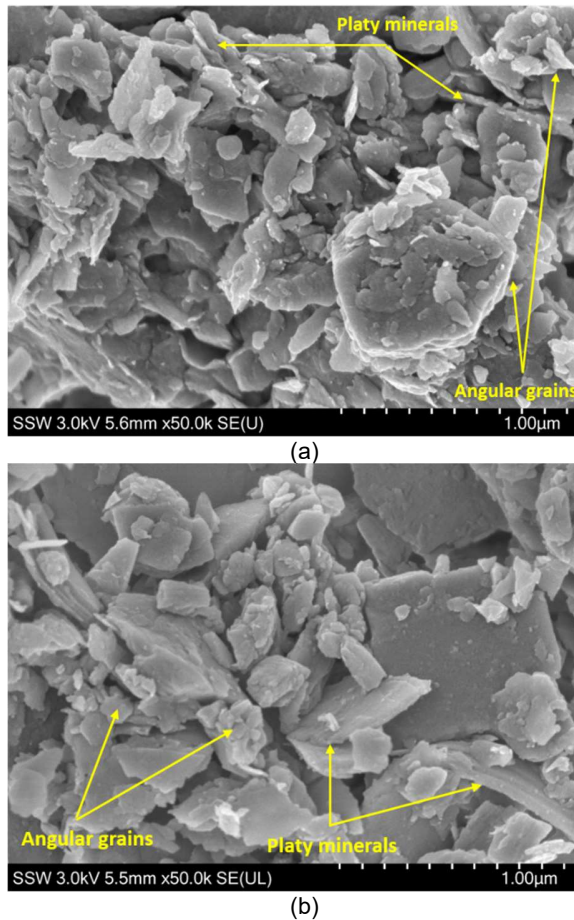


Figure 4. SEM images of (a) Desbiens and (b) Albanel clays with a band length of 1µm

### 11.3 Undrained strength and stress state

#### 4.3.1 Monotonic shearing behaviour

Undrained triaxial tests on isotropically-consolidated samples of Desbiens and Albanel clays were conducted in the overconsolidated range of stresses (i.e.,  $OCR = 2.8 - 14$ ). Failure took place at low strains of 1.0 – 3.5%. The details of the test are shown in Table 2. The clays presented high deviatoric stresses and low pore pressures due to their overconsolidated nature. The stress paths of the clays are plotted with other Eastern Canadian clays and are shown in Figure 5. All clays used for comparison were tested in the overconsolidated range of stresses. Stress paths of Desbiens and Albanel, as well as SJV (Vaid et al. 1978) showed dilative behaviours. This is typical of overconsolidated clays and further highlights the actual overconsolidated nature of Laflamme clays. The stress paths of Champlain clays from St Leon (Flon 1982) and St Jude (Locat et al. 2019) showed a more contractive nature as is typical of clays from this sedimentary basin. This is because overconsolidation in Champlain clays is an apparent preconsolidation due to cementation (Torrance 2017) which can break during shearing, while their natural uncemented fabric is normally consolidated. Since their natural water contents were close to their liquid limits, the Champlain clays generate high positive excess pore water pressures leading to a contractive shearing behavior.



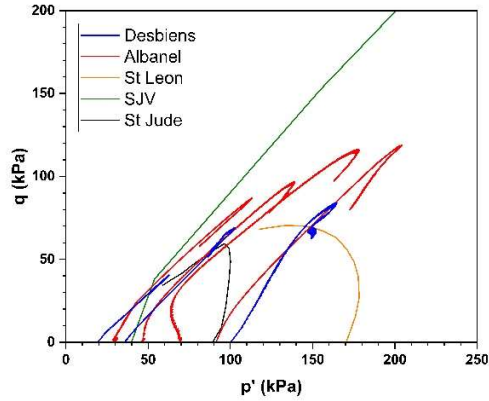


Figure 5. Stress paths of Desbiens and Albanel clays along with other Eastern Canadian clays (Vaid et al. 1978; Flon 1982 and Locat et al. 2019)

A comparison between highly overconsolidated clays such as London clay and soft sensitive clays by Lefebvre (1981) highlighted their key differences in triaxial compression tests. In this context, the LSJ clays of this study behaved like an overconsolidated London clay rather than a soft structured clay. They exhibited highly dilatant behaviours as opposed to the contractive behaviour of other soft clays in Figure 5. Similar behaviour was also observed in an overconsolidated Norwegian ('Emmerstad') clay (Thakur et al. 2014). Skempton (1964) describes the mechanism of progressive slope failures in overconsolidated clays as an increase of mean effective stress with shearing due to dilatancy and therefore overstressing the underlying clay layers to failure. It may also be observed that the stress states in Laflamme clays (Desbiens, Albanel and SJV) are higher than Champlain clays (St Leon and St Jude) due to overconsolidation and preloading.

The shearing behavior of clays of this study are evaluated further based on Skempton's pore pressure parameter at failure,  $A_f = \Delta u_f / \Delta \sigma_f$  (Skempton 1954). The variation of  $A_f$  with OCR as shown by Bishop and Henkel (1957) for Weald clay is reproduced in Figure 6 along with other Eastern Canadian clays as well as the results of this study. The figure shows extremely low  $A_f$  values (-0.04-0.12) in Laflamme clays (Desbiens, Albanel and SJV) in comparison to Champlain clays (St Leon and St Jude) indicating their overconsolidation and dilatancy. Furthermore, the experimental data and the empirical reduction of  $A_f$  with increasing OCR suggested by Bishop and Henkel (1957) seem to be inapplicable to the sensitive clays of the Laflamme basin. This is seen in the case of clays from this study and SJV, both belonging to the Laflamme basin, where their high OCR does not reflect the corresponding  $A_f$  as proposed by Bishop and Henkel (1957).

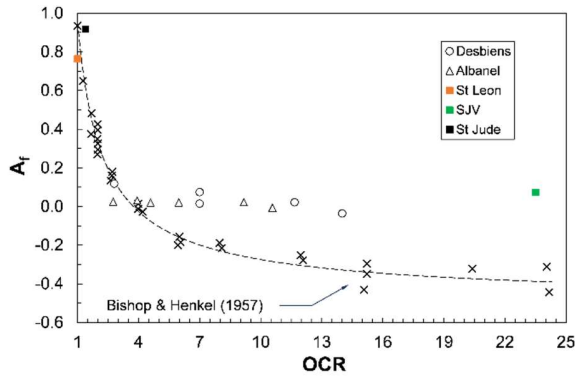


Figure 6.  $A_f$ -OCR relations of Desbiens and Albanel clays along with other Eastern Canadian clays

The peak stress ratio ( $\tau_p / \sigma'_{3c}$ ) is plotted against OCR for Desbiens and Albanel clays along with other Eastern Canadian clays in Figure 7. Here the peak shear stress,  $\tau_p$ , is assumed to be half of  $\Delta \sigma_f$ . The higher stress ratios of Laflamme clays by virtue of their overconsolidation is seen in Figure 7.

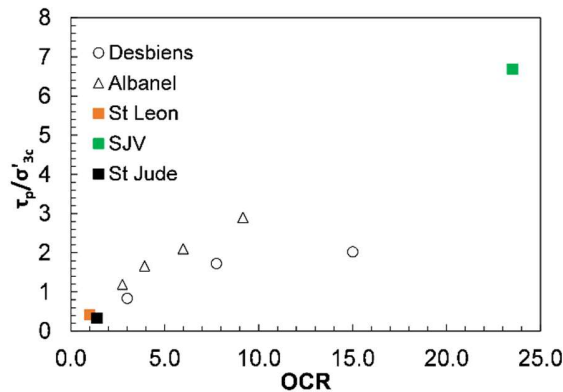


Figure 7. Stress ratios of Desbiens and Albanel clays along with other Eastern Canadian clays

#### 4.3.2 Remoulded shear strength

Remoulded undrained shear strengths were measured at different depths in Desbiens clays and all the boreholes in Albanel clays. According to the  $I_L$ - $s_{ur}$  correlation of Leroueil et al. (1983) and Locat and Demers (1988),  $s_{ur}$  for Desbiens and Albanel clays should be in the range of 2.1 - 3.3 kPa based on their  $I_L$  values (0.6 - 1). However, as mentioned before, it has been shown by Levesque et al. (2007) that these correlations underpredict  $s_{ur}$  of Laflamme clays. This is shown in Figure 8, where most of the results of this study, especially those for Albanel clays and SJV clays fall above the correlations. The Champlain clays of St Leon and St Jude follow this trend and the criterion for retrogressive flowslides with  $s_{ur} \approx 1$  kPa. Since Desbiens and SJV are known for retrogressive failures, it may be assumed that even when  $s_{ur}$  is above 1 kPa, for a retrogressive flowslide to occur, the  $s_{ur}$  need only be low enough for the remoulded clay to move out of the crater and leave an unsupported backscarp.

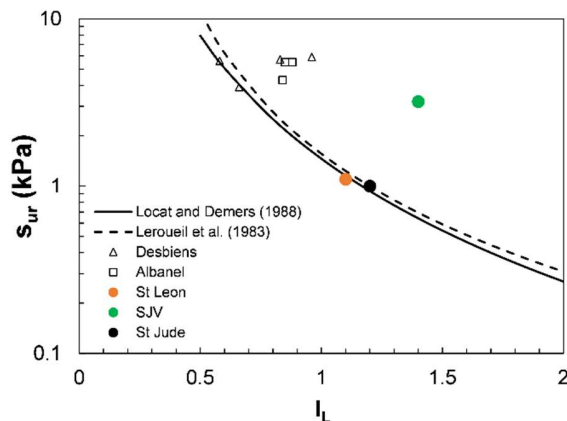


Figure 8. Comparison of remoulded undrained strengths of Desbiens and Albanel clays along with other Eastern Canadian clays with empirical trends of Locat and Demers (1988) and Leroueil et al. (1983)

## 12 CONCLUSIONS

A comparative analysis of geotechnical parameters from Champlain and Laflamme clays was carried out in this study. The experimental results of Laflamme clays from Desbiens and Albanel sites were primarily used for this analysis. For the comparative study, data on certain Eastern Canadian clays from literatures were relied upon. The study highlights certain differences in the behaviour of Champlain clays in comparison to Laflamme clays. Laflamme clays have lower clay fractions and liquid limits in comparison to Champlain clays. They do not have clay aggregations in the microstructure as in the Champlain clays and exhibit dilatant behaviour under undrained loading as opposed to a contractive failure in Champlain clays. They also possess higher strength ratios and remoulded strengths compared to Champlain clays. The primary reason for these differences is attributed to the depositional history of sediments in both regions with the Laflamme clays being more preloaded and overconsolidated. This study also highlights the importance of taking the geological history of sensitive clay sediments into consideration before conducting hazard assessment studies in sensitive clay landslides. In this particular study, only few Eastern Canadian clays were considered but it may be assumed that they represent the properties of the respective sedimentary basins.

### 13 REFERENCES

- American Society of Testing and Materials, (2021). Standard Test Method for Particle Size Distribution of Fine-Grained Soils Using the Sedimentation (Hydrometer) Analysis. ASTM Designation D7928-21e1.
- American Society of Testing and Materials, (2019). Standard Test Methods for Laboratory Determination of Water (Moisture) Content of Soil and Rock by Mass. ASTM Designation D 2216-19.
- American Society of Testing and Materials, (2018). Standard Test Methods for Liquid Limit, Plastic Limit and Plasticity Index of Soils. ASTM Designation D4318-17.
- American Society of Testing and Materials, (2011). Standard Test Method for Consolidated Undrained Triaxial Compression Test Method for Cohesive Soils. ASTM Designation D4767-11.
- American Society of Testing and Materials, (2000a). Standard Test Method for Specific Gravity of Soils. ASTM Designation D 854-00.
- Bishop, A. W., & Henkel, D. J. (1957). The measurement of soil properties in the triaxial test.
- Bouchard, R., Dion, D. J., & Tavenas, F. (1983). Origine de la préconsolidation des argiles du Saguenay, Québec. *Canadian Geotechnical Journal*, 20(2), 315-328.
- Chatillon, M. (1974). A literature review of stability of slopes in Champlain clay.
- Delage, P. (2010). A microstructure approach to the sensitivity and compressibility of some Eastern Canada sensitive clays. *Géotechnique*, 60(5), 353-368.
- Demers, D., Robitaille, D., Locat, P., & Potvin, J. (2014). Inventory of large landslides in sensitive clay in the province of Québec, Canada: preliminary analysis. *Landslides in sensitive clays: from geosciences to risk management*, 77-89.
- Flon, P. 1982. *Energie de remaniement et regression des coulees d'argile*. M.Sc. thesis, Dept. Civil Eng., Laval University, Quebec, Canada.
- Lefebvre, G., & Rochelle, P. L. (1974). The analysis of two slope failures in cemented Champlain clays. *Canadian Geotechnical Journal*, 11(1), 89-108.
- Lefebvre, G. (1981). Strength and slope stability in Canadian soft clays. *Canadian Geotechnical Journal*, 18(3), 420-442.
- Leroueil, S., Tavenas, F. and Le Bihan, J.P. (1983). Propriétés caractéristiques des argiles de l'est du Canada. *Canadian Geotechnical Journal* 20(4), 681-705.
- Levesque, C. L., Locat, J., & Leroueil, S. (2007). Characterisation of postglacial sediments of the Saguenay Fjord, Quebec, Canada. *Characterisation and engineering properties of natural soils*, 2645-2677.
- Liu, J., Afroz, M., & Ahmad, A. (2021). Experimental investigation of the impact of salinity on Champlain Sea clay. *Marine Georesources & Geotechnology*, 39(4), 494-504.
- Locat, A., Locat, P., Michaud, H., Hébert, K., Leroueil, S., & Demers, D. (2019). Geotechnical characterization of the Saint-Jude clay, Quebec, Canada. *AIMS Geosciences*, 5, 273-302.
- Locat, J., and St-Gelais, D. (2014). Nature of sensitive clays from Quebec. *Landslides in Sensitive Clays: From Geosciences to Risk Management*, 25-37.
- Locat, J., and Demers, D. (1988). Viscosity, yield stress, remolded strength, and liquidity index relationships for sensitive clays. *Canadian Geotechnical Journal* 25(4), 799-806.
- Quigley, R. M. (1980). Geology, mineralogy, and geochemistry of Canadian soft soils: a geotechnical perspective. *Canadian Geotechnical Journal*, 17(2), 261-285.
- Quinn, P. E. (2009). Large landslides in sensitive clay in eastern Canada and the associated hazard and risk to linear infrastructure, Ph.D. thesis (Vol. 71, No. 11).
- Rochelle, P. L., Chagnon, J. Y., & Lefebvre, G. (1970). Regional geology and landslides in the marine clay deposits of eastern Canada. *Canadian Geotechnical Journal*, 7(2), 145-156.
- Shan, Z., Zhang, W., Wang, D., & Wang, L. (2021). Numerical investigations of retrogressive failure in sensitive clays: revisiting 1994 Sainte-Monique slide, Quebec. *Landslides*, 18, 1327-1336.
- Skempton, A. W. (1954). The pore-pressure coefficients A and B. *Geotechnique*, 4(4), 143-147.
- Skempton, A. W. (1964). Long-term stability of clay slopes. *Geotechnique*, 14(2), 77-102.
- Thakur, V., Jostad, H. P., Kornbrenke, H. A., & Degago, S. A. (2014). How well do we understand the undrained strain softening response in soft sensitive clays? *Landslides in Sensitive Clays: From Geosciences to Risk Management*, 291-303.
- Torrance, J. K. (2017). Chemistry: an essential key to understanding high sensitivity and quick clays and to addressing landslide risk. In *Landslides in sensitive clays* (pp. 35-44), Springer, Cham
- Vaid, Y.P., Robertson, P. K., & Campanella, R. G. (1979). Strain rate behaviour of Saint-Jean-Vianney clay. *Canadian Geotechnical Journal*, 16(1), 34-42.